Olfaction and neurodegeneration: olfactory proteotyping across proteinopathies

Memoria presentada por

Mercedes Lachén Montes

para optar al grado de doctor por la Universidad Pública de Navarra

Pamplona-Iruña, 2019

Diseño de portada: **Unidad de Comunicación y Diseño de Navarrabiomed**

upna
Universidad Pública de Navarra
Nafarroako Unibertsitate Publikoa

Olfaction and neurodegeneration: olfactory proteotyping across proteinopathies

Los Dres. Enrique Santamaría Martínez y Joaquín Fernández Irigoyen INFORMAN que la presente memoria de tesis doctoral elaborada por Mercedes Lachén Montes ha sido realizada bajo su dirección y cumple con las condiciones exigidas por la legislación vigente para optar al grado de Doctor.

Y para que así conste, firman la presente en Pamplona, 21 de noviembre de 2018.

Enrique Santamaría Martínez

Joaquín Fernández Irigoyen

A mis padres, Marta y Mariano

Agradecimientos

En primer lugar, quiero agradecer al centro de investigación Navarrabiomed y a la Universidad Pública de Navarra por acogerme durante estos años y haberme permitido disponer de los recursos, medios y financiación necesarios para realizar mi tesis doctoral. También gracias a mi tutor Iñaki Encío por su disponibilidad y tiempo dedicado.

Pero no estaría escribiendo este apartado de agradecimientos de no ser por mis directores, Quique y Jokin, que confiaron en mí desde el primer momento para realizar esta tesis. Sobre todo, quiero agradecerles que me dieran esta oportunidad, no tan fácil de conseguir a día de hoy. Su apoyo y dedicación ha sido constante a lo largo de estos años. Gracias por su implicación en mi aprendizaje diario, por enseñarme a pensar y a pelearme con el 5600. Gracias porque he podido aprender de todo con los dos, desde los entresijos de la espectrometría de masas y la biología molecular, hasta el descubrimiento de nuevas bebidas. En este sentido, creo que es justo agradecerles también por todas las invitaciones que he recibido de su parte. Espero que esto no cambie.

En los cuatro años que llevo en Navarrabiomed son muchas las personas con las he tenido la oportunidad de cruzarme y me gustaría agradecer a todas aquellas que, poniendo su granito de arena, han contribuido a que esta investigación haya llegado a buen curso. Gracias a los departamentos de Gestión y Administración, a Maribel, y especial mención a las chicas de la Unidad de Comunicación y Diseño y en concreto a María, por todo lo que me ha ayudado para que esta tesis quede así de bonita. Me gustaría dar las gracias también a las chicas de Oncohematología, en especial a Cris, Estela y Miriam, que se volcaron en enseñarme de todo ese año que compartimos poyata. Gracias por vuestra amistad. Gracias a Xabi, por intentar explicarme conceptos de bioinformática desde su pantalla triple. Gracias también a todo el departamento de Proteómica de la Universidad de Ginebra por hacer de mi estancia allá una experiencia tan enriquecedora. Y por último, quiero acordarme de todos mis compañeros de otros grupos de investigación. Es una alegría ver cómo este centro ha crecido tanto y se ha

llenado de tan buena gente. Gracias a todos los que me han echado una mano cuando han podido, gracias por el buen rollo que se respira nada más cruzar las puertas y gracias por esas comidas que se convierten en cenas, recenas y subsecuentes cierres de locales nocturnos.

En cuanto a las chicas de Proteómica, el equipo que hemos formado estos años ha sido inmejorable. Gracias a Karina por ser la mejor boss del laboratorio que se pueda tener y por odiar juntas a Cadena 100, hartas de escuchar las mismas canciones. Gracias a Andrea, por haber recorrido este camino juntas enfrentándonos a los mismos problemas y por alumbrar con su luz cuando nos perdermos por el bosque. Gracias a Irene, por todos sus consejos y porque pelearse con el masas acompañado, siempre es mejor. No me olvido de Iranzu, que, aunque ya no es proteómica oficialmente, le agradezco la frescura y humildad que transmite cada día. También a Vicky, por el tiempo dedicado a enseñarme sobre la parte neuropatológica de esta tesis. Y gracias a Maialen por su gran implicación en este proyecto y contagiar sus ganas de aprender más y más. A todas, gracias por haberme ayudado siempre que habéis podido. Pero sobre todo, gracias por hacer que venir a trabajar sea tan fácil y divertido.

Mi camino hacia la investigación comenzó allá por 2009 cuando empecé a estudiar Bioquímica en la Universidad de Navarra. Sin duda alguna, lo mejor que encontré allí son mis queridas monadas: Ekhine, Irati, Libe, Miren, Patri y Tere. Es imposible haber tenido mejor suerte. Gracias a todas por todos estos años en los que, a pesar de vivir cada una en una punta (¡volved ya, malditas!), nos reencontramos y es como si estuviéramos a punto de coger el Ryanair para irnos a Bruselas, bien cubiertas de capas de ropa, o en Madrid, esquivando redes de pescar, o cogiendo el Euskotren a horas infernales, con caídas incluidas. Gracias por todo vuestro apoyo y ánimos en esas épocas de dudas existenciales.

Por supuesto, gracias a mis amigas: Izas, Ley, Lucía, Marta y Oihane (o lo que es lo mismo Sask, Panxi, Luzo, Mart o la Calvo, (tenía que ponerlo) y Poyo). Toda una vida juntas da para mucho lo que agradecer. Gracias por tener la cita del sábado por la noche como algo inamovible

e inexcusable, y por ser, siempre, de lo mejor de la semana. Gracias por todas las necesidades creadas, por todos los viajes habidos y por haber (¡y los que nos quedan!), por los litros de alcohol ingeridos (aunque sean cada vez menos…), por el milka, nestle jungly, y nocilla consumidos (menos mal que han ido a menos), por todo. Porque los amigos son la familia que se elige y yo no podría haber elegido mejor.

Por último, a mi familia. Que aunque somos pocos, cundimos mucho: mis tíos, mis abuelos, mis sobrinas, mi hermana Marta y Miguel, mis padres y Pablo. Gracias a mi abuela Mariasun por pensar que soy la mejor en todo aunque todavía no me haya visto en el periódico. Gracias a mi tío Ramón por guiarme y enseñarme tanto sobre este campo, siempre dispuesto a ayudarme, aunque a veces sea un poco pesado. Gracias a mis sobrinas Marta, Marina y Maitena por ser la alegría de la casa. Gracias a mi hermana por ayudarme a maquetar este trabajo, por todos sus sabios consejos de vida, aunque a veces ‘’se haga la madre’’ y todos los vampiros isleños vividos. Por supuesto, gracias a mis padres, porque sin ellos no habría llegado hasta aquí. Gracias por apoyarme siempre y siempre haberme dejado hacer lo que he querido.

Y gracias a Pablo. Por todo. Por intentar entender mi tesis y el mundo de la investigación, aunque le pille tan de lejos. Por ser el que más me aguanta (aunque yo le aguanto mucho también a él). Gracias por enseñarme tantas cosas, entre ellas a ser más inconformista. Gracias por estar ahí siempre, apoyándome en todas mis decisiones y sobre todo, animándome a superarme cada día.

A continuación, se exponen los **7 artículos** que constituyen esta tesis por orden cronológico junto a la relación de autores y el papel desempeñado por cada uno de ellos, las revistas en las que se han publicado o están pendientes de publicación y el factor de impacto de las mismas. El material suplementario de cada uno de los artículos se encuentra adjunto en el CD incluído en el dorso del libro.

Publicación 1:

An early dysregulation of FAK and MEK/ERK signaling pathways precedes the β-amyloid deposition in the olfactory bulb of APP/PS1 mouse model of Alzheimer's disease

Mercedes Lachén-Montes (MLM), Andrea González-Morales (AGM), Xabier Martínez de Morentin (XMM), Estela Pérez-Valderrama (EPV), Karina Ausín (KA), María Victoria Zelaya (MVZ), Antonio Serna (AS), Ester Aso (EA), Isidro Ferrer (IF), Joaquín Fernández-Irigoyen (JFI), Enrique Santamaría (ES)

Journal of Proteomics (2016), FI: 3.867

- MLM, EPV: preparación de la muestra y análisis proteómico.
- MVZ, EA, IF: selección de muestras y análisis inmunohistoquímico/neuropatológico
- MLM, AGM, EPV y KA: experimentos de validación y rutas de supervivencia
- AS, JFI y ES: espectrometría de masas e interpretación de los datos
- XMM: análisis bioinformático
- JFI y ES: diseño y supervisión del estudio y obtención de financiación
- ES: escritura manuscrito

Publicación 2:

Progressive modulation of the human olfactory bulb transcriptome during Alzheimer's disease evolution: novel insights into the olfactory signaling across proteinopathies

Mercedes Lachén-Montes, María Victoria Zelaya, Víctor Segura (VS), Joaquín Fernández-Irigoyen, Enrique Santamaría

Oncotarget (2017), FI: 5.168

- MLM: preparación de la muestra y extracción de RNA
- MLM, MVZ: selección de muestras y análisis inmunohistoquímico/neuropatológico
- VS: análisis estadístico y bioinformática
- MLM, JFI y ES: interpretación de los datos
- JFI y ES: diseño y supervisión del estudio y obtención de financiación
- ES: escritura manuscrito

Publicación 3:

Olfactory bulb neuroproteomics reveals a chronological perturbation of survival routes and a disruption of prohibitin complex during Alzheimer's disease progression

Mercedes Lachén-Montes, Andrea González-Morales, María Victoria Zelaya, Estela Pérez-Valderrama, Karina Ausín, Isidro Ferrer, Joaquín Fernández-Irigoyen, Enrique Santamaría

Scientific Reports (2017), FI: 4.259

- MLM, EPV: preparación de la muestra y análisis proteómico.
- MVZ e IF: selección de muestras y análisis inmunohistoquímico/neuropatológico
- MLM, AGM, EPV y KA: experimentos de validación y caracterización de pathways
- MLM, JFI y ES: espectrometría de masas, interpretación de los datos y análisis bioinformático
- JFI y ES: diseño y supervisión del estudio y obtención de financiación
- ES, MLM: escritura manuscrito

Publicación 4:

Network-driven proteogenomics unveils an aging-related imbalance in the olfactory IκB alpha-NFκB p65 complex functionality in Tg2576 Alzheimer's disease mouse model

Maialen Palomino, Mercedes Lachén-Montes, Andrea González-Morales, Karina Ausín, Alberto Pérez-Mediavilla (APM), Joaquín Fernández-Irigoyen, Enrique Santamaría

International Journal of Molecular Science (2017), FI: 3.226

- MP: preparación de la muestra y análisis proteómico.
- APM: selección de muestras y análisis inmunohistoquímico.
- MP, MLM, AGM y KA: experimentos de validación
- MP, MLM, JFI y ES: espectrometría de masas e interpretación de los datos
- MP, MLM: análisis bioinformático
- JFI y ES: diseño y supervisión del estudio y obtención de financiación
- ES: escritura manuscrito

Publicación 5:

Unveiling the olfactory proteostatic disarrangement in Parkinson's disease by proteome-wide profiling

Mercedes Lachén-Montes, Andrea González-Morales, Ibon Iloro (II), Felix Elortza (FE), Isidre Ferrer, Djordje Gveric (DG), Joaquín Fernández-Irigoyen, Enrique Santamaría

Neurobiology of Aging (2018), FI: 4.454

- MLM: preparación de la muestra y análisis proteómico.
- DG e IF: selección de muestras y análisis neuropatológico
- IL, FE: MALDI imaging
- MLM, AGM: experimentos de validación
- MLM, JFI y ES: espectrometría de masas, interpretación de los datos y análisis bioinformático
- JFI y ES: diseño y supervisión del estudio y obtención de financiación
- ES, MLM: escritura manuscrito

Publicación 6: (Submitted)

Early onset molecular derangements in the olfactory bulb of the Alzheimer's disease Tg2576 mice: novel insights into the stress-responsive olfactory kinase dynamics in Alzheimer's disease

Mercedes Lachén-Montes, Andrea González-Morales, Maialen Palomino-Alonso, Karina Ausin, Marta Gómez-Ochoa (MGO), María Victoria Zelaya, Isidro Ferrer, Alberto Pérez-Mediavilla, Joaquín Fernández-Irigoyen, Enrique Santamaría

Frontiers in Aging Neuroscience (2018), FI: 3.582

- MP: preparación de la muestra y análisis proteómico.
- APM, IF y MGO: selección de muestras y análisis inmunohistoquímico.
- MP, MLM, AGM y KA: experimentos de validación
- MP, MLM, JFI y ES: espectrometría de masas e interpretación de los datos
- MP, MLM: análisis bioinformático
- JFI y ES: diseño y supervisión del estudio y obtención de financiación
- ES: escritura manuscrito

Publicación 7: (Submitted)

The olfactory bulb proteotype differs across frontotemporal dementia spectrum: focus on progressive supranuclear palsy and frontotemporal lobar degeneration TDP43 proteinopathy

Mercedes Lachén-Montes, Andrea González-Morales, Domitille Schvartz (DS), María Victoria Zelaya, Karina Ausin, Joaquín Fernández-Irigoyen, Jean Charles Sánchez (JCS), Enrique Santamaría

International Journal of Molecular Sciences (2018), FI: 3.687

- MLM, DS: preparación de la muestra y análisis proteómico.
- MVZ: selección de muestras y análisis neuropatológico.
- MLM, AGM: experimentos de validación
- DS y JCS: espectrometría de masas
- MLM, JFI y ES: interpretación de los datos y análisis bioinformático
- JCS, JFI y ES: diseño y supervisión del estudio y obtención de financiación
- ES, MLM: escritura manuscrito

A continuación, se exponen brevemente las ayudas y financiaciones que han permitido el desarrollo de esta tesis:

- **Olfato y neurodegeneración: detección y categorización de alteraciones moleculares en el bulbo olfatorio como innovación diagnóstica de taupatías y sinucleopatías**

  MINECO (SAF2014-59340)

- **Perfil transcriptómico y proteómico del bulbo olfatorio en neurodegeneración: monitorización de mediadores proteicos en diferentes estadios de la enfermedad de Alzheimer**

  FUNDACION BANCARIA LA CAIXA

- **OLFAPROT: Aplicación de técnicas proteómicas sobre el bulbo olfatorio como innovación diagnóstica en la enfermedad de Alzheimer**

  FUNDACION CAJA NAVARRA (70027)

- **Desarrollo de biosensores para la enfermedad de Alzheimer**

  DEPARTAMENTO DE SALUD. GOBIERNO DE NAVARRA (72/2015)

- **BIOPTSENS: Sistema portátil para la detección rápida de biomarcadores asociados a la enfermedad de Alzheimer**

  DEPARTAMENTO DE DESARROLLO ECONÓMICO GOBIERNO DE NAVARRA

- **Ayudas para la formación de Personal Investigador de la Universidad Pública de Navarra para la realización de tesis doctorales 2017**

  UNIVERSIDAD PÚBLICA DE NAVARRA

- **Ayudas a profesionales para la formación continuada en Ciencias de la Salud**

  DEPARTAMENTO DE SALUD DEL GOBIERNO DE NAVARRA

- **Ayudas a la movilidad de doctorandos UPNA 2016-2017-2018**

  UNIVERSIDAD PÚBLICA DE NAVARRA – LA CAIXA

Por otra parte, agradecemos al **Biobanco de Cerebros del Complejo Hospitalario de Navarra, al Biobanco de la Universidad de Navarra-CIMA, al Parkinson's Brain Bank (Imperial College of London), Banc de Teixits Neurologics (Biobanc-Hospital Clinic-IDIBAPS) y al Biobanco de Cerebros de IDIBELL** por su colaboración en la obtención y cesión de muestras humanas y los datos clínicopatológicos asociados.

INDEX

ABSTRACT

It has been established that smell impairment is a common early feature of neurodegenerative diseases (NDs). In fact, there is a spectrum of olfactory dysfunction ranging from severe loss, as seen in Alzheimer's disease (AD) and Parkinson's disease (PD), to little olfactory deficits, as seen in frontotemporal dementias (FTD). That is why, ***it is likely that differential disruption of a common neuropathological substrates might be causing these differences in olfactory functionality***. The olfactory bulb (OB) is the first site for the processing of olfactory information and the ***deposition of pathological substrates such as amyloid peptides (Aß), α-synuclein or the hyperphosphorylated form of tau has been suggested as a potential origin of olfactory deficits***. However, it remains unknown whether these protein aggregates represent a cause or consequence of the neurodegenerative process ocurring in the OB.

In this thesis, a high-throughput comparative molecular analysis of OBs derived from: a) two familial AD mouse models; and b) 4 different NDs including AD, PD, frontotemporal lobar degeneration with TAR DNA-binding protein 43 deposits (FTLD-TDP43) and progressive supranuclear palsy (PSP) subjects, has been performed in order to characterize the neuropathophysiological mechanisms occurring in this structure during the neurodegenerative process. This wide analysis has shown great disarrangements in the OB proteostasis across AD and PD stages, where 20% of the quantified proteome was differentially expressed, while a minor deregulation was observed in FTLD-TDP43 and PSP subjects, where ~1% of the quantified proteome was affected. Interestingly, ***both commonalities and differences were observed in the proteomic signature across the NDs at the OB level***. On the other hand, ***olfactory molecular disarrangements were observed at early AD stages and prior to the appearance of both Aß plaques and memory impairments*** in two different mouse models. Finally, the use of olfactory proteomics as a resource for the discovery of neurodegeneration biomarkers has been demonstrated, identifying *Glucosamine-6-phosphate isomerase 2* (GNPDA2) as a potential biomarker candidate for PD.

RESUMEN

La disfunción olfatoria es un síntoma temprano y común en diversas enfermedades neurodegenerativas (ENs). Según el grado de disfunción olfatoria que presentan, existen ENs con disfunción olfatoria pronunciada, como la enfermedad de Alzheimer (EA) y la enfermedad de Parkinson (EP), y otras con déficits más leves, como ocurre en las demencias frontotemporales. ***Se ha sugerido que la existencia de un sustrato patológico común actuando mediante diferentes mecanismos en este amplio espectro de ENs podría ser el causante de estas diferencias en el déficit olfatorio.*** El bulbo olfatorio (BO) es la primera estructura del cerebro responsable de procesar la información olfatoria y ***el depósito de sustratos neuropatológicos como el péptido amiloide o la forma hiperfosforilada de la proteína tau en esta región se ha propuesto también como posible origen de este síntoma.*** Sin embargo, se desconoce si los agregados neuropatológicos son causa o consecuencia del proceso neurodegenerativo que ocurre en esta región.

En esta tesis se ha realizado un análisis molecular de alto rendimiento en BOs procedentes de: a) dos modelos animales de la EA; y b) sujetos diagnosticados con cuatro ENs incluyendo la EA, la EP, la degeneración lobar fronto-temporal con depósitos de *TAR DNA-binding protein* (FTLD-TDP43) y la parálisis supranuclear progresiva (PSP), con el objetivo de caracterizar los mecanismos neuropatofisiológicos que ocurren en esta región durante el proceso neurodegenerativo. Este amplio análisis ha demostrado que existe una gran alteración en la proteostasis del BO durante la EA y la EP, donde los resultados mostraron un 20% del proteoma cuantificado diferencialmente expresado. Por otra parte, en el caso de los sujetos diagnosticados con FTLD-TDP43 y PSP, el número de alteraciones fue mucho menor, constituyendo alrededor del 1% del proteoma cuantificado. Es interesante resaltar que se han encontrado ***tanto similitudes como diferencias en los mediadores proteicos diferencialmente expresados entre las ENs analizadas y la población control***. Por otra parte, el estudio en los dos modelos animales de EA ha demostrado que, ***a nivel de BO, existen alteraciones moleculares previas a la aparición de placas amiloides y deficits cognitivos***. Finalmente, se ha demostrado

la utilidad de la proteómica dirigida a estructuras olfatorias como fuente de biomarcadores en ENs. De hecho, se propone la proteína *Glucosamine-6-phosphate isomerase 2* (GNPDA2) como potencial biomarcador de la EP.

ABBREVIATIONS

AC: Adenylyl cyclase

AD: Alzheimer´s disease

AKT: Protein kinase B

ALS: Amyotrophic lateral sclerosis

AON: Anterior olfactory nucleus

APP: Amyloid precursor protein

Aβ: Beta-amyloid

BAD: Blc2-associated agonist of cell death

bvFTD: behavioural variant of frontotemporal dementia

CACYBP: Calcyclin biding protein

CamkIIa: Ca2+/CaM-dependent protein kinase type II subunit alpha

CERAD: Consortium to establish a registry for Alzheimer's disease

CJD: Creutzfeldt-Jakob disease

CNGA2: Cyclic-nucleotide gated channel

CNDP2: Cytosolic nonspecific dipeptidase 2

CPNE: Copine-6

CREB: cAMP response element-binding

c-JUN: AP-1 transcription factor subunit

CSF: Cerebrospinal fluid

CT: Computerized tomography

DA: Dopaminergic neurons

DPP6: Dipeptidyl aminopeptidase-like protein 6

EGFR: Epidermal growth factor receptor

ENS: Enteric nervous system

ERK: Extracellular signal regulated kinase

FAK: Focal adhesion kinase

FDA: Food and Drug Administration

FDR: False discovery rate

fMRI: Functional magnetic resonance imaging

FTD: Frontotemporal dementia

FTLD: Frontotemporal lobar degeneration

FTLD-tau: Frontotemporal lobar degeneration with tau deposits

FTLD-TDP43: Frontotemporal lobar degeneration with TDP43 deposits

FTLD-FUS: Frontotemporal lobar degeneration with fus inclusions

FUS: Fused in sarcoma

Gdap: Ganglioside induced differentiation associated protein 1

GPCRs: G-protein coupled receptors

GEP: Gene expression profiling

GNPDA2: Glucosamine 6 phosphate isomerase 2

GRN: Granulin

HC: Healthy controls

HPP: Human Proteome Project

IPA: Ingenuity pathway analysis

iTRAQ: isobaric tags for relative and absolute quantitation

LBs: Lewy bodies

LCM: Laser capture microdissection

LC-MS/MS: Liquid chromatography tandem mass spectrometry

LC-ESI-Q-TOF MS: Liquid chromatography-electrospray ionization-quadrupole-time of flight mass spectrometry

LTS: Lewy-type alpha-synucleinopathy

MALDI: Matrix Assisted Laser Desorption/Ionization

MAPT: Microtubule-associated protein tau

MARCKS: myristoylated alanine rich C kinase substrate

MCI: Mild cognitive impairment

MEK: dual specificity mitogen activated protein kinase kinase

MMTS: M-methylmethanethiosulfonate

MS: mass spectrometry

MRI: Magnetic resonance imaging

NDs: Neurodegenerative diseases

Ndufs2: NADH deshydrogenase iron sulfur protein 2

NGS: Next-generation sequencing

NIA-RIA: National Institute of the Alzheimer's Association

NFT: Neurofibrillary tangles

nfvPPA: nonfluent variant primary progressive aphasia

OB: Olfactory bulb

OE: Olfactory epithelium

ORs: Olfactory receptors

OSNs: Olfactory sensory neurons

OT: Olfactory tract

PART: Primary age related tauopathy

PD: Parkinson's disease

PDK1: Phosphoinositide-dependent protein kinase 1

PET: Positron emission tomography

PIP2: Phosphatidylinositol 4,5 bisphosphate

Pip4k2a: Phosphatidylinositol 5-phosphate 4 kinase type 2 alpha

p38 MAPK: p38 Mitogen activated protein kinase

PMCA2: plasma membrane calcium transporting ATPase 2Phb1: Prohibitin-1

Phb2: Prohibitin-2

PKA: protein kinase A

PKC: Protein kinase C

PMI: Post-mortem interval

PP5: Serine/threonine protein phosphatase 5

PS1: Presenilin 1

PSP: Progressive supranuclear palsy

RACK1: Receptor of activated protein C kinase 1

sAD: sporadic Alzheimer's disease

SAPK/JNK: stress activated protein kinase/jun-amino terminal kinase

SCGN: Secretagogin

Smap1: Stromal membrane-associated protein 1

SEK/MKK4: Mitogen activated protein kinase kinase 4

SN: Substantia nigra

STAT3: Signal transducer and activator of transcription 3

svPPA: semantic variant primary progressive aphasia

TAARS: Trace amine-associated receptors

TDP43: TAR DNA binding protein 43

TFG-beta: Transforming growth factor beta

Tom1: Target of Myb protein

UPSIT: University of Pennsylvania Smell Identification Test

VIM: Vimentin

WT: Wild-type

INTRODUCTION

1. The olfactory system

The olfactory system is part of the sensory system used for smelling and responsible for the processing of the information related to identity, concentration, and quality of chemical stimuli. It comprises sensory structures such as the olfactory epithelium (OE) and other brain regions such as the olfactory bulb (OB) and the olfactory tract (OT) (Figure I1).

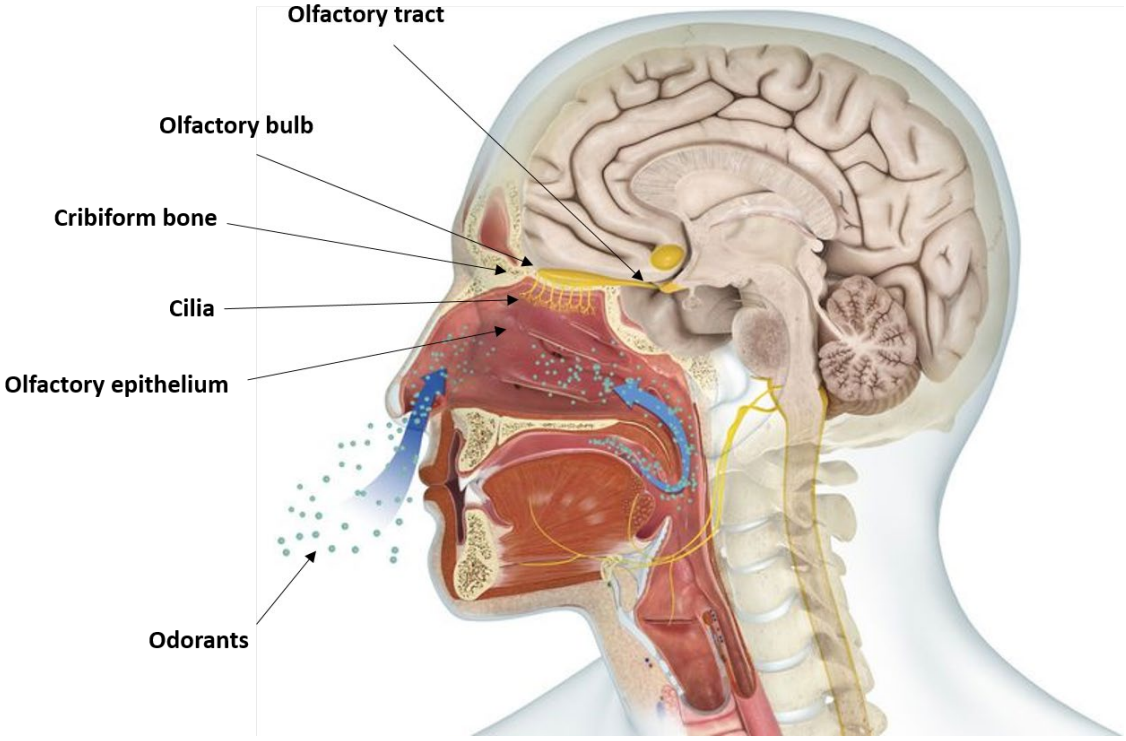

Figure I1: Overview of the olfactory system.
Adapted from https://www.thoughtco.com/olfactory-system-4066176

1.1. Anatomy and physiology of olfactory structures

Olfactory epithelium

The chemical stimuli i.e. the molecular odorants enter through the nasal cavity and arrive to the olfactory mucosa. This region is located in the superior and posterior part of the nasal cavity, close to the cribiform plate. The olfactory mucosa comprises the OE and its lamina propria. The first is a pseudostratified epithelium that contains olfactory sensory neurons

(OSNs). The OSNs are bipolar neurons responsible for the detection of molecular odorants and the OE is full of millions of these cells. They possess a thin dendritic rod that contains specialized cilia covered in specialized receptors for odour detection, providing the transduction surface for the odorous stimuli. The axons of the OSNs leave the OE and join in bundles in the lamina propria gathering into larger fascicles and then traversing the skull base through the opening of the cribiform plate and entering into the olfactory bulb (OB) [1, 2].

The Bowman's gland, which lies in the lamina propria underneath the epithelial layer, together with the supporting cells of the OE, secrete the mucous covering the epithelium. This mucous is mainly aqueous, however, the binding cavities of the olfactory receptors (ORs) are somewhat hydrophobic. The secretion of odorant-binding proteins increases the solubility of the hydrophobic molecules, allowing them to reach the ORs in the mucous layer. There are also some enzymes in this region that break down the odorant molecules facilitating their interaction with the ORs [2].

Underlying the OE, there is a niche of basal stem cells. Unusually, the OE undergoes a continue process of neurogenesis in which the OSN population is renewed constantly [3]. This regularly turnover and new development and maturation of OSNs is unique to the mammalian olfactory system and it is due to the damage that this region suffers because of its exposure to environmental agents (airborne toxins, harsh chemicals, viruses). Current research is now exploring this unique capacity of these cells for its use as therapies in other neuronal types [4-6].

In the OE, the OSNs cilia comprise the well-known OR proteins [7]. There are two families of odorant receptors: the canonical ORs and the trace amine-associated receptors (TAARS) [8]. The first one comprises a large family of G-protein coupled receptors (GPCRs) predicted to have a seven-transmembrane domain topology. This family represents 2-3% of the human genome and it is highly variable. Humans have around 800 ORs, however, 400 are pseudogenes, leaving about 400 ORs that code for functional receptors. In fact, this family is poorly characterized at

proteomic level, belonging mainly to the group of proteins of which there is only information concerning their transcripts (PE2, according to the NextProt database) [9]. The OSNs express just one of those ORs and OSNs expressing the same OR are broadly dispersed throughout the OE being distributed not uniformly. Only some subgroups seem to be confined to several broad regions within the nasal cavity. However, the functional relevance of these zonal-expression pattern is still unknown.

OSNs need to respond to many different odorants. That is why, the OR gene family is characterized by a huge diversity in the transmembrane domains predicted to interact with the odorant molecules. Also, this diversity allows the different receptive ranges of these ORs. Each OR has a distinct receptive range in its response to odorants and different response profiles to high or low concentrations of odours. Thus, odour information is encoded by distinct patterns of OSNs activation. However, it is important to note that there is lack of information regarding the match of ORs to its ligand. Apparently, OSNs respond to many different odorants, and each odorant can interact with multiple receptors [10].

The second family of odorant receptors expressed in the OSNs is the TAARs [11]. This family responds mainly to amines and also consist in seven transmembrane GPCRs. In human, this family is composed by six intact members. As in ORs, OSNs only expressed one type of TAAR, localized in their cilia and projecting to the glomeruli in the OB. In both types of receptors, the olfactory signals transduction pathway begins with the binding of the molecular odorants to their receptor (Figure I2). This binding makes the receptor to undergo a conformational change, allowing to function as a guanine nucleotide exchange factor. The receptor activates its associated G-protein (Golf) and dissociating from its beta and gamma subunits, activates adenylyl cyclase III (ACIII). The cascade continues with the accumulation of cAMP that binds and opens the cyclic-nucleotide gated channel (CNGA2). This channel allows the influx of positive calcium and sodium from the mucous layer, initiating the depolarization along the neuron. This depolarization is increased with the binding of the calcium to the chloride channels that leads

to the efflux of Cl- ions. This propagated ion action potential leads to the final release of neurotransmitters at its synapse with the OB [12]. To rapidly turn off the response to a stimulus and to prepare for the next one, the intracellular calcium binds to the calcium-binding protein calmodulin, which afterwards binds to CNGA2, decreasing its affinity for cAMP and therefore, stopping the calcium influx. Also, calmodulin activates CAMKII that results in the phosphorylation of ACIII, which decreases the cAMP production. Additionally, the molecular odorants are removed and degraded by the enzymes in the mucous flow [12].

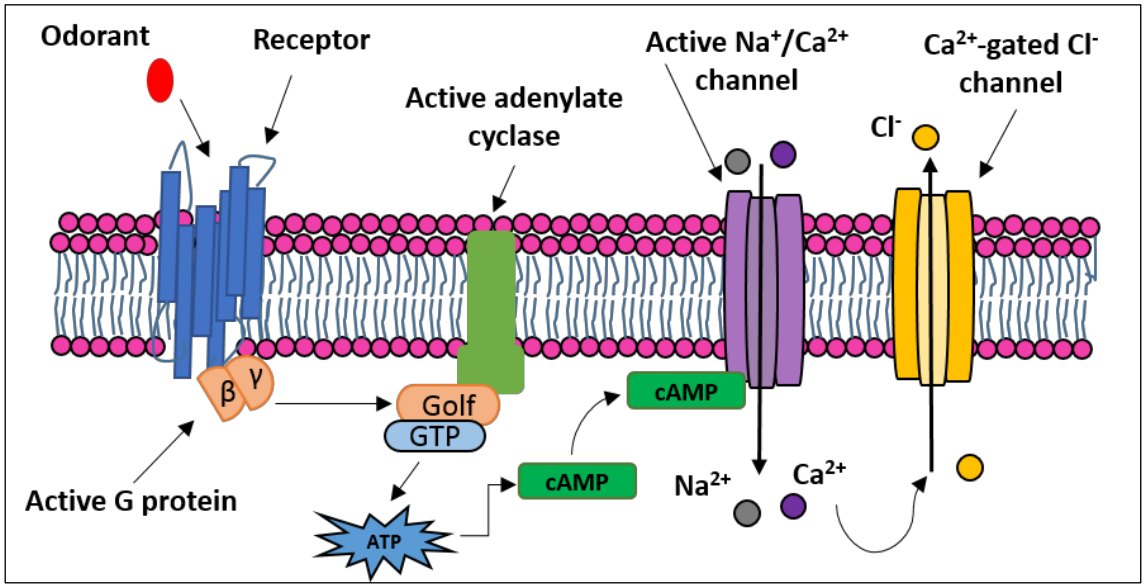

Figure I2: Olfactory transduction signal cascade.

Olfactory bulb

The OB is the first brain region to process the odour information [13]. The OB is a well-defined structure, located in the ventral surface of each frontal lobe above the cribiform plate. It is composed by concentric layers with different cellular types (Figure I3 and I4).

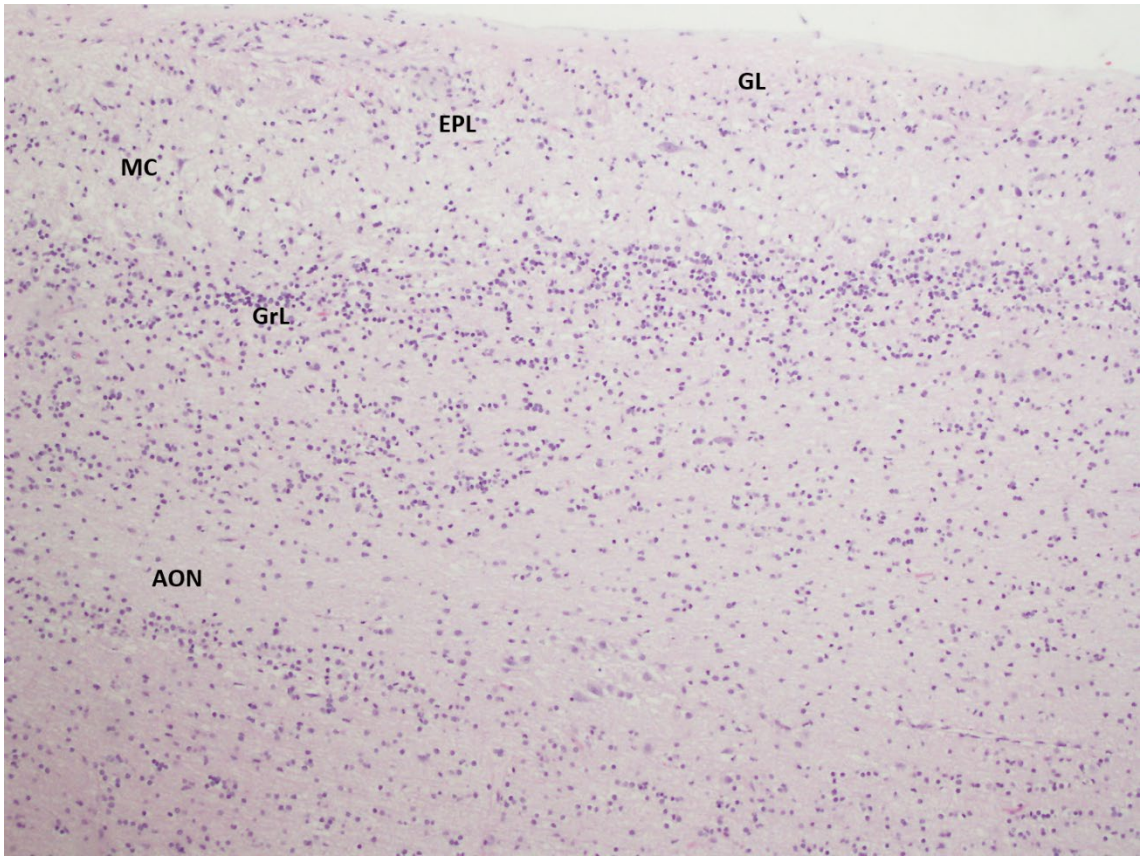

Figure I3. Hematoxylin-eosine figure representing the panoramic view of the OB cell layers. GL: glomerular layer; EPL: external plexiform layer; MC: mitral cell layer; GrL: granular cell layer; AON: anterior olfactory nucleus (40X).

In the glomerular layer, the main anatomical structures are the glomeruli. Each OSN sends one axon to one glomerulus. Because each OSN expresses one type of ORs, pre-synaptic glomerular-activation patterns are a direct reflection of the tuning properties of the OR. Within the glomeruli, the axons of the OSNs synapse with the dendrites of different neuronal populations, such as the mitral and tufted cells and the periglomerular interneurons. Incoming sensory information passes to the mitral and tufted cells that provide the output to higher central olfactory regions. Each glomerulus has around 20-50 mitral and tufted cells. These cells interact with periglomerular cells, forming dendrodendritic synapses and inhibiting their synaptic relay of OSNs information. They also interact with granule cells, located in the deeper external plexiform layer of the OB and without axons, forming also dendrodendritic synapses

that modulate negatively their activity. Thus, in the OB, the physiology is determined by the spatial nature of the input. Each mitral cell has a dendrite in only a single glomerulus, thus, the activity of the mitral cells is spatially distributed such that odorants are represented in the OB by a distributed pattern of mitral cell activity. The nature of interneuron connectivity then leads to a sharpening of the response of the mitral cells both in time and space, with the effect of narrowing the responses of the mitral cells to a smaller number of odorant molecules compared to the sensory neurons [14].

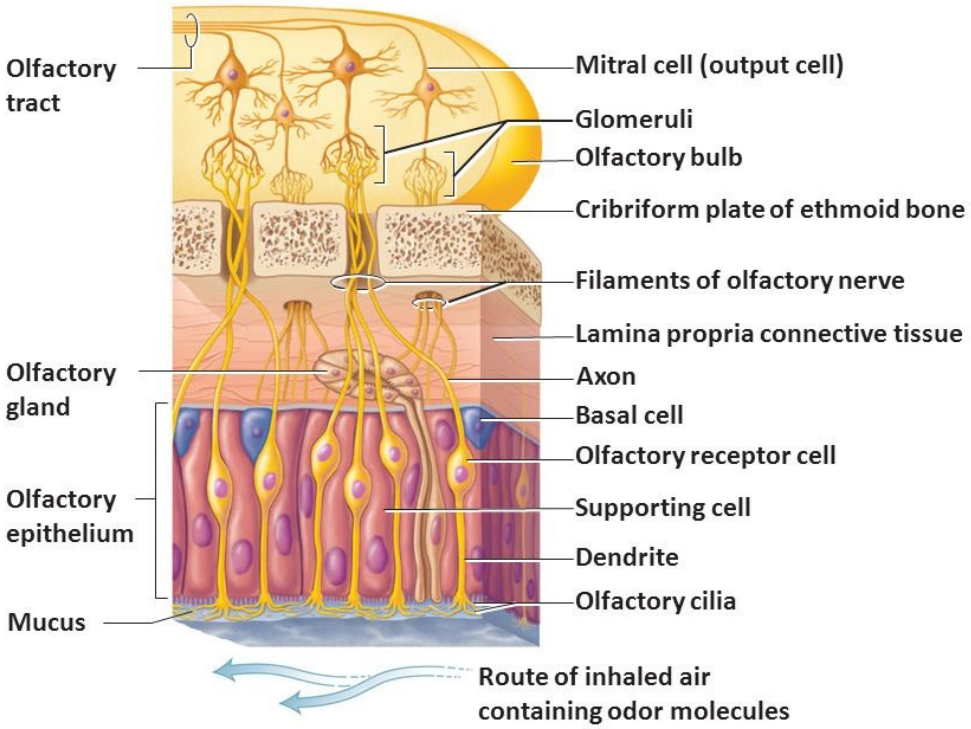

Figure I4: Scheme of the cell layers composing the OB. Image taken from lifeinharmony.me/anatomy-of-the-nose-smell

Olfactory tract

The OT is composed mainly by the afferent axons coming from the mitral and tufted cells in the OB. This region connects the odorant output to other central brain regions such as the piriform cortex, the amygdala and enthorinal cortex. It lies in the olfactory sulcus on the inferior

surface of the frontal lobe and is divided in two striae, a medial olfactory stria and a lateral olfactory stria. The OT appears to end in the antero-lateral part of the olfactory tubercle, the dorsal and external parts of the anterior olfactory nucleus (AON), and the frontal and temporal parts of the prepyriform area, the corticol-medial group amygdaloid nuclei and the nucleus of the stria terminalis [15].

1.2. Neuronal connections with other brain regions

The sensory information processed in the OB targets different regions in the brain implicated in memory and emotion including the piriform cortex, the AON, the nucleus of LOT, the periamygdaloid cortex, the olfactory tubercle, the anterior and posterior cortical amygdala and the entorhinal cortex. Interestingly, these structures, except the olfactory tubercle, send descending projections back to the OB (to interneurons at the granule and periglomerular level). This feature distinguishes this system from other sensorial systems, suggesting that the OB is not a merely passive conduit but might act also as a filter of some sort. Thus, these centrifugal projections seem to play an important role of behaviour modulation [16].

The primary olfactory cortex

The primary olfactory cortex includes regions such as the AON, the olfactory tubercle, the piriform cortex, the periamygdaloid cortex, the lateral enthorinal cortex, the cortical amygdaloid nuclei, the ventral tenia tecta, and the nucleus of the lateral olfactory tract [17]. Most OB projections target the piriform cortex. Interestingly, the OB projections to the piriform cortex are distributed randomly. This is surprising viewing the extreme organization that occurs in earlier stages of the olfactory signal transduction. Moreover, the anterior piriform cortex receives more afferent inputs from the OB and fewer associational inputs than the posterior division. This suggests that the anterior piriform cortex encodes odour identity, while the posterior form compares the odour to store information and is capable of detecting correlations between olfactory subjects. The second largest brain structure that receives OB projections is

the AON. The pars externa region of the AON receives projections from the ipsilateral OB and projects to the contralateral OB. These interbulbar connections implicate this structure in interhemispheric processing of odour information, especially in olfactory memories. There is evidence that bi-nasal mechanisms operate in the spatial localization of odours, and the AON may be responsible of this feature [18].

The secondary olfactory areas

The piriform cortex mainly projects to the amygdala, entorhinal cortex, dorsomedial nucleus of the thalamus, hypothalamus, ventral putamen, orbitofrontal cortex, and insular cortex. The orbitofrontal cortex is the main region and in fact is often referred as the secondary olfactory cortex itself. It receives both connections from the piriform cortex and indirect connections from through the dorsomedial nucleus of the thalamus. Lesions in this region result in deficits in odour discrimination and identification [19].

1.3. Functionality of the olfactory system

The sense of smell has been usually neglected in the clinical practice. Until very recently, the efforts that were made to understand human olfaction were mainly focused in the study of lesions in this region. Thanks to the development of imaging techniques such as the functional magnetic resonance imaging (fMRI) or the positron emission tomography (PET), it is now possible to know the activation patterns associated to a particular cognitive process allowing the identification of the neural networks specifically activated by chemosensory stimuli, here in particular, concerning the olfactory system [20]. For instance, we know that when the molecular odorants are delivered to subjects, the right orbitofrontal cortex is activated (sometimes the piriform also is activated) and independently which side of the nose is stimulated [21]. Moreover, when subjects perform specific olfactory tasks, it is possible to reveal information regarding successive steps of odour processing. The piriform cortex appears to be involved in odour recognition memory, as indicated by strong bilateral PET activity in long term, rather than

in short-term recognition tasks [22]. Other structures of the medial temporal lobe such as the hippocampus and the perirhinal and the parahippocampal regions are currently of interest in several aspects of memory such as associative vs. non-associative memory, or recollection vs. familiarity [23]. Besides, these same regions are activated during odour discrimination [24], familiarity judgements [25], and during familiar odour stimulation [26]. Concerning odour identification, the activation of the left inferior temporal gyrus has been demonstrated. This region is responsible for making edibility judgements and naming odours [24]. However, activation during familiarity has also been observed, pointing out the fact that odour familiarity is also important for odour naming.

Another characteristic to take into account in relationship with odour stimulation is odour pleasantness. Interestingly, it has also been demonstrated that while highly aversive odours activate the left orbitofrontal cortex and amygdala bilaterally, less aversive odours only activate the left orbitofrontal cortex [27]. The left orbitofrontal cortex, temporal pole, and superior frontal gyrus are activated in PET scans when subjects are presented with emotionally, olfactory, visual, and auditory stimuli [28]. This suggests that pleasant and unpleasant emotional judgements call upon the same core network in the left hemisphere regardless of the sensory modality. On the other hand, odour and taste intensity have been shown to be associated with activation of the amygdala and piriform cortex [29]. However, activity within the left amygdala and piriform cortex is also found to be significantly correlated with subjective ratings of perceived aversiveness, but not with perceived intensity [30]. This is due to the fact that unpleasant odours can induce intense negative emotional reactions (e.g., disgust) whereas pleasant odours rarely induce intense emotional reaction (e.g., euphoria). This is consistent with the hypothesis that the amygdala mediates both negative and positive emotions, and that differences in activity of this area stem from the intensity of the induced emotion [21]. In contrast to the amygdala, the left orbitofrontal cortex is activated when subjects are specifically asked to judge whether an odour is pleasant or unpleasant compared to passively smelling these

same odorants [30]. This finding suggests that the left orbitofrontal cortex is involved in the conscious assessment of the emotional quality of odours. Hence, orbitofrontal cortex activation during passive detection of mildly pleasant and unpleasant is probably evoked by spontaneous hedonic judgements [31].

2. Olfactory dysfunction in neurodegenerative diseases

Olfactory impairment is a common occurrence during aging [32]. In fact, it has been reported that, in case of healthy people over 60 years old, 16% of the cases are affected [33] and this percentage increases as we grow old [34]. This deficit is caused by different changes in the anatomy of the olfactory system, such as a decrease in the number of ORs in the OE [35] and, in central level, a progressive loss of neurons [35]. The presence of neuropathological features such as neurofibrillary tangles (NFT) and amyloid plaques in this region has also been demonstrated. However, in case of amyloid plaques, there are usually found in a diffuse way, different to those found in Alzheimer's disease (AD) patient's brains [35]. At the level of the OB, a progressive atrophy occurs that leads to a loss of function. The volume of this region maintains its shape until the fourth decade of life and starting to reduce in the sixth [36]. Overall, this translates in an increment in the threshold to detect a wide variety of substances, a decrease in the odour perception and difficulty to name the different odours [37]. The specific causes of this functional decline are still unknown. Different factors might influence the ability to smell such as exercise and physical activity, genetic factors, head trauma, smoking and, nutrition. Moreover, exposure to toxic substances or viral infections can also damage the olfactory region [38]. In fact, numerous theories link the exposure to different pathogens with the development of neurological diseases such as Parkinson's disease (PD) [39].

Smell impairment is a common feature in NDs, particularly exaggerated in AD and PD, but being also present in other less prevalent such as frontotemporal dementias (FTD), or amyotrophic

lateral sclerosis (ALS) [40-43]. This deficit reaches the 90% of the patients in case of AD and PD [41, 44] and moreover, this symptom appears at very early stages of the disease, being even suggested as a preclinical sign of neurodegeneration [45]. Nevertheless, in clinical practice, the sense of smell is usually neglected. This is unfortunate because olfactory deficits assumed in healthy people might be actually the early symptoms of a neurological disorder. In this sense, tests of olfactory function have been included in the battery diagnostic tools for AD and PD [46, 47]. Interestingly, a recently published study aimed to classify distinct neurological disorders given the score of patients being tested with an olfactory test (the University of Pennsylvania Smell Identification Test (UPSIT)) [48]. This test consists in 40 different odorants and patients are supposed to identify, recognize or distinguish them [49]. The results showed that AD and PD are located in the group with more severe smell deficit, while the FTD spectrum one was much mild. However, the aberrant molecular mechanisms occurring at the level of the olfactory system remain unknown. In the following sections, the olfactory dysfunction occurring in a group of NDs including AD, PD and FTD will be described.

2.1. Alzheimer's disease

AD pathogenesis

AD represents 50-70% of worldwide dementias, being the most prevalent one. The Alzheimer's Association estimates that in 2050 the people suffering from AD will reach 26 million. These data together with those who estimate that in 2050 one in three person will be older than 65 years old, point out how the health-care systems might be economically affected because of this issue and the urgency to find not only curative treatments for this disease but also predictive biomarkers that could help the patients and their families in the life planning and decision making [50].

Only a small number of patients, around 5% of them, develop early-onset AD (< 65 years) due to the inheritance of autosomal dominant mutations in genes whose protein products lead

to the production of pathological Aβ peptides [51, 52]. Otherwise, the majority develop sporadic late-onset AD (> 65 years), being aging the more important risk factor to develop this disease. Other risk factors include low level of education, severe head injury, diabetes and obesity [50].

Concerning the specific causes that lead to the development of the typically well-known symptoms in these patients such as memory loss, disorientation or behaviour changes, there are two pathological hallmarks supposed to provoke the neuronal loss (Figure I5). The first one has to do with the production of Aβ peptides. The amyloid precursor protein (APP) is a transmembrane protein that can be processed by the family of secretases. All healthy brains produce Aβ peptides but there are usually quickly removed by clearance mechanisms. However, a wrong processing leads to the overproduction, aggregation and accumulation of more hydrophobic Aβ peptides, with a 40-42 aminoacids length. Those peptides easily tend to aggregate forming assemblies ranging from oligomers to protofibrils, fibrils and, amyloid plaques. These inclusions localized extracellularly interact with cell-surface membranes and receptors, altering signal-transduction cascades, disturbing neuronal activities and potentiating the release of neurotoxic mediators by immune cells such as microglia [53]. The other important hallmark in the AD pathogenesis is the microtubule-associated protein tau (MAPT) hyperphosphorylation. The role of this protein is related with the stabilization of the microtubules, main component of the cytoskeleton. In AD, tau hyperphosphorylation leads to the formation of paired helical filaments and the NFT afterwards [54]. These intracellular inclusions disrupt the correct transport of molecules inside of the neuron leading to neuronal death. Which of the two pathological deposits is firstly involved in the disease development still remains on debate. What is clear is that these two pathological hallmarks lead to alterations in synaptic plasticity and neuronal integrity, causing dementia in AD.

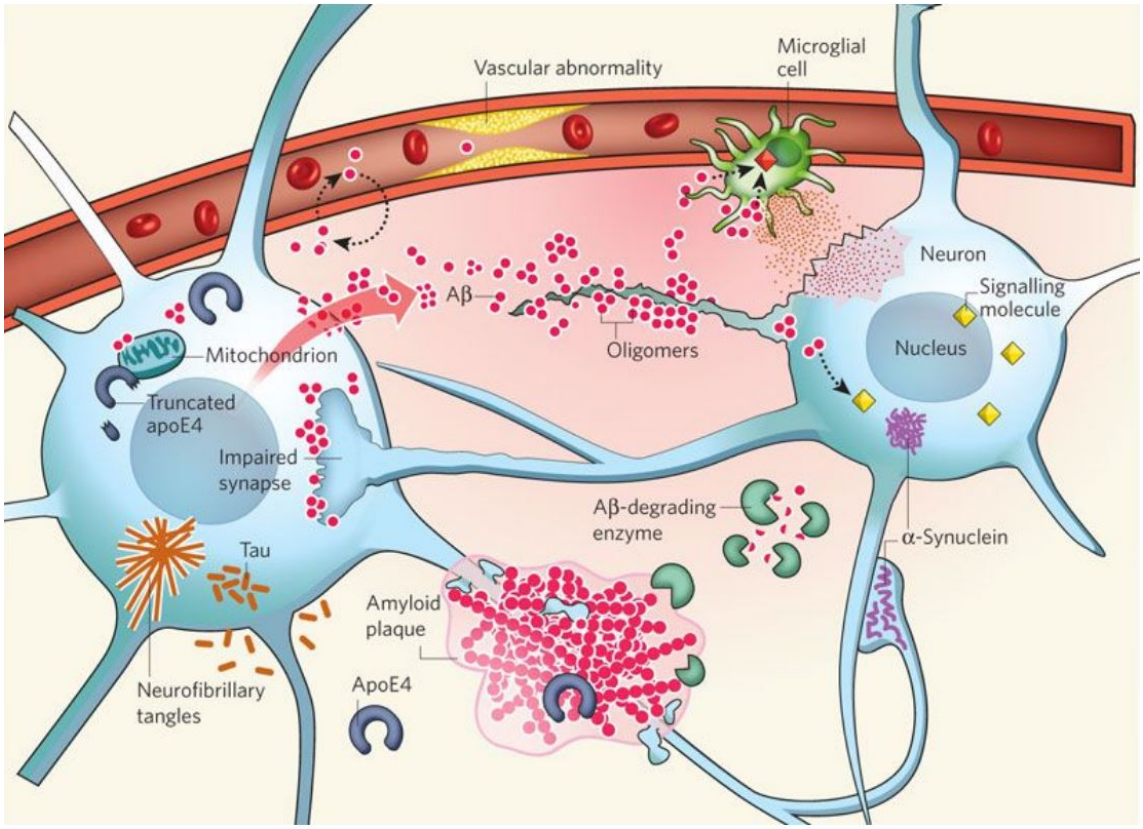

Figure I5: Overview of the general AD pathological mechanisms. The increased production of Aβ together with the abnormal behaviour of secretases and the decreased activity of Aβ-degrading enzymes, lead to the aggregation and accumulation of Aβ oligomers constituting the amyloid plaques. These oligomers impair synaptic functions interacting with cell-surface membrane receptors, altering signal-transduction cascades and even triggering the release of neurotoxic mediators by microglia. On the other hand, the hyperphosphorylation of tau provoques the formation of large intra-neuronal aggregates (NFT), which displace intracellular organelles. Figure taken from Lennart M, *Nature* 2009, 461, 895-897.

AD diagnosis and treatment

Unfortunately, there is no diagnostic tool that could tell whether a patient does or does not suffer from AD. The definitive diagnosis is performed once the patient has died with the neuropathological study of brain regions. For now, the clinical diagnosis is based on the exhaustive analysis of the medical history, objective cognitive assessment tests (MMSE: Mini Mental State Exam, or Mini-cog) [55], neurological tests (reflexes, coordination, speech) or through brain imaging tools MRI or computerized tomography (CT), usually used to discard other

possible conditions that may be the cause of brain damage such as tumours, strokes or head traumas [56].

As mentioned before, AD is characterized by the presence of NFTs and amyloid plaques. However, the neuronal loss occurring during AD progression, does not always correlate with the density or number of NFT and amyloid plaques. That is why, the diagnostic based on these two criteria might not mirror cognitive decline. Currently, there are three pathological criteria for AD diagnosis: Braak's criterion [57], Consortium to establish a registry for Alzheimer's disease (CERAD) criterion [58], and their combination or National Institute of the Alzheimer's Association (NIA-RIA) criterion [59]. The first one, Braak's criterion is based on the distribution of NFTs, starting in the transentorhinal area (Stage I), and then spreading to entorhinal region in stage II. In stage III, NFTs extend to the hippocampus and increase in number till stage IV. In stage V, the neocortex is then affected and finally, in stage VI, the primary cortex gets involved. The CERAD criterion requires Bielschowsky staining of the second frontal gyrus at the level of the caudateputamen complex, the first temporal gyrus at the level of the amygdala and the supramarginal gyrus with parietooccipital sulcus. The maximum density of neuritic plaques is calculated and the cases are classified into stage A, less than 2; stage B, approximately 6; and stage C, more than 30 neuritic plaques per 100 x light microscopic field. Finally, the NIA-RIA criterion is a combination of the above criteria.

Concerning the treatment, unfortunately, therapeutic options able to cure AD are still lacking. Instead, palliative treatments are given to patients in order to diminish or delay the disease's symptoms. Given the fact that it has been previously suggested that the AD symptoms could be due to deficits in acetylcholine levels, few of the drugs approved by the Food and Drug Administration (FDA) have been designed to inhibit reversibly the acetylcholinesterase (donepezil, rivagstimine and galantamine). Another sought effect is to avoid the excessive

excitotoxicity produced by the neurotransmitter glutamate with non-competitive inhibitors of NMDA receptors such as the drug memantine [60].

2.2. Parkinson's disease

PD pathogenesis

PD is the second most prevalent neurodegenerative disease after AD [61] with approximately 0.3% of the population being affected [62]. According to the UK Brain Bank Criteria, the clinical presentation of PD is based mainly on motor symptoms such as tremor at rest, rigidity, bradykinesia, and postural instability [63]. However, PD patients may also present other non-motor symptoms (some of them even precede diagnosis) such as sleep disorders [64], depression [65], constipation [66] and, olfactory dysfunction [67]. Interestingly, both the enteric nervous system (ENS) and the OB have been proposed as the gateways to the environment triggering the pathogenesis of PD [68].

Although the exact cause of PD is still not clear, it is assumed that is the result of combination of environmental factors together with genetic predisposition or susceptibility. It is well- known though that PD pathogenesis is characterized by the severe loss of pigmented dopaminergic neurons in the substantia nigra (SN) that project to the basal ganglia [69]. However, the neuronal loss found in this region is common to other denominated parkinsonian disorders. PD can be distinguish through the presence or absence of Lewy pathology. Lewy bodies (LBs) are intraneuronal inclusions composed of aggregates of the protein α-synuclein. This protein is usually localized in the presynaptic terminal and although its physiological role is still poorly understood, it may play an important role in the synaptic vesicle release and therefore, in the neurotransmitter release (such as dopamine) [70]. Pathological α-synuclein becomes misfolded and this abnormal aggregation promotes its aggregation and also pathological post-translational modifications such as phosphorylation [71]. It has been proposed that pathological α-synuclein is localized and accumulated inside of cytoplasmic inclusions, thus,

not capable of enrich the presynaptic terminals. Additionally, other several mechanisms have been proposed as consequences of α-synuclein toxicity. For instance, some studies suggest that pathological α-synuclein in its oligomeric form might also disrupt the cellular homeostasis creating pores in the cell membrane, increasing the permeability and influx of extracellular ions [72]. Failure in degradation cascades such as the ubiquitin-proteasome system or the autophagy-lysosomal pathway and mitochondrial and endoplasmic reticulum impairments have also been related with oligomeric α-synuclein formation [73-75]. Finally, α-synuclein cell to cell propagation or spreading is now being suggested as one of the most pathological hallmarks of PD. In fact, it has been demonstrated that *in vitro* α-synuclein oligomers induce transmembrane seeding of α-synuclein aggregation in primary neuronal cultures and those are likely to be secreted in exosomes and then spread to neighbour neurons [76]. The physiological and pathological roles of α-synuclein are summarized in Figure I6.

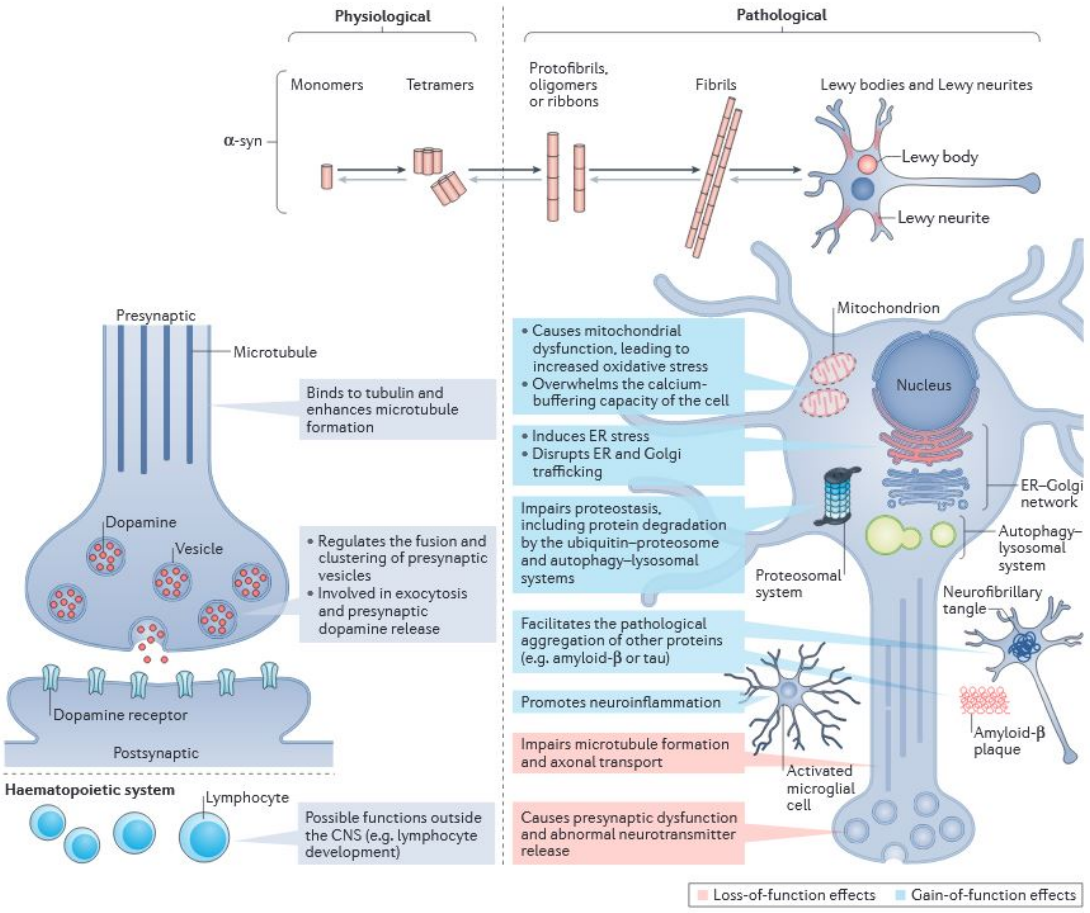

Figure I6: Overview of the physiological and pathological roles of α-synuclein. The monomeric and tetrameric forms of α-synuclein have been proposed to function in the physiological or healthy state, having a role in the presynaptic neurotransmitter release (dopamine), among others. The pathological forms of α-synuclein (protofibrils, oligomers, ribbons and fibrils) result in loss-of-function effects, including impaired neurotransmitter release, microtubule formation, ER stress, mitochondrial dysfunction, enhanced neuroinflammation, etc. Figure taken from Koprich J. B et al. *Nature Reviews Neuroscience*, 2017. 18(9), 515-529.

PD diagnosis and treatment

Just as in AD, there is no specific test to diagnose PD. The neurologist will diagnose PD according to the medical history of the patient, the exhaustive analysis of signs and symptoms and the physical evaluation. Again, brain imaging tools are usually used mainly to discard other possible causes of the brain damage and responsible for the patient symptoms. Additionally, patients with PD suspicion, might be treated with carbidopa or levodopa, a drug composed of L-

Dopa, the dopamine precursor. A significant improvement after the treatment in the patient symptoms could confirm PD diagnosis [62]. In sporadic PD, the neuropathological criteria for PD post-mortem diagnosis is mainly based in two key histopathological hallmarks: neuronal loss in the SN and Lewy pathology [69]. Concerning this second feature, Braak and colleagues used the spreading of Lewy pathology to specifically describe the PD progression in different stages. Following this scheme, they describe PD progression in six neuropathological stages, defined by the development of inclusion bodies formed either by branching Lewy neurites with spindle or thread-like form, or by granular aggregations as LBs in the somata of the involved nerve cells. The AON and the OB together with the dorsal motor nucleus of the vagus in the medulla are firstly affected in stage 1. The locus coeruleus neurons in the pons and the neurons in the SN follow (stage 2) and then, in stage 3, the process reaches the upper limit of the pontine tegmentum and enters the basal portions of the midbrain and forebrain. Finally, in the later stages, the spreading reaches the basal forebrain, the amygdala and the medial temporal lobe structures and cortical areas [77]. Additionally, it is important to note that Lewy pathology has also been detected at the level of the enteric plexus of the gastrointestinal tract [78]. Besides, McKeith and colleagues proposed a new revised scheme for the pathologic evaluation of LBs and Lewy neurites using α-synuclein immunohistochemistry describing a regional involvement progression. They classified the cases into brainstem predominant, limbic (transitional) and neocortical subtypes [79].

There is not a curative treatment for PD. For now, the treatment could ameliorate the patient symptoms, especially the temblors. As mentioned before, some of these drugs approved by the FDA are dopamine precursors that are processed in the brain and transformed into dopamine (levadopa, carbodopa). Others are dopamine agonists that instead of making dopamine, mimic its effects on the brain (pramiprexol or ropinirol) [62].

2.3. Frontotemporal lobar degeneration spectrum

Pathogenesis

Frontotemporal lobar degeneration (FTLD) is a group of clinically, genetically, and pathologically heterogeneous neurodegenerative disorders that are distinguished by progressive deterioration and selective neuronal loss and gliosis in the frontal and temporal lobes [80]. FTLD is considered a presenile dementia and its prevalence is estimated between 10 and 30 per 100.000 individuals between ages of 45 and 65 [81]. From a clinical point view, FTLD often exhibits frontotemporal dementia (FTD) and patient's phenotype is characterized by progressive changes in behaviour, executive dysfunction, and/or language impairment. In fact, FTD might be clinically classified in three major syndromes. Hence, patients diagnosed with the behavioural variant of frontotemporal dementia (bvFTD) exhibit insidious changes in personality, interpersonal conduct, and emotional modulation [82]. On the other hand, those that present progressive changes in language function belong to the other two groups, semantic variant primary progressive aphasia (svPPA) and nonfluent variant primary progressive aphasia (nfvPPA) [83]. It is important to note that in the past decade, there has been remarkable progress in the understanding of the molecular mechanisms underlying FTLD, including the discovery of the most common FTD-causing genes and the identification of the major pathological proteins. First, compared with other neurodegenerative disorders such as AD, the familial component has more importance in FTLD. Thus, positive family history is observed in 40-50% of FTLD cases [84] and described mutations mainly include *MAPT*, granulin (*GRN*), and *C9ORF72*, which together explain the 17% of familial FTLD [84]. On the other hand, thanks to the immunohistochemistry analysis, FTLD spectrum may be defined as a proteinopathy and can be neuropathologically classified based on the identification of the protein that accumulates in neurons and glia [85]. The distinct forms have been named according to the presence of protein inclusions: a) FTLD-tau is characterized by inclusions of hyperphosphorylated tau in neurons and

glial cells [86] and it includes different forms such as Pick's disease, characterized by severe cortical atrophy and brain weight decrease [87], and progressive supranuclear palsy (PSP), in which patients reported symptoms are impaired balance, movement slowness, subtle personality changes, bulbar symptoms and impaired eye motion [88]; b) FTLD-TDP43, defined by positive ubiquitin immunohistochemistry neurites and neuronal and glia inclusions of TAR DNA binding protein 43 (TDP43) [86], and c) FTLD-FUS, which includes those cases with tau and TDP43 negative and positive FUS immunohistochemical staining [86]. In summary, these findings have enhanced the knowledge about FTLD spectrum. Nevertheless, further studies in human FTLD material and animal models are needed to establish the specific molecular mechanisms governing FTLD appearance.

Diagnosis and treatment

For now, only clinical diagnosis is available for patients suffering from FTLD and it is associated with the clinically relevant findings related with specific cognitive, behavioural, and socio-emotional deficits seen in these syndromes [89]. As in AD and PD, definitive and precise diagnosis occurs when the macroscopic neuropathological characterization is accomplished. In this sense, the immunohistochemical staining techniques allow to classify FTLD spectrum disorders based on the predominant neuropathological protein: FTLD-tau, FTLD-TDP43, and FTLD-FUS. However, the correlation with the specific clinicopathological symptoms remains to be elucidated. The current diagnose of FTD is mainly based on multiparametric test, including imaging [90] and cognitive [91] and genetic analysis [92]. Concerning FTLD treatment, to date, there are no specific drugs able to cure FTLD. Pharmacological strategies focus on neurotransmitter replacement and treatment of behavioural, motor and cognitive symptoms of FTD, including selective serotonin reuptake inhibitors (SSRIs), atypical antipsychotics, acetylcholinesterase inhibitors and glutamate NMDA receptor antagonists [83].

2.4. Smell impairment in Alzheimer's disease, Parkinson's disease and frontotemporal lobar degeneration spectrum

Smell impairment in AD

There are many studies that describe olfactory deficits in AD patients [48, 93]. This symptom is presented as a progressive worsening of the olfactory function with difficulties in detecting, recognizing and remembering odorants [94]. In this sense, recent studies demonstrate a high correlation between the cognitive status and baseline olfactory test scores [95]. Moreover, even amnestic individuals with mild cognitive impairment (MCI) and early AD patients display significant deficits in olfactory identification tests when compared to healthy elderly people [96]. However, although around 85-90% of the patients suffer from olfactory dysfunction, the majority of them are unaware until they perform an actual olfactory test. That is why, this lack of complaints of olfactory decline indicate that, although impairments in the sense of smell may occur in early and even preclinical stages of AD, the use of olfactory test as a unique tool for the prediction of AD progression from normal aging is still limited.

Lots of evidence suggests that olfactory impairments are due to central sensorineural dysfunction. Brain imaging studies have been able to correlate odour identification deficits with smaller hippocampal volume in individuals with MCI and early AD [97]. Lower scores obtained in olfactory tests are associated with a higher AD pathology in central olfactory structures such as the entorhinal cortex or the hippocampus [98]. Moreover, deficits in olfaction have been associated with decreased activation of central odour processing structures measured by functional imaging [99]. Early loss of noradrenergic neurons in the locus coeruleus and cholinergic neurons in the nucleus basalis of Meynert, regions that also participate in the modulation of odour information processing, could have an impact in this olfactory deficits in AD subjects [100].

On the other hand, it has also been demonstrated that both the human olfactory system and the brain areas with extensive connections to the olfactory system have pathological deposits of Aβ plaques and NFT [93, 101]. NFTs have been observed in the AON and the number and density increased as long as did the dementia [102]. In fact, Attems *et al*. demonstrated that: a) the deposition of the two pathological proteins Aβ and the hyperphosphorylated form of the protein tau in two of the main peripheral olfactory structures such as the OB and the OT increases as the disease progresses and b) what is happening in the olfactory system reflects what is occurring in other affected brain regions such as hippocampus. Despite this, it is important to note that there still exists a little controversy regarding the presence of these amyloid deposits or plaques and there are some studies that have failed to detect amyloid plaques in the OB [103]. Braak and colleagues defined six neuropathological stages for AD based on the localization of NFTs [57]. Accordingly, olfactory structures are already affected in early stages of the disease, prior to the appearance of cognitive symptoms [104]. NFTs are firstly located in the transentorhinal region and entorhinal cortex (stage 1). In this stage, some studies describe tau pathology already in all the layers of the OB [105] and in the OT [101] and others at stage 2 [106]. In the same stage 1, some publications point that tau pathology is also present in AON [107]. The periamygdaloid cortex and anterior amygdala are involved in the stage 2 and then, NFTs reach limbic regions and progress to the amygdala and thalamus at stage 4. Finally, isocortex at stage 5 and sensory, motor and, visual cortex at stage 6 are affected.

Neuronal death has also been postulated as potential contributor of olfactory deficits in AD. In this sense, neuronal cell loss has been observed in both the OB and the entorhinal cortex of AD subjects [103, 108]. However, it is unclear whether this cell loss is actually a consequence of accumulation of the pathology.

Nowadays, animal models play a crucial role for the study of NDs. In particular, several murine models have been developed to model AD [109]. Interestingly, olfactory dysfunction has

also been study in some of them. The deposition of non-fibrillary Aβ peptides in the olfactory system has been observed in the Tg2576 mouse model [110]. These transgenic mice overexpress the 695-amino acid isoform of human Alzheimer Aβ precursor protein containing a Lys670 --> Asn, Met671 --> Leu mutation with learning and memory impairments appearing at 9 months of age [111]. Interestingly, Aβ deposits were found in the olfactory system earlier than in other brain regions, supporting the theory that human OB is damaged at very early AD stages [110]. Another well-known experimental model used to mimic AD is the APP/PS1 transgenic mouse [112]. In fact, a recent publication evaluated both olfactory capability using two olfactory behaviour tests and the amyloid deposition through the olfactory system in this model. However, although the results showed a clear impairment in olfactory functionality, authors did not delve into the potential molecular mechanisms causing this deficit [113]. Another study aimed to analyse the neurogenic process in the OB in the same mouse model. Their findings suggested that this process is altered in transgenic animals, probably due to a differential vulnerability among interneuron populations carrying Aβ inclusions [114]. In addition, an interesting approach was performed by Kempf S.J and colleagues where, using 12 month-APP/PS1 mice, changes in the global phosphorylation and sialylated N-glycosylation patterns, and in particular, in synaptic functions associated with dendritic spine morphology, neurite outgrowth, long-term potentiation, cAMP response element-binding (CREB) signalling and cytoskeletal dynamics in the neocortex and, more importantly, in the OB were observed [115]. Finally, although in lesser extent compared to other brain regions such as hippocampus and cortex, alteration in metabolic processes related to purine metabolism, bioenergetics failures and dyshomeostasis of amino acids were observed at the level of the OB [116]. Altogether, these findings corroborate the potential implication of olfactory dysfunction in AD progression.

Smell impairment in PD

Olfactory deficits are present in almost 90% of PD patients [41] and is considered one of the earliest neurological signs of PD, occurring even before the appearance of the classical motor symptoms by at least 4 years [48, 93, 117]. In fact, there are tens of published studies that using different olfactory tests have probed the common hyposmia in these patients [47] and these olfaction tests have been proposed as a diagnostic tool for prodromal PD by the International Parkinson and Movement Disorder Society [118].

PD patients experiment deficits in odour detection, discrimination and identification [47, 119]. Interestingly, a recent publication by Doty and colleagues classified idiopathic PD as a disease with severe olfactory deficits when patients were submitted to take the UPSIT test [48]. Usually, PD patients do not suffer from a complete anosmia (total loss of smell) but from hyposmia (reduced sense of smell). These deficits are enough to differentiate them from healthy controls when taken olfactory tests and even better than some clinical motor tests [120] or single-photon emission CT imaging of dopamine transporter do. However, there is lack of specificity. For instance, olfactory dysfunction in PD is equivalent to that of early-stage of AD. Many studies have investigated whether smell impairment could be used as a biomarker for motor dysfunction or cognitive deficits. The earliest studies suggested that olfactory dysfunction is stable during PD progression [121]. On the other hand, more recent studies have observed that marked changes in olfactory threshold and odour discrimination alterations correlate with more rapid disease progression [122, 123].

The origin of olfactory loss in PD remains unknown, however, it is believed that has to do with both peripheral and central olfactory structures. Following the Braak neuropathological stages for PD, based on α-synuclein deposits, Lewy bodies and Lewy neurites are firstly (stage 1) found in the OB, the AON [124, 125] and the vagal and glossopharyngeal nerves [126]. In the OB, α-synuclein deposits are found in interneurons, in the internal plexiform layer, and less

frequently in mitral and tufted cells. Nevertheless, although less likely to develop α-synuclein deposits than other neurons, these two cellular types may have an important role in the propagation of α-synuclein allowing the transfer of small seed to connected regions. In the second stage, α-synuclein deposits are already located in the locus coeruleus. Later on, at stage 3 and more, α-synuclein inclusions in the OB and in the AON become denser. Moreover, they are also found in other olfactory regions such as the piriform cortex and the cortical amygdala and more slightly in the olfactory tubercle and entorhinal cortex [77, 127]. Finally, a recent publication has again demonstrated, as in AD, that α-synuclein deposits in the OB and in the OT increase as long as the disease progresses and that this deposits reflect what is happening in other brain regions [93]. In fact, the injection of α-synuclein fibrils in mice OBs is now being used as prodromal PD experimental model [128]. Using this approach, Graham S.F and colleagues observed a progressive synucleopathy propagation of α-synuclein deposits in the brain and serum. Metabolomic analysis showed alterations in taurine and hypotaurine metabolism, bile acid biosynthesis, glicine, serine and threonine metabolisms, and in the citric acid cycle [129].

Concerning possible cell loss in the olfactory system of PD subjects, the information available is scarce. A mean reduction cell loss was found in the AON of the OB and the OT in PD subjects interestingly correlating their olfactory deficits [130]. Other regions connected to olfactory structures that are also affected by neuronal loss are the locus coeruleus and amygdala [131, 132]. Finally, changes in the OB volume have also been described in PD post-portem samples. Both left and right OB were decreased in PD subjects compared to healthy controls [133]. But again, no study has been published assessing the molecular changes occurring in this region during human PD progression.

Smell impairment in FTLD spectrum

Odour impairment and its relationship with FTLD spectrum has not been elucidated. Recent evidence suggests that odour identification is impaired in the frontal variant of FTD [134-139].

Interestingly, Tonacci's group has recently published a full review of the latest studies linking olfactory dysfunction and FTD [139]. Although the literature concerning this topic is still scarce, this review concludes that a clear association between olfactory deficits symptoms and FTD/FTLD exists. Nonetheless, the molecular mechanisms underlying this degenerative process are still lacking. Doty R (2017) ordered neurological disorders in terms of relative differences in UPSIT scores comparing the results with age-matched controls [48]. Hence, FTD displayed 32.7% difference from controls, while PSP displayed one of the lowest results with 12.1% difference from controls. However, so far, little attention has been paid to the potential role of olfactory dysfunction in the pathogenesis of FTLD and a possible correlation with the identified pathological proteins such as tau, TDP43 and FUS. In Pick's disease, Pick's bodies, which are mainly formed by tau inclusions, have been found in the AON and in a lesser extent in the OB [140]. On the other hand, a recent research in a FTLD-taupathy mouse model (rTg4510) has exhibited evident neurochemical alterations in the OB at 5 months of age. The results showed alterations in oxidative stress, glutaminergic and GABAergic neurotransmissions, and in neuronal and membrane integrity [141]. Finally, considering that the impaired cellular plasticity that occurs at the level of the OB could be due to alterations in neuroinflammatory processes, Kohl and colleagues demonstrated that there is an increase in microglial activation in this region [142]. Interestingly, this study was performed using a great number of human samples, including other NDs, confirming again the potential role that olfactory system has in these disorders. In this sense, our group has also previously reported common disturbances at the level of OB in post-mortem samples from subjects with AD, Lewy body disease (LBD) and, interestingly, FTLD-TDP43 and PSP. Thus, common olfactory targets such as Copine-6 (CPNE6), Visilin-like protein 1 (VILIP1), Dipeptidyl aminopeptidase-like protein (DPP6) and protein RUFY3 (RIPX) were suggested as potential mediators in the olfactory impairment occurring in neurological disorders [143]. Concerning TDP43 deposits, main research has been focused on its relationship with ALS.

In fact, recent investigations have shown TDP43 inclusions in olfactory regions including AON and the OB [144].

2.5. The olfactory bulb as the entry site for pathological protein aggregates in neurodegeneration

Together, AD and PD affect over 50 million people in the world and, as mentioned before, most of the patients develop the sporadic form of the disease. Although the exact causes responsible for the appearance of both diseases remain unknown, the presence of misfolded protein aggregates in affected regions of the nervous system are thought to provoke neuronal dysfunction in both pathologies. For many years, it has been believed that the molecular mechanisms underlying AD and PD are cell-autonomous. This means that the formation for instance of tau or α-synuclein aggregates occurs in each cell independently of what is occurring in the neighbouring neurons. However, recent studies suggest that cell-to-cell transmission of neuropathological proteins could be a common mechanism for the onset and progression of NDs [145-147]. Thus, inclusions are believed to form in a small group of cells and then spread in a deterministic manner to other distant brain regions, being the formation of Aβ, tau and α-synuclein first aggregates stochastic. This mechanism is characteristic of human prion diseases, such as Creutzfeldt-Jakob disease (CJD) and that is why, the prion concept applied to human NDs is now growing on evidence [146]. Nevertheless, it is important to note that in contrast to CJD, transmission between individuals in AD and PD has not been probed yet. It remains to be demonstrated whether this lack of infectivity of AD and PD might be because of the more fragile nature of Aβ peptides, tau and α-synuclein.

As mentioned, mounting evidence supports the spreading of Aβ pathology as the potential cause of AD progression [148-151]. For instance, it has been demonstrated that intracerebral or peripheral injection of susceptible transgenic mice or rats with extracts containing Aβ aggregates

causes the deposition of the same on brain regions [152-154] and these deposits spread away from the inoculation [155, 156]. This observation has been recently corroborated by Ruiz-Riquelme and colleagues, with the added value that their results also demonstrate that APP overexpression is unnecessary for the prion-like induction of Aβ deposition [151]. Moreover, studies concerning Tau aggregates transference cell to cell have been also published in the last few years [157-162]. Many efforts are being made to better understand the actual mechanisms responsible for the Aβ and tau propagation [163]. For instance, transfer neuron to neuron across trans-synaptic connections via exosomes has been proposed [149, 164]. However, other studies point that trans-synaptic propagation may not be the only way to spread these pathological proteins and a potential role of glia has also been suggested [165].

On the other hand, the prion hypothesis has been similarly proposed as a crucial event in the Lewy pathology. In fact, several animal models have been developed to asses α-synuclein propagation [166]. A-synuclein pathology appears in brain regions anatomically close to the injection site after intracerebral, intramuscular, or intravenous inoculation of brain homogenates from PD patients or α-synuclein fibrils in different mice models [167-171]. Interestingly, this has also been demonstrated when inoculating α-synuclein fibrils into the OB of wild-type mice. Rey N. L *et al.* reported a progressive spreading of α-synuclein aggregates after inoculating α-synuclein pre-formed fibrils into the OB of three-month-old wild type mice. First, they described more than 40 brain regions where α-synuclein pathology was present at a 12-month time point after injection. These include not only olfactory system regions, but also regions such as hypothalamus, cortical regions, locus coeruleus and SN [128]. This work has been continued reaching 18 and 23-month post-injection in the same model. Interestingly, a reduction in the density of α-synuclein fibrils was observed in some of the previously affected brain regions. Moreover, no additional brain regions showed α-synuclein aggregates. More importantly, exploring neural cell death in the olfactory system, authors did not find a severe cell loss in the OB, being unable to find a connection between cell death in the OB region and

the behavioural deficits observed in this model concerning olfaction functionality [172]. Thus, further studies are needed to understand which molecular mechanisms are responsible for the olfactory deficit observed after α-synuclein fibrils inoculation. It is important to note also, that not only α-synuclein injection in the OB has been described as entry site for neurodegenerative pathology, but also injected Aβ peptides in this region have been shown to wide spread to other brain regions via neural connections. Recently, He B and colleagues injected Aβ1-42 monomers and oligomers, showing a rapid spreading from the injection site to other interconnected brain regions also triggering neuronal apoptosis [150]. Altogether, these studies support the hypothesis of the prion concept connected to the mechanisms of neurodegeneration and, more importantly, the notion that the OB being one of the earliest regions affected in AD and PD, becoming one of the potential entry sites for prion-like propagation in NDs.

3. Omic tools for the study of olfaction deficits during neurodegeneration

The human brain is extremely complex, not only because of the huge number of different regions in which it can be divided, but also because of the great number of cellular types that reside in all its structures [173]. With around 86 billion neurons and an equal number of glial cells, there are hundreds of distinct cellular types according to their morphology, molecular and electrophysiological properties. This immense heterogeneity makes the study of the molecular profiles within the specific neuronal types and their connectivity in the different brain regions a real challenge even for high-throughput omic analysis.

3.1. Transcriptomics approaches

In the last decade, research combining transcriptomics and NDs has evolved considerably. The employment of complementary DNA microarray is usually used to identify deregulated

biological pathways and more importantly, potential therapeutic biomarkers. A large number of probes can be used at the same time allowing to differentiate healthy samples from sick ones. Moreover, next-generation sequencing (NGS) is now also available, being able to sequence an entire human genome in a single day. One of the goals of these high-throughput transcriptomics approaches is to measure and compare gene expression profiles between two or more samples and identify differentially expressed genes. Thus, identifying the molecular pathways in which these differentially expressed genes are implicated, may help to understand the pathophysiology of neurological diseases. Finally, novel alternative RNA splicing mechanisms occurring at this level can be also described. In the next headline, some of the transcriptomic studies focusing on the olfactory system in neurological diseases are described. Moreover, some recent research using transcriptomics approaches in NDs using human samples is summarized in Table I1.

Transcriptomics in neurodegenerative diseases

Molecular disturbances concerning gene regulation and expression can result in development of NDs such as AD, PD and others. Being the most common neurodegenerative disease, various gene expression profiling (GEP) studies have been published aiming to find therapeutic targets or even diagnostic biomarkers for AD. Due to its relevance in the pathogenesis, most of the transcriptomic studies have been performed mainly in the hippocampus and in the cortex regions (Table I1). In fact, two studies in whose the impairment of various brain regions in AD is analysed, highlight that the greatest number of deregulated genes is located precisely in these two regions [174, 175]. Moreover, those studies applying a stage-dependent analysis have concluded that is between the mild to moderate dementia where the greatest changes occur [176]. Concerning the functional categories in whose these aberrantly expressed genes are implicated, various are related with intracellular calcium signalling and neuroinflammation [175, 177-179]. More recent studies have also found

significant reductions in genes regulating mitochondrial respiration, redox homeostasis and neuronal plasticity [180]. In addition, as a novelty, Qiu and colleagues identified 103 piRNAs (Piwi-interacting RNA) deregulated in the prefrontal cortex of patients with AD. These non-coding RNA are known to interact with Piwi proteins and function as a complex to regulate cellular activities by RNA silencing [181]. Here, these piRNA, being mostly brain specific, are suggested as potential risk biomarkers for AD.

In the case of PD, the main pathological hallmark is the selective degeneration and death of dopaminergic neurons in the SN. That is why, although there is evidence that other brain regions are also affected during PD progression, many of the transcriptomic research in this disease has been focussed in the SN [182-188]. In Table I1, a summary of some of the PD studies in this and other brain regions using transcriptomic approaches is shown. Concerning the general results obtained across the different PD brain studies, it is important to note that there is a lack of consensus in the differentially expressed gene lists obtained even in the same tissues. However, when it comes to implication in functional biological categories, this variability greatly improves. Consistently, the majority of the studies performed in SN pointed dysregulation in pathways related to dopamine metabolism, oxidative stress, mitochondrial function, neuroinflammation, vesicular transport and synaptic transport, among others. In addition, several studies have confirmed downregulated levels of genes related to dopamine metabolism such as *SLC6A3* or *SLC18A2* [189, 190]. Altogether, these findings support the well-established PD hallmark of altered dopamine metabolism. On the other hand, the role of mitochondrial dysfunction in PD pathogenesis has also been settled down and transcriptomic studies have confirmed the implication of aberrantly expressed mitochondrial-related genes. Significant downregulation of genes coding for components of the electron transport chain complex or mitochondrial membrane translocases as well as the upregulation of oxidative damage response proteins has been observed [183, 184, 191]. Other reports have also shown the implication of aberrant synaptic functionality. For instance, genes associated with synaptic vesicle dynamics

and neurotransmission have been reported to be altered, not only at the level of SN, but also in other brain regions such as striatum and cerebral cortex [185, 189, 192].

To overcome the drawbacks of using tissue samples, such as the heterogeneity of cell populations analysed at the same time and the fact that, usually, this post-mortem samples belong to patients with late stages of the disorder, the use of peripheral fluids entails clear advantages for the discovery of disease biomarkers. Several studies monitoring transcriptomic changes in blood cells have revealed alterations in immune system pathways, inflammation, protein chaperones, programmed cell death, and, as in brain tissues, mitochondrial function in both AD and PD [193-196]. Others have used CSF instead. CSF choice entails a notably advantage as it reflects more precisely what is happening in the brain due to its proximity. A recent study using CSF as target sample has suggested *DNMT1*, *PTPRC* and the mitochondrial genes *NDUFV2* and *LRPPRC* as potential biomarkers of PD in CSF [197].

Brain area	Subjects	Analytic platform	Reference
Substantia nigra	6 PD and 8 HC	GE CodeLink Human 20k	Miller RM et al, Neurobiol Dis 2006
Dopaminergic neurons from substantia nigra	8 PD and 8 HC	GeneChip® Human X3P expression arrays, Affymetrix	Cantuti-Castelvetri et al, 2007
Cortex and hippocampus	33 AD and 14 HC	Affymetrix Human Genome U133 Plus 2,0 microarrays	Liang WS et al, Physiol genomics 2008
Cortex and hippocampus	6 early AD and 8 HC	Affymetrix Human Genome HG-U133A	Williams C et al, PloS One 2009
Temporal cortex	5 AD and 5 HC	Affymetrix GeneChip Human Genome U133 Plus 2,0	Bronner IF et al, PloS One 2009
14 cortical areas and hippocampus	104 AD and 26 HC	Affymetrix HG-U133 A&B Human genome GeneChip® sets	Haroutunian V et al, Neurobiol, Aging 2009
Substantia nigra	10 PD and 9 HC	HU-133A arrays	Simunovic F et al, Brain 2009
Substantia nigra	41 PD and 39 HC	Illumina WG6v1 expression chips	Elstner M et al, Ann Neurol, 2009
Substantia nigra	4 PD and 4 HC	Agilent custom-made 22K 60-mer	Bossers K et al, Brain Pathol, 2009
Temporal cortex	12 AD and 8 HC	Affymetrix GeneChip Human Exon 1,0 ST Arrays	Tan MG et al, J Neurosci Res 2010
Prefrontal cortex	21 AD	Agilent 44K Whole Human Genome arrays	Bossers K et al, Brain 2010
Putamen	31 PD and 31 HC	Affymetrix Human U133A2,0 Arrays	Naydenov AV et al, Acta Neuropathol 2010
Dopaminergic neurons from substantia nigra	11 PD and 11 HC	Illumina WG6v1 expression chips	Elstner Met al, Acta Neuropathol, 2011
Temporal, frontal and parietal cortex	55 AD and 22 HC	Affymetrix HG-U133A chip	Horesh Y et al, Eur J Neurol et al, 2011
Blood	11 ALS and 11 HC	Agilent Human Whole Genome 4 × 44k Array	Mougeot JL C et al, BMC Medical Genomics 2011
Temporal cortex	6 AD and 9 HC	Affymetrix GeneChip Fluidics Station 450	Tollervey J R et al, Genome Res 2011
Microvessels from temporal, frontal and parietal cortex	12 AD and 12 HC	Agilent Human 4 × 44 K arrays	Wang S et al, J Alzheimer Dis 2012
Substantia nigra	12 PD and 7 HC	Illumina WG8v2 expression chips	Durrenberger P, F et al, Parkinson Dis 2012
Putamen	5 PD and 5 HC	Affimetrix Exon 1,0 ST Array	Botta-Orfila T et al, Neurobiol Dis 2012
Broadman area 8	27 PD and 26 HC	Agilent Human 44k	Dumitriu A et al, PLoS Genet 2012
Spinal cord	12 ALS and 11 HC	Affymetrix Human U133 Plus 2 GeneChips	Figueroa Romero C et al, PLoS One 2012
Skeletal muscle	7 ALS and 7HC	GeneChip Human Genome Focus Array, Affymetrix	Bernardini C et al, PLoS One2013
Substantia nigra	8 PD and 8 HC	TaqMan Human miRNA A v2,0	Kim W et al, Neurobiol Aging 2014
Locus coeruleus	8 PD and 5 HC	Agilent Human 44k	Corradini BR et al, Biomed Res Int 2014
Frontal cortex	16 PD and 14 HC	Affimetrix Gene 1,0 ST Array, Illumina TruSeq SBS v3-HS	Riley BE et al, PLoS One 2014
Blood	4 PD and 4 HC	HumanHT-12 v4 Expression BeadChip Ki	Alieva A et al, Biomed Res Int 2014
Substantia nigra	8 PD and 8 HC	TaqMan Human miRNA A v2,0	Briggs C E et al, Brain Res 2015
Cortex, hippocampus and cerebellum	4 AD and 4 HC	RNAseq	Magistri M et al, J Alzheimer Dis 2015
Blood	40 PD and 20 HC	HG – U133A 2,0	Calligaris R et al, BMC Genomics 2015
Blood	51 PD and 45 HC	Multiple platforms	Santiago J A et al, Proc Natl Acad Sci U,S,A 2015
CSF	27 PD and 30 HC	NEB Directional RNA-Seq kit	Hossein-Nezhad A et al, J Parkinsons Dis 2016
Broadman area 8	29 PD and 44 HC	Agilent Human 44k	Dumitriu A et al, BMC Med Genomis 2016
Broadman area 8	29 PD and 33 HC	Illumina TruSeq Small RNA kit	Hoss A G et al, Front, Aging, Neurosci 2016
Putamen	12 PD and 12 HC	NanoString nCounter v2miRNA	Nair VD & Ge Y Neurosci Lett 2016
Substantia nigra	50 PD and 43 HC	Multiple platforms	Cruz-Monteagudo M et al, BMC Med Genomics 2016
Hippocampus	6 AD and 6 HC	RNAseq	Mastroeni D et al, PloS One 2017
Prefrontal cortex	6 AD and 6 HC	Arraystar HG19 piRNA array	Qiu W et al, Neurobiol Aging 2017
Temporal lobe	12 AD and 3 HC	RNAseq	Barbash S et al, Neurobiol Dis 2017
Locus coeruleus	8 AD and 11 HC	Custom-designed microarray	Kelly S C et al, Acta Neurathol Commun, 2017
Spinal cord and frontal cortex	18 ALS and 23 HC	GeneChip® Human Gene 2,0 ST Array	Andres-Benito, P et al, Aging, 2017
Blood	35PD and 23 HC	GeneChip Transcriptome Array (MTA) 1,0 (Affymetrix	Miki Y et al, Neurobiol Aging 2018
Skin biopsy	4 PD and 4 HC	HiSeq 2000, Illumina	González C I et al, Neurobiol Aging 2018
Choroid plexus	7 AD, 4 FTD, 3 HD and 6 HC	Affymetrix GeneChip microarray GEO platform GPL 10379	Stopa E G et al, Fluids Barriers CNS, 2018

Table I1. Compilation of recent research using transcriptomic approaches to study NDs pathogenesis in human samples. (HC: healthy control; PD: Parkinson's disease; AD: Alzheimer's disease; ALS: Amyotrophic lateral sclerosis, FTD: frontotemporal dementia)

3.2. Proteomics approaches

Over the last decades, the field of proteomics has undergone a rapid development in important aspects such as mass spectrometer platforms improvements, peptide identification algorithms and bioinformatics. In neuroscience, this has supposed a great progress concerning the understanding of the enormous complexity of the nervous system at molecular level [198-204]. In this section, a brief compilation of neuroproteomics studies is presented [205]. Besides, a compilation of NDs studies using proteomic approaches in human samples is summarized in Table I2.

Proteomics in Alzheimer's disease

The advent of proteomics has opened a huge field for the identification of new biomarkers for the early diagnosis and treatment of AD [206]. In Table I2, there is a compilation of some of the proteomics studies that have been published during the last decade related with AD using human samples. Most of them have chosen the frontal cortex and the hippocampus as target areas. In 2014, Musunuri and colleagues used multiplexed MS with stable isotope dimethyl labelling to study the differential proteome in the temporal cortex of AD subjects. Among the 69 proteins that were found differentially expressed, most of them were involved in metabolic processes, inflammatory and stress responses and synaptic functions [207]. It is well-known that synaptic plasticity impairment is one the main features in the pathogenesis of AD. Interestingly, Sweet and colleagues focused on the synaptic fraction of the cortex from AD subjects. Quantifying 191 synaptic proteins, they concluded that while there is profound loss of synaptic proteins in the entorhinal cortex during AD progression, the disease leads to altered synaptic protein homeostasis in the dorsolateral prefrontal cortex. This was consistent with previous findings related with synaptic transmission in this region [208]. Finally, Drummond and colleagues performed a cell-type specific proteomic approach overcoming the limitation of whole tissue studies. Using laser capture microdissection (LCM) and isolating neuron

populations identified by cresyl violet in temporal cortex from 2 AD subjects, among the 399 identified proteins, 77% of them were confirmed as neuronal proteins and 50% had been previously related with AD. Although this study does not suggest potential players in AD pathogenesis, it reflects the substantial improvement that LCM might bring to brain proteomic studies [209]. In fact, a quantitative proteomic study combining LCM with LC-MS/MS was performed in human hippocampus from 35 AD subjects and 5 healthy controls (HC). This study revealed significant differences in 372 proteins and their activity was related to cytoskeletal dynamics, the extracellular matrix, response to cellular stress and, again, synaptic signalling [210]. Accordingly, the hippocampus is one of the most vulnerable regions in AD [211] and fair reflection of this is the great number of proteomic studies that have been performed in this region [210, 212, 213]. Kim and colleagues performed a proteome-wide characterization of the signalling interactions occurring in the CA4 and dentate gyrus of the hippocampus. They identified 113 altered proteins in AD compared to control tissues and five of them were cross-validated by immunoblotting, selected reaction monitoring and MALDI imaging (*MDH2, PCLO, TRRAP, YWHAZ,* and *MUC19 isoform 5*), suggesting them as potential biomarkers for AD.

Biomarkers for AD are urgently needed, especially to identify individuals in preclinical stages of the disease. For that, biological fluids are always preferred due mainly to their less invasive availability. To this purpose, the cerebrospinal fluid (CSF) offers several advantages such as its continuity with the brain and its narrower dynamic range of protein concentration compared to plasma. In fact, p-Tau and the Aβ are both well-established markers of AD in CSF [214]. Thus, some proteomic approaches have been performed using CSF as biological sample [215-219]. Another advantage using CSF is the greater number of samples that can be analysed in the same study and more importantly, CSF samples from MCI patients can also be added to the analysis. In this preclinical stage, patients present measurable symptoms of cognitive decline that often precede to AD. Thereby, one of the main goals of this research is to identify biomarkers that could finger those MCI patients that likely will progress to AD. In this sense,

Skillbäck and colleagues proposed the secreted growth factor pleiotrophin as a novel biomarker in AD. Interestingly, while pleiotrophin levels were increased in AD samples, there were decreased in those from MCI patients. Moreover, this observation correlated with established biomarkers such as tau and Aβ, suggesting an association with disease progression [219]. Another similar study using two independent AD cohorts suggested two neurosecretory proteins as potential biomarkers for AD (*VGF* and *NPTXR*) and both candidates, mainly expressed in the nervous system, have a role in synaptic plasticity and function [220, 221]. Interestingly, this group applied a similar approach to selected reaction monitoring to validate their candidates in the two patient cohorts. This discovery proteomic approach allows the analysis of hundreds of samples quantifying specific analytes with high analytical precision and could be a useful tool for the discovery of AD biomarkers in fluid samples.

Proteomics in Parkinson's disease

As in AD, proteomic strategies have emerged as potent tools to unravel the molecular mechanisms involved in the pathogenesis of PD and to identify potential diagnostic, prognostic and therapeutic biomarkers [222]. Some of the latest studies published in the context of proteomics in human PD are summarized in Table I2. The affection of the SN in PD is responsible for most of the debilitating symptoms of the disease. Thus, some groups have focused their comparative studies in this region finding involvement of oxidative stress in the pathogenesis of PD [223, 224]. The frontal cortex has also been a recurrent target region in the study of PD pathogenesis. For instance, using an isotope labelling technique to compare protein profiles quantitatively in patients with different stages of PD, Shi and colleagues revealed mitochondrial defects and oxidative stress occurring in this region and suggested a chaperone involved in mitochondrial energy generation, mortalin, as potential player in the disease [225]. Two more recent studies in the same region confirmed these findings [191, 226]. Dumitriu and colleagues identified 283 differentially expressed proteins mapping mostly in the biological process

category ''mitochondrial electron transport'' and ''respiratory electron transport'' in the canonical pathway category [191]. Licker and colleagues pointed out novel interactors in the pathogenesis of PD at the level of SN, such as *CNDP2* (cytosolic nonspecific dipeptidase 2). This results support the well accepted consensus of impaired mitochondrial function being an important feature in PD pathogenesis [227]. Another substrate that contributes to this mitochondrial abnormalities in the SN is PARkin-Interacting Substrate (PARIS). In this sense, Kim H and colleagues performed a LC-MS/MS approach in the SN of PD subjects aiming to identify PARIS target molecules altered in this region. For that, they applied a label free LC-MS/MS approach in various brain regions from AAV-PARIS mice model, including the SN. From the 5 candidate molecules that were altered in all the regions, they afterwards confirmed that PARIS transcriptionally suppressed one of them, a protein related with the pentose phosphate pathway, the transketolase (*TKT*). Moreover, they confirmed a reduction in the protein levels of *TKT* in the SN from PD patients [228]. This study is another great example of how proteomics is a useful tool to make steps forward in the understanding of PD pathogenesis.

Concerning the biomarker discovery, most of PD proteomic studies have relied in the analysis of CSF. In all cases the aim has always been to find and stablish a robust biomarker signature for the early PD diagnosis [229-231]. In this sense, targeted proteomics methods have been widely used for the discovery of new disease biomarkers. For instance, Yang and colleagues applied targeted mass spectrometry approach to develop a sensitive and quantitative α-synuclein assay. Analysing 60 clinical samples from patients with PD, they developed and optimized an assay to quantify α-synuclein in CSF, suggesting it as promising biomarker for this illness [231]. On the other hand, a non-targeted proteomic approach was applied to analyse the proteome profile of mononuclear cells coming from CSF. In this study, 16 proteins were differentially expressed with respect to the healthy controls, including proteins related with cytoskeletal function, signal transduction, antioxidant activities [230].

Proteomics in FTLD spectrum

As mentioned before, FTLD consists in a wide heterogeneous group of diseases, with similar clinical features and illness progression, making their diagnosis elusive. Concerning proteomic research, although there are still few, some groups have focused their attention in the search of FTLD biomarkers [232]. For instance, Gozal's group identified 54 upregulated and 19 downregulated proteins when combining LCM and LC-MS/MS on hippocampal dentate gyrus from three different FTLD patients compared to three healthy controls [233]. Martins-de-Souza and colleagues identified 107 differentially expressed proteins across prefrontal cortex, cerebellum, and occipital lobe. These proteins were involved in processes such as energy metabolism and cellular transport [234]. Moreover, being the ubiquitinated and phosphorylated TDP-43 protein one of the major pathological proteins in FTLD, Herskowitz and colleagues employed IMAC and LC-MS/MS aiming to identify dysregulated phosphorylation events. Seven hundred eighty six phosphopeptides were identified in frontal cortex revealing six proteins with significant changes in FTLD phosphoproteome (*NDRG2, GFAP, MAP1A, PRKCG, reticulon 4,* and *HSP90AA1)* [235]. Finally, to overcome the drawback of using post-mortem samples, two-dimensional gel electrophoresis was used by Davidsson and colleagues in 15 CSF samples from FTD patients. This study revealed six differentially expressed proteins in CSF from FTD patients [236]. Due to their brain proximity and the possibility of analysing presymptomatic disease stages and even disease progression, CSF represents a valid alternative for the study of new biomarkers for early and differential diagnosis of FTLD.

Brain area	Subjects	Analytic platform	Reference
CSF	15 FTD and 12 HC	2D-E MS/MS	Davidsson P et al, *Brain Res Mol Brain Res* 2002
Substantia nigra	4 PD and 4 HC	2D-E MS/MS	Basso M et al. *Proteomics* 2004
Substantia nigra	5 PD and 5 HC	LC-MS/MS	Jin J et al, *MCP* 2006
Substantia nigra	5 PD and 5 HC	2D-E MS/MS	Werner C J et al. *Proteome Science* 2008
Frontal cortex	7 PSP and 7 HC	LC-MS/MS	Martinez A et al, *J Neural Transm* 2008
Frontal cortex	15 PD and 5 HC	2D-E MS/MS	Shi M et al, *J Neuropathol Exp Neurol* 2008
Frontal cortex	10 FTLD and 10 HC	LC-MS/MS	Gozal Y M. et al, *J Proteome Res* 2009
Frontal gyrus	15 PD and 5 HC	LCM combined with LC-MS/MS	Shi M et al, *AJP* 2009
Synaptosomal fractions	15 PD and 5 HC	Maldi TOF	Shi M et al, Am *J Pathol* 2009
Frontal cortex and hippocampus	4 FTLD and 4 HC	LC-MS/MS	Herskowitz J H et al, J Proteome Res 2010
Inferior patietal lobule	12 preclinical AD and 12 HC	2D-E-MS/MS	Aluise C D et al, *Neurobiol Dis*. 2011
Locus coeruleus	6 PD and 6 HC	LC-MS/MS	van Dijk K D et al, *Brain Pathology* 2011
Hippocampus	3 FTLD and 3 HC	LCM combined with LC-MS/MS	Gozal Y M et al, *Front Neurol* 2011
Cortex	10 AD and 10 HC	LC-MS/MS	Andreev V P et al, *J Proteome Res* 2012
Substantia nigra	6 PD and 4 HC	2D-E MS/MS	Licher V et al, *Journal of Proteomics* 2012
Prefrontal cortex, cerebellum and occipital lobe	5 FTLD and 7 HC	LC-MS/MS	Martins-de-Souza D et al, *J Proteome Res* 2012
CSF	14 AD and 5 HC	LC-MS/MS	Ringman J M et al, *Arch Neurol* 2012
Hippocampus	3 AD and 3 HC	LC-MS/MS	Begcevic I et al, *Clin Proteomics* 2013
Neocortex	10 AD and 10 HC	LC-MS/MS	Musunuri S et al, *J Proteome Res.* 2014
Prefrontal cortex	2 AD	LC-MS/MS	Drummond E S et al, *Sci Rep.* 2015
Hippocampus	5 AD and 5 HC	LC-MS/MS	Kim J H et al, *Sci Rep.* 2015
CSF	10 AD and 10 HC	LC-MS/MS	Hendrickson R C et al, *PLoS One* 2015
CSF	17 PD and 15 HC	2D-E-MS/MS	Xing L et al, *Int J Clin Exp Pathol* 2015
Hippocampus	35 AD and 5 HC	LCM coupled to LC-MS/MS	Hondius D C et al, *Alzheimer & Dementia* 2016
Hippocampus	4 AD and 4 HC	LC-MS/MS	Ayyadevara S et al, *Aging Cell* 2016
Prefrontal cortex	59 AD and 12 HC	LC-MS/MS	Sweet R A et al, *Mol Cell Proteomics* 2016
Middle frontal gyrus	6 asymptomatic AD, 11 MCI, 13 AD and 5 HC	LC-MS/MS	Hales C M et al, *Proteomics* 2016
CSF	20 FTD and 10 HC	LC-MS/MS	Teunissen C E et al, *Azlheimers Dement* 2016
Frontal cortex	12 PD and 12 HC	LC-MS/MS	Dumitriu et al, *BMC Medical Genomics* 2016
CSF	88 MCI and 19 HC	MRM	Paterson R W et al, *Trans Phsychiatry* 2016
CSF	8 MCI and 4 AD	LC-MS/MS	Wang J et al, *Proteomics Clin Appl* 2016
Grey matter of frontal gyrus	10 AD and 10 HC	LC-MS/MS	Wang S et al, *J Pathol* 2017
Lenses	3 PD and 3 HC	LC-MS/MS	Klettner A et al. *Mov Disord.* 2017
Amyloid plaques	22 familial AD and 22 sporadic AD	LCM combined with LC-MS/MS	Drummond E S et al, *Acta Neuropathol.* 2017
Prefrontal cortex	21 PDD, 19 DLB and 21 HC	LC-MS/MS	Datta A et al, *Molecular brain* 2017
CSF	15 PD and 15 HC	MRM	Yang L et al, Proteomics Clin Appl 2017
Hippocampus, entorhinal cortex	6 AD and 6 HC	LC-MS/MS	Xu J et al, *bioRxiv* 2018
Prefrontal cortex	20 AD and 15 HC	LC-MS/MS	Seyfried N et al, *Cell Syst* 2018
Prefrontal cortex	8 PDD, 7 DLB, 9 AD and 8 HC	LC-MS/MS	Bereczki E et al, *Brain* 2018
Frontal cortex	19 ALS and 10 HC	LC-MS/MS	Umoh M E et al, *EMBO Mol Med* 2018

Table I2: Compilation of recent research using proteomic approaches to study NDs pathogenesis in human samples. (HC: healthy control; PD: Parkinson's disease; PDD: Parkinson's disease dementia; AD: Alzheimer's disease; ALS: Amyotrophic lateral sclerosis, FTD: frontotemporal dementia; FTLD: frontotemporal lobar degeneration; DLB: dementia with Lewy bodies; LC-MS/MS: liquid chromatography tandem mass spectrometry; LCM: laser capture microdissection)

3.3. Olfactory transcriptomics and proteomics

Transcriptomics in olfaction

Unfortunately, although the molecular mechanisms responsible for the early olfactory dysfunction remain poorly understood, few studies have been published using a transcriptomic approach focused on the olfactory system, and even less using human samples [237, 238].

Recently, Olender and colleagues applied RNAseq with the aim to characterize the human olfactory epithelia. They were able to identify not only around 400 intact ORs genes, but also nearly 200 olfactory-enriched non-receptors transcripts, from which 80% had not been previously implicated in chemosensory function [239]. As mentioned before, olfactory recognition is mediated by a large family of ORs. These ORs are located in the cilia of the olfactory sensory neurons in the olfactory epithelium. Although it is estimated that humans express around 400 functional ORs [8], they belong to one of the largest families of missing proteins, the human GPCRs (PE2-4). In fact, according to the nextProt 2017 release, only two of them have been identified at protein level with strong evidence of detection by MS [9]. On the other hand, some efforts have been made to understand the molecular mechanisms responsible for the OB projection neuron development. For instance, Kawasawa and colleagues performed a wide transcriptome analysis targeting purified mouse OB projections neurons and, using RNA-seq, they were able to find 388 genes that temporally changed their expression only in projection neurons [240]. Additionally, a similar approach was used by Li H et al. but with Drosophila olfactory projection neurons [241]. Although these studies have not been performed in human samples yet, they provide useful information to understand the spatiotemporal dynamics during OB projection neuron development. Finally, an interesting approach was performed by Wang M and colleagues to study the olfactory decline that occurs during aging. In particular, they focused their attention on the study of long-non-coding RNAs studying three groups of mice with different ages (2, 6 and 20 months of age) and their findings suggested that olfactory impairment may be consequence of the aberrant expression of some of them [242]. Nevertheless, correlation with olfactory dysfunction in NDs is lacking in this study. Altogether, we can conclude that further studies are needed to decipher which genes are responsible for the olfactory deficit that occurs in human neurological diseases.

Proteomics in olfaction

As mentioned before, the anatomy of the human olfactory system is highly complex with different functional regions, such as those in charge of odour perception (OE), those where the signal transduction is performed (OB and OT) and those responsible for the recognition, discrimination and identification of odours (olfactory cortical areas). Following this path, the OE is the site where the odorants bind, specifically in the cilia and thanks to the excitation of the OSNs and in this sense, with the aim to better understanding the olfactory mechanisms from the beginning, some studies have characterized the olfactory cilia proteome using mass spectrometry approaches. Although the majority of the studies in this region have been performed in animal models, there are few that have been done obtaining human olfactory cells by rapid nasal biopsy. However, these studies have only been performed in healthy volunteers and with the aim to just make a wide description of the molecular mechanisms occurring in this region in normal physiology. Simoes and colleagues published an extensively characterization of normal nasal epithelium using subcellular fractionation coupled to 2D-LC-MS/MS and were able to identify 1482 proteins. Interestingly, 64% of them were associated to the membrane fraction [243]. On the other hand, using LC-ESI-Q-TOF MS, Casado and colleagues identified 111 proteins in the nasal mucus of 10 volunteers. Most of this proteome was involved in innate and acquire immunity, pointing out the role of this extract in the prevention and protection against infections and other contaminants [244].

Otherwise, more proteomic studies have been published focussing on the OB. Nevertheless, few of them have been performed in human samples. Fernández et al. described deeply this region providing a functional analysis of the 1466 proteins identified [173]. The activity of these proteins was mainly involved in hydrolase and phosphatase activities. Afterwards, the same region was studied in order to decipher the molecular mechanisms occurring in the AD neurodegenerative process. Using an iTRAQ approach, Zelaya et al.

described an imbalance in splicing factors, alterations in toxic and protective mechanisms of Aβ peptides, interrupted cycling of neurotransmitters, and disturbances in mitochondrial functionality and neuron-neuron adhesions at the level of the OB [143]. Finally, Dammali and colleagues published an exhaustive description of the OB and OT proteomes, identifying 7750 and 6055 proteins, respectively, and combining two fractionation methods (high pH reverse phase liquid chromatography and SDS-PAGE) followed by liquid chromatography tandem-mass spectrometry (LC-MS/MS) analysis [245, 246]. However, both reports were again performed in healthy subjects. Evidently, there is a lack of research studies focused on the role of the OB in the pathogenesis of NDs. That is why, this PhD project aims to provide new insights into the molecular mechanisms potentially responsible for the olfactory dysfunction occurring in neurological processes.

References

[1] Leopold, D. A., Hummel, T., Schwob, J. E., Hong, S. C*., et al.*, Anterior distribution of human olfactory epithelium. *Laryngoscope* 2000, *110*, 417-421.
[2] Munger, S. D., Leinders-Zufall, T., Zufall, F., Subsystem organization of the mammalian sense of smell. *Annu Rev Physiol* 2009, *71*, 115-140.
[3] Feron, F., Perry, C., McGrath, J. J., Mackay-Sim, A., New techniques for biopsy and culture of human olfactory epithelial neurons. *Arch Otolaryngol Head Neck Surg* 1998, *124*, 861-866.
[4] Marshall, C. T., Lu, C., Winstead, W., Zhang, X*., et al.*, The therapeutic potential of human olfactory-derived stem cells. *Histol Histopathol* 2006, *21*, 633-643.
[5] Young, E., Westerberg, B., Yanai, A., Gregory-Evans, K., The olfactory mucosa: a potential source of stem cells for hearing regeneration. *Regen Med* 2018.
[6] Roche, P., Alekseeva, T., Widaa, A., Ryan, A*., et al.*, Olfactory Derived Stem Cells Delivered in a Biphasic Conduit Promote Peripheral Nerve Repair In Vivo. *Stem Cells Transl Med* 2017, *6*, 1894-1904.
[7] Buck, L., Axel, R., A novel multigene family may encode odorant receptors: a molecular basis for odor recognition. *Cell* 1991, *65*, 175-187.
[8] Spehr, M., Munger, S. D., Olfactory receptors: G protein-coupled receptors and beyond. *J Neurochem* 2009, *109*, 1570-1583.
[9] Baker, M. S., Ahn, S. B., Mohamedali, A., Islam, M. T*., et al.*, Accelerating the search for the missing proteins in the human proteome. *Nat Commun* 2017, *8*, 14271.
[10] Araneda, R. C., Peterlin, Z., Zhang, X., Chesler, A., Firestein, S., A pharmacological profile of the aldehyde receptor repertoire in rat olfactory epithelium. *The Journal of Physiology* 2004, *555*, 743-756.
[11] Liberles, S. D., Buck, L. B., A second class of chemosensory receptors in the olfactory epithelium. *Nature* 2006, *442*, 645-650.
[12] Ronnett, G. V., Moon, C., G proteins and olfactory signal transduction. *Annu Rev Physiol* 2002, *64*, 189-222.

[13] Mori, K., Nagao, H., Yoshihara, Y., The olfactory bulb: coding and processing of odor molecule information. *Science* 1999, *286*, 711-715.
[14] Leon, M., Johnson, B. A., Olfactory coding in the mammalian olfactory bulb. *Brain Res Brain Res Rev* 2003, *42*, 23-32.
[15] Sarnat, H. B., Yu, W., Maturation and Dysgenesis of the Human Olfactory Bulb. *Brain Pathol* 2016, *26*, 301-318.
[16] McLean, J. H., Harley, C. W., Olfactory learning in the rat pup: a model that may permit visualization of a mammalian memory trace. *Neuroreport* 2004, *15*, 1691-1697.
[17] Carmichael, S. T., Clugnet, M. C., Price, J. L., Central olfactory connections in the macaque monkey. *J Comp Neurol* 1994, *346*, 403-434.
[18] Benignus, V. A., Prah, J. D., Olfaction: anatomy, physiology and behavior. *Environmental Health Perspectives* 1982, *44*, 15-21.
[19] Trimmer, C., Mainland, J. D., in: Conn, P. M. (Ed.), *Conn's Translational Neuroscience*, Academic Press, San Diego 2017, pp. 363-377.
[20] Royet, J. P., Plailly, J., Lateralization of olfactory processes. *Chem Senses* 2004, *29*, 731-745.
[21] Francis, S., Rolls, E. T., Bowtell, R., McGlone, F.*, et al.*, The representation of pleasant touch in the brain and its relationship with taste and olfactory areas. *Neuroreport* 1999, *10*, 453-459.
[22] Dade, L. A., Zatorre, R. J., Jones-Gotman, M., Olfactory learning: convergent findings from lesion and brain imaging studies in humans. *Brain* 2002, *125*, 86-101.
[23] Squire, L. R., Stark, C. E., Clark, R. E., The medial temporal lobe. *Annu Rev Neurosci* 2004, *27*, 279-306.
[24] Kareken, D. A., Mosnik, D. M., Doty, R. L., Dzemidzic, M., Hutchins, G. D., Functional anatomy of human odor sensation, discrimination, and identification in health and aging. *Neuropsychology* 2003, *17*, 482-495.
[25] Plailly, J., Bensafi, M., Pachot-Clouard, M., Delon-Martin, C.*, et al.*, Involvement of right piriform cortex in olfactory familiarity judgments. *Neuroimage* 2005, *24*, 1032-1041.
[26] Savic, I., Berglund, H., Passive perception of odors and semantic circuits. *Hum Brain Mapp* 2004, *21*, 271-278.
[27] Zald, D. H., Donndelinger, M. J., Pardo, J. V., Elucidating dynamic brain interactions with across-subjects correlational analyses of positron emission tomographic data: the functional connectivity of the amygdala and orbitofrontal cortex during olfactory tasks. *J Cereb Blood Flow Metab* 1998, *18*, 896-905.
[28] Royet, J. P., Zald, D., Versace, R., Costes, N.*, et al.*, Emotional responses to pleasant and unpleasant olfactory, visual, and auditory stimuli: a positron emission tomography study. *J Neurosci* 2000, *20*, 7752-7759.
[29] Anderson, A. K., Christoff, K., Stappen, I., Panitz, D.*, et al.*, Dissociated neural representations of intensity and valence in human olfaction. *Nat Neurosci* 2003, *6*, 196-202.
[30] Royet, J. P., Plailly, J., Delon-Martin, C., Kareken, D. A., Segebarth, C., fMRI of emotional responses to odors: influence of hedonic valence and judgment, handedness, and gender. *Neuroimage* 2003, *20*, 713-728.
[31] Zald, D. H., Pardo, J. V., Emotion, olfaction, and the human amygdala: amygdala activation during aversive olfactory stimulation. *Proc Natl Acad Sci U S A* 1997, *94*, 4119-4124.
[32] Boyce, J. M., Shone, G. R., Effects of ageing on smell and taste. *Postgraduate Medical Journal* 2006, *82*, 239-241.
[33] Rouby, C., Thomas-Danguin, T., Vigouroux, M., Ciuperca, G.*, et al.*, The lyon clinical olfactory test: validation and measurement of hyposmia and anosmia in healthy and diseased populations. *Int J Otolaryngol* 2011, *2011*, 203805.
[34] Devanand, D. P., Tabert, M. H., Cuasay, K., Manly, J.*, et al.*, Olfactory identification deficits and MCI in a multi-ethnic elderly community sample. *Neurobiology of aging* 2010, *31*, 1593-1600.
[35] Kovacs, T., Mechanisms of olfactory dysfunction in aging and neurodegenerative disorders. *Ageing Res Rev* 2004, *3*, 215-232.

[36] Buschhuter, D., Smitka, M., Puschmann, S., Gerber, J. C*., et al.*, Correlation between olfactory bulb volume and olfactory function. *Neuroimage* 2008, *42*, 498-502.
[37] Murphy, C., Schubert, C. R., Cruickshanks, K. J., Klein, B. E*., et al.*, Prevalence of olfactory impairment in older adults. *Jama* 2002, *288*, 2307-2312.
[38] Dando, S. J., Mackay-Sim, A., Norton, R., Currie, B. J*., et al.*, Pathogens penetrating the central nervous system: infection pathways and the cellular and molecular mechanisms of invasion. *Clin Microbiol Rev* 2014, *27*, 691-726.
[39] Hawkes, C. H., Del Tredici, K., Braak, H., Parkinson's disease: a dual-hit hypothesis. *Neuropathol Appl Neurobiol* 2007, *33*, 599-614.
[40] Barresi, M., Ciurleo, R., Giacoppo, S., Foti Cuzzola, V*., et al.*, Evaluation of olfactory dysfunction in neurodegenerative diseases. *J Neurol Sci* 2012, *323*, 16-24.
[41] Doty, R. L., Olfactory dysfunction in Parkinson disease. *Nat Rev Neurol* 2012, *8*, 329-339.
[42] Franks, K. H., Chuah, M. I., King, A. E., Vickers, J. C., Connectivity of Pathology: The Olfactory System as a Model for Network-Driven Mechanisms of Alzheimer's Disease Pathogenesis. *Frontiers in Aging Neuroscience* 2015, *7*, 234.
[43] Ruan, Y., Zheng, X. Y., Zhang, H. L., Zhu, W., Zhu, J., Olfactory dysfunctions in neurodegenerative disorders. *J Neurosci Res* 2012, *90*, 1693-1700.
[44] Rahayel, S., Frasnelli, J., Joubert, S., The effect of Alzheimer's disease and Parkinson's disease on olfaction: a meta-analysis. *Behav Brain Res* 2012, *231*, 60-74.
[45] Doty, R. L., The olfactory vector hypothesis of neurodegenerative disease: is it viable? *Ann Neurol* 2008, *63*, 7-15.
[46] Miller, D. B., O'Callaghan, J. P., Biomarkers of Parkinson's disease: present and future. *Metabolism* 2015, *64*, S40-46.
[47] Doty, R. L., Olfaction in Parkinson's disease and related disorders. *Neurobiol Dis* 2012, *46*, 527-552.
[48] Doty, R. L., Olfactory dysfunction in neurodegenerative diseases: is there a common pathological substrate? *Lancet Neurol* 2017, *16*, 478-488.
[49] Doty, R. L., Shaman, P., Kimmelman, C. P., Dann, M. S., University of Pennsylvania Smell Identification Test: a rapid quantitative olfactory function test for the clinic. *Laryngoscope* 1984, *94*, 176-178.
[50] Reitz, C., Mayeux, R., Alzheimer disease: epidemiology, diagnostic criteria, risk factors and biomarkers. *Biochem Pharmacol* 2014, *88*, 640-651.
[51] Mucke, L., *Nature*, England 2009, pp. 895-897.
[52] Bettens, K., Sleegers, K., Van Broeckhoven, C., Current status on Alzheimer disease molecular genetics: from past, to present, to future. *Hum Mol Genet* 2010, *19*, R4-r11.
[53] Roberson, E. D., Scearce-Levie, K., Palop, J. J., Yan, F*., et al.*, Reducing endogenous tau ameliorates amyloid beta-induced deficits in an Alzheimer's disease mouse model. *Science* 2007, *316*, 750-754.
[54] Goedert, M., Tau protein and the neurofibrillary pathology of Alzheimer's disease. *Trends Neurosci* 1993, *16*, 460-465.
[55] McKhann, G. M., Knopman, D. S., Chertkow, H., Hyman, B. T*., et al.*, The diagnosis of dementia due to Alzheimer's disease: recommendations from the National Institute on Aging-Alzheimer's Association workgroups on diagnostic guidelines for Alzheimer's disease. *Alzheimers Dement* 2011, *7*, 263-269.
[56] Staffaroni, A. M., Elahi, F. M., McDermott, D., Marton, K*., et al.*, Neuroimaging in Dementia. *Semin Neurol* 2017, *37*, 510-537.
[57] Braak, H., Braak, E., Neuropathological stageing of Alzheimer-related changes. *Acta Neuropathol* 1991, *82*, 239-259.
[58] Mirra, S. S., Heyman, A., McKeel, D., Sumi, S. M*., et al.*, The Consortium to Establish a Registry for Alzheimer's Disease (CERAD). Part II. Standardization of the neuropathologic assessment of Alzheimer's disease. *Neurology* 1991, *41*, 479-486.

[59] Hyman, B. T., Trojanowski, J. Q., Consensus recommendations for the postmortem diagnosis of Alzheimer disease from the National Institute on Aging and the Reagan Institute Working Group on diagnostic criteria for the neuropathological assessment of Alzheimer disease. *J Neuropathol Exp Neurol* 1997, *56*, 1095-1097.
[60] Massoud, F., Gauthier, S., Update on the Pharmacological Treatment of Alzheimer's Disease. *Current Neuropharmacology* 2010, *8*, 69-80.
[61] Dorsey, E. R., Constantinescu, R., Thompson, J. P., Biglan, K. M.*, et al.*, Projected number of people with Parkinson disease in the most populous nations, 2005 through 2030. *Neurology* 2007, *68*, 384-386.
[62] Rizek, P., Kumar, N., Jog, M. S., An update on the diagnosis and treatment of Parkinson disease. *Cmaj* 2016, *188*, 1157-1165.
[63] Fernandez, H. H., 2015 Update on Parkinson disease. *Cleve Clin J Med* 2015, *82*, 563-568.
[64] Iranzo, A., Molinuevo, J. L., Santamaria, J., Serradell, M.*, et al.*, Rapid-eye-movement sleep behaviour disorder as an early marker for a neurodegenerative disorder: a descriptive study. *Lancet Neurol* 2006, *5*, 572-577.
[65] Reichmann, H., Schneider, C., Lohle, M., Non-motor features of Parkinson's disease: depression and dementia. *Parkinsonism Relat Disord* 2009, *15 Suppl 3*, S87-92.
[66] Jost, W. H., Gastrointestinal dysfunction in Parkinson's Disease. *J Neurol Sci* 2010, *289*, 69-73.
[67] Patel, R. M., Pinto, J. M., Olfaction: anatomy, physiology, and disease. *Clin Anat* 2014, *27*, 54-60.
[68] Klingelhoefer, L., Reichmann, H., Pathogenesis of Parkinson disease--the gut-brain axis and environmental factors. *Nat Rev Neurol* 2015, *11*, 625-636.
[69] Dickson, D. W., Braak, H., Duda, J. E., Duyckaerts, C.*, et al.*, Neuropathological assessment of Parkinson's disease: refining the diagnostic criteria. *Lancet Neurol* 2009, *8*, 1150-1157.
[70] Burre, J., Sharma, M., Tsetsenis, T., Buchman, V.*, et al.*, Alpha-synuclein promotes SNARE-complex assembly in vivo and in vitro. *Science* 2010, *329*, 1663-1667.
[71] Dickson, D. W., Alpha-synuclein and the Lewy body disorders. *Curr Opin Neurol* 2001, *14*, 423-432.
[72] Reynolds, N. P., Soragni, A., Rabe, M., Verdes, D.*, et al.*, Mechanism of membrane interaction and disruption by alpha-synuclein. *J Am Chem Soc* 2011, *133*, 19366-19375.
[73] Klucken, J., Poehler, A. M., Ebrahimi-Fakhari, D., Schneider, J.*, et al.*, Alpha-synuclein aggregation involves a bafilomycin A 1-sensitive autophagy pathway. *Autophagy* 2012, *8*, 754-766.
[74] Di Maio, R., Barrett, P. J., Hoffman, E. K., Barrett, C. W.*, et al.*, alpha-Synuclein binds to TOM20 and inhibits mitochondrial protein import in Parkinson's disease. *Sci Transl Med* 2016, *8*, 342ra378.
[75] Colla, E., Jensen, P. H., Pletnikova, O., Troncoso, J. C.*, et al.*, Accumulation of toxic alpha-synuclein oligomer within endoplasmic reticulum occurs in alpha-synucleinopathy in vivo. *J Neurosci* 2012, *32*, 3301-3305.
[76] Danzer, K. M., Kranich, L. R., Ruf, W. P., Cagsal-Getkin, O.*, et al.*, Exosomal cell-to-cell transmission of alpha synuclein oligomers. *Mol Neurodegener* 2012, *7*, 42.
[77] Braak, H., Ghebremedhin, E., Rub, U., Bratzke, H., Del Tredici, K., Stages in the development of Parkinson's disease-related pathology. *Cell Tissue Res* 2004, *318*, 121-134.
[78] Fumimura, Y., Ikemura, M., Saito, Y., Sengoku, R.*, et al.*, Analysis of the adrenal gland is useful for evaluating pathology of the peripheral autonomic nervous system in lewy body disease. *J Neuropathol Exp Neurol* 2007, *66*, 354-362.
[79] McKeith, I. G., Dickson, D. W., Lowe, J., Emre, M.*, et al.*, Diagnosis and management of dementia with Lewy bodies: third report of the DLB Consortium. *Neurology* 2005, *65*, 1863-1872.
[80] Sobue, G., Ishigaki, S., Watanabe, H., Pathogenesis of Frontotemporal Lobar Degeneration: Insights From Loss of Function Theory and Early Involvement of the Caudate Nucleus. *Front Neurosci* 2018, *12*, 473.

[81] Bennion Callister, J., Pickering-Brown, S. M., Pathogenesis/genetics of frontotemporal dementia and how it relates to ALS. *Exp Neurol* 2014, *262 Pt B*, 84-90.
[82] Piguet, O., Hornberger, M., Mioshi, E., Hodges, J. R., Behavioural-variant frontotemporal dementia: diagnosis, clinical staging, and management. *Lancet Neurol* 2011, *10*, 162-172.
[83] Seltman, R. E., Matthews, B. R., Frontotemporal lobar degeneration: epidemiology, pathology, diagnosis and management. *CNS Drugs* 2012, *26*, 841-870.
[84] Sieben, A., Van Langenhove, T., Engelborghs, S., Martin, J. J.*, et al.*, The genetics and neuropathology of frontotemporal lobar degeneration. *Acta Neuropathol* 2012, *124*, 353-372.
[85] Li, Y. Q., Tan, M. S., Yu, J. T., Tan, L., Frontotemporal Lobar Degeneration: Mechanisms and Therapeutic Strategies. *Mol Neurobiol* 2016, *53*, 6091-6105.
[86] Mackenzie, I. R., Neumann, M., Bigio, E. H., Cairns, N. J.*, et al.*, Nomenclature and nosology for neuropathologic subtypes of frontotemporal lobar degeneration: an update. *Acta Neuropathol* 2010, *119*, 1-4.
[87] Yamamoto, K., Ogihara, T., [Pick's disease]. *Nihon Rinsho* 2016, *74*, 476-481.
[88] Richardson, J. C., Steele, J., Olszewski, J., SUPRANUCLEAR OPHTHALMOPLEGIA, PSEUDOBULBAR PALSY, NUCHAL DYSTONIA AND DEMENTIA. A CLINICAL REPORT ON EIGHT CASES OF "HETEROGENOUS SYSTEM DEGENERATION". *Trans Am Neurol Assoc* 1963, *88*, 25-29.
[89] Bott, N. T., Radke, A., Stephens, M. L., Kramer, J. H., Frontotemporal dementia: diagnosis, deficits and management. *Neurodegenerative disease management* 2014, *4*, 439-454.
[90] Diehl-Schmid, J., Onur, O. A., Kuhn, J., Gruppe, T., Drzezga, A., Imaging frontotemporal lobar degeneration. *Curr Neurol Neurosci Rep* 2014, *14*, 489.
[91] Osher, J. E., Wicklund, A. H., Rademaker, A., Johnson, N., Weintraub, S., The mini-mental state examination in behavioral variant frontotemporal dementia and primary progressive aphasia. *Am J Alzheimers Dis Other Demen* 2007, *22*, 468-473.
[92] Ferrari, R., Hardy, J., Momeni, P., Frontotemporal dementia: from Mendelian genetics towards genome wide association studies. *J Mol Neurosci* 2011, *45*, 500-515.
[93] Attems, J., Walker, L., Jellinger, K. A., Olfactory bulb involvement in neurodegenerative diseases. *Acta Neuropathol* 2014, *127*, 459-475.
[94] Peters, J. M., Hummel, T., Kratzsch, T., Lotsch, J.*, et al.*, Olfactory function in mild cognitive impairment and Alzheimer's disease: an investigation using psychophysical and electrophysiological techniques. *Am J Psychiatry* 2003, *160*, 1995-2002.
[95] Masurkar, A. V., Devanand, D. P., Olfactory Dysfunction in the Elderly: Basic Circuitry and Alterations with Normal Aging and Alzheimer's Disease. *Current geriatrics reports* 2014, *3*, 91-100.
[96] Bahar-Fuchs, A., Moss, S., Rowe, C., Savage, G., Awareness of olfactory deficits in healthy aging, amnestic mild cognitive impairment and Alzheimer's disease. *Int Psychogeriatr* 2011, *23*, 1097-1106.
[97] Kjelvik, G., Saltvedt, I., White, L. R., Stenumgård, P.*, et al.*, The brain structural and cognitive basis of odor identification deficits in mild cognitive impairment and Alzheimer's disease. *BMC Neurology* 2014, *14*, 168-168.
[98] Wilson, R. S., Arnold, S. E., Schneider, J. A., Boyle, P. A.*, et al.*, Olfactory impairment in presymptomatic Alzheimer's disease. *Ann N Y Acad Sci* 2009, *1170*, 730-735.
[99] Wang, J., Eslinger, P. J., Doty, R. L., Zimmerman, E. K.*, et al.*, Olfactory Deficit Detected by fMRI in Early Alzheimer's Disease. *Brain research* 2010, *1357*, 184-194.
[100] D'Souza, R. D., Vijayaraghavan, S., Paying attention to smell: cholinergic signaling in the olfactory bulb. *Front Synaptic Neurosci* 2014, *6*, 21.
[101] Christen-Zaech, S., Kraftsik, R., Pillevuit, O., Kiraly, M.*, et al.*, Early olfactory involvement in Alzheimer's disease. *Can J Neurol Sci* 2003, *30*, 20-25.
[102] Price, J. L., Davis, P. B., Morris, J. C., White, D. L., The distribution of tangles, plaques and related immunohistochemical markers in healthy aging and Alzheimer's disease. *Neurobiol Aging* 1991, *12*, 295-312.

[103] Struble, R. G., Clark, H. B., Olfactory bulb lesions in Alzheimer's disease. *Neurobiol Aging* 1992, *13*, 469-473.
[104] Attems, J., Lintner, F., Jellinger, K. A., Olfactory involvement in aging and Alzheimer's disease: an autopsy study. *J Alzheimers Dis* 2005, *7*, 149-157; discussion 173-180.
[105] Kovacs, T., Cairns, N. J., Lantos, P. L., beta-amyloid deposition and neurofibrillary tangle formation in the olfactory bulb in ageing and Alzheimer's disease. *Neuropathol Appl Neurobiol* 1999, *25*, 481-491.
[106] Tsuboi, Y., Wszolek, Z. K., Graff-Radford, N. R., Cookson, N., Dickson, D. W., Tau pathology in the olfactory bulb correlates with Braak stage, Lewy body pathology and apolipoprotein epsilon4. *Neuropathol Appl Neurobiol* 2003, *29*, 503-510.
[107] Kovacs, T., Cairns, N. J., Lantos, P. L., Olfactory centres in Alzheimer's disease: olfactory bulb is involved in early Braak's stages. *Neuroreport* 2001, *12*, 285-288.
[108] Gomez-Isla, T., Price, J. L., McKeel, D. W., Jr., Morris, J. C*., et al.*, Profound loss of layer II entorhinal cortex neurons occurs in very mild Alzheimer's disease. *J Neurosci* 1996, *16*, 4491-4500.
[109] LaFerla, F. M., Green, K. N., Animal models of Alzheimer disease. *Cold Spring Harb Perspect Med* 2012, *2*.
[110] Wesson, D. W., Levy, E., Nixon, R. A., Wilson, D. A., Olfactory dysfunction correlates with amyloid-beta burden in an Alzheimer's disease mouse model. *J Neurosci* 2010, *30*, 505-514.
[111] Hsiao, K., Chapman, P., Nilsen, S., Eckman, C*., et al.*, Correlative memory deficits, Abeta elevation, and amyloid plaques in transgenic mice. *Science* 1996, *274*, 99-102.
[112] Borchelt, D. R., Thinakaran, G., Eckman, C. B., Lee, M. K*., et al.*, Familial Alzheimer's disease-linked presenilin 1 variants elevate Abeta1-42/1-40 ratio in vitro and in vivo. *Neuron* 1996, *17*, 1005-1013.
[113] Yao, Z. G., Hua, F., Zhang, H. Z., Li, Y. Y., Qin, Y. J., Olfactory dysfunction in the APP/PS1 transgenic mouse model of Alzheimer's disease: Morphological evaluations from the nose to the brain. *Neuropathology* 2017, *37*, 485-494.
[114] De la Rosa-Prieto, C., Saiz-Sanchez, D., Ubeda-Banon, I., Flores-Cuadrado, A., Martinez-Marcos, A., Neurogenesis, Neurodegeneration, Interneuron Vulnerability, and Amyloid-beta in the Olfactory Bulb of APP/PS1 Mouse Model of Alzheimer's Disease. *Front Neurosci* 2016, *10*, 227.
[115] Kempf, S. J., Metaxas, A., Ibanez-Vea, M., Darvesh, S*., et al.*, An integrated proteomics approach shows synaptic plasticity changes in an APP/PS1 Alzheimer's mouse model. *Oncotarget* 2016, *7*, 33627-33648.
[116] Gonzalez-Dominguez, R., Garcia-Barrera, T., Vitorica, J., Gomez-Ariza, J. L., Region-specific metabolic alterations in the brain of the APP/PS1 transgenic mice of Alzheimer's disease. *Biochim Biophys Acta* 2014, *1842*, 2395-2402.
[117] Alves, J., Petrosyan, A., Magalhães, R., Olfactory dysfunction in dementia. *World Journal of Clinical Cases : WJCC* 2014, *2*, 661-667.
[118] Postuma, R. B., Berg, D., Stern, M., Poewe, W*., et al.*, MDS clinical diagnostic criteria for Parkinson's disease. *Mov Disord* 2015, *30*, 1591-1601.
[119] Kranick, S. M., Duda, J. E., Olfactory dysfunction in Parkinson's disease. *Neurosignals* 2008, *16*, 35-40.
[120] Bohnen, N. I., Studenski, S. A., Constantine, G. M., Moore, R. Y., Diagnostic performance of clinical motor and non-motor tests of Parkinson disease: a matched case-control study. *Eur J Neurol* 2008, *15*, 685-691.
[121] Quinn, N. P., Rossor, M. N., Marsden, C. D., Olfactory threshold in Parkinson's disease. *J Neurol Neurosurg Psychiatry* 1987, *50*, 88-89.
[122] Hawkes, C., Shah, M., Findley, L., Olfactory function in essential tremor: a deficit unrelated to disease duration or severity. *Neurology* 2003, *61*, 871-872; author reply 872.
[123] Berendse, H. W., Roos, D. S., Raijmakers, P., Doty, R. L., Motor and non-motor correlates of olfactory dysfunction in Parkinson's disease. *J Neurol Sci* 2011, *310*, 21-24.

[124] Braak, H., Rub, U., Gai, W. P., Del Tredici, K., Idiopathic Parkinson's disease: possible routes by which vulnerable neuronal types may be subject to neuroinvasion by an unknown pathogen. *J Neural Transm (Vienna)* 2003, *110*, 517-536.
[125] Braak, H., Del Tredici, K., Rub, U., de Vos, R. A.*, et al.*, Staging of brain pathology related to sporadic Parkinson's disease. *Neurobiol Aging* 2003, *24*, 197-211.
[126] Del Tredici, K., Rub, U., De Vos, R. A., Bohl, J. R., Braak, H., Where does parkinson disease pathology begin in the brain? *J Neuropathol Exp Neurol* 2002, *61*, 413-426.
[127] Hubbard, P. S., Esiri, M. M., Reading, M., McShane, R., Nagy, Z., Alpha-synuclein pathology in the olfactory pathways of dementia patients. *J Anat* 2007, *211*, 117-124.
[128] Rey, N. L., Steiner, J. A., Maroof, N., Luk, K. C.*, et al.*, Widespread transneuronal propagation of alpha-synucleinopathy triggered in olfactory bulb mimics prodromal Parkinson's disease. *J Exp Med* 2016, *213*, 1759-1778.
[129] Graham, S. F., Rey, N. L., Yilmaz, A., Kumar, P.*, et al.*, Biochemical Profiling of the Brain and Blood Metabolome in a Mouse Model of Prodromal Parkinson's Disease Reveals Distinct Metabolic Profiles. *J Proteome Res* 2018, *17*, 2460-2469.
[130] Pearce, R. K., Hawkes, C. H., Daniel, S. E., The anterior olfactory nucleus in Parkinson's disease. *Mov Disord* 1995, *10*, 283-287.
[131] German, D. C., Manaye, K. F., White, C. L., 3rd, Woodward, D. J.*, et al.*, Disease-specific patterns of locus coeruleus cell loss. *Ann Neurol* 1992, *32*, 667-676.
[132] Harding, A. J., Stimson, E., Henderson, J. M., Halliday, G. M., Clinical correlates of selective pathology in the amygdala of patients with Parkinson's disease. *Brain* 2002, *125*, 2431-2445.
[133] Li, J., Gu, C. Z., Su, J. B., Zhu, L. H.*, et al.*, Changes in Olfactory Bulb Volume in Parkinson's Disease: A Systematic Review and Meta-Analysis. *PLoS One* 2016, *11*, e0149286.
[134] Heyanka, D. J., Golden, C. J., McCue, R. B., 2nd, Scarisbrick, D. M.*, et al.*, Olfactory deficits in frontotemporal dementia as measured by the Alberta Smell Test. *Appl Neuropsychol Adult* 2014, *21*, 176-182.
[135] Luzzi, S., Snowden, J. S., Neary, D., Coccia, M.*, et al.*, Distinct patterns of olfactory impairment in Alzheimer's disease, semantic dementia, frontotemporal dementia, and corticobasal degeneration. *Neuropsychologia* 2007, *45*, 1823-1831.
[136] McLaughlin, N. C., Westervelt, H. J., Odor identification deficits in frontotemporal dementia: a preliminary study. *Arch Clin Neuropsychol* 2008, *23*, 119-123.
[137] Pardini, M., Huey, E. D., Cavanagh, A. L., Grafman, J., Olfactory function in corticobasal syndrome and frontotemporal dementia. *Arch Neurol* 2009, *66*, 92-96.
[138] Orasji, S. S., Mulder, J. L., de Bruijn, S. F., Wirtz, P. W., Olfactory dysfunction in behavioral variant frontotemporal dementia. *Clin Neurol Neurosurg* 2016, *141*, 106-110.
[139] Tonacci, A., Billeci, L., Olfactory Testing in Frontotemporal Dementia: A Literature Review. *Am J Alzheimers Dis Other Demen* 2018, *33*, 342-352.
[140] Yoshimura, N., Olfactory bulb involvement in Pick's disease. *Acta Neuropathol* 1988, *77*, 202-205.
[141] Kim, J., Choi, I. Y., Duff, K. E., Lee, P., Progressive Pathological Changes in Neurochemical Profile of the Hippocampus and Early Changes in the Olfactory Bulbs of Tau Transgenic Mice (rTg4510). *Neurochem Res* 2017, *42*, 1649-1660.
[142] Kohl, Z., Schlachetzki, J. C., Feldewerth, J., Hornauer, P.*, et al.*, Distinct Pattern of Microgliosis in the Olfactory Bulb of Neurodegenerative Proteinopathies. *Neural Plast* 2017, *2017*, 3851262.
[143] Zelaya, M. V., Perez-Valderrama, E., de Morentin, X. M., Tunon, T.*, et al.*, Olfactory bulb proteome dynamics during the progression of sporadic Alzheimer's disease: identification of common and distinct olfactory targets across Alzheimer-related co-pathologies. *Oncotarget* 2015, *6*, 39437-39456.
[144] Takeda, T., Iijima, M., Uchihara, T., Ohashi, T.*, et al.*, TDP-43 Pathology Progression Along the Olfactory Pathway as a Possible Substrate for Olfactory Impairment in Amyotrophic Lateral Sclerosis. *J Neuropathol Exp Neurol* 2015, *74*, 547-556.

[145] Guo, J. L., Lee, V. M. Y., Cell-to-cell transmission of pathogenic proteins in neurodegenerative diseases. *Nature medicine* 2014, *20*, 130-138.
[146] Goedert, M., NEURODEGENERATION. Alzheimer's and Parkinson's diseases: The prion concept in relation to assembled Abeta, tau, and alpha-synuclein. *Science* 2015, *349*, 1255555.
[147] Rey, N. L., Wesson, D. W., Brundin, P., The olfactory bulb as the entry site for prion-like propagation in neurodegenerative diseases. *Neurobiol Dis* 2018, *109*, 226-248.
[148] Watts, J. C., Condello, C., Stohr, J., Oehler, A.*, et al.*, Serial propagation of distinct strains of Abeta prions from Alzheimer's disease patients. *Proc Natl Acad Sci U S A* 2014, *111*, 10323-10328.
[149] Sardar Sinha, M., Ansell-Schultz, A., Civitelli, L., Hildesjo, C.*, et al.*, Alzheimer's disease pathology propagation by exosomes containing toxic amyloid-beta oligomers. *Acta Neuropathol* 2018, *136*, 41-56.
[150] He, B., Zheng, M., Liu, Q., Shi, Z.*, et al.*, Injected Amyloid Beta in the Olfactory Bulb Transfers to Other Brain Regions via Neural Connections in Mice. *Mol Neurobiol* 2018, *55*, 1703-1713.
[151] Ruiz-Riquelme, A., Lau, H. H. C., Stuart, E., Goczi, A. N.*, et al.*, Prion-like propagation of beta-amyloid aggregates in the absence of APP overexpression. *Acta Neuropathol Commun* 2018, *6*, 26.
[152] Eisele, Y. S., Obermuller, U., Heilbronner, G., Baumann, F.*, et al.*, Peripherally applied Abeta-containing inoculates induce cerebral beta-amyloidosis. *Science* 2010, *330*, 980-982.
[153] Langer, F., Eisele, Y. S., Fritschi, S. K., Staufenbiel, M.*, et al.*, Soluble Abeta seeds are potent inducers of cerebral beta-amyloid deposition. *J Neurosci* 2011, *31*, 14488-14495.
[154] Rosen, R. F., Fritz, J. J., Dooyema, J., Cintron, A. F.*, et al.*, Exogenous seeding of cerebral beta-amyloid deposition in betaAPP-transgenic rats. *J Neurochem* 2012, *120*, 660-666.
[155] Eisele, Y. S., Bolmont, T., Heikenwalder, M., Langer, F.*, et al.*, Induction of cerebral beta-amyloidosis: intracerebral versus systemic Abeta inoculation. *Proc Natl Acad Sci U S A* 2009, *106*, 12926-12931.
[156] Ye, L., Hamaguchi, T., Fritschi, S. K., Eisele, Y. S.*, et al.*, Progression of Seed-Induced Abeta Deposition within the Limbic Connectome. *Brain Pathol* 2015, *25*, 743-752.
[157] Clavaguera, F., Bolmont, T., Crowther, R. A., Abramowski, D.*, et al.*, Transmission and spreading of tauopathy in transgenic mouse brain. *Nat Cell Biol* 2009, *11*, 909-913.
[158] Ahmed, Z., Cooper, J., Murray, T. K., Garn, K.*, et al.*, A novel in vivo model of tau propagation with rapid and progressive neurofibrillary tangle pathology: the pattern of spread is determined by connectivity, not proximity. *Acta Neuropathol* 2014, *127*, 667-683.
[159] Clavaguera, F., Akatsu, H., Fraser, G., Crowther, R. A.*, et al.*, Brain homogenates from human tauopathies induce tau inclusions in mouse brain. *Proc Natl Acad Sci U S A* 2013, *110*, 9535-9540.
[160] Clavaguera, F., Hench, J., Lavenir, I., Schweighauser, G.*, et al.*, Peripheral administration of tau aggregates triggers intracerebral tauopathy in transgenic mice. *Acta Neuropathol* 2014, *127*, 299-301.
[161] Boluda, S., Iba, M., Zhang, B., Raible, K. M.*, et al.*, Differential induction and spread of tau pathology in young PS19 tau transgenic mice following intracerebral injections of pathological tau from Alzheimer's disease or corticobasal degeneration brains. *Acta Neuropathol* 2015, *129*, 221-237.
[162] Wu, J. W., Hussaini, S. A., Bastille, I. M., Rodriguez, G. A.*, et al.*, Neuronal activity enhances tau propagation and tau pathology in vivo. *Nat Neurosci* 2016, *19*, 1085-1092.
[163] Fuster-Matanzo, A., Hernandez, F., Avila, J., Tau Spreading Mechanisms; Implications for Dysfunctional Tauopathies. *Int J Mol Sci* 2018, *19*.
[164] Wang, Y., Balaji, V., Kaniyappan, S., Kruger, L.*, et al.*, The release and trans-synaptic transmission of Tau via exosomes. *Mol Neurodegener* 2017, *12*, 5.
[165] Asai, H., Ikezu, S., Tsunoda, S., Medalla, M.*, et al.*, Depletion of microglia and inhibition of exosome synthesis halt tau propagation. *Nat Neurosci* 2015, *18*, 1584-1593.

[166] Rey, N. L., George, S., Brundin, P., Review: Spreading the word: precise animal models and validated methods are vital when evaluating prion-like behaviour of alpha-synuclein. *Neuropathol Appl Neurobiol* 2016, *42*, 51-76.
[167] Luk, K. C., Kehm, V., Carroll, J., Zhang, B.*, et al.*, Pathological alpha-synuclein transmission initiates Parkinson-like neurodegeneration in nontransgenic mice. *Science* 2012, *338*, 949-953.
[168] Masuda-Suzukake, M., Nonaka, T., Hosokawa, M., Oikawa, T.*, et al.*, Prion-like spreading of pathological alpha-synuclein in brain. *Brain* 2013, *136*, 1128-1138.
[169] Sacino, A. N., Brooks, M., Thomas, M. A., McKinney, A. B.*, et al.*, Intramuscular injection of alpha-synuclein induces CNS alpha-synuclein pathology and a rapid-onset motor phenotype in transgenic mice. *Proc Natl Acad Sci U S A* 2014, *111*, 10732-10737.
[170] Paumier, K. L., Luk, K. C., Manfredsson, F. P., Kanaan, N. M.*, et al.*, Intrastriatal injection of pre-formed mouse alpha-synuclein fibrils into rats triggers alpha-synuclein pathology and bilateral nigrostriatal degeneration. *Neurobiol Dis* 2015, *82*, 185-199.
[171] Dehay, B., Vila, M., Bezard, E., Brundin, P., Kordower, J. H., Alpha-synuclein propagation: New insights from animal models. *Mov Disord* 2016, *31*, 161-168.
[172] Rey, N. L., George, S., Steiner, J. A., Madaj, Z.*, et al.*, Spread of aggregates after olfactory bulb injection of alpha-synuclein fibrils is associated with early neuronal loss and is reduced long term. *Acta Neuropathol* 2018, *135*, 65-83.
[173] Fernandez-Irigoyen, J., Labarga, A., Zabaleta, A., de Morentin, X. M.*, et al.*, Toward defining the anatomo-proteomic puzzle of the human brain: An integrative analysis. *Proteomics Clin Appl* 2015, *9*, 796-807.
[174] Katsel, P., Li, C., Haroutunian, V., Gene expression alterations in the sphingolipid metabolism pathways during progression of dementia and Alzheimer's disease: a shift toward ceramide accumulation at the earliest recognizable stages of Alzheimer's disease? *Neurochem Res* 2007, *32*, 845-856.
[175] Katsel, P., Tan, W., Haroutunian, V., Gain in brain immunity in the oldest-old differentiates cognitively normal from demented individuals. *PLoS One* 2009, *4*, e7642.
[176] Haroutunian, V., Katsel, P., Schmeidler, J., Transcriptional vulnerability of brain regions in Alzheimer's disease and dementia. *Neurobiol Aging* 2009, *30*, 561-573.
[177] Tan, M. G., Chua, W. T., Esiri, M. M., Smith, A. D.*, et al.*, Genome wide profiling of altered gene expression in the neocortex of Alzheimer's disease. *J Neurosci Res* 2010, *88*, 1157-1169.
[178] Youn, H., Jeoung, M., Koo, Y., Ji, H.*, et al.*, Kalirin is under-expressed in Alzheimer's disease hippocampus. *J Alzheimers Dis* 2007, *11*, 385-397.
[179] Wang, S., Qaisar, U., Yin, X., Grammas, P., Gene expression profiling in Alzheimer's disease brain microvessels. *J Alzheimers Dis* 2012, *31*, 193-205.
[180] Kelly, S. C., He, B., Perez, S. E., Ginsberg, S. D.*, et al.*, Locus coeruleus cellular and molecular pathology during the progression of Alzheimer's disease. *Acta Neuropathol Commun* 2017, *5*, 8.
[181] Zuo, L., Wang, Z., Tan, Y., Chen, X., Luo, X., piRNAs and Their Functions in the Brain. *Int J Hum Genet* 2016, *16*, 53-60.
[182] Cantuti-Castelvetri, I., Keller-McGandy, C., Bouzou, B., Asteris, G.*, et al.*, Effects of gender on nigral gene expression and parkinson disease. *Neurobiol Dis* 2007, *26*, 606-614.
[183] Simunovic, F., Yi, M., Wang, Y., Macey, L.*, et al.*, Gene expression profiling of substantia nigra dopamine neurons: further insights into Parkinson's disease pathology. *Brain* 2009, *132*, 1795-1809.
[184] Elstner, M., Morris, C. M., Heim, K., Lichtner, P.*, et al.*, Single-cell expression profiling of dopaminergic neurons combined with association analysis identifies pyridoxal kinase as Parkinson's disease gene. *Ann Neurol* 2009, *66*, 792-798.
[185] Bossers, K., Meerhoff, G., Balesar, R., van Dongen, J. W.*, et al.*, Analysis of gene expression in Parkinson's disease: possible involvement of neurotrophic support and axon guidance in dopaminergic cell death. *Brain Pathol* 2009, *19*, 91-107.
[186] Durrenberger, P. F., Grunblatt, E., Fernando, F. S., Monoranu, C. M.*, et al.*, Inflammatory Pathways in Parkinson's Disease; A BNE Microarray Study. *Parkinsons Dis* 2012, *2012*, 214714.

[187] Kim, W., Lee, Y., McKenna, N. D., Yi, M.*, et al.*, miR-126 contributes to Parkinson's disease by dysregulating the insulin-like growth factor/phosphoinositide 3-kinase signaling. *Neurobiol Aging* 2014, *35*, 1712-1721.
[188] Briggs, C. E., Wang, Y., Kong, B., Woo, T. U.*, et al.*, Midbrain dopamine neurons in Parkinson's disease exhibit a dysregulated miRNA and target-gene network. *Brain Res* 2015, *1618*, 111-121.
[189] Miller, R. M., Kiser, G. L., Kaysser-Kranich, T. M., Lockner, R. J.*, et al.*, Robust dysregulation of gene expression in substantia nigra and striatum in Parkinson's disease. *Neurobiol Dis* 2006, *21*, 305-313.
[190] Cruz-Monteagudo, M., Borges, F., Paz, Y. M. C., Cordeiro, M. N.*, et al.*, Efficient and biologically relevant consensus strategy for Parkinson's disease gene prioritization. *BMC Med Genomics* 2016, *9*, 12.
[191] Dumitriu, A., Golji, J., Labadorf, A. T., Gao, B.*, et al.*, Integrative analyses of proteomics and RNA transcriptomics implicate mitochondrial processes, protein folding pathways and GWAS loci in Parkinson disease. *BMC Med Genomics* 2016, *9*, 5.
[192] Riley, B. E., Gardai, S. J., Emig-Agius, D., Bessarabova, M.*, et al.*, Systems-based analyses of brain regions functionally impacted in Parkinson's disease reveals underlying causal mechanisms. *PLoS One* 2014, *9*, e102909.
[193] Alieva, A., Shadrina, M. I., Filatova, E. V., Karabanov, A. V.*, et al.*, Involvement of endocytosis and alternative splicing in the formation of the pathological process in the early stages of Parkinson's disease. *Biomed Res Int* 2014, *2014*, 718732.
[194] Calligaris, R., Banica, M., Roncaglia, P., Robotti, E.*, et al.*, Blood transcriptomics of drug-naive sporadic Parkinson's disease patients. *BMC Genomics* 2015, *16*, 876.
[195] Santiago, J. A., Potashkin, J. A., Network-based metaanalysis identifies HNF4A and PTBP1 as longitudinally dynamic biomarkers for Parkinson's disease. *Proc Natl Acad Sci U S A* 2015, *112*, 2257-2262.
[196] Han, G., Wang, J., Zeng, F., Feng, X.*, et al.*, Characteristic transformation of blood transcriptome in Alzheimer's disease. *J Alzheimers Dis* 2013, *35*, 373-386.
[197] Hossein-Nezhad, A., Fatemi, R. P., Ahmad, R., Peskind, E. R.*, et al.*, Transcriptomic Profiling of Extracellular RNAs Present in Cerebrospinal Fluid Identifies Differentially Expressed Transcripts in Parkinson's Disease. *J Parkinsons Dis* 2016, *6*, 109-117.
[198] Craft, G. E., Chen, A., Nairn, A. C., Recent advances in quantitative neuroproteomics. *Methods* 2013, *61*, 186-218.
[199] Moya-Alvarado, G., Gershoni-Emek, N., Perlson, E., Bronfman, F. C., Neurodegeneration and Alzheimer's disease (AD). What Can Proteomics Tell Us About the Alzheimer's Brain? *Mol Cell Proteomics* 2016, *15*, 409-425.
[200] Hosp, F., Mann, M., A Primer on Concepts and Applications of Proteomics in Neuroscience. *Neuron* 2017, *96*, 558-571.
[201] Bayes, A., Grant, S. G., Neuroproteomics: understanding the molecular organization and complexity of the brain. *Nat Rev Neurosci* 2009, *10*, 635-646.
[202] Kitchen, R. R., Rozowsky, J. S., Gerstein, M. B., Nairn, A. C., Decoding neuroproteomics: integrating the genome, translatome and functional anatomy. *Nature neuroscience* 2014, *17*, 1491-1499.
[203] Sharma, K., Schmitt, S., Bergner, C. G., Tyanova, S.*, et al.*, Cell type- and brain region-resolved mouse brain proteome. *Nat Neurosci* 2015, *18*, 1819-1831.
[204] Scifo, E., Calza, G., Fuhrmann, M., Soliymani, R.*, et al.*, Recent advances in applying mass spectrometry and systems biology to determine brain dynamics. *Expert Rev Proteomics* 2017, *14*, 545-559.
[205] Lachen-Montes, M., Fernandez-Irigoyen, J., Santamaria, E., Deconstructing the molecular architecture of olfactory areas using proteomics. *Proteomics Clin Appl* 2016, *10*, 1178-1190.
[206] Veenstra, T. D., Global and targeted quantitative proteomics for biomarker discovery. *J Chromatogr B Analyt Technol Biomed Life Sci* 2007, *847*, 3-11.

[207] Musunuri, S., Wetterhall, M., Ingelsson, M., Lannfelt, L*., et al.*, Quantification of the brain proteome in Alzheimer's disease using multiplexed mass spectrometry. *J Proteome Res* 2014, *13*, 2056-2068.
[208] Sweet, R. A., MacDonald, M. L., Kirkwood, C. M., Ding, Y*., et al.*, Apolipoprotein E*4 (APOE*4) Genotype Is Associated with Altered Levels of Glutamate Signaling Proteins and Synaptic Coexpression Networks in the Prefrontal Cortex in Mild to Moderate Alzheimer Disease. *Mol Cell Proteomics* 2016, *15*, 2252-2262.
[209] Drummond, E. S., Nayak, S., Ueberheide, B., Wisniewski, T., Proteomic analysis of neurons microdissected from formalin-fixed, paraffin-embedded Alzheimer's disease brain tissue. *Sci Rep* 2015, *5*, 15456.
[210] Hondius, D. C., van Nierop, P., Li, K. W., Hoozemans, J. J*., et al.*, Profiling the human hippocampal proteome at all pathologic stages of Alzheimer's disease. *Alzheimers Dement* 2016, *12*, 654-668.
[211] Lace, G., Savva, G. M., Forster, G., de Silva, R*., et al.*, Hippocampal tau pathology is related to neuroanatomical connections: an ageing population-based study. *Brain* 2009, *132*, 1324-1334.
[212] Ho Kim, J., Franck, J., Kang, T., Heinsen, H*., et al.*, Proteome-wide characterization of signalling interactions in the hippocampal CA4/DG subfield of patients with Alzheimer's disease. *Sci Rep* 2015, *5*, 11138.
[213] Ayyadevara, S., Balasubramaniam, M., Parcon, P. A., Barger, S. W*., et al.*, Proteins that mediate protein aggregation and cytotoxicity distinguish Alzheimer's hippocampus from normal controls. *Aging Cell* 2016, *15*, 924-939.
[214] Blennow, K., Hampel, H., Weiner, M., Zetterberg, H., Cerebrospinal fluid and plasma biomarkers in Alzheimer disease. *Nat Rev Neurol* 2010, *6*, 131-144.
[215] Ringman, J. M., Schulman, H., Becker, C., Jones, T*., et al.*, Proteomic Changes in Cerebrospinal Fluid of Presymptomatic and Affected Persons Carrying Familial Alzheimer Disease Mutations. *Archives of neurology* 2012, *69*, 96-104.
[216] Hendrickson, R. C., Lee, A. Y., Song, Q., Liaw, A*., et al.*, High Resolution Discovery Proteomics Reveals Candidate Disease Progression Markers of Alzheimer's Disease in Human Cerebrospinal Fluid. *PLoS One* 2015, *10*, e0135365.
[217] Paterson, R. W., Heywood, W. E., Heslegrave, A. J., Magdalinou, N. K*., et al.*, A targeted proteomic multiplex CSF assay identifies increased malate dehydrogenase and other neurodegenerative biomarkers in individuals with Alzheimer's disease pathology. *Transl Psychiatry* 2016, *6*, e952.
[218] Wang, J., Cunningham, R., Zetterberg, H., Asthana, S*., et al.*, Label-free quantitative comparison of cerebrospinal fluid glycoproteins and endogenous peptides in subjects with Alzheimer's disease, mild cognitive impairment, and healthy individuals. *Proteomics Clin Appl* 2016, *10*, 1225-1241.
[219] Skillback, T., Mattsson, N., Hansson, K., Mirgorodskaya, E*., et al.*, A novel quantification-driven proteomic strategy identifies an endogenous peptide of pleiotrophin as a new biomarker of Alzheimer's disease. *Sci Rep* 2017, *7*, 13333.
[220] Dodds, D. C., Omeis, I. A., Cushman, S. J., Helms, J. A., Perin, M. S., Neuronal pentraxin receptor, a novel putative integral membrane pentraxin that interacts with neuronal pentraxin 1 and 2 and taipoxin-associated calcium-binding protein 49. *J Biol Chem* 1997, *272*, 21488-21494.
[221] Levi, A., Ferri, G. L., Watson, E., Possenti, R., Salton, S. R., Processing, distribution, and function of VGF, a neuronal and endocrine peptide precursor. *Cell Mol Neurobiol* 2004, *24*, 517-533.
[222] Robinson, P. A., Understanding the molecular basis of Parkinson's disease, identification of biomarkers and routes to therapy. *Expert Rev Proteomics* 2010, *7*, 565-578.
[223] Basso, M., Giraudo, S., Corpillo, D., Bergamasco, B*., et al.*, Proteome analysis of human substantia nigra in Parkinson's disease. *Proteomics* 2004, *4*, 3943-3952.

[224] Werner, C. J., Heyny-von Haussen, R., Mall, G., Wolf, S., Proteome analysis of human substantia nigra in Parkinson's disease. *Proteome Sci* 2008, *6*, 8.
[225] Shi, M., Jin, J., Wang, Y., Beyer, R. P.*, et al.*, Mortalin: a protein associated with progression of Parkinson disease? *J Neuropathol Exp Neurol* 2008, *67*, 117-124.
[226] Licker, V., Cote, M., Lobrinus, J. A., Rodrigo, N.*, et al.*, Proteomic profiling of the substantia nigra demonstrates CNDP2 overexpression in Parkinson's disease. *J Proteomics* 2012, *75*, 4656-4667.
[227] Larsen, S. B., Hanss, Z., Kruger, R., The genetic architecture of mitochondrial dysfunction in Parkinson's disease. *Cell Tissue Res* 2018.
[228] Kim, H., Kang, H., Lee, Y., Park, C. H.*, et al.*, Identification of transketolase as a target of PARIS in substantia nigra. *Biochem Biophys Res Commun* 2017, *493*, 1050-1056.
[229] Trezzi, J. P., Galozzi, S., Jaeger, C., Barkovits, K.*, et al.*, Distinct metabolomic signature in cerebrospinal fluid in early parkinson's disease. *Mov Disord* 2017, *32*, 1401-1408.
[230] Xing, L., Wang, D., Wang, L., Lan, W., Pan, S., Differential proteomics analysis of mononuclear cells in cerebrospinal fluid of Parkinson's disease. *Int J Clin Exp Pathol* 2015, *8*, 15462-15466.
[231] Yang, L., Stewart, T., Shi, M., Pottiez, G.*, et al.*, An alpha-synuclein MRM assay with diagnostic potential for Parkinson's disease and monitoring disease progression. *Proteomics Clin Appl* 2017, *11*.
[232] Agresta, A. M., De Palma, A., Bardoni, A., Salvini, R.*, et al.*, Proteomics as an innovative tool to investigate frontotemporal disorders. *Proteomics Clin Appl* 2016, *10*, 457-469.
[233] Gozal, Y. M., Dammer, E. B., Duong, D. M., Cheng, D.*, et al.*, Proteomic analysis of hippocampal dentate granule cells in frontotemporal lobar degeneration: application of laser capture technology. *Front Neurol* 2011, *2*, 24.
[234] Martins-de-Souza, D., Guest, P. C., Mann, D. M., Roeber, S.*, et al.*, Proteomic analysis identifies dysfunction in cellular transport, energy, and protein metabolism in different brain regions of atypical frontotemporal lobar degeneration. *J Proteome Res* 2012, *11*, 2533-2543.
[235] Herskowitz, J. H., Seyfried, N. T., Duong, D. M., Xia, Q.*, et al.*, Phosphoproteomic analysis reveals site-specific changes in GFAP and NDRG2 phosphorylation in frontotemporal lobar degeneration. *J Proteome Res* 2010, *9*, 6368-6379.
[236] Davidsson, P., Sjogren, M., Andreasen, N., Lindbjer, M.*, et al.*, Studies of the pathophysiological mechanisms in frontotemporal dementia by proteome analysis of CSF proteins. *Brain Res Mol Brain Res* 2002, *109*, 128-133.
[237] Hanchate, N. K., Kondoh, K., Lu, Z., Kuang, D.*, et al.*, Single-cell transcriptomics reveals receptor transformations during olfactory neurogenesis. *Science* 2015, *350*, 1251-1255.
[238] Shao, X., Lakhina, V., Dang, P., Cheng, R. P.*, et al.*, Olfactory sensory axons target specific protoglomeruli in the olfactory bulb of zebrafish. *Neural Dev* 2017, *12*, 18.
[239] Olender, T., Keydar, I., Pinto, J. M., Tatarskyy, P.*, et al.*, The human olfactory transcriptome. *BMC Genomics* 2016, *17*, 619.
[240] Kawasawa, Y. I., Salzberg, A. C., Li, M., Sestan, N.*, et al.*, RNA-seq analysis of developing olfactory bulb projection neurons. *Mol Cell Neurosci* 2016, *74*, 78-86.
[241] Li, H., Horns, F., Wu, B., Xie, Q.*, et al.*, Classifying Drosophila Olfactory Projection Neuron Subtypes by Single-Cell RNA Sequencing. *Cell* 2017, *171*, 1206-1220.e1222.
[242] Wang, M., Liu, W., Jiao, J., Li, J.*, et al.*, Expression Profiling of mRNAs and Long Non-Coding RNAs in Aged Mouse Olfactory Bulb. *Sci Rep* 2017, *7*, 2079.
[243] Simoes, T., Charro, N., Blonder, J., Faria, D.*, et al.*, Molecular profiling of the human nasal epithelium: A proteomics approach. *J Proteomics* 2011, *75*, 56-69.
[244] Casado, B., Pannell, L. K., Iadarola, P., Baraniuk, J. N., Identification of human nasal mucous proteins using proteomics. *Proteomics* 2005, *5*, 2949-2959.
[245] Dammalli, M., Dey, G., Madugundu, A. K., Kumar, M.*, et al.*, Proteomic Analysis of the Human Olfactory Bulb. *Omics* 2017, *21*, 440-453.

[246] Dammalli, M., Dey, G., Kumar, M., Madugundu, A. K.*, et al.*, Proteomics of the Human Olfactory Tract. *Omics* 2018, *22*, 77-87.

HYPOTHESIS AND OBJECTIVES

Olfactory dysfunction is a common early feature of neurodegenerative diseases (NDs) occurring in particular of Alzheimer's disease (AD), Lewy body diseases (LBD), and Parkinson's disease (PD), and to a lesser extent in other NDs such as frontotemporal dementias (FTD). These deficits have been related to the deposition of pathological proteins, such as Aβ, α-synuclein, hyperphosphorylated tau protein, and neurofilament protein in the olfactory bulb/tract (OB) as well as in the olfactory epithelium (OE), inducing a complex cascade of molecular processes leading to cell death. Recent studies of olfactory dysfunction have considered its potential as an early biomarker for the diagnosis of neurodegenerative disorders and their disease progression but the molecular disturbances that occur specifically in the OB in different tauopathies and synucleopathies are yet to be determined. The main hypothesis of this project postulates that there is a distinctive profile in the transcriptome and proteome level in the OB during the neurodegenerative process that may be common or dissimilar between different NDs and neurological intact subjects and may provide clues to understand hitherto unknown triggering mechanisms.

To achieve this aim the next **objectives** are proposed:

1. Molecular characterization of the OB proteostasis in neurological disorders with high olfactory deficits
   - 1.1. High-throughput analysis in AD murine models: APP/PS1 and Tg2576 mice
   - 1.2. High-throughput and stage-dependent analysis of the OB from AD and PD subjects:
     - 1.2.1 Initial AD (Braak I-II); Intermediate AD (Braak III-IV); Advanced AD (Braak V-VI)
     - 1.2.2 PD (LBD limbic stage); PD (LBD early-neocortical stage); PD (LBD neocortial stage)
   - 1.3. Stage-dependent pathway analysis and proteome-interaction networks
   - 1.4. Kinase activation dynamics

2. Molecular characterization of the OB proteostasis in neurological disorders with mild olfactory deficits
    2.1. High-throughput analysis of the OB from subjects with frontotemporal dementia (FTD)
        2.1.1 Progressive supranuclear palsy (PSP)
        2.1.2 Frontotemporal lobar degeneration TDP-43 proteinopathy (FTLD-TDP43)
    2.2. Pathway analysis and intersection with Tau and TDP43 interactomes
    2.3. Kinase activation dynamics
3. Identification of common deregulated protein mediators across tauopathies and synucleinopathies
4. Monitoring of potential secretable biomarkers derived from olfactory proteomic datasets

CHAPTER 1

An early dysregulation of FAK and MEK/ERK signaling pathways precedes the β-amyloid deposition in the olfactory bulb of APP/PS1 mouse Model of Alzheimer's Disease

Mercedes Lachén-Montes[1], Andrea González-Morales[1], Xabier Martínez de Morentin[2], Estela Pérez-Valderrama[2], Karina Ausín[2], María Victoria Zelaya[1], Antonio Serna[3], Ester Aso[4], Isidro Ferrer[4], Joaquín Fernández-Irigoyen[1,2], Enrique Santamaría[1,2]

[1] *Clinical Neuroproteomics Group, Navarrabiomed Biomedical Research Center, Instituto de Investigación Sanitaria de Navarra (IdiSNA), Pamplona, Spain*

[2] *Proteomics Unit, Navarrabiomed Biomedical Research Center, Proteored-ISCIII, Instituto de investigación Sanitaria de Navarra (IdiSNA), Pamplona, Spain*

[3] *Sciex. Valgrande 8, Edificio Thanworth II, Alcobendas, Madrid, Spain*

[4] *Institut de Neuropatologia, IDIBELL-Hospital Universitari de Bellvitge, Universitat de Barcelona, L'Hospitalet de Llobregat, Spain, CIBERNED (Centro de Investigación Biomédica en Red de Enfermedades Neurodegenerativas), Spain.*

Abstract

Olfactory dysfunction is an early event of Alzheimer's disease (AD). However, the mechanisms associated to AD neurodegeneration in olfactory areas are unknown. Here we used double-transgenic amyloid precursor protein/presenilin 1 (APPswe/PS1dE9) mice and label-free quantitative proteomics to analyze early pathological effects on the olfactory bulb (OB) during AD progression. Prior to β-amyloid plaque formation, 9 modulated proteins were detected on 3-month-old APP/PS1 mice while 16 differential expressed proteins were detected at 6 months, when β-amyloid plaques appear, indicating a moderate imbalance in cytoskeletal rearrangement, and synaptic plasticity in APP/PS1 OBs. Moreover, β-amyloid induced an inactivation of focal adhesion kinase (FAK) together with a transient activation of MEK1/2, leading to inactivation of ERK1/2 in 6-months APP/PS1 OBs. In contrast, the analysis of human OBs revealed a late activation of FAK in advanced AD stages, whereas ERK1/2 activation was enhanced across AD staging respect to controls. This survival potential was accompanied by the inhibition of the proapototic factor BAD in the OB across AD phenotypes. Our data contribute to a better understanding of the early molecular mechanisms that are modulated in AD neurodegeneration, highlighting significant differences in the regulation of survival pathways between APP/PS1 mice and sporadic human AD.

Introduction

Alzheimer's disease (AD) is the most common form of dementia in the elderly, being a disorder of unknown and variable aetiology. Two major forms of AD have been recognized, a familial (genetic) form, with early-onset of dementia comprising an incidence of 5% in people younger than 60 years and an sporadic late-onset variety affecting most AD patients [1]. It is generally thought that one of the driving force of AD pathology is the formation of toxic Aβ peptides cleaved from amyloid precursor protein (APP) followed by a cascade of secondary pathologies eventually leading to synaptic loss and neuronal death. APP is proteolyzed in a sequential manner by the enzymatic actions of beta and gamma secretases, where the catalytic core of presenilin 1 (PS1) plays a pivotal role [2]. Mutations in the *PS1* gene are the major cause of familial AD, leading to an increased production of the highly neurotoxic 42 amino acid variant of the Aβ peptide [2].

Several transgenic mice expressing human APP and PS1mutations have been created in order to understand the development of AD [3]. Double-transgenic APP/PS1 mice express a chimeric mouse/human APP (Mo/HuAPP695swe) and a mutant human PS1-dE9 [4]. Both AD-associated mutations are under control of the mouse prion protein promoter directing both mutated proteins mainly to the CNS neurons, and result in age-dependent amyloid plaque depositions in mouse brain. The APPswe-mutated APP is a favorable substrate for β-secretase, whereas the PS1dE9 mutation alters β-secretase cleavage, thereby promoting overproduction of Aβ42 [4]. This mouse model is extensively employed in AD research given that it reproduces well some of the neuropathological and cognitive deficits observed in human AD, with a phenotype characterized by deposition of Aβ plaques, glial activation, and deficits in cognitive functions [5]. APP/PS1 mice develop a multisystemic disease of the central nervous system [4, 6, 7] accompanied by progression of memory and cognitive deficits [8]. At 3 months of age, APP/PS1 mice develop few neocortical amyloid plaques that increase in number and distribution across

AD stages through entorhinal cortex, amygdala, and hippocampus [9]. At this stage, a robust up-regulation of protein components of the extracellular matrix occurs in hippocampal synaptosomes in parallel of an impairment in hippocampal long-term potentiation [10]. Deposition of Aβ plaques is accompanied by a redox imbalance leading to alterations in the ubiquitin-proteasome system and mitochondrial homeostasis [9]. Moreover, global alterations in specific biological functions such as molecular transport, lipid metabolism, autophagy, and oxidative stress have been partially characterized in the cerebral cortex of 5-month-old APP/PS1 mice [11]. Additionally, impaired memory and learning performance appear from the age of 6 months onwards in APP/PS1 mice [9]. Interestingly, part of these symptoms may be restored by direct injection into the hippocampus of the extracellular matrix inactivating enzyme chondroitinase ABC, indicating the pivotal role of extracellular matrix in memory loss [10]. Between 6 and 12 months of age, an acute de-regulation of cytokines and mediators of immune response also appear in cortical areas of APP/PS1 mice respect to WT littermates [12].

Some studies suggest that olfactory impairment is an early event of AD, preceding the appearance of symptoms such as memory loss, and dementia [13]. A reduction in olfactory performance, OB atrophy, olfactory pathological changes, and OB molecular alterations have been detected in AD subjects with respect to control individuals [14-17]. Reduced volumes of the OB and piriform cortex have been also detected in the APP/PS1 transgenic mice [18]. Specifically, APP/PS1 mice present a reduction in the area of the OB granule cell layer as revealed by morphometric measurements [19]. Olfactory recognition test has pointed out that APP/PS1 model shows a deficit in retention of familiar odors [19]. At molecular level, APP/PS1 mice have showed an imbalance in the OB metabolic homeostasis, mainly due to the alteration in normal levels of a plethora of metabolites and lipids such as amino acids, acylcarnitines, phospholipids, and fatty acids [20, 21].

We consider that deciphering the early proteome-wide alterations that occurs in the OB derived from APP/PS1 mice might reveal novel stage-dependent molecular alterations during the AD progression. In this study, we have used mass-spectrometry based quantitative proteomics in order to increase our knowledge about the early pathophysiological mechanisms that are disturbed at the level of OB prior to Aβ burden. For that, a time-dependent proteome expression profiling was performed at 3 and 6 months of age, revealing a slight and progressive proteome modulation in the OB. Although apoptosis was not induced, the activation status of Fak/Src and Mek/Erk signaling pathways was impaired not only in the OB of APP/PS1 mice but also in OB tissue derived from AD subjects, indicating an early imbalance in survival routes at the level of OB during AD progression. Our data reflect the progressive effect of APP overproduction and Aβ accumulation on the OB proteome, contributing to the understanding of the abnormal olfactory-driven behaviors and olfactory sensory impairment that appear during the AD neurodegeneration in the OB.

Materials and methods

Materials - The following reagents and materials were used: anti-caspase 9, anti-cleaved-caspase3 (Asp175), anti-Bcl2, anti-Bcl-xL, anti-Phb1, anti-Phb2, anti-pAkt (Ser473), anti-Akt, anti-pMEK1/2 (Ser217/221), anti-MEK1/2, anti-pERK1/2 (Thr202/Tyr204), anti-ERK1/2, anti-pFAK (Tyr576/577), anti-FAK, and anti-pBAD (Ser112) were purchased from Cell signaling. Anti-GAPDH (Ref.CB1001) were obtained from Merck Millipore. Electrophoresis reagents were purchased from Biorad and trypsin from Promega.

Animals- The generation of mice expressing a chimeric mouse/human APP (Mo/HuAPPswe), and a human exon-9-deleted variant of PS1 (PS1-dE9) has been previously described [4]. In our colony, APP/PS1 transgenic mice developed a few cortical Aβ plaques at the age of three months and began to have deficits in learning and memory at the age of 6 months [9]. The animals were kept under controlled temperature, humidity and light conditions with food and water provided ad libitum. Animal care procedures were conducted in accordance with the European Community Council Directive (2010/63/EU) and approved by the local ethics committee. Twenty animals, divided into four groups, were used for the proteomic study, with at least 5 wild-type and 5 APP/PS1 transgenic mice per stage (3 and 6-month-old). For histological analysis, three different OB sections from 5 wild-type and 5 APP/PS1 transgenic mice per stage (3 and 6-month-old) were used.

β-amyloid Immunohistochemistry- Fixed tissue samples derived from murine OBs were embedded in paraffin, and coronal sections, 4 µm thick, were cut with a microtome. De-waxed sections were incubated with 98% formic acid (3 min) and then treated with citrate buffer (20 min) to enhance antigenicity. Then endogenous peroxidases were blocked by incubation in 10% methanol-1% H2O2 solution (15 min). Sections were blocked with 3% normal horse serum solution and then incubated at 4ºC overnight with the primary antibody against total Aβ (clone 6F/3D 1:50, Dako, Glostrup, Denmark). Sections were subsequently rinsed and incubated with

biotinylated secondary antibody (Dako). Peroxidase reaction was visualized with diaminobenzidine and H2O2. Sections were lightly counterstained with hematoxylin. After staining, the sections were dehydrated and cover-slipped for observation under a Nikon Eclipse E800 microscope (Nikon Imaging Inc., Tokyo, Japan). The OB total Aβ burden was calculated as the percentage of the area of amyloid deposition in plaques with respect to the total area in pictures taken from 3 different sections of the each animal brain. Aβ quantification was calculated using the Analysis tool of the Adobe® Photoshop® CS4 software (Adobe Systems Inc., San Jose, CA, USA). Five APP/PS1 animals per age (3 and 6 months) were analyzed.

Human samples- According to the Spanish Law 14/2007 of Biomedical Research inform written consent form of the Neurological Tissue Bank of Navarra Health Service was obtained for research purposes from relatives of patients included in this study. Nine AD cases were distributed into different groups according to specific consensus diagnostic criteria [22-24]: low, intermediate, and high neuropathological changes (n = 3/group) (Supplementary Table 1). Three cases from elderly subjects with no history or histological findings of any neurological disease were used as a control group. All human brains considered in this study had a post-mortem interval (PMI) lower than 10 hours (Supplementary Table 1). One hemisphere (usually the left) with the corresponding OB was fixed in 10% formalin for morphological studies. After fixation (21-25 days), representative brain areas from cortical and subcortical areas, brainstem, cerebellum and spinal cord were taken and embedded in paraffin in order to make a neuropathological diagnosis. Neuropathological assessment was performed according to standardized neuropathological scoring/grading systems, including Thal phases of β-amyloid deposition, Braak staging of neurofibrillary lesions, Consortium to Established a Registry for Alzheimer's Disease, National Institute on Aging-Alzheimer's Association (NIA-AA) guidelines, and primary age-related tauopathy (PART) criteria [22-26]. β-Amyloid and phospho-Tau immunostaining were performed in the OB of AD and control cases. The OBs were embedded in paraffin and 4-µm-thick sagital sections were stained with hematoxylin-eosin and 3-µm-thick

sagital sections were processed for immunohistochemical analysis. Formalin-fixed sections (3-5 µm-thick) were mounted on slides and deparaffinized. After conducting a routine antigen retrieval protocol, tissue sections were immunohistochemically labelled overnight with a mouse monoclonal anti-human PHF-TAU antibody (clone AT-8, Innogenetics) and a mouse monoclonal (S6F/3D) anti β-amyloid antibody (Leica). The reaction product was visualized using an automated slide immunostainer (Leica Bond Max) with Bond Polymer Refine Detection (Leica Biosystems Newcastle Ltd). Analysis of OB for specific protein deposits aggregates was carried out in a light microscope (Olympus BX51) blinded to pathological diagnosis. A semiquantitative assessment was performed according to Kovacs T et al. [27]. We consider compact deposit with central core as mature plaques and granular or fibrillar deposit as diffuse plaques. Moreover, Aβ immunopositivity was scored on a 4-tiered scale as: (-) negative, (+) 1-2 isolated Aβ depositions, (++) 3-4 Aβ depositions, and (+++) > 4 Aβ depositions (Supplementary Table 1). We also described different patterns of deposits and its intensity for Phospho-Tau immunostaining: neurofibrillary tangles, neuropil threads and neuritic plaques (n.d: not determined; +: low; ++: intermediate; +++ high) (Supplementary Table 1). All preparations were examined by two independent pathologists.

Sample preparation for proteomic analysis – Murine OB specimens were homogenized in lysis buffer containing 7 M urea, 2 M thiourea, 4% (v/v) CHAPS, 50 mM DTT. The homogenates were spinned down at 100.000 x g for 1 h at 15ºC. Protein concentration was measured in the supernatants with the Bradford assay kit (Bio-rad).

Label free LC-MS/MS – Protein extracts were precipitated with methanol/choloroform, and pellets dissolved in 6M Urea, Tris 100mM pH 7.8. Protein quantitation was performed with the Bradford assay kit (Bio-Rad). Protein enzymatic cleavage (10ug) was carried out with trypsin (Promega; 1:20, w/w) at 37°C for 16 h as previously described [28]. Peptides mixtures were separated by reverse phase chromatography using an Eksigent nanoLC ultra 2D pump fitted with

a 75 µm ID column (Eksigent 0.075 x 250). Samples were first loaded for desalting and concentration into a 0.5 cm length 100 µm ID precolumn packed with the same chemistry as the separating column. Mobile phases were 100% water 0.1% formic acid (FA) (buffer A) and 100% Acetonitrile 0.1% FA (buffer B). Column gradient was developed in a 240 min two step gradient from 5% B to 25% B in 210 min and 25%B to 40% B in 30 min. Column was equilibrated in 95% B for 9 min and 5% B for 14 min. During all process, precolumn was in line with column and flow maintained all along the gradient at 300 nl/min. Eluting peptides from the column were analyzed using an Sciex 5600 Triple-TOF system. Information data acquisition was acquired upon a survey scan performed in a mass range from 350 m/z up to 1250 m/z in a scan time of 250 ms. Top 35 peaks were selected for fragmentation. Minimum accumulation time for MS/MS was set to 100 ms giving a total cycle time of 3.8 s. Product ions were scanned in a mass range from 230 m/z up to 1500 m/z and excluded for further fragmentation during 15 s.

Peptide Identification and Quantification – MS/MS data acquisition was performed using Analyst 1.5.2 (AB Sciex) and spectra files were processed through Protein Pilot ™ Software (v.4.0.8085-ABSciex) using Paragon™ Algorithm (v.4.0.0.0) [29] for database search, Progroup™ for data grouping, and searched against the concatenated target-decoy UniProt proteome reference mouse database (Proteome ID: UP000000589; 50691 proteins, December 2015). False discovery rate was performed using a non lineal fitting method [30] and displayed results were those reporting a 1% Global false discovery rate or better. The peptide quantification was performed using the Progenesis LC–MS software (ver. 2.0.5556.29015, Nonlinear Dynamics). Using the accurate mass measurements from full survey scans in the TOF detector and the observed retention times, runs were aligned to compensate for between-run variations in our nanoLC separation system. To this end, all runs were aligned to a reference run automatically chosen by the software, and a master list of features considering m/z values and retention times was generated. The quality of these alignments was manually supervised with the help of quality scores provided by the software. The peptide identifications were exported from Protein Pilot

and imported in Progenesis LC– MS where they were matched to the respective features. Output data files were managed using R scripts for subsequent statistical analyses and representation. Proteins identified by site (identification based only on a modification), reverse proteins (identified by decoy database) and potential contaminants were filtered out. Proteins quantified with at least one unique peptide, an ANOVA *p*-value lower than 0.05, and an absolute fold changes of <0.77 (down-regulation) or >1.3 (up-regulation) in linear scale were considered to be significantly differentially expressed. MS raw data and search results files have been deposited to the ProteomeXchange Consortium (http://proteomecentral.proteomexchange.org) via the PRIDE partner repository [31] with the dataset identifiers PXD003683.

Immunoblotting analysis - Equal amounts of protein (10 µg) were resolved in 12.5% SDS-PAGE gels. OB proteins derived from mice and humans were electrophoretically transferred onto nitrocellulose membranes for 45 min at 120 V. Membranes were probed with primary antibodies at 1:1000 dilution in 5% nonfat milk or BSA. After incubation with the appropriate horseradish peroxidase-conjugated secondary antibody (1:5000), the immunoreactivity was visualized by enhanced chemiluminiscence (Perkin Elmer). Equal loading of the gels was assessed by Ponceau staining and hybridization with a GAPDH specific antibody (Calbiochem).

Results and discussion

Although it is widely believed that OB perturbations are responsible for olfactory dysfunction in NDs [32], few studies have examined this area using high throughput molecular technologies [14]. Different neuroproteomic studies have been attempted to discover novel protein mediators associated with AD pathogenesis in brain areas differentially affected by the disease across AD models [10, 11, 33-40]. However, to our knowledge, this is the first study to characterize early AD-associated molecular changes in the OB derived from an AD model using MS-based quantitative proteomics.

Proteome changes in the OB of APP/PS1 mice

APP/PS1 transgenic mice suffer from cognitive impairment accompanied by β-amyloid plaques that increase with disease progression [9]. At 3 months of age, APP/PS1 mice showed β-amyloid mainly located in the walls of the blood vessels at the level of the OB (figure 1A, and C). However, a small portion of β-amyloid plaques are observed in the OB of APP/PS1 mice at 6 months of age (figure 1B, and D), when memory decline and impaired learning are manifested [9]. The amyloid burden was significantly higher in APP/PS1 mice aged 6 months than in animals aged 3 months ($p<0.001$) (figure 1E). No amyloid deposition was observed in WT mice at both time points (data not shown). This temporal profile is very similar to the β-amyloid deposition observed in the cortex of APP/PS1 mice [9]. To determine olfactory protein expression changes induced by β-amyloid, a label-free MS-based approach was performed on OB tissue derived from 3 and 6-month-old APP/PS1 mice and WT littermate controls in order to reveal novel information about the OB site-specific proteomic signature at early stages of AD pathology. 1105 and 1125 proteins were quantified at 3 and 6-months respectively (Figure 1F and Supplementary tables 2-5).

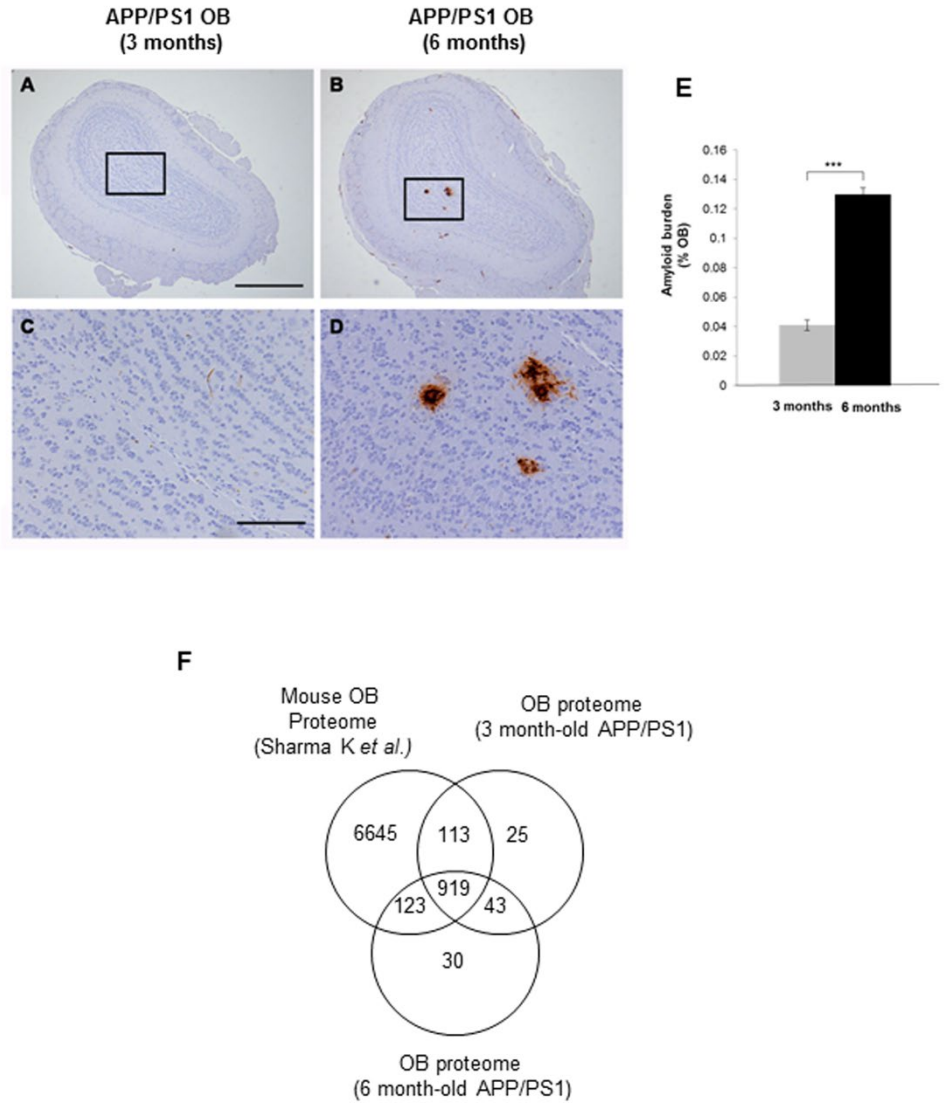

Figure 1. β-amyloid increase in number with disease progression. Representative images of β-amyloid plaques in the OB of APP/PS1 mice aged 3 (A,C), and 6 months (B,D). Scale bars: 500 µm (upper) and 100 µm (lower) (left). Quantitation of β-amyloid burden in the OB of APP/PS1 mice aged 3, and 6 months (E). Data are expressed as the mean values ± standard error of the mean (SEM) of five animal per age (3 sections per case). *** $P < 0.001$ (Student's t; 3 months vs 6 months). F) Intersection of proteins derived from proteomic expression profiling of mouse OB [41] and our study.

Among 1253 quantified proteins, 1155 gene-products (92%) has been previously identified in proteomic characterizations of the mouse OB [41], being 962 proteins (77%) longitudinally

quantified in APP/PS1 OB (Figure 1F). In addition, differential analysis revealed 25 de-regulated proteins in APP/PS1 OBs with respect to WT OBs (Figure 2). Among the proteome quantified, 8 proteins were up-regulated and 1 was down-regulated in 3-month-old APP/PS1 OBs (Figure 2A, Table 1), when olfactory deficits are manifested [19] and prior to the appearance of β-amyloid plaques (figure 1C). On the other hand, 11 proteins were over-expressed and 5 were under-expressed in 6-month-old APP/PS1 mice (Figure 2B, Table 1), when impaired memory and learning performance are manifested [9]. The up-regulation of our intrinsic positive control (Amyloid beta A4 protein) was the unique differential protein detected in both time points. Differentially expressed proteins in 3-month-old APP/PS1 OB were unchanged at the age of 6 months, while 12 differential proteins detected at the age of 6 months, were unchanged in 3-month-old APP/PS1 OB. However, it was not possible to obtain robust quantitative information for 4 differential proteins (*Snd1*, *Try10*, *Gdap1*, and *Fam214a*) in 3-month-old APP/PS1 OB samples. Data mining of MS-generated proteomic data suggested a moderate imbalance in cytoskeletal rearrangement, mitochondrial homeostasis, and synaptic plasticity in the OB of APP/PS1 mice. We have investigated whether our differential proteomic fingerprint identified in the OB of APP/PS1 mice has been partially reflected in previous transcriptomic and proteomic studies performed in different brain structures across AD models [33-40, 42-46]. According to our integrative meta-analysis (Supplementary table 6), most of the differential OB proteins has not been previously reported as differentially expressed genes/proteins in animal models of AD.

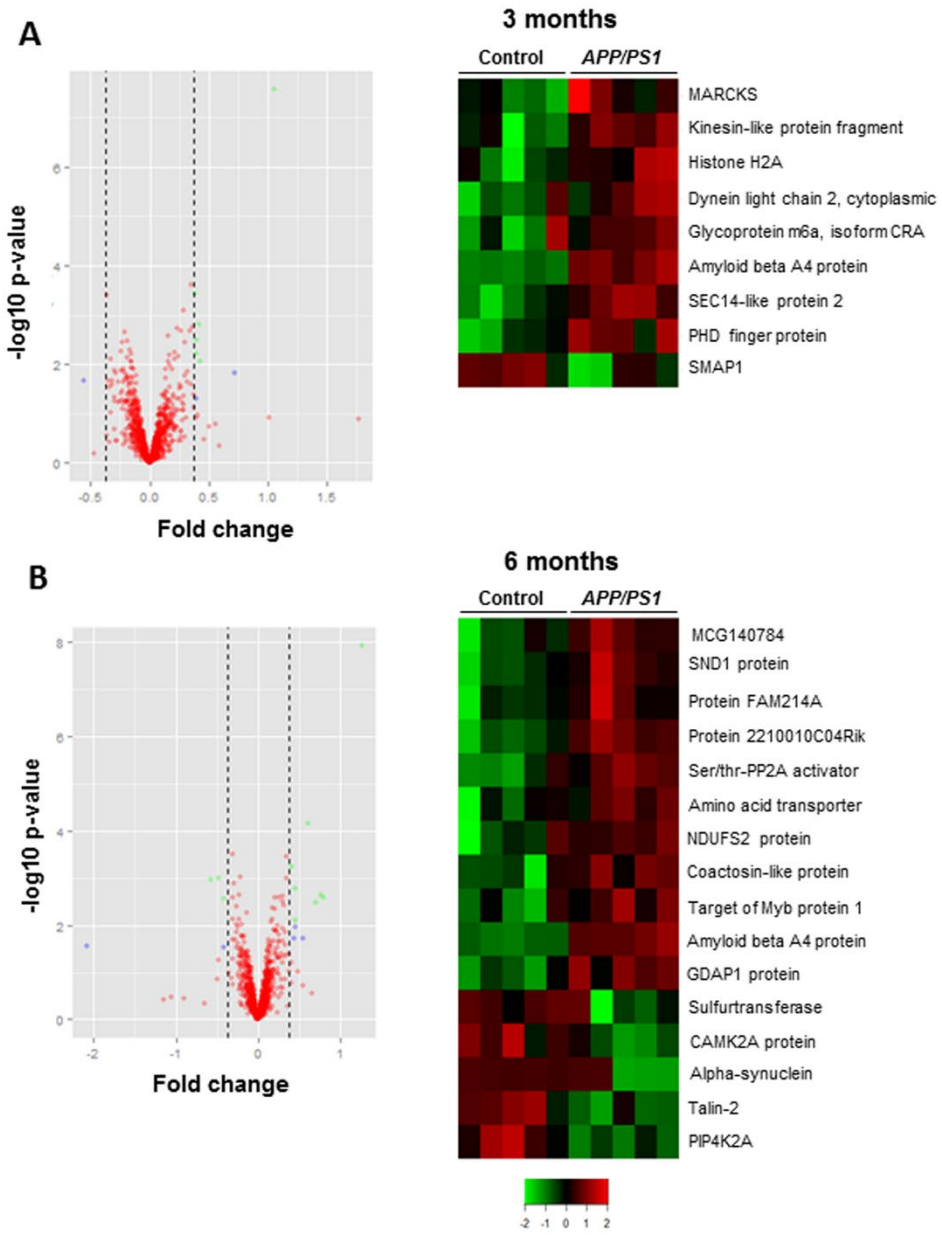

Figure 2. Differentially expressed proteins in the OB from APP/PS1 mice at 3 and 6 months of age. A) Volcano plots representing the fold-change of identified proteins with associated P values from the pair-wise quantitative comparisons of wild type OB vs APP/PS1 OB (3 months, left plot). Heat map representing the degree of change for the differentially expressed proteins at 3 months ($P < 0.05$) between control and APP/PS1 OBs (5 independent mice per group) (right panel). B) Volcano plots representing the fold-change of identified proteins with associated P values from the pair-wise quantitative comparisons of wild type OB vs APP/PS1 OB (6 months, left plot). Heat map representing the degree of change for the differentially expressed proteins at 6 months ($P < 0.05$) between control and APP/PS1 OBs (5 independent mice per group) (right

panel). Legend (bottom) indicates color-coded fold-change scale. Red and green, up- and down-regulated proteins, respectively.

Protein Names	Accession	Gene name	Unique peptides	score	Fold Change	P-value
Up-regulated olfactory proteins in 3-month-old APP/PS1						
Amyloid beta A4 protein	P12023	App	5	48	2.09	0.0000
SEC14-like protein 2	Q99J08	Sec14l2	2	18	1.31	0.0004
Kinesin-like protein (Fragment)	F8VQ42	Kif2a	1	9	1.34	0.0016
PHD finger protein 24	Q80TL4	Phf24	2	11	1.32	0.0031
Histone H2A	Q149V4	Hist2h2ac	2	124	1.31	0.0060
Myristoylated alanine-rich C-kinase substrate (MARCKS)	P26645	Marcks	13	269	1.34	0.0087
Dynein light chain 2, cytoplasmic	Q9D0M5	Dynll2	1	57	1.65	0.0154
Glycoprotein m6a, isoform CRA_b	Q542P2	Gpm6a	4	80	1.32	0.0489
Down-regulated olfactory proteins in 3-month-old APP/PS1						
Stromal membrane-associated protein 1 (SMAP1)	Q91VZ6	Smap1	2	41	0.68	0.0214
Up-regulated olfactory proteins in 6-month-old APP/PS1						
Amyloid beta A4 protein	P12023	App	6	65	2.40	0.0000
Protein 2210010C04Rik	Q9CPN9	2210010C04Rik	1	10	1.53	0.0001
Serine/threonine-protein phosphatase 2A activator	P58389	Ppp2r4	2	50	1.37	0.0017
Staphylococcal nuclease domain-containing protein 1 (SND1)	Q78PY7	Snd1	1	14	1.70	0.0023
MCG140784	Q792Z1	Try10	1	12	1.73	0.0025
Coactosin-like protein	Q544F6	Cotl1	3	60	1.62	0.0033
Ganglioside-induced differentiation-associated protein 1 (GDAP1)	O88741	Gdap1	2	21	1.32	0.0006
Target of Myb protein 1	O88746	Tom1	2	45	1.37	0.0080
Protein FAM214A	Q69ZK7	Fam214a	1	4	1.36	0.0107
Amino acid transporter	Q5SSP3	Slc1a4	2	27	1.35	0.0193
NADH dehydrogenase [ubiquinone] iron-sulfur protein 2, mit.	Q91WD5	Ndufs2	2	165	1.47	0.0195
Down-regulated olfactory proteins in 6-month-old APP/PS1						
Alpha-synuclein	O55042	Snca	6	217	0.24	0.0272
Sulfurtransferase	Q3UW66	Mpst	2	47	0.75	0.0294
Phosphatidylinositol 5-phosphate 4-kinase type-2 alpha (PIP4K2A)	Q544E3	Pip4k2a	2	45	0.72	0.0010
Talin-2	E9PUM4	Tln2	3	54	0.67	0.0011
Ca2+/CaM-dependent protein kinase type II subunit alpha (CAMK2A)	F8WIS9	Camk2a	7	286	0.75	0.0028

Tabla 1: Differential expressed proteins in the OB of APP/PS1 mice at 3 and 6 months of age

Deregulated proteins in the OB of 3-month-old APP/PS1 mice

Sec14-like protein 2 is involved in the binding and transport of alpha-tocopherol to the mitochondria [47] where it protects against lipid peroxidation, neuron loss, and mitochondrial dysfunction [48-50]. Interestingly, alpha-tocopherol has been related to AD neuropathology [51] decreasing the β-amyloid deposition [48, 52], indicating that the up-regulation of Sec14-like protein 2 in APP/PS1 mice may be an early protective mechanism of Aβ aggregate-induced neurotoxicity in olfactory cells. A large body of evidence have demonstrated alterations in axonal transport in animal models of AD [53]. Analysis of the mechanisms that underlie axonal transport deficits in AD has point out that dyneins and kinesins play a pivotal role in the movement of cytoskeletal structures that occur during axonal degeneration [54]. In accordance with previous data, the up-regulation of kinesin in APP/PS1 mice might indicate an imbalance in

the axonal transport at the level of OB due to early cytoskeletal rearrangements. Moreover, the increment in dynein light chain 2 also indicates a potential impairment in the axonal mitochondrial mobility process in the OB of APP/PS1 mice [55]. The over-expression of Myristoylated alanine-rich C kinase substrate (MARCKS) in APP/PS1 OB may be a consequence of β-amyloid generation [56]. MARCKS is a marker for activation of protein kinase C, and changes in its phosphorylation state have been reported in microglia associated with senile plaques from AD patients [57]. Moreover, MARCKS has been proposed as a β-amyloid inducer, modulating phosphatidylinositol 4,5 bisphosphate (PIP2) levels and actin movement, causing endocytosis [58]. Glycoprotein m6a is involved in neurite and filopodia outgrowth mediated by mitogen-activated protein kinase (MAPK) and Src signaling pathways [59-61]. Stromal membrane-associated protein 1 (Smap1) also mediates in neurite outgrowth [62]. Moreover, Smap1 acts on ADP-ribosylation factor 6, interacts with clathrin and regulates clathrin-dependent endocytosis [63], suggesting that the de-regulation in m6a and Smap1 protein levels in APP/PS1 OB cells points out an early readjustment in neuronal plasticity and filopodia motility.

Deregulated proteins in the OB of 6-month-old APP/PS1 mice

At 6 months of age, β-amyloid continues causing an alteration in specific protein mediators involved in cytoskeletal rearrangements, leading to an imbalance in intracellular signaling, vesicular trafficking, and structural stabilization at the level of OB. Coactosin-like protein, also deregulated in cortical and hippocampal neurons in APP (E693Δ) transgenic mice [64], regulates cytoskeleton dynamics by protecting F-actin from the disassembly mediated by cofilin [65]. Previous studies have demonstrated that β-amyloid oligomers activates cofilin in order to induce loss of cell surface β-1 integrin, disruption of F-actin/focal talin, and depletion of F-actin-associated post-synaptic proteins [66]. In our model, β-amyloid induces a down-regulation of Talin expression in the OB. Talin colocalizes with APP on the surface of cortical neurons [67], recruiting and activating focal adhesion proteins like Focal Adhesion Kinase (FAK) [68, 69]. It is

well known that β-amyloid deposition produced in APP/PS1 mice is accompanied by altered mitochondria and increase oxidative damage [9]. At the level of OB, we have observed an over-expression of ganglioside-induced differentiation-associated protein 1 (Gdap1) and NADH dehydrogenase iron-sulfur protein 2 (Ndufs2) in APP/PS1 mice. Gdap1 is involved in the regulation of the mitochondrial network by promoting mitochondrial fission [70] while Ndufs2 protein is a core subunit of the Complex I involved in the mitochondrial OXPHOS machinery. To complement the potential mitochondrial impairment in the APP/PS1 OB, the expression of prohibitin proteins (Phb1, Phb2) was examined. Phb complex regulates mitochondria ultrastructure, assembly/stabilization of OXPHOS complexes, and ROS formation [71]. Although loss of Phb complex impairs mitochondrial architecture and leads to neurodegeneration [72], protein expression levels of Phb1 and Phb2 were unchanged in APP/PS1 mice (data not shown), indicating that the potential mitochondrial dysfunction that occur in the OB is not induced by a Phb depletion. In parallel, the down-regulation of Ca^{2+}/CaM-dependent protein kinase type II subunit alpha (Camk2a), Phosphatidylinositol 5-phosphate 4 kinase type 2 alpha (Pip4k2a), sulfurtransferase (Mpst), and target of Myb protein 1 (Tom1) suggests a dysfunctional synaptic plasticity in the OB of APP/PS1 mice. Tom1 is essential for membrane recruitment of clathrin [73], necessary to mediate synaptic vesicle endocytosis [74]. The sulfurtransferase (Mpst) is an important producer of hydrogen sulfide in the brain [75]. This molecule is considered a neuroprotective synaptic modulator, facilitating long-term potentiation [76, 77], and ameliorating homocysteine-induced AD-like pathology and synaptic disorder [78]. Moreover, Pip4k2a participates in the synthesis of phosphatidylinositol 4,5 bisphosphate (PIP2) [79]. Previous studies revealed that presenilin mutations linked to familial AD and oligomeric β-amyloid peptides cause an imbalance in PIP2 metabolism [80, 81], suggesting that the down-regulation of Pip4k2a may produce an incorrect modulation of PIP2 levels, leading to a dysregulation of ion channels and membrane trafficking in the OB of APP/PS1 mice. In summary,

our proteomic data point out a moderate cytoskeletal disruption accompanied by an impairment in synaptic plasticity in the OB of APP/PS1 mice.

Death and survival routes in the OB of APP/PS1 mice

To complement our proteomic analysis, survival and apoptotic pathways were mapped in order to monitor the effect of β-amyloid burden on neuronal viability in the OB of APP/PS1 mice. For that, steady-state levels of survival proteins like Bcl-2, and Bcl-xL and the activation status of phospho-BAD (Ser112), caspase-3, -9, and -12 were measured in protein extracts from APP/PS1 OBs at 3 and 6 months. The stepwise characterization of constitutive pro- and anti-apoptotic factors revealed no activation of endoplasmic reticulum or mitochondrial apoptotic pathways at the level of OB (data not shown). However, the alteration of Talin-2 and Ser/Thr PP2A activator protein levels detected by proteomics, suggests that the activation of survival pathways critically involved in neuronal energy impairment and neurodegeneration like FAK/PI3K/Akt and MAP kinase pathways [82] may be affected in the OB of APP/PS1 transgenic mice. Previous studies have pointed out an interdependence of Talin levels with FAK-dependent effects [68]. The down-regulation of Talin observed in the OB of APP/PS1 mice suggests that FAK is not correctly recruited to adhesion sites [69]. Although Akt activation status was unchanged in APP/PS1 OBs (Figure 3A), the sustained dephosphorylation of FAK at tyr576/577 residues indicates that its activation is compromised in the OB of APP/PS1 mice (Figure 3A). Several reasons may explain this event. The recruitment of Src family kinases results in the phosphorylation of both tyrosines in the catalytic domain of FAK to obtain maximal kinase activity [83], suggesting that FAK dephosphorylation may be due to inactivation of Src kinases. Moreover, the phosphatase PTEN, which is altered in AD [84], may prevent the activation of FAK required to induce the MAPK/ERK pathway, and this lack of activation leads to neurodegeneration [82]. Although the influence of FAK dysregulation on the development of AD has not been completely elucidated, several reports have revealed a potential link. In addition to the participation of FAK in integrin signal

transduction related to neuronal guidance and neuritogenesis [85], it has been demonstrated that: i) neuronal FAK regulates apoptosis in AD [86], ii) its absence influences the onset of dementia [85], iii) abnormal gamma-secretase complexes lacking presenilin 1 affect its phosphotyrosine content [87], and iv) phosphorylation of FAK is dysregulated in cells co-transfected by Swedish mutant of APP695 gene plus ΔE9 deleted presenilin1 genes [88]. Although the particular mechanism still needs to be further explored, our results point out an early alteration in pathways of cell adhesion and motility in the OB of APP/PS1 mice because of the inactive state of FAK. On the other hand, the up-regulation of a PP2A activator may indicate a potential activation of this phosphatase. Since it has been demonstrated that transient activation of PP2A slows down the transmission of survival signals through dephosphorylation of MAP kinases [89, 90], subsequent experiments were performed in order to analyze the interaction of β-amyloid with MAP kinase pathway in the OB of APP/PS1 mice. At 3 months of age, β-amyloid induced the phosphorylation of MEK1/2 in the OB of APP/PS1 mice, maintaining the activation status of ERK1/2 unchanged (Figure 3B). In contrast, β-amyloid promoted the dephosphorylation of MEK1/2 and ERK1/2 in 6-months APP/PS1 OBs (Figure 3B), indicating a sequential interaction of β-amyloid with MAP kinase pathway in the OB region.

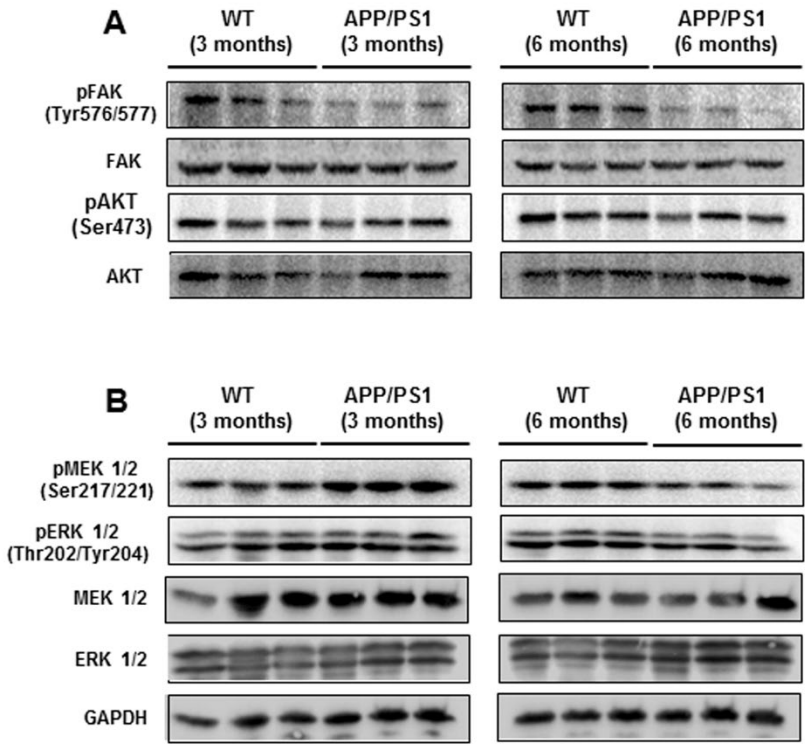

Figure 3. Survival pathways deregulated in the OB from APP/PS1 mice at 3 and 6 months of age. A) Levels and residue-specific phosphorylation of FAK/PI3K/Akt pathway in the OB of 3-months (left) and 6-months (right) APP/PS1 mice. B) Levels and residue-specific phosphorylation of MAP kinase pathway in the OB of 3-months (left) and 6-months (right) APP/PS1 mice. Representative Western blot gels (n = 3/experimental group) are shown.

Death and survival routes in the OB of sAD subjects

Within sporadic Alzheimer's disease (sAD), much effort has been spent on studying the role of β-amyloid in human disease pathogenesis but the available information is insufficient to fully understand the disease progression at the level of olfactory areas [14]. To investigate whether FAK and MAP kinase pathways altered in the OB of APP/PS1 mice were also associated with human sAD, the activation state of the corresponding survival pathways was measured by Western blotting in OBs from sAD subjects with different neuropathological grading (Supplementary table 1). An increment in OB total and phosphorylated protein levels of MEK1/2

was detected in initial and advanced AD stages (figure 4A and 4C) while the phosphorylation state of ERK1/2 was increased in initial, intermediate, and advanced AD stages respect to control OBs (figure 4A-C). Moreover, an increase in FAK phosphorylation was exclusively detected in advanced AD stages (figure 4C). This activation of FAK could mediate cell cycle activation, thereby leading to neurodegeneration and cell death [91-93]. Despite ERK is a well-defined pro-survival factor, neuronal ERK has been reported to be involved in the induction of cell death, APP processing, and Tau phosphorylation [94-96]. β–amyloid induces ERK1/2 abnormalities as shown in human AD brains, murine AD models, and AD in vitro systems [97-99]. According to our data obtained at the level of the OB, studies conducted in human AD brains [97] and APP/PS1 mice [98] have demonstrated stage-dependent ERK activity levels with increased or reduced amounts of ERK phosphorylation. Both ERK hyper- or hypo-phosphorylation induced by β–amyloid have been proposed as drivers of synaptic dysfunction in AD, possibly at different stages of the neurodegenerative process [100]. Regarding apoptotic pathways, no differences were observed in OB protein levels of survival proteins (Bcl-2, and Bcl-xL) and effector caspases (caspase-3, -9, and -12) between control and human sAD OBs (data not shown). Unlike the molecular information derived from APP/PS1 mice, an inhibition of the proapoptotic factor BAD by phosphorylation at Ser112 was evidenced in human OB across AD phenotypes. The nonphosphorylated BAD isoform is the responsible for the heterodimerization with Bcl-xL to promote cell death [101]. Despite Ser112 of BAD is considered a canonical target of active Akt to modulate this checkpoint for apoptosis [102], phosphorylated Akt at Ser473 (active form) was unchanged across AD grading respect to control OBs (data not shown). The persistent activation of ERK1/2 together with the inhibition of BAD [103] could contribute to the activation of neuroprotective mechanisms against β-amyloid toxicity in the OB of AD subjects.

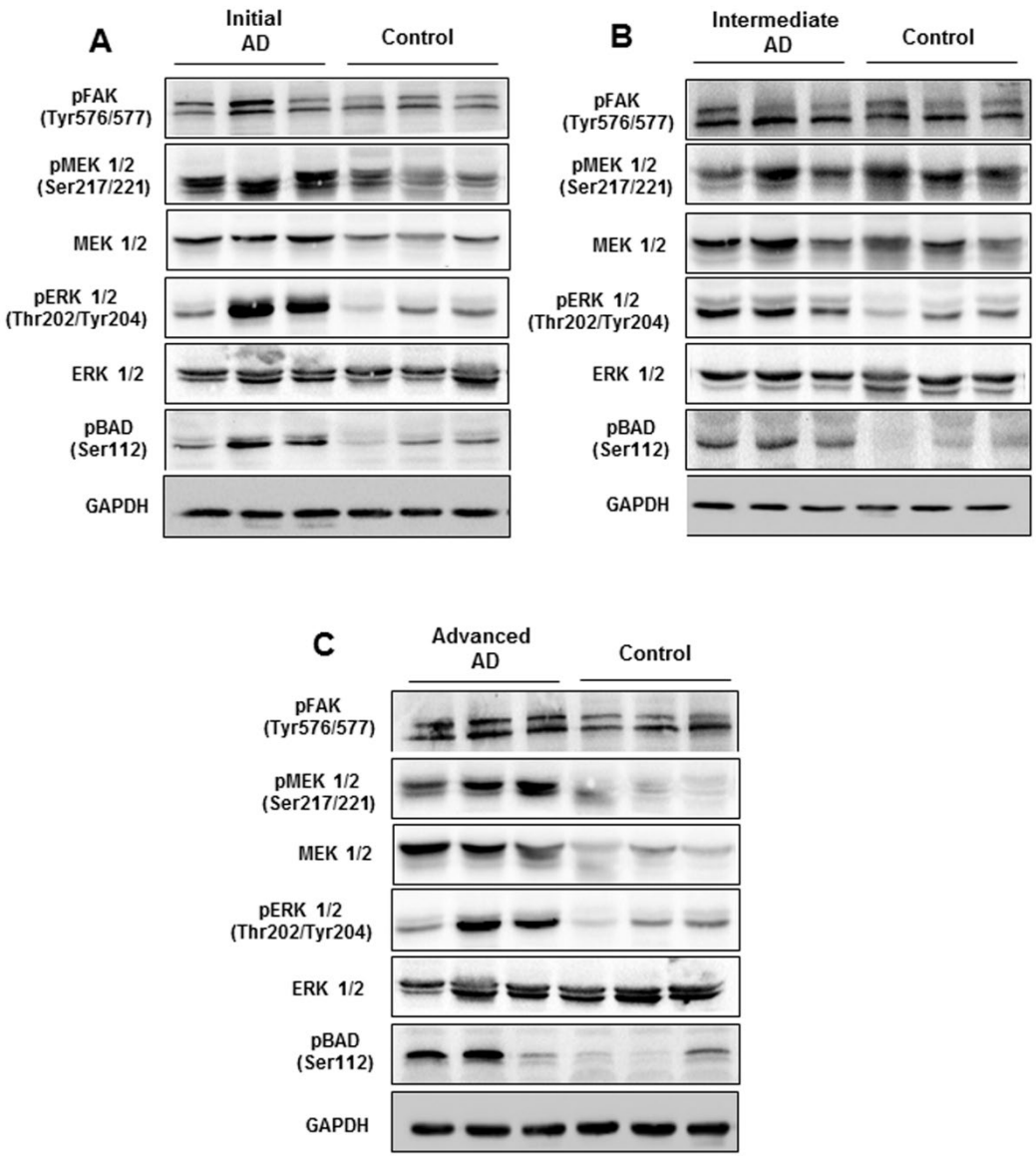

Figure 4. Survival pathways deregulated in human OB across AD staging. OB levels and residue-specific phosphorylation of FAK, MAP kinases, and BAD in initial AD stages (A), intermediate AD stages (B), and advanced AD stages (C). Representative Western blot gels (n=3/clinical background) are shown.

Conclusions

Overall, our present study carried out in OB derived from AD subjects and APP/PS1 mice allows a side-by-side comparisons and identification of similarities and differences in olfactory signaling in relation to species and stage of sAD progression. The different molecular signatures indicate that β-amyloid affects similar survival pathways in the OB of APP/PS1 mice and human sAD but the tangled regulatory mechanisms that govern the survival of olfactory cells significantly differ between species. This is not an unexpected observation, because the AD progression in APP/PS1 mice is reminiscent of, but not identical to sAD. This may be explained, in part, by specie- and stage-dependent inflammatory responses [12], differences in iron regulation and glial response [104], differences in molecular mechanisms associated to β-amyloidogenesis, and the lack of intraneuronal neurofibrillary tangles in the APP/PS1 transgenic AD model [9].

References

[1] Bettens K, Sleegers K, Van Broeckhoven C. Current status on Alzheimer disease molecular genetics: from past, to present, to future. Hum Mol Genet. 2010;19:R4-R11.

[2] Steiner H. The catalytic core of gamma-secretase: presenilin revisited. Curr Alzheimer Res. 2008;5:147-57.

[3] Woodruff-Pak DS. Animal models of Alzheimer's disease: therapeutic implications. J Alzheimers Dis. 2008;15:507-21.

[4] Borchelt DR, Thinakaran G, Eckman CB, Lee MK, Davenport F, Ratovitsky T, et al. Familial Alzheimer's disease-linked presenilin 1 variants elevate Abeta1-42/1-40 ratio in vitro and in vivo. Neuron. 1996;17:1005-13.

[5] Malm T, Koistinaho J, Kanninen K. Utilization of APPswe/PS1dE9 Transgenic Mice in Research of Alzheimer's Disease: Focus on Gene Therapy and Cell-Based Therapy Applications. Int J Alzheimers Dis. 2011;2011:517160.

[6] Blanchard V, Moussaoui S, Czech C, Touchet N, Bonici B, Planche M, et al. Time sequence of maturation of dystrophic neurites associated with Abeta deposits in APP/PS1 transgenic mice. Exp Neurol. 2003;184:247-63.

[7] Savonenko A, Xu GM, Melnikova T, Morton JL, Gonzales V, Wong MP, et al. Episodic-like memory deficits in the APPswe/PS1dE9 mouse model of Alzheimer's disease: relationships to beta-amyloid deposition and neurotransmitter abnormalities. Neurobiol Dis. 2005;18:602-17.

[8] Webster SJ, Bachstetter AD, Nelson PT, Schmitt FA, Van Eldik LJ. Using mice to model Alzheimer's dementia: an overview of the clinical disease and the preclinical behavioral changes in 10 mouse models. Front Genet. 2014;5:88.

[9] Aso E, Lomoio S, Lopez-Gonzalez I, Joda L, Carmona M, Fernandez-Yague N, et al. Amyloid generation and dysfunctional immunoproteasome activation with disease progression in animal model of familial Alzheimer's disease. Brain Pathol. 2012;22:636-53.

[10] Vegh MJ, Heldring CM, Kamphuis W, Hijazi S, Timmerman AJ, Li KW, et al. Reducing hippocampal extracellular matrix reverses early memory deficits in a mouse model of Alzheimer's disease. Acta Neuropathol Commun. 2014;2:76.

[11] Lv J, Ma S, Zhang X, Zheng L, Ma Y, Zhao X, et al. Quantitative proteomics reveals that PEA15 regulates astroglial Abeta phagocytosis in an Alzheimer's disease mouse model. J Proteomics. 2014;110:45-58.

[12] Lopez-Gonzalez I, Schluter A, Aso E, Garcia-Esparcia P, Ansoleaga B, F LL, et al. Neuroinflammatory signals in Alzheimer disease and APP/PS1 transgenic mice: correlations with plaques, tangles, and oligomeric species. J Neuropathol Exp Neurol. 2015;74:319-44.

[13] Kovacs T, Cairns NJ, Lantos PL. Olfactory centres in Alzheimer's disease: olfactory bulb is involved in early Braak's stages. Neuroreport. 2001;12:285-8.

[14] Zelaya MV, Perez-Valderrama E, de Morentin XM, Tunon T, Ferrer I, Luquin MR, et al. Olfactory bulb proteome dynamics during the progression of sporadic Alzheimer's disease: identification of common and distinct olfactory targets across Alzheimer-related co-pathologies. Oncotarget. 2015;6:39437-56.

[15] Attems J, Jellinger KA. Olfactory tau pathology in Alzheimer disease and mild cognitive impairment. Clin Neuropathol. 2006;25:265-71.

[16] Arnold SE, Lee EB, Moberg PJ, Stutzbach L, Kazi H, Han LY, et al. Olfactory epithelium amyloid-beta and paired helical filament-tau pathology in Alzheimer disease. Ann Neurol. 2010;67:462-9.

[17] Talamo BR, Rudel R, Kosik KS, Lee VM, Neff S, Adelman L, et al. Pathological changes in olfactory neurons in patients with Alzheimer's disease. Nature. 1989;337:736-9.

[18] Lau JC, Lerch JP, Sled JG, Henkelman RM, Evans AC, Bedell BJ. Longitudinal neuroanatomical changes determined by deformation-based morphometry in a mouse model of Alzheimer's disease. Neuroimage. 2008;42:19-27.

[19] Rey NL, Jardanhazi-Kurutz D, Terwel D, Kummer MP, Jourdan F, Didier A, et al. Locus coeruleus degeneration exacerbates olfactory deficits in APP/PS1 transgenic mice. Neurobiol Aging. 2012;33:426 e1-11.

[20] Gonzalez-Dominguez R, Garcia-Barrera T, Vitorica J, Gomez-Ariza JL. Region-specific metabolic alterations in the brain of the APP/PS1 transgenic mice of Alzheimer's disease. Biochim Biophys Acta. 2014;1842:2395-402.

[21] Gonzalez-Dominguez R, Garcia-Barrera T, Vitorica J, Gomez-Ariza JL. Metabolomic screening of regional brain alterations in the APP/PS1 transgenic model of Alzheimer's disease by direct infusion mass spectrometry. J Pharm Biomed Anal. 2015;102:425-35.

[22] Braak H, Alafuzoff I, Arzberger T, Kretzschmar H, Del Tredici K. Staging of Alzheimer disease-associated neurofibrillary pathology using paraffin sections and immunocytochemistry. Acta Neuropathol. 2006;112:389-404.

[23] Alafuzoff I, Arzberger T, Al-Sarraj S, Bodi I, Bogdanovic N, Braak H, et al. Staging of neurofibrillary pathology in Alzheimer's disease: a study of the BrainNet Europe Consortium. Brain Pathol. 2008;18:484-96.

[24] Montine TJ, Phelps CH, Beach TG, Bigio EH, Cairns NJ, Dickson DW, et al. National Institute on Aging-Alzheimer's Association guidelines for the neuropathologic assessment of Alzheimer's disease: a practical approach. Acta Neuropathol. 2012;123:1-11.

[25] Thal DR, Rub U, Orantes M, Braak H. Phases of A beta-deposition in the human brain and its relevance for the development of AD. Neurology. 2002;58:1791-800.

[26] Crary JF, Trojanowski JQ, Schneider JA, Abisambra JF, Abner EL, Alafuzoff I, et al. Primary age-related tauopathy (PART): a common pathology associated with human aging. Acta Neuropathol. 2014;128:755-66.

[27] Kovacs T, Cairns NJ, Lantos PL. beta-amyloid deposition and neurofibrillary tangle formation in the olfactory bulb in ageing and Alzheimer's disease. Neuropathol Appl Neurobiol. 1999;25:481-91.

[28] Shevchenko A, Tomas H, Havlis J, Olsen JV, Mann M. In-gel digestion for mass spectrometric characterization of proteins and proteomes. Nat Protoc. 2006;1:2856-60.

[29] Shilov IV, Seymour SL, Patel AA, Loboda A, Tang WH, Keating SP, et al. The Paragon Algorithm, a next generation search engine that uses sequence temperature values and feature probabilities to identify peptides from tandem mass spectra. Mol Cell Proteomics. 2007;6:1638-55.

[30] Tang WH, Shilov IV, Seymour SL. Nonlinear fitting method for determining local false discovery rates from decoy database searches. J Proteome Res. 2008;7:3661-7.

[31] Vizcaino JA, Deutsch EW, Wang R, Csordas A, Reisinger F, Rios D, et al. ProteomeXchange provides globally coordinated proteomics data submission and dissemination. Nat Biotechnol. 2014;32:223-6.

[32] Attems J, Walker L, Jellinger KA. Olfactory bulb involvement in neurodegenerative diseases. Acta Neuropathol. 2014;127:459-75.

[33] Robinson RA, Joshi G, Huang Q, Sultana R, Baker AS, Cai J, et al. Proteomic analysis of brain proteins in APP/PS-1 human double mutant knock-in mice with increasing amyloid beta-peptide deposition: insights into the effects of in vivo treatment with N-acetylcysteine as a potential therapeutic intervention in mild cognitive impairment and Alzheimer's disease. Proteomics. 2011;11:4243-56.

[34] Cao Z, Robinson RA. Proteome characterization of splenocytes from an Abetapp/ps-1 Alzheimer's disease model. Proteomics. 2014;14:291-7.

[35] Martin B, Brenneman R, Becker KG, Gucek M, Cole RN, Maudsley S. iTRAQ analysis of complex proteome alterations in 3xTgAD Alzheimer's mice: understanding the interface between physiology and disease. PLoS One. 2008;3:e2750.

[36] Ciavardelli D, Silvestri E, Del Viscovo A, Bomba M, De Gregorio D, Moreno M, et al. Alterations of brain and cerebellar proteomes linked to Abeta and tau pathology in a female triple-transgenic murine model of Alzheimer's disease. Cell Death Dis. 2010;1:e90.

[37] Chou JL, Shenoy DV, Thomas N, Choudhary PK, Laferla FM, Goodman SR, et al. Early dysregulation of the mitochondrial proteome in a mouse model of Alzheimer's disease. J Proteomics. 2011;74:466-79.

[38] Rhein V, Song X, Wiesner A, Ittner LM, Baysang G, Meier F, et al. Amyloid-beta and tau synergistically impair the oxidative phosphorylation system in triple transgenic Alzheimer's disease mice. Proc Natl Acad Sci U S A. 2009;106:20057-62.

[39] Nilsson P, Loganathan K, Sekiguchi M, Winblad B, Iwata N, Saido TC, et al. Loss of neprilysin alters protein expression in the brain of Alzheimer's disease model mice. Proteomics. 2015;15:3349-55.

[40] Shevchenko G, Wetterhall M, Bergquist J, Hoglund K, Andersson LI, Kultima K. Longitudinal characterization of the brain proteomes for the tg2576 amyloid mouse model using shotgun based mass spectrometry. J Proteome Res. 2012;11:6159-74.

[41] Sharma K, Schmitt S, Bergner CG, Tyanova S, Kannaiyan N, Manrique-Hoyos N, et al. Cell type- and brain region-resolved mouse brain proteome. Nat Neurosci. 2015;18:1819-31.

[42] Jackson HM, Soto I, Graham LC, Carter GW, Howell GR. Clustering of transcriptional profiles identifies changes to insulin signaling as an early event in a mouse model of Alzheimer's disease. BMC Genomics. 2013;14:831.

[43] Dickey CA, Loring JF, Montgomery J, Gordon MN, Eastman PS, Morgan D. Selectively reduced expression of synaptic plasticity-related genes in amyloid precursor protein + presenilin-1 transgenic mice. J Neurosci. 2003;23:5219-26.

[44] Gatta V, D'Aurora M, Granzotto A, Stuppia L, Sensi SL. Early and sustained altered expression of aging-related genes in young 3xTg-AD mice. Cell Death Dis. 2014;5:e1054.

[45] Wirz KT, Bossers K, Stargardt A, Kamphuis W, Swaab DF, Hol EM, et al. Cortical beta amyloid protein triggers an immune response, but no synaptic changes in the APPswe/PS1dE9 Alzheimer's disease mouse model. Neurobiol Aging. 2013;34:1328-42.

[46] Bouter Y, Kacprowski T, Weissmann R, Dietrich K, Borgers H, Brauss A, et al. Deciphering the molecular profile of plaques, memory decline and neuron loss in two mouse models for Alzheimer's disease by deep sequencing. Front Aging Neurosci. 2014;6:75.

[47] Zingg JM, Kempna P, Paris M, Reiter E, Villacorta L, Cipollone R, et al. Characterization of three human sec14p-like proteins: alpha-tocopherol transport activity and expression pattern in tissues. Biochimie. 2008;90:1703-15.

[48] Nishida Y, Ito S, Ohtsuki S, Yamamoto N, Takahashi T, Iwata N, et al. Depletion of vitamin E increases amyloid beta accumulation by decreasing its clearances from brain and blood in a mouse model of Alzheimer disease. J Biol Chem. 2009;284:33400-8.

[49] Bostanci MO, Bas O, Bagirici F. Alpha-tocopherol decreases iron-induced hippocampal and nigral neuron loss. Cell Mol Neurobiol. 2010;30:389-94.

[50] Navarro A, Bandez MJ, Lopez-Cepero JM, Gomez C, Boveris A. High doses of vitamin E improve mitochondrial dysfunction in rat hippocampus and frontal cortex upon aging. Am J Physiol Regul Integr Comp Physiol. 2011;300:R827-34.

[51] Morris MC, Schneider JA, Li H, Tangney CC, Nag S, Bennett DA, et al. Brain tocopherols related to Alzheimer's disease neuropathology in humans. Alzheimers Dement. 2015;11:32-9.

[52] Yang SG, Wang WY, Ling TJ, Feng Y, Du XT, Zhang X, et al. alpha-Tocopherol quinone inhibits beta-amyloid aggregation and cytotoxicity, disaggregates preformed fibrils and decreases the production of reactive oxygen species, NO and inflammatory cytokines. Neurochem Int. 2010;57:914-22.

[53] Gotz J, Ittner LM, Kins S. Do axonal defects in tau and amyloid precursor protein transgenic animals model axonopathy in Alzheimer's disease? J Neurochem. 2006;98:993-1006.

[54] Kanaan NM, Pigino GF, Brady ST, Lazarov O, Binder LI, Morfini GA. Axonal degeneration in Alzheimer's disease: when signaling abnormalities meet the axonal transport system. Exp Neurol. 2013;246:44-53.

[55] Chen YM, Gerwin C, Sheng ZH. Dynein light chain LC8 regulates syntaphilin-mediated mitochondrial docking in axons. J Neurosci. 2009;29:9429-38.

[56] Murphy A, Sunohara JR, Sundaram M, Ridgway ND, McMaster CR, Cook HW, et al. Induction of protein kinase C substrates, Myristoylated alanine-rich C kinase substrate (MARCKS) and MARCKS-related protein (MRP), by amyloid beta-protein in mouse BV-2 microglial cells. Neurosci Lett. 2003;347:9-12.

[57] Kimura T, Yamamoto H, Takamatsu J, Yuzuriha T, Miyamoto E, Miyakawa T. Phosphorylation of MARCKS in Alzheimer disease brains. Neuroreport. 2000;11:869-73.

[58] Su R, Han ZY, Fan JP, Zhang YL. A possible role of myristoylated alanine-rich C kinase substrate in endocytic pathway of Alzheimer's disease. Neurosci Bull. 2010;26:338-44.

[59] Formoso K, Billi SC, Frasch AC, Scorticati C. Tyrosine 251 at the C-terminus of neuronal glycoprotein M6a is critical for neurite outgrowth. J Neurosci Res. 2015;93:215-29.

[60] Formoso K, Garcia MD, Frasch AC, Scorticati C. Filopodia formation driven by membrane glycoprotein M6a depends on the interaction of its transmembrane domains. J Neurochem. 2011;134:499-512.

[61] Brocco MA, Fernandez ME, Frasch AC. Filopodial protrusions induced by glycoprotein M6a exhibit high motility and aids synapse formation. Eur J Neurosci. 2010;31:195-202.

[62] Tong CW, Wang JL, Jiang MS, Hsu CH, Chang WT, Huang AM. Novel genes that mediate nuclear respiratory factor 1-regualted neurite outgrowth in neuroblastoma IMR-32 cells. Gene. 2013;515:62-70.

[63] Tanabe K, Torii T, Natsume W, Braesch-Andersen S, Watanabe T, Satake M. A novel GTPase-activating protein for ARF6 directly interacts with clathrin and regulates clathrin-dependent endocytosis. Mol Biol Cell. 2005;16:1617-28.

[64] Takano M, Maekura K, Otani M, Sano K, Nakamura-Hirota T, Tokuyama S, et al. Proteomic analysis of the brain tissues from a transgenic mouse model of amyloid beta oligomers. Neurochem Int. 2012;61:347-55.

[65] Kim J, Shapiro MJ, Bamidele AO, Gurel P, Thapa P, Higgs HN, et al. Coactosin-like 1 antagonizes cofilin to promote lamellipodial protrusion at the immune synapse. PLoS One. 2014;9:e85090.

[66] Woo JA, Zhao X, Khan H, Penn C, Wang X, Joly-Amado A, et al. Slingshot-Cofilin activation mediates mitochondrial and synaptic dysfunction via Abeta ligation to beta1-integrin conformers. Cell Death Differ. 2015;22:1069-70.

[67] Storey E, Beyreuther K, Masters CL. Alzheimer's disease amyloid precursor protein on the surface of cortical neurons in primary culture co-localizes with adhesion patch components. Brain Res. 1996;735:217-31.

[68] Michael KE, Dumbauld DW, Burns KL, Hanks SK, Garcia AJ. Focal adhesion kinase modulates cell adhesion strengthening via integrin activation. Mol Biol Cell. 2009;20:2508-19.

[69] Wang P, Ballestrem C, Streuli CH. The C terminus of talin links integrins to cell cycle progression. J Cell Biol. 2011;195:499-513.

[70] Pareyson D, Saveri P, Sagnelli A, Piscosquito G. Mitochondrial dynamics and inherited peripheral nerve diseases. Neurosci Lett. 2015;596:66-77.

[71] Artal-Sanz M, Tavernarakis N. Prohibitin and mitochondrial biology. Trends Endocrinol Metab. 2009;20:394-401.

[72] Merkwirth C, Martinelli P, Korwitz A, Morbin M, Bronneke HS, Jordan SD, et al. Loss of prohibitin membrane scaffolds impairs mitochondrial architecture and leads to tau hyperphosphorylation and neurodegeneration. PLoS Genet. 2012;8:e1003021.

[73] Seet LF, Hong W. Endofin recruits clathrin to early endosomes via TOM1. J Cell Sci. 2005;118:575-87.

[74] Smith SM, Renden R, von Gersdorff H. Synaptic vesicle endocytosis: fast and slow modes of membrane retrieval. Trends Neurosci. 2008;31:559-68.

[75] Miyamoto R, Otsuguro K, Yamaguchi S, Ito S. Contribution of cysteine aminotransferase and mercaptopyruvate sulfurtransferase to hydrogen sulfide production in peripheral neurons. J Neurochem. 2014;130:29-40.

[76] Shibuya N, Tanaka M, Yoshida M, Ogasawara Y, Togawa T, Ishii K, et al. 3-Mercaptopyruvate sulfurtransferase produces hydrogen sulfide and bound sulfane sulfur in the brain. Antioxid Redox Signal. 2009;11:703-14.

[77] Kamat PK, Kalani A, Tyagi N. Role of hydrogen sulfide in brain synaptic remodeling. Methods Enzymol. 2015;555:207-29.

[78] Kamat PK, Kyles P, Kalani A, Tyagi N. Hydrogen Sulfide Ameliorates Homocysteine-Induced Alzheimer's Disease-Like Pathology, Blood-Brain Barrier Disruption, and Synaptic Disorder. Mol Neurobiol. 2015.

[79] Rameh LE, Tolias KF, Duckworth BC, Cantley LC. A new pathway for synthesis of phosphatidylinositol-4,5-bisphosphate. Nature. 1997;390:192-6.

[80] Landman N, Jeong SY, Shin SY, Voronov SV, Serban G, Kang MS, et al. Presenilin mutations linked to familial Alzheimer's disease cause an imbalance in phosphatidylinositol 4,5-bisphosphate metabolism. Proc Natl Acad Sci U S A. 2006;103:19524-9.

[81] Berman DE, Dall'Armi C, Voronov SV, McIntire LB, Zhang H, Moore AZ, et al. Oligomeric amyloid-beta peptide disrupts phosphatidylinositol-4,5-bisphosphate metabolism. Nat Neurosci. 2008;11:547-54.

[82] Gupta A, Dey CS. PTEN, a widely known negative regulator of insulin/PI3K signaling, positively regulates neuronal insulin resistance. Mol Biol Cell. 2012;23:3882-98.

[83] Calalb MB, Polte TR, Hanks SK. Tyrosine phosphorylation of focal adhesion kinase at sites in the catalytic domain regulates kinase activity: a role for Src family kinases. Mol Cell Biol. 1995;15:954-63.

[84] Sonoda Y, Mukai H, Matsuo K, Takahashi M, Ono Y, Maeda K, et al. Accumulation of tumor-suppressor PTEN in Alzheimer neurofibrillary tangles. Neurosci Lett. 2010;471:20-4.

[85] Armendariz BG, Masdeu Mdel M, Soriano E, Urena JM, Burgaya F. The diverse roles and multiple forms of focal adhesion kinase in brain. Eur J Neurosci. 2014;40:3573-90.

[86] Zhang C, Lambert MP, Bunch C, Barber K, Wade WS, Krafft GA, et al. Focal adhesion kinase expressed by nerve cell lines shows increased tyrosine phosphorylation in response to Alzheimer's A beta peptide. J Biol Chem. 1994;269:25247-50.

[87] Waschbusch D, Born S, Niediek V, Kirchgessner N, Tamboli IY, Walter J, et al. Presenilin 1 affects focal adhesion site formation and cell force generation via c-Src transcriptional and posttranslational regulation. J Biol Chem. 2009;284:10138-49.

[88] Sheng B, Song B, Zheng Z, Zhou F, Lu G, Zhao N, et al. Abnormal cleavage of APP impairs its functions in cell adhesion and migration. Neurosci Lett. 2009;450:327-31.

[89] Chen J, Martin BL, Brautigan DL. Regulation of protein serine-threonine phosphatase type-2A by tyrosine phosphorylation. Science. 1992;257:1261-4.

[90] Letourneux C, Rocher G, Porteu F. B56-containing PP2A dephosphorylate ERK and their activity is controlled by the early gene IEX-1 and ERK. EMBO J. 2006;25:727-38.

[91] Williamson R, Scales T, Clark BR, Gibb G, Reynolds CH, Kellie S, et al. Rapid tyrosine phosphorylation of neuronal proteins including tau and focal adhesion kinase in response to amyloid-beta peptide exposure: involvement of Src family protein kinases. J Neurosci. 2002;22:10-20.

[92] Grace EA, Busciglio J. Aberrant activation of focal adhesion proteins mediates fibrillar amyloid beta-induced neuronal dystrophy. J Neurosci. 2003;23:493-502.

[93] Caltagarone J, Jing Z, Bowser R. Focal adhesions regulate Abeta signaling and cell death in Alzheimer's disease. Biochim Biophys Acta. 2007;1772:438-45.

[94] Dehvari N, Isacsson O, Winblad B, Cedazo-Minguez A, Cowburn RF. Presenilin regulates extracellular regulated kinase (Erk) activity by a protein kinase C alpha dependent mechanism. Neurosci Lett. 2008;436:77-80.

[95] Subramaniam S, Zirrgiebel U, von Bohlen Und Halbach O, Strelau J, Laliberte C, Kaplan DR, et al. ERK activation promotes neuronal degeneration predominantly through plasma membrane damage and independently of caspase-3. J Cell Biol. 2004;165:357-69.

[96] Cheung EC, Slack RS. Emerging role for ERK as a key regulator of neuronal apoptosis. Sci STKE. 2004;2004:PE45.

[97] Russo C, Dolcini V, Salis S, Venezia V, Zambrano N, Russo T, et al. Signal transduction through tyrosine-phosphorylated C-terminal fragments of amyloid precursor protein via an enhanced interaction with Shc/Grb2 adaptor proteins in reactive astrocytes of Alzheimer's disease brain. J Biol Chem. 2002;277:35282-8.

[98] Liu MY, Wang S, Yao WF, Zhang ZJ, Zhong X, Sha L, et al. Memantine improves spatial learning and memory impairments by regulating NGF signaling in APP/PS1 transgenic mice. Neuroscience. 2014;273:141-51.

[99] Balleza-Tapia H, Pena F. Pharmacology of the intracellular pathways activated by amyloid beta protein. Mini Rev Med Chem. 2009;9:724-40.

[100] Origlia N, Arancio O, Domenici L, Yan SS. MAPK, beta-amyloid and synaptic dysfunction: the role of RAGE. Expert Rev Neurother. 2009;9:1635-45.

[101] Zha J, Harada H, Yang E, Jockel J, Korsmeyer SJ. Serine phosphorylation of death agonist BAD in response to survival factor results in binding to 14-3-3 not BCL-X(L). Cell. 1996;87:619-28.

[102] del Peso L, Gonzalez-Garcia M, Page C, Herrera R, Nunez G. Interleukin-3-induced phosphorylation of BAD through the protein kinase Akt. Science. 1997;278:687-9.

[103] Stein TD, Johnson JA. Lack of neurodegeneration in transgenic mice overexpressing mutant amyloid precursor protein is associated with increased levels of transthyretin and the activation of cell survival pathways. J Neurosci. 2002;22:7380-8.

[104] Meadowcroft MD, Connor JR, Yang QX. Cortical iron regulation and inflammatory response in Alzheimer's disease and APPSWE/PS1DeltaE9 mice: a histological perspective. Front Neurosci. 2015;9:255.

CHAPTER 2

Progressive Modulation of the Human Olfactory Bulb Transcriptome during Alzheimer´s Disease Evolution: novel insights into the olfactory signaling across proteinopathies

Mercedes Lachén-Montes[1,2], María Victoria Zelaya[1,2,3], Víctor Segura[2,4], Joaquín Fernández-Irigoyen[1,2,5]§, Enrique Santamaría[1,2,5]§

[1] *Clinical Neuroproteomics Group, Navarrabiomed, Departamento de Salud, Universidad Pública de Navarra, Pamplona, Spain*

[2] *IDISNA, Navarra Institute for Health Research, Pamplona, Spain*

[3] *Pathological Anatomy Department, Navarra Hospital Complex, Pamplona, Spain*

[4] *Bioinformatics Unit, Center for Applied Medical Research, University of Navarra, 31008, Pamplona, Spain.*

[5] *Proteored-ISCIII, Proteomics Unit, Navarrabiomed, Departamento de Salud, Universidad Pública de Navarra, Pamplona, Spain*

Abstract

Alzheimer´s disease (AD) is characterized by progressive dementia, initially presenting olfactory dysfunction. Despite the olfactory bulb (OB) is the first central structure of the olfactory pathway, we lack a complete molecular characterization of the transcriptional events that occurs in this olfactory area during AD progression. To address this gap in knowledge, we have assessed the genome-wide expression in postmortem OBs from subjects with varying degree of AD pathology. A stage-dependent deregulation of specific pathways was observed, revealing transmembrane transport, and neuroinflammation as part of the functional modules that are disrupted across AD grading. Potential drivers of neurodegeneration predicted by network-driven transcriptomics were monitored across different types of dementia, including progressive supranuclear palsy (PSP), mixed dementia, and frontotemporal lobar degeneration (FTLD). Epidermal growth factor receptor (EGFR) expression was significantly increased in the OB of AD and mixed dementia subjects. Moreover, a significant increment in the activation of signal transducer and activator of transcription 3 (STAT3) was exclusively detected in advanced AD stages, whereas total STAT3 levels were specifically overexpressed in mixed dementia. Furthermore, transcription factors deregulated in the OB of mixed dementia subjects such as cAMP Responsive Element Binding Protein 1 (CREB1) and AP-1 Transcription Factor Subunit (c-Jun) were not differentially modulated at olfactory level across AD grading. On the other hand, olfactory expression of this signal transducer panel was unchanged in PSP and FTLD subjects. Taken together, this study unveils cross-disease similarities and differences for specific signal transducers, providing mechanistic clues to the intriguing divergence of AD pathology across proteinopathies.

Introduction

Although olfactory involvement may also appear in healthy non-demented elderly subjects [1], olfactory dysfunction is present in up to 90% of AD patients [2]. Some studies suggest that olfactory dysfunction is an early event of AD, preceding the appearance of typical AD symptoms, such as memory loss, and dementia. The olfactory bulb (OB) is the first central structure of the olfactory pathway in the brain [3]. An OB atrophy and a significant reduction in olfactory performance have been detected in AD respect to control subjects using MRI and PET technologies [4, 5]. From a neuropathological point of view, olfactory centres are involved in early Braak stages [6], and OB pathology correlates with cortical AD pathology [7-9]. In view of these data, an in depth biochemical characterization of the neurodegeneration that occurs in the OB is mandatory as a first step for understanding early smell impairment in AD. Although neuroanatomical, volumetric, and histological approaches have been the gold standard techniques employed to characterize the OB functionality, little attention has been focused specifically on the molecular composition of the OB from the perspective of high throughput molecular technologies [10, 11]. Different transcriptomic studies have been attempted to discover novel regulatory mechanisms associated with AD pathogenesis in brain areas differentially affected by the disease [12]. Nevertheless, no study to date has addressed whether specific patterns of gene expression is associated to the development of human AD-related pathology at olfactory level in a stage-dependent manner. We consider that deciphering the progressive transcriptome-wide alterations that occurs in the OB derived from human AD cases with different Braak staging, might help develop early diagnosis and identify potential therapeutic targets for AD. In this study, we have analyzed the progressive modulation of the OB transcriptome across neuropathological stages of AD, in order to increase our knowledge about the pathophysiological mechanisms that are disturbed during the AD neurodegeneration in the OB. 249 differential genes were detected between controls and AD-related phenotypes,

pinpointing specific pathways, gene interaction networks, and potential novel therapeutic targets that are modulated in specific AD stages. Interestingly, the OB transcriptome exploration in parallel with a cross-disease analysis including different proteinopathies, has revealed distinct modulation of specific signal transducers, providing new avenues of research into the role of olfactory signaling across different types of dementias.

Results and discussion

During the last decade, gene expression profiling of postmortem tissue has greatly increased our knowledge about the pathophysiological mechanisms that occur in affected brain structures during AD progression [12]. With the aim to identify downstream aberrant gene expression related to beta-amyloid and Tau deposits across AD phenotypes, the temporal lobe–hippocampus and the frontal–prefrontal cortex has been the most studied areas [12-16]. However, loss of smell is involved in early stages of AD, partially due to an imbalance in the OB functionality [17]. Albeit olfactory impairment is considered an important clinical marker and predictor of AD progression [18], the mechanisms governing this dysfunction are still poorly understood. Transcriptome profiling has revealed multiple metabolic alterations in the OB of a rat AD model [19], however, the progression of the disease in rodent models does not correlate well with human AD [20], being necessary genome-wide studies in human olfactory tissue with neuropathologically well-defined AD-associated changes (Figure 1).

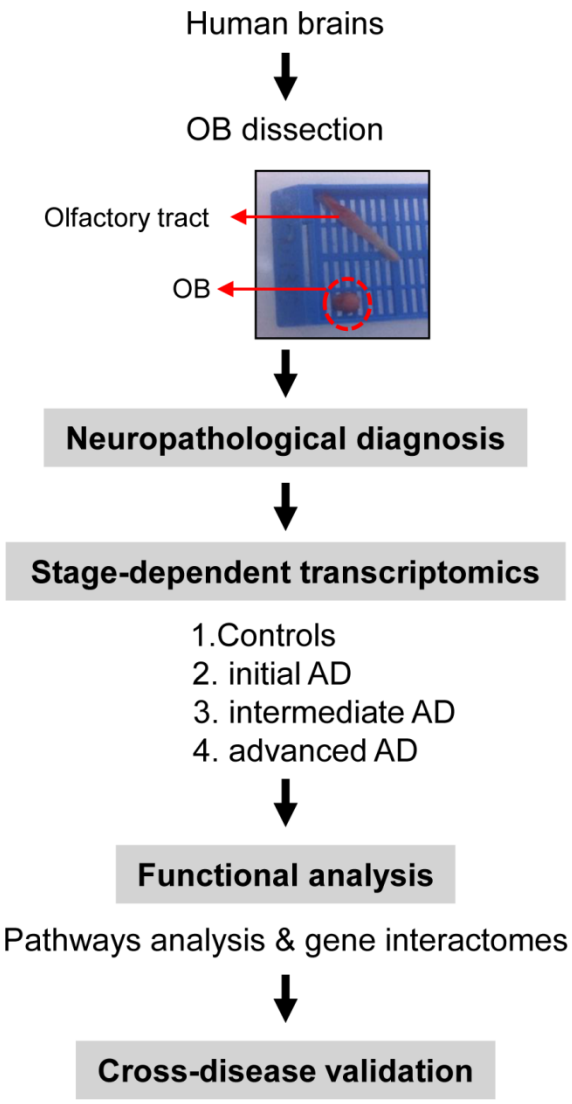

Figure 1. An overview of the workflow used for the characterization of OB transcriptome during AD evolution.

			Duration	PMI	Pathological diagnosis	IHQ: βA in OB		IHQ: TAU in OB	
Cases	age	sex	(years)	(hours)	NIA-AA criteria	MP	DP	Tangles	neurites
Control									
C1	72	M		9	Thal 1 Cerad 1 no tau deposit	-	-	-	+
C2	103	M		3	No protein deposit+vascular disease	-	-	-	+
C3	81	F		3.3	PART (Braak I)+vascular disase	-	-	-	+
C4	61	M		8	PART (Braak I)	-	-	+	-
Initial AD									
I1	88	M	1	3.45	AD (A2B1C2)	++	+	++	++
I2	85	F	8	2	AD (A2B1C1)	-	-	+	+
I3	80	M	5	3	AD (A2B1C1)	++	++	++	+++
I4	75	F	n.d	6	AD (A1B1C1)	-	-	+	+
I5	72	F	n.d	4	AD (A1B1C1)	-	-	+	+
intermediate AD									
M1	85	M	12	3.3	AD (A2B2C2)	-	+	+++	+++
M2	97	F	9	n.d	AD (A2B2C2)	n.d	n.d	n.d	n.d
M3	77	M	17	1.5	AD (A2B2C1)	-	-	++	++
M4	86	F	9	3	AD (A2B2C2)	-	+	++	++
Advanced AD									
A1	77	F	16	4	AD (A2B3C3)	+	+++	+++	+++
A2	70	M	4	2.5	AD (A3B3C3)	++	+++	++	+++
A3	89	M	13	3	AD (A2B3C3)	+	+++	+++	+++
A4	86	M	8	2.5	AD (A3B3C3)	+	-	+	++
A5	93	M	3	2.4	AD (A3B3C3)	+	+++	+++	+++

Table 1. Summary of selected cases included in this study. The neuropathological assessment was performed according to Thal phases, adapted CERAD score, NIA-AA guidelines and PART criteria. Aβ immunopositivity was scored on a 4-tiered scale as: (-) negative, (+) 1-2 isolated Aβ depositions, (++) 3-4 Aβ depositions, and (+++) >4 Aβ depositions. Graduation of phospho-TAU deposit: (-) negative +: low; ++: intermediate; +++ high. PMI: post-mortem interval; n.d: not determined; MP: Mature plaques; DP: Diffuse plaques.

OB transcriptome dynamics during AD progression

The immunohistochemical study of β-amyloid and phospho-Tau protein in the cases included in this study, allowed us to confirm the presence of neuropathological proteins in the OB of subjects with distinct stages of AD (Figure 2), confirming the involvement of OB in pre-clinical stages of the disease.

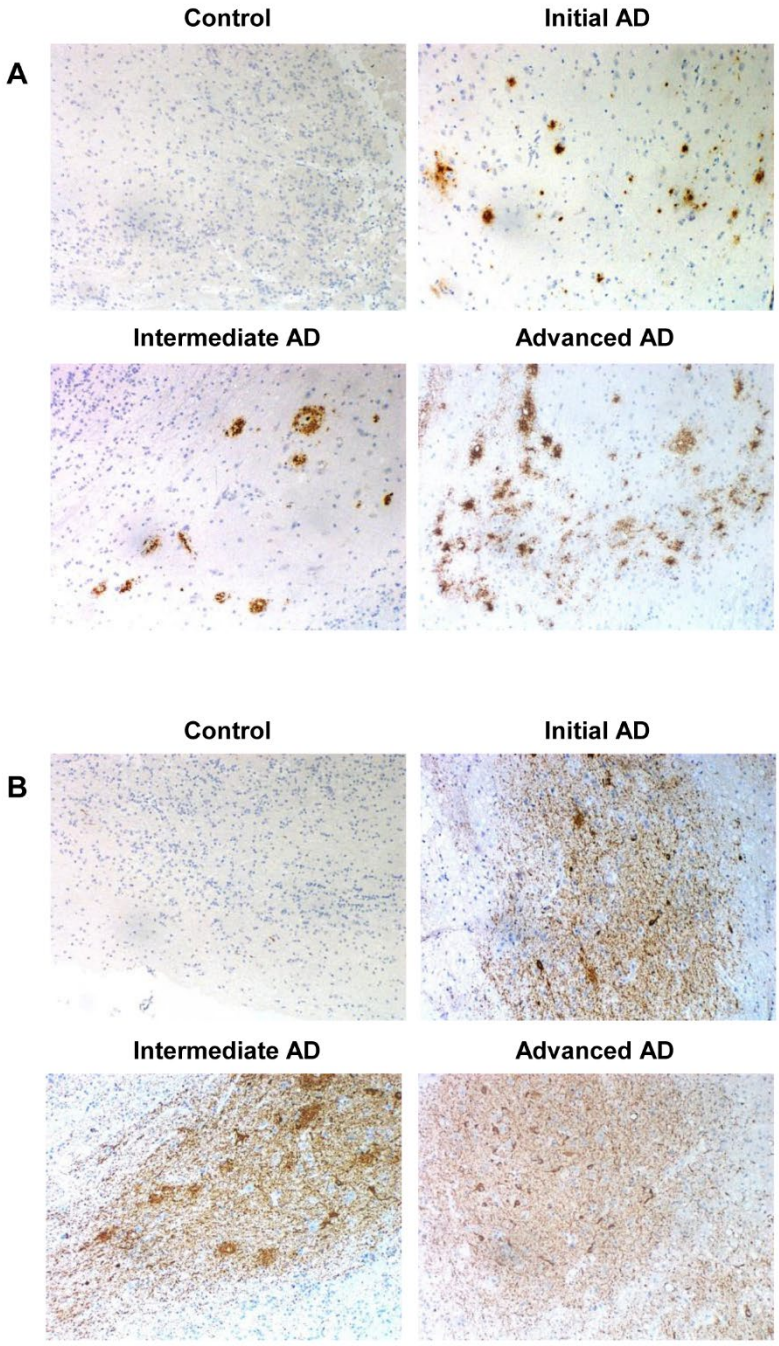

Figure 2. Representative immunohistochemical analysis of β-amyloid and phospho-Tau in the OB across AD stages. A) Control: negative staining of β-amyloid in the anterior olfactory nucleus (AON). Low AD: mild compact deposits of β-amyloid in the AON. Intermediate AD: sparse neuritic plaques of β-amyloid in the AON. High AD: mild neuritic and diffuse plaques of β-amyloid in the AON. B) Control: isolated neuropil threads of phospho-Tau protein in the glomerular layer of the OB. Initial AD: Moderate neuropil threads and tangles of phospho-Tau protein. Intermediate AD: Severe deposit of neuropil threads of phospho-Tau protein. Advanced AD: Severe neuropil threads and tangles of phospho-Tau protein in the AON (All images are 20x).

To further understand the olfactory molecular background contributing to the progression of AD, we have performed a differential OB transcriptome analysis in order to detect early and stage-dependent molecular events underlying the progression of the disease at olfactory level (Figure 1). As shown in Figure 3, 103, 78, and 105 differentially expressed protein-coding genes were detected in initial, intermediate, and advanced AD stages respectively (Supplementary table 2). In our sample set, the distribution between up-regulated and down-regulated protein coding-genes was very similar across AD grading (Figure 3A). As expected, we detected a substantial heterogeneity within the same Braak staging. This may be due to unpredictable confounders such as clinical, environmental, behavioral and agonal factors (i.e medication, substance abuse and health status prior to death) [21]. However, 10 genes were modulated across all stages (Figure 3B), suggesting a potential role during AD progression (Table 2), although we can not discard that this subset of olfactory genes may be also primary related to the neurodegenerative process that occur in other neurodegenerative diseases with common smell impairment. Some of these genes are involved in synaptic plasticity (*EGFLAM*), zinc transporter (*SLC39A11*), retinoid carrier (*LCN10*), and sodium and carbohydrate transport (*SLC5A11*). Other differential expressed genes overlapped between initial-intermediate stages, intermediate-advanced stages, and initial-advanced stages (Table 2). We have investigated whether the differential OB transcriptomic fingerprint has been partially reflected in previous transcriptomic studies performed in different brain structures across AD pathology [15, 22-27]. According to our integrative meta-analysis (Supplementary table 3), most of the differential OB genes have not been previously proposed as differential molecular features in hippocampal structures affected by the disease, serving as a foundation for new areas of investigation into the role of olfactory signaling in human AD. However, due to the OB pathology correlates with cortical AD pathology [7-9], we compared our differential gene sets with the differential expressed genome that previously showed significant expression correlation to Braak stage and cerebral atrophy in prefrontal cortex from AD subjects [16]. Thirteen OB differential genes in

initial stages (*KLC1, RAB7L1, C8orf46, GRM8, DCC, TMEM9, DDA1, HPCAL1, C15orf37, SYT13, VIP, RGS4, SST*), seven differential expressed OB genes in intermediate stages (*OR2T2, LOR, DCLRE1C, HMOX2, UBE2NL, SYT13*), and eight differential OB genes in advanced stages (*ZNF443, PHF17, CEP68, UIMC1, SMAD5, ELF1, PTPN2, CASP1*) present a significant expression correlation to Braak staging at cortical level [16]. Moreover, twenty OB early-deregulated genes (*C15orf37, C8orf46, DCC, DDA1, GIMAP7, GRM8, HPCAL1, KLC1, PDE10A, RASAL1, RGS4, SST,TMEM204, TMEM9, VIP, TMSB15B, RAB7L1, SYT13, EGFLAM, SLC39A11*), sixteen OB intermediate-affected genes (*TMSB15B, RAB7L1, SYT13, ESAM, EGFLAM, SLC39A11, CTXN3, DCLRE1C, GTF3C6, HLA-DRA, HMOX2, LOR, NBPF1, OR2T2, RASL11B, SNRPN*), and fifteen OB advanced-deregulated genes (*EGFLAM, SLC39A11, ESAM, CASP1, CD58, CEP68, CHRM4, ELF1, PHF17, PTPN2, SERPINH1, SMAD5, TUBA1A, UIMC1, ZNF443*) showed a good correlation with cerebral atrophy [16]. Although our stage-dependent analysis presents a limited number of study population, these data shed new light on the potential coordinated regulation of specific gene modules across AD-related brain structures, reinforcing the molecular correlation between OB and cortical AD pathology beyond the presence and distribution of beta-amyloid and phospho-Tau protein [7-9]. Using data mining-based methods for proteome-scale protein-protein interaction predictions [28], we have generated the potential interactome for human APP (β-amyloid precursor protein) and Tau protein (Supplementary table 4), detecting some OB differentially expressed protein-coding genes as potential APP and/or Tau interactors. Specifically, differentially expressed genes in initial stages like *RASAL1*, *TUBB4A*, and *BTK* genes are potential APP interactors, whereas *MAPK8IP1*, and *HSPA1B* genes (deregulated in advanced stages) may be potential Tau interactors. Although these predictive assumptions should be experimentally validated, this information may be useful to generate new working hypothesis to clarify the relationship between both neuropathologic substrates in AD at olfactory level. *KLC1* gene (Kinesin 2) is a common interactor between both neuropathological substrates (Supplementary table 4). Moreover, *RASAL1*, *TUBB4A*, and *KLC1* are also deregulated in cortical areas from AD patients

[24, 27], being *KLC1* a modifier of the beta-amyloid accumulation [29]. Interestingly, kinesin 2 protein levels were significantly increased in the OB from initial and advanced AD stages (Supplementary Figure 1). In addition, *HSPA1B* gene (up-regulated in advanced AD at the level of OB) is also up-regulated at protein level in hippocampus from AD subjects [30]. *RASAL1* and *TUBB4A* genes (up-regulated in initial AD at the level of OB) are down-regulated in hippocampal proteome at all pathologic stages of AD [30]. All these evidences suggest that AD pathology modulates the gene/protein expression of most APP and Tau interactors mentioned in this study in a spatial and stage-dependent manner across AD brains.

		INITIAL AD		INTERMEDIATE AD		ADVANCED AD	
Gene name	Gene description	p-Val	FC	p-Val	FC	p-Val	FC
EGFLAM	EGF-like, fibronectin type III and laminin G domains	0.002	0.48	0.003	0.48	0.009	0.55
LOC391636	chromosome 9 open reading frame 78 pseudogene	0.000	0.55	0.003	0.62	0.000	0.57
RN5S344	RNA, 5S ribosomal 344	0.003	0.60	0.003	0.59	0.000	0.41
SCARNA2	small Cajal body-specific RNA 2	0.004	0.72	0.002	0.68	0.010	0.25
FLJ39739	uncharacterized FLJ39739	0.007	1.33	0.005	1.37	0.004	1.37
MRPL23-AS1	MRPL23 antisense RNA 1 (non-protein coding)	0.004	1.34	0.009	1.32	0.000	1.53
SLC39A11	solute carrier family 39 (metal ion transporter), member 11	0.002	1.54	0.001	1.70	0.000	1.98
LCN10	lipocalin 10	0.009	1.61	0.002	1.82	0.000	2.00
CCHCR1	coiled-coil alpha-helical rod protein 1	0.000	1.74	0.004	1.48	0.004	1.46
SLC5A11	solute carrier family 5 (sodium/glucose cotransporter), member 11	0.001	2.30	0.002	2.30	0.010	1.89
TMSB15B	thymosin beta 15B	0.006	0.72	0.006	0.71	n.s	n.s
SLIT3	slit homolog 3 (Drosophila)	0.005	1.46	0.008	1.45	n.s	n.s
RNU7-76P	RNA, U7 small nuclear 76 pseudogene	0.003	1.54	0.010	1.47	n.s	n.s
HCRTR1	hypocretin (orexin) receptor 1	0.003	1.55	0.007	1.51	n.s	n.s
TMEM186	transmembrane protein 186	0.006	1.55	0.008	1.55	n.s	n.s
RAB7L1	RAB7, member RAS oncogene family-like 1	0.003	1.58	0.007	1.52	n.s	n.s
SYT13	synaptotagmin XIII	0.002	1.74	0.010	1.57	n.s	n.s
SNORD116-27	small nucleolar RNA, C/D box 116-27	n.s	n.s	0.000	0.42	0.003	0.53
YTHDC1	YTH domain containing 1	n.s	n.s	0.008	0.56	0.006	0.56
TREX2	three prime repair exonuclease 2	n.s	n.s	0.002	0.59	0.002	0.60
TK2	thymidine kinase 2, mitochondrial	n.s	n.s	0.001	0.61	0.007	0.68
IP6K3	inositol hexakisphosphate kinase 3	n.s	n.s	0.004	1.40	0.004	1.38
ESAM	endothelial cell adhesion molecule	n.s	n.s	0.006	1.44	0.005	1.44
RRP7B	ribosomal RNA processing 7 homolog B (S. cerevisiae)	0.006	0.20	n.s	n.s	0.001	0.11
SNORA36B	small nucleolar RNA, H/ACA box 36B	0.001	0.36	n.s	n.s	0.001	0.38
ZNF45	zinc finger protein 45	0.009	0.73	n.s	n.s	0.004	0.70
PPP1R13L	protein phosphatase 1, regulatory subunit 13 like	0.006	1.34	n.s	n.s	0.002	1.40

Table 2. Common differentially expressed genes across AD staging.

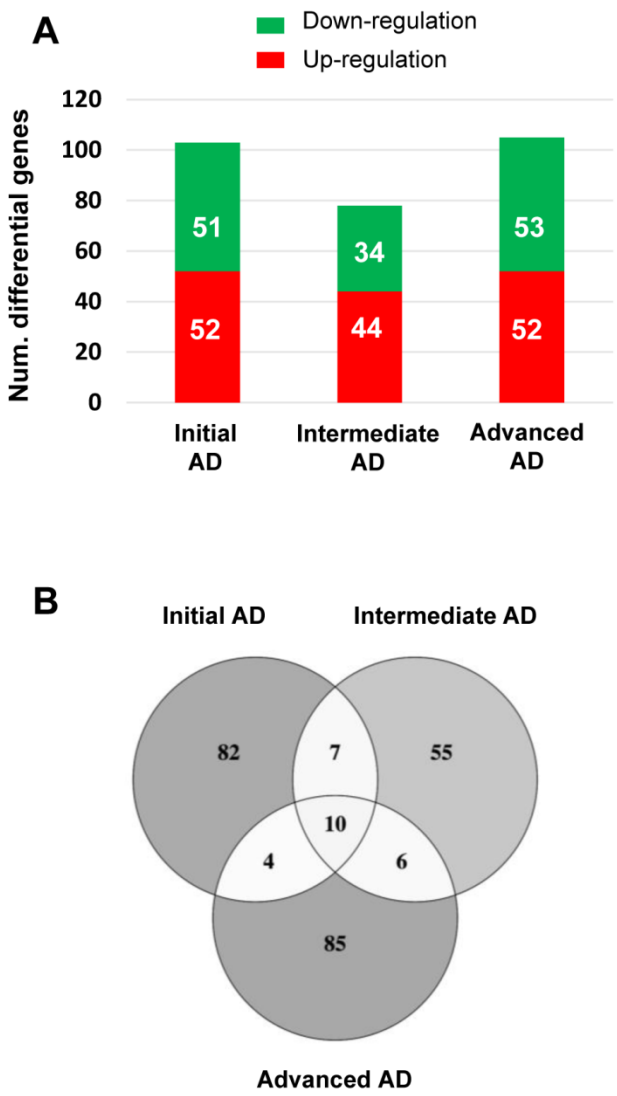

Figure 3. Differentially expressed genes in the OB across AD-related phenotypes. A) Differential olfactory transcriptome distribution across AD stages. B) Venn diagram of common and unique differential genes between AD stages. The distribution of common and distinct protein-coding genes in low, intermediate, and high AD stages is shown.

Although the analysis of the OB transcriptome provides a unique window into their biochemistry and dysfunction across AD stages, there are potential limitations of our study that warrant discussion. We have processed all cellular layers present in the bulk OB, giving novel insight into the gene-expression in this olfactory area. However, the OB is composed by intermixed multiple cell types with intricate architecture and connectivity [31], and information about specific-cell

types where mRNAs originated from is lost in our dataset. The implementation of novel workflows that allow the exploration of olfactory cell-type specific transcriptomes [32] would complement the output of our nonbiased profiling of the OB transcriptome, minimizing the effect of multiple neuronal microenvironments, and deciphering the specific role of each olfactory neuronal population during AD progression.

Progressive modulation of olfactory pathways across AD staging

To obtain a functional genomic perspective, differential transcriptomes were analyzed for higher-level organization of genes into common biological pathways using the Reactome database [33] (Supplementary table 5). As shown in Figure 4, our results point out a stage-dependent deregulation of specific pathways. Gene clusters involved in hemostasis, metabolism of carbohydrates, and metabolism of proteins were mapped across AD stages (Figure 4A), confirming previous observations obtained at protein level using proteomic workflows [34]. Moreover, a de-regulation of genes involved in signal transduction, immune system, and molecular transport was also evidenced across AD staging (Figure 4A), reinforcing the idea that cellular signaling and neuroinflammation are common driving forces of AD pathology across brain structures [12]. Gastrin-CREB signaling is involved in neurogenesis and cognitive impairment at hippocampal level [35], suggesting that the slight alteration in this pathway in initial-intermediate stages (Figure 4B) might play a role in the disruption of olfactory neurogenesis that occur in AD [36]. In addition, OB *HLA-DR* genes involved in MHC class II presentation pathway were up-regulated in intermediate stages (Figure 4B), in accordance with previous transcriptomic experiments performed in cortical structures from AD patients [16, 24, 27]. In line with these findings, an increase in HLA-DR immunopositive microglia across all layers of the cortex has been detected in post-mortem AD brains [37]. A deregulation of sensory perception of smell has been proposed from transcriptomic information extracted from prefrontal cortex derived from AD subjects [16]. Accordingly, olfactory receptor (OR) gene

dysregulation has been demonstrated in entorhinal and frontal cortex during AD progression [38]. In our case, we found several de-regulated OR genes during AD progression at the level of OB (Figure 4B). In particular, *OR5M1*, and *OR2T2* genes were down-regulated in intermediate stages, while *OR2T8*, and *OR6J1* genes were over-expressed in advanced stages (supplementary table 2). These data suggest that the presence of neuropathological substrates at the level of OB triggers a minor alteration in the OR transcriptome across AD stages, being necessary further developments that enable the analysis of OR family at protein level in the context of AD [11, 39, 40]. Moreover, a slight deregulation of a subset of functional categories was observed in specific AD stages. As shown in Figure 4C, degradation of extracellular matrix, signaling by PDGF, and DAP12 were specifically mapped in initial stages. In line with our observations, gene modules regulated by PDGF, and DAP12 (or TYROBP) are disrupted in cortical structures from AD subjects [16]. Specifically, TYROBP expression is restricted to cells involved in the innate immunity [41], and is one of the causal regulator of the activated immune system network in late-onset AD [16]. On the other hand, metabolism of lipids, and aminoacids together with TCR signaling by ZAP-70 were exclusively detected in intermediate stages (Figure 4C). In advanced stages, gene clusters related to transcription, HSF1 activation, and ER to Golgi transport were specifically deregulated (Figure 4C).

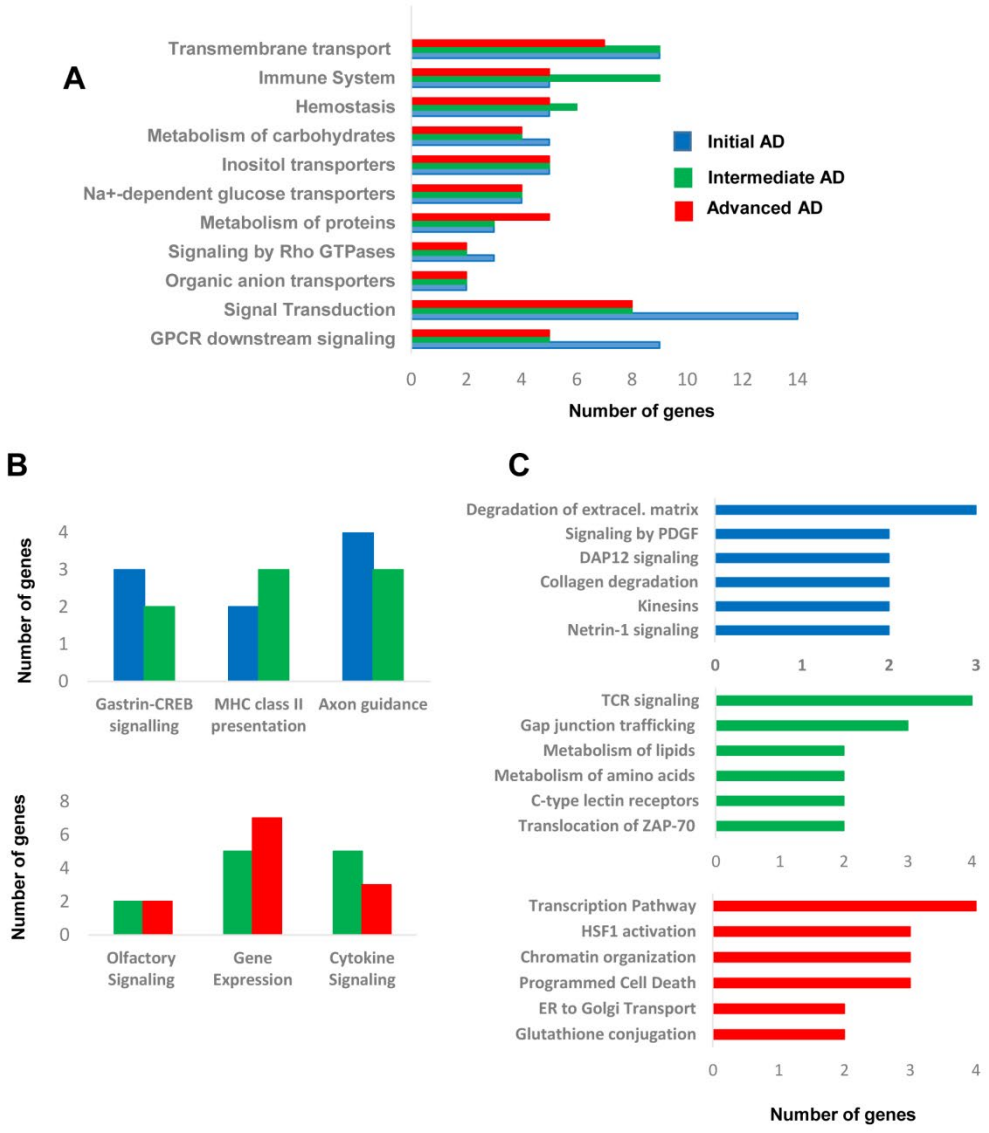

Figure 4. Functional metrics of the differential OB transcriptome across AD staging. Specific pathway analysis for the differential OB transcriptome detected in each AD stage is shown. Blue, green, and red bars correspond to functional deregulated categories in low, intermediate, and high AD stages respectively.

Modulation of gene interactome networks in the OB across AD stages

To explore the cooperative action among differentially expressed genes, we performed gene-scale interaction networks merging the olfactory genes that tend to be de-regulated across AD staging. Using IPA software, a gene interactome map has been constructed for each AD stage

(Figures 5-7). In this case, the integrative network-based approach allowed us to: i) elucidate the biological function and molecular context of the deregulated genes in each neuropathological stage, ii) establish a framework to map interaction between deregulated genes and network modules across AD grading, and iii) to define potential causal regulators of the stage-dependent networks that may be considered as gene targets to modulate the disease progression at olfactory level. In initial AD stages, the top deregulated pathways proposed by IPA were estrogen biosynthesis (p-value: 7,12E-03), cAMP-mediated signaling (p-value: 1,02E-02), and Gi Signaling (p-value: 1,15E-02), suggesting a central function of EGFR in the functional network (Figure 5). In intermediate stages, communication between innate and adaptive immune cells (p-value. 1,59E-03), and antigen presentation pathway (p-value: 5,02E-03) were the top deregulated pathways, being TGF-beta, and CREB1 potential nodes of the network (Figure 6). In advanced stages, the functional module composed by STAT3, c-Jun, and APP nodes appears as one of the main axis in the network (Figure 7).

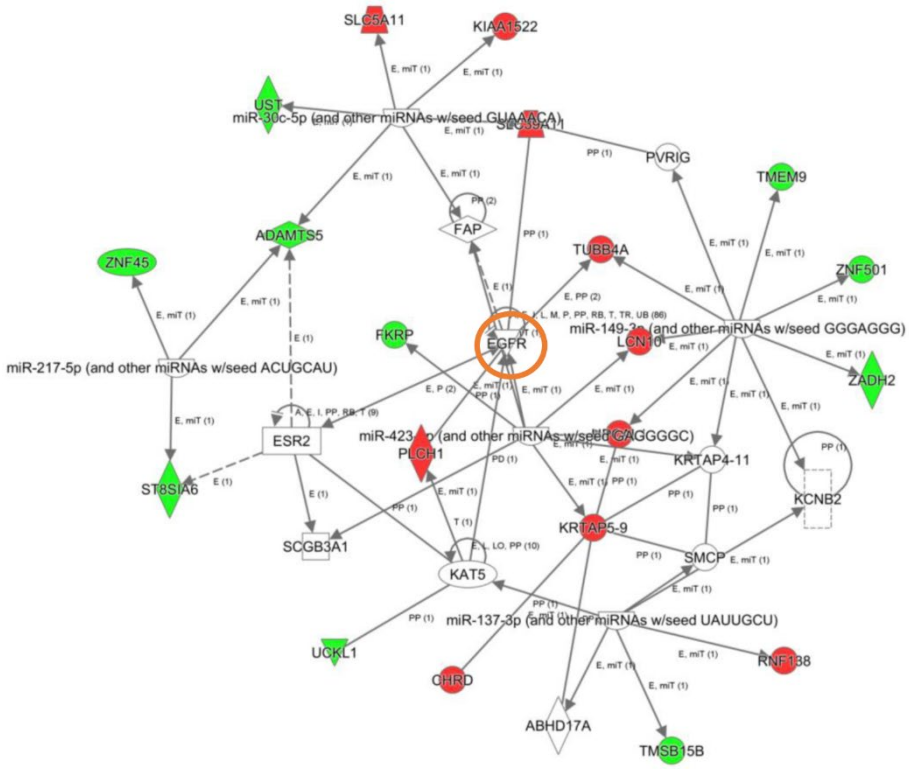

Figure 5. High-scoring gene interactome map for early differentially expressed genes in the OB during AD progression. Visual representation of the relationships between differential expressed genes and functional interactors in low stage. Dysregulated genes are highlighted in red (up-regulated) and green (down-regulated). Continuous and discontinuous lines represent direct and indirect interactions respectively. The complete legend including main features, molecule shapes, and relationships is found at http://ingenuity.force.com/ipa/articles/Feature_Description/Legend.

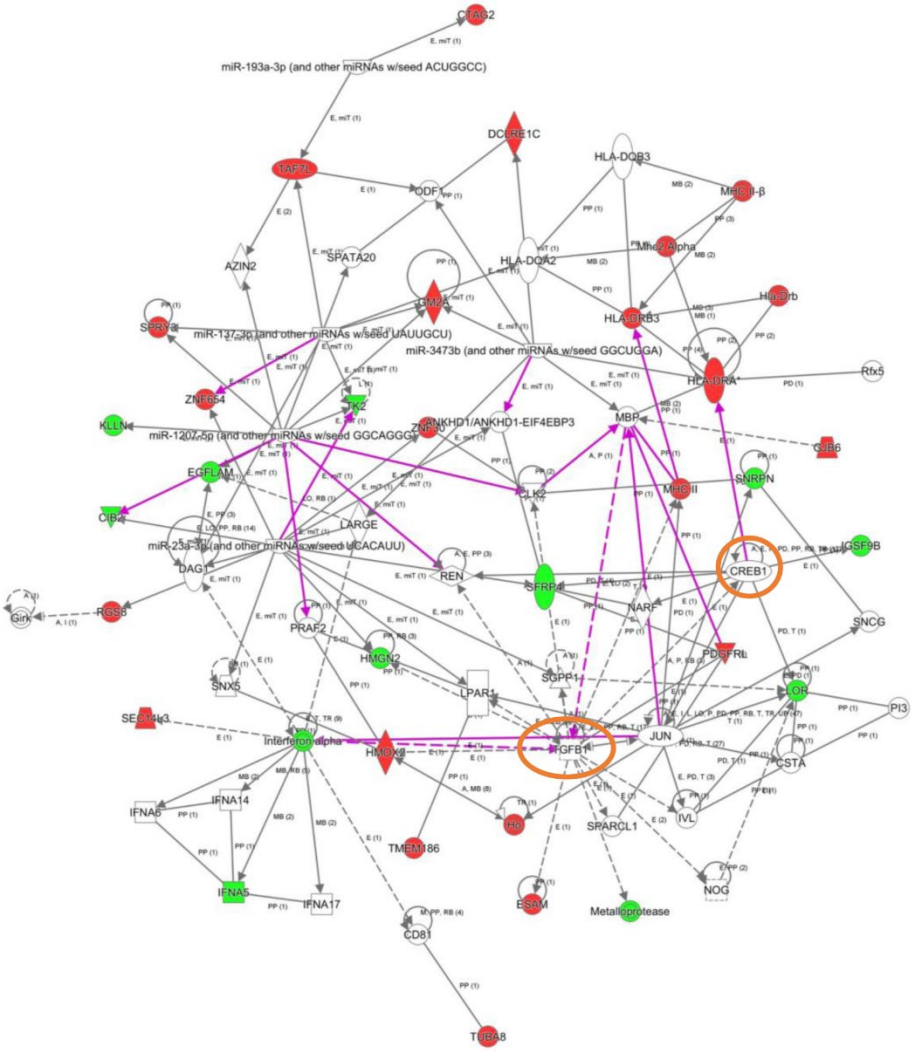

Figure 6. High-scoring gene interactome map for OB differentially expressed genes in intermediate AD stages. Visual representation of the relationships between differential expressed genes and functional interactors in intermediate stages. In this case, two networks were merged to facilitate the global interpretation (purple lines correspond to novel functional links after merging). Dysregulated genes are highlighted in red (up-regulated) and green (down-regulated). Continuous and discontinuous lines represent direct and indirect interactions respectively. The complete legend including main features, molecule shapes, and relationships may be found at http://ingenuity.force.com/ipa/articles/Feature_Description/Legend.

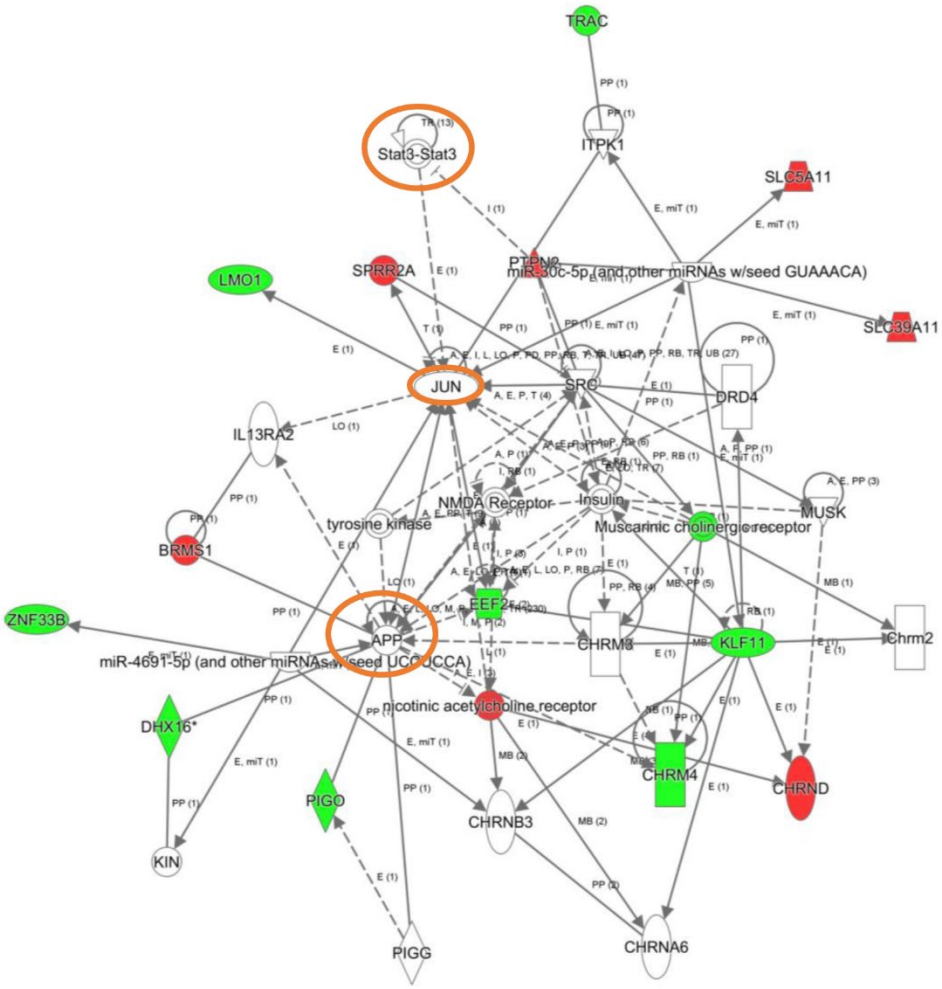

Figure 7. High-scoring gene interactome map for OB differentially expressed genes in high AD stages. Visual representation of the relationships between differential expressed genes and functional interactors is shown. Dysregulated genes are highlighted in red (up-regulated) and green (down-regulated). Continuous and discontinuous lines represent direct and indirect interactions respectively. The complete legend including main features, molecule shapes, and relationships may be found at http://ingenuity.force.com/ipa/articles/Feature_Description/Legend.

Protein expression of predictive interactome hubs across AD grading: Focus on olfactory EGFR, CREB1, TGF-beta, c-Jun and STAT3

Even though changes in their expression were not detected in our transcriptomic workflow, the alteration of some of their targets may be compatible with a dysregulation of their functionality during AD progression at the level of OB. For that, subsequent experiments were performed in

order to monitor the OB protein expression of these signal transducers across AD stages. Although a deficient EGFR signaling affects the OBs in mice, being necessary for olfactory learning, and discrimination [42-44], an increment in olfactory EGFR protein expression was significantly detected in initial and advanced AD stages (Figure 8). Interestingly, intense EGFR expression has been also observed in hippocampal and cortical neuritic plaques from patients with pathologically confirmed AD [45], suggesting that abnormal EGFR signaling could contribute to cognitive impairment in AD [46]. CREB1 is at a central converging point of activated pathways during the processes of synaptic strengthening and memory formation, and targeted therapeutic strategies focusing on augmentation of CREB-mediated transcription might prove beneficial for the enhancement of both processes in initial stages of AD [47-49]. Disruption of these mechanisms in AD results in a reduction of CREB1 activation with accompanying memory impairment [50, 51]. At olfactory level, most of the well-known activity-dependent CREB target genes such as *C-FOS*, *FOSB*, *BDNF*, *NR4A2*, and *EGR1* [50] were unchanged across AD stages (with the exception of *CYR61* that was up-regulated in advanced stages) (Supplementary table 2). This transcriptomic fingerprint might partially corroborate the unmodified activation state of phosphorylated CREB (Ser133) observed at olfactory level during AD progression (Supplementary Figure 2). In relation to the predictive findings observed in Figure 7, it has been proposed that activated STAT3 is involved in the responsiveness of microglia to beta amyloid [52], being a common inducer of astrocyte reactivity in AD [53]. Moreover, STAT3 has been recently proposed as an upstream regulator in late onset AD at cortical level [27]. Accordingly, we observed an increment in the phosphorylation state of STAT3 (Y705) in advanced AD stages (Figure 8). In accordance with previous studies, the late STAT3 activation observed in the OB suggests an impairment in the differentiation process of olfactory neurons in advanced stages of the disease [54]. On the other hand, other hubs proposed by the interaction network analysis such as TGF-beta and c-Jun presented unmodified protein levels across AD grading (Supplementary Figure 2)

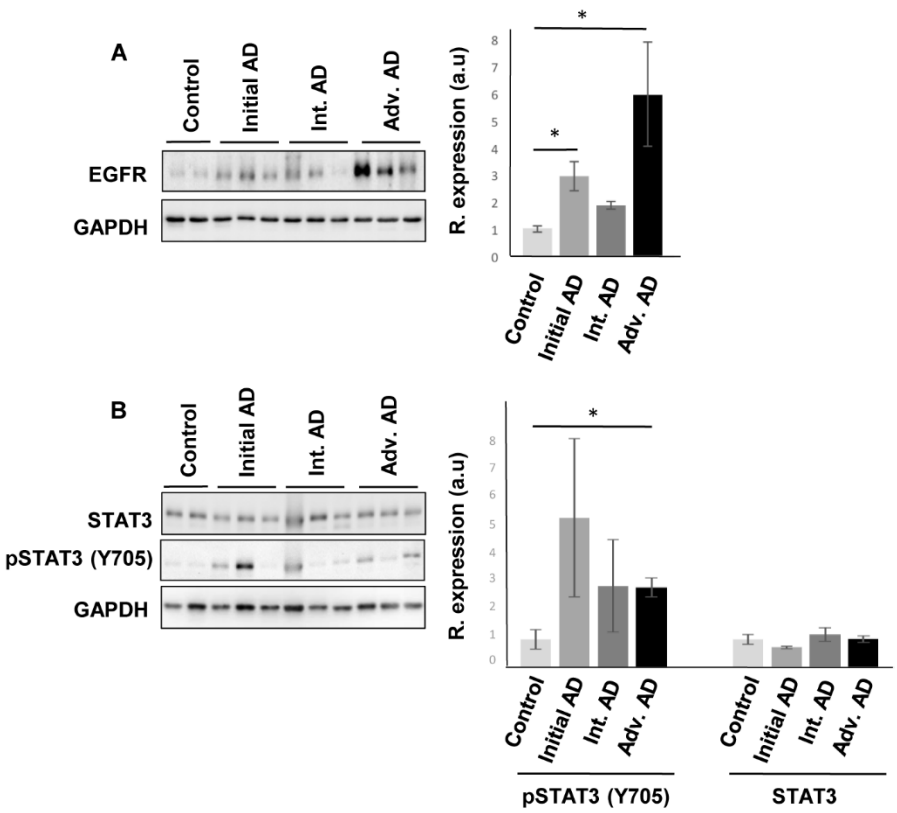

Figure 8. Olfactory bulb protein expression of EGFR, and STAT3 across AD staging. A) Representative Western blot gels to detect olfactory EGFR across AD grading. B) Protein expression of Total STAT3, and active STAT3 (Y705) in the OB during AD progression. Right panels shows histograms of band densities. Data are presented as mean ± SEM from 3 independent OB samples per group. *P < 0.05 vs control group.

Protein expression of olfactory EGFR, CREB1, TGF-beta, c-Jun and STAT3 across Alzheimer-related co-pathologies

In contrast to the common separate investigation of neurological diseases, targeted cross-disease studies comparing shared molecular relationships may give new insights into possible olfactory perturbations common for all or some neurological disorders. In order to detect novel molecular features shared by different Alzheimer-related co-pathologies at olfactory level, we have evaluated the OB protein expression of EGFR, CREB1, TGF-beta, c-Jun, and STAT3 across

several AD-related diseases (n=28 OB samples). We have included pathologies with common smell impairment like FTLD [55, 56], PSP where olfactory loss occurs to a lesser extent or is absent [2, 57, 58], and mixed dementia. Mixed dementia is a condition in which AD and vascular dementia occur at the same time, and both separate disorders often display olfactory dysfunction [59, 60]. As shown in Figure 9, EGFR protein levels were also increased in the OB derived from mixed dementia subjects (Figure 9A). As previously observed in AD, OB TGF-beta levels were unchanged across PSP, FTLD, and mixed dementia (Figure 9B). In contrast, OB protein levels of STAT3 and CREB1 were significantly increased only in mixed dementia, without apparent shifts in their activation status (Figure 9D and 9E). Differently from AD, olfactory c-Jun protein levels were exclusively increased in mixed dementia (Figure 9C). c-Jun up-regulation has also been reported in entorhinal cortex and hippocampus from AD subjects and also in AD transgenic mice [61-63]. Mechanistically, the c-Jun N terminal kinase (JNK)/c-Jun cascade exerts its influence in aberrant processes of AD pathogenesis such as Tau hyperphosphorylation, amyloid aggregation, and synaptic dysfunction in murine models of AD [64-66]. According to previous studies [67, 68], the c-Jun overexpression observed in the OB of mixed dementia subjects could contribute to some AD-related neuropathologies present in vascular dementia such as beta amyloid-induced neuroinflammation and vascular insufficiencies.

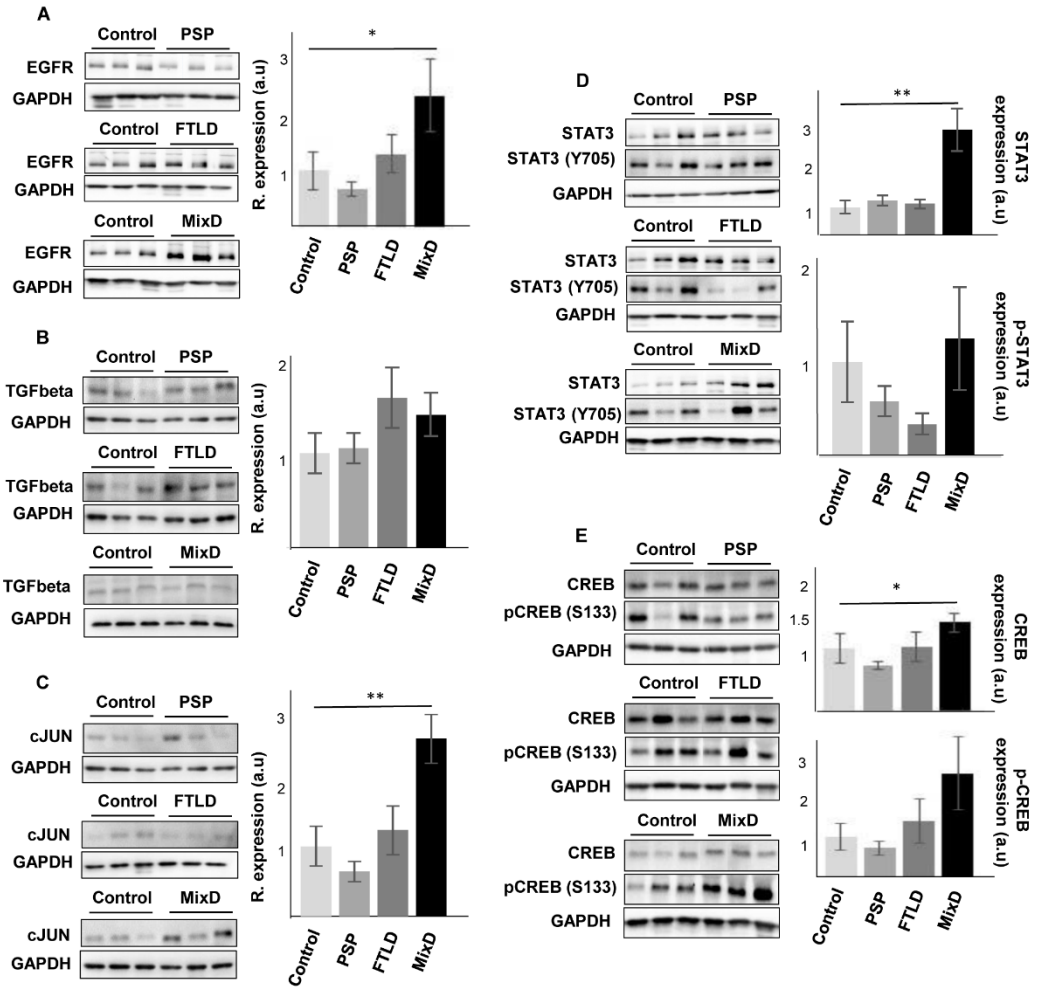

Figure 9. Olfactory bulb protein expression of EGFR, CREB1, TGF-beta, c-Jun and STAT3 across proteinopathies. OB Protein expression was documented by Western blot. a) EGFR expression, b) TGF-beta expression, c) c-Jun expression, d) STAT3/phospho-STAT3 (Y705) expression, and e) CREB/phospho-CREB (S133) expression, in PSP, FTLD, and mixed dementia subjects. Graphs represent histograms of band densities. Data are presented as mean ± SEM from: Controls (n = 4 cases), PSP (n = 9 cases), FTLD (n = 6 cases), and mixed dementia (mix AD VD) (n = 9 cases). *P < 0.05 vs control group; ** P < 0.01 vs control group.

Conclusion

Summing up, we have performed a stage-dependent comprehensive analysis of differential expression of OB coding transcripts during AD progression. To the best of our knowledge, this is the first study to characterize in depth, potential AD-associated transcriptional changes in the human OB. We performed gene set enrichment analysis to find the most relevant pathways and gene regulatory networks that are progressively modulated during AD progression. More importantly, using a discovery platform combining neuropathological diagnosis, OB transcriptome exploration, functional interaction data, together with a cross-disease analysis, a divergent olfactory expression of specific signal transducers has been observed across AD-related co-pathologies, serving as a foundation for new research areas into the role of olfactory signaling across different types of dementias.

Materials and methods

Materials - The following antibodies and materials were used: anti-GAPDH (Calbiochem), anti-EGFR (Millipore), anti-CREB, anti-phospho CREB (S133), anti-STAT3, anti-phospho STAT3 (Y705), anti-c-Jun (Cell signaling), and anti-TGF-beta (Abcam). Electrophoresis reagents were purchased from Biorad.

Human samples - According to the Spanish Law 14/2007 of Biomedical Research, inform written consent form of the Neurological Tissue Bank of Navarra Health Service was obtained for research purposes from relatives of patients included in this study. The study was conducted in accordance with the Declaration of Helsinki and all assessments, post-mortem evaluations, and procedures were previously approved by the Clinical Ethics Committee of Navarra Health Service. Fourteen AD cases were distributed into different groups according to specific consensus diagnostic criteria [69-71]: low, intermediate, and high AD neuropathological changes (n = 4-5/group). Four cases from elderly subjects with no history or histological findings of any neurological disease were used as a control group. All human brains considered in this study had a post-mortem interval (PMI) lower than 10 hours (Table 1). Brain processing and the neuropathological study for protein deposits aggregates beta-amyloid and phospho-Tau were performed as previously described [34]. For the discovery phase, neuropathological assessment was performed according to standardized neuropathological scoring/grading systems, including Thal phases of beta-amyloid deposition, Braak staging of neuro fibrillary lesions, Consortium to Established a Registry for Alzheimer's Disease, National Institute on Aging-Alzheimer's Association (NIA-AA) guidelines, and primary age-related tauopathy (PART) criteria [69-73]. For the cross-disease analysis, different clinical backgrounds were considered: Progressive supranuclear palsy (PSP) (n = 9 cases; 4F/5M; median age: 74 years), frontotemporal lobar degeneration (FTLD) (n = 6; 3F/3M; median age: 81 years), mixed dementia (mix AD VD) (n = 9 cases; 4F/5M; median age: 85 years), and additional controls (n = 4; 1F/3M; median age: 80

years). In these cases, neuropathological assessment was performed according to standardized neuropathological guidelines: Mackenzie criteria for FTLD pathology [74], NINDS-AIREN criteria for vascular dementia [75], and NINDS criteria for PSP [76]. 80% of the OB samples included in the cross-disease phase had a PMI lower than 10 hours (Supplementary Table 1).

Microarray hybridization and data analysis - For OB mRNA extraction, the Maxwell® 16 simplyRNA Kit (Promega) was used. The sense cDNA was prepared from 1 ng of total RNA and then fragmented and biotinylated using Affymetrix GeneChip® WT Pico Kit (PN902623). Labeled sense cDNA was hybridized to the Affymetrix Human Gene 2.0 ST chip according to the manufacturer protocols and using GeneChip® Hybridization, Wash and Stain Kit. Genechips were scanned with the Affymetrix GeneChip® Scanner 3000. For microarray data analysis, both background correction and normalization were done using RMA (Robust Multichip Average) algorithm [77]. Then, a filtering process was performed to eliminate low expression probe sets. Applying the criterion of an expression value of 16 in at least 2 samples for each experimental condition, 28353 probe sets were selected. R/Bioconductor was used for preprocessing and statistical analysis. For analysis of genes related to pathological changes, individuals with AD pathology were compared to non-demented controls. LIMMA (Linear Models for Microarray Data) was used to find out the probe sets that showed significant differential expression between controls and AD stages. We first used a threshold criteria of False Discovery Rate (FDR) < 5% to select differentially expressed genes. As in other transcriptomic studies performed in AD brains [15, 78], we did not achieve significant results using this criteria, so we worked with a p-value < 0.01 (without using any method for multiple testing correction). Microarray data files were submitted to the GEO (Gene Expression Omnibus) database and are available under accession number GSE93885.

The differential expression of RNAs was functionally analyzed through the use of Reactome [33], and QIAGEN's Ingenuity® Pathway Analysis (IPA) (QIAGEN Redwood City,

www.qiagen.com/ingenuity), in order to detect and infer differentially activated/deactivated pathways as a result of AD phenotypes. IPA software comprises curated information from databases of experimental and predictive origin, enabling discovery of highly represented functions, pathways, and interactome networks.

Western blotting - Equal amounts of protein (10 µg) were resolved in 12.5% SDS-PAGE gels. OB proteins derived from human samples were electrophoretically transferred onto nitrocellulose membranes for 45 min at 120 V. Equal loading of the gels was assessed by Ponceau staining. Membranes were probed with primary antibodies at 1:1000 dilution in 5% nonfat milk or BSA. After incubation with the appropriate horseradish peroxidase-conjugated secondary antibody (1:5000), antibody binding was detected by a Chemidoc™MP Imaging System (Bio-Rad) after incubation with an enhanced chemiluminescence substrate (Perkin Elmer). All Band intensities were measured with Image Lab Software Version 5.2 (Bio-Rad) and normalized to GAPDH.

References

1. Bahar-Fuchs A, Chetelat G, Villemagne VL, Moss S, Pike K, Masters CL, Rowe C and Savage G. Olfactory deficits and amyloid-beta burden in Alzheimer's disease, mild cognitive impairment, and healthy aging: a PiB PET study. J Alzheimers Dis. 2010; 22(4):1081-1087.

2. Attems J, Walker L and Jellinger KA. Olfactory bulb involvement in neurodegenerative diseases. Acta Neuropathol. 2014; 127(4):459-475.

3. Doty RL. The olfactory vector hypothesis of neurodegenerative disease: is it viable? Ann Neurol. 2008; 63(1):7-15.

4. Thomann PA, Dos Santos V, Seidl U, Toro P, Essig M and Schroder J. MRI-derived atrophy of the olfactory bulb and tract in mild cognitive impairment and Alzheimer's disease. J Alzheimers Dis. 2009; 17(1):213-221.

5. Forster S, Vaitl A, Teipel SJ, Yakushev I, Mustafa M, la Fougere C, Rominger A, Cumming P, Bartenstein P, Hampel H, Hummel T, Buerger K, Hundt W and Steinbach S. Functional representation of olfactory impairment in early Alzheimer's disease. J Alzheimers Dis. 2010; 22(2):581-591.

6. Kovacs T, Cairns NJ and Lantos PL. Olfactory centres in Alzheimer's disease: olfactory bulb is involved in early Braak's stages. Neuroreport. 2001; 12(2):285-288.

7. Attems J and Jellinger KA. Olfactory tau pathology in Alzheimer disease and mild cognitive impairment. Clin Neuropathol. 2006; 25(6):265-271.

8. Arnold SE, Lee EB, Moberg PJ, Stutzbach L, Kazi H, Han LY, Lee VM and Trojanowski JQ. Olfactory epithelium amyloid-beta and paired helical filament-tau pathology in Alzheimer disease. Ann Neurol. 2010; 67(4):462-469.

9. Talamo BR, Rudel R, Kosik KS, Lee VM, Neff S, Adelman L and Kauer JS. Pathological changes in olfactory neurons in patients with Alzheimer's disease. Nature. 1989; 337(6209):736-739.

10. Lotsch J, Schaeffeler E, Mittelbronn M, Winter S, Gudziol V, Schwarzacher SW, Hummel T, Doehring A, Schwab M and Ultsch A. Functional genomics suggest neurogenesis in the adult human olfactory bulb. Brain Struct Funct. 2014.

11. Lachen-Montes M, Fernandez-Irigoyen J and Santamaria E. Deconstructing the molecular architecture of olfactory areas using proteomics. Proteomics Clin Appl. 2016; 10(12):1178-1190.

12. Cooper-Knock J, Kirby J, Ferraiuolo L, Heath PR, Rattray M and Shaw PJ. Gene expression profiling in human neurodegenerative disease. Nat Rev Neurol. 2012; 8(9):518-530.

13. Katsel P, Li C and Haroutunian V. Gene expression alterations in the sphingolipid metabolism pathways during progression of dementia and Alzheimer's disease: a shift toward ceramide accumulation at the earliest recognizable stages of Alzheimer's disease? Neurochem Res. 2007; 32(4-5):845-856.

14. Katsel P, Tan W and Haroutunian V. Gain in brain immunity in the oldest-old differentiates cognitively normal from demented individuals. PLoS One. 2009; 4(10):e7642.

15. Silva AR, Grinberg LT, Farfel JM, Diniz BS, Lima LA, Silva PJ, Ferretti RE, Rocha RM, Filho WJ, Carraro DM and Brentani H. Transcriptional alterations related to neuropathology and clinical manifestation of Alzheimer's disease. PLoS One. 2012; 7(11):e48751.

16. Zhang B, Gaiteri C, Bodea LG, Wang Z, McElwee J, Podtelezhnikov AA, Zhang C, Xie T, Tran L, Dobrin R, Fluder E, Clurman B, Melquist S, Narayanan M, Suver C, Shah H, et al. Integrated systems approach identifies genetic nodes and networks in late-onset Alzheimer's disease. Cell. 2013; 153(3):707-720.

17. Rey NL, Wesson DW and Brundin P. The olfactory bulb as the entry site for prion-like propagation in neurodegenerative diseases. Neurobiol Dis. 2016.

18. Roberts RO, Christianson TJ, Kremers WK, Mielke MM, Machulda MM, Vassilaki M, Alhurani RE, Geda YE, Knopman DS and Petersen RC. Association Between Olfactory Dysfunction and Amnestic Mild Cognitive Impairment and Alzheimer Disease Dementia. JAMA Neurol. 2016; 73(1):93-101.

19. Zhu YY, Ni DF and Xu CM. Gene expression profiles in the olfactory bulb from a rat model of Alzheimer's disease. J Alzheimers Dis. 2009; 18(3):581-593.

20. Masurkar AV and Devanand DP. Olfactory Dysfunction in the Elderly: Basic Circuitry and Alterations with Normal Aging and Alzheimer's Disease. Curr Geriatr Rep. 2014; 3(2):91-100.

21. Leite RE and Grinberg LT. Closing the gap between brain banks and proteomics to advance the study of neurodegenerative diseases. Proteomics Clin Appl. 2015.

22. Xu PT, Li YJ, Qin XJ, Scherzer CR, Xu H, Schmechel DE, Hulette CM, Ervin J, Gullans SR, Haines J, Pericak-Vance MA and Gilbert JR. Differences in apolipoprotein E3/3 and E4/4 allele-specific gene expression in hippocampus in Alzheimer disease. Neurobiol Dis. 2006; 21(2):256-275.

23. Liang WS, Dunckley T, Beach TG, Grover A, Mastroeni D, Ramsey K, Caselli RJ, Kukull WA, McKeel D, Morris JC, Hulette CM, Schmechel D, Reiman EM, Rogers J and Stephan DA. Altered neuronal gene expression in brain regions differentially affected by Alzheimer's disease: a reference data set. Physiol Genomics. 2008; 33(2):240-256.

24. Parachikova A, Agadjanyan MG, Cribbs DH, Blurton-Jones M, Perreau V, Rogers J, Beach TG and Cotman CW. Inflammatory changes parallel the early stages of Alzheimer disease. Neurobiol Aging. 2007; 28(12):1821-1833.

25. Bossers K, Wirz KT, Meerhoff GF, Essing AH, van Dongen JW, Houba P, Kruse CG, Verhaagen J and Swaab DF. Concerted changes in transcripts in the prefrontal cortex precede neuropathology in Alzheimer's disease. Brain. 2010; 133(Pt 12):3699-3723.

26. Tan MG, Chua WT, Esiri MM, Smith AD, Vinters HV and Lai MK. Genome wide profiling of altered gene expression in the neocortex of Alzheimer's disease. J Neurosci Res. 2010; 88(6):1157-1169.

27. Li X, Long J, He T, Belshaw R and Scott J. Integrated genomic approaches identify major pathways and upstream regulators in late onset Alzheimer's disease. Sci Rep. 2015; 5:12393.

28. Kotlyar M, Pastrello C, Pivetta F, Lo Sardo A, Cumbaa C, Li H, Naranian T, Niu Y, Ding Z, Vafaee F, Broackes-Carter F, Petschnigg J, Mills GB, Jurisicova A, Stagljar I, Maestro R, et al. In silico prediction of physical protein interactions and characterization of interactome orphans. Nat Methods. 2015; 12(1):79-84.

29. Morihara T, Hayashi N, Yokokoji M, Akatsu H, Silverman MA, Kimura N, Sato M, Saito Y, Suzuki T, Yanagida K, Kodama TS, Tanaka T, Okochi M, Tagami S, Kazui H, Kudo T, et al. Transcriptome analysis of distinct mouse strains reveals kinesin light chain-1 splicing as an amyloid-beta accumulation modifier. Proc Natl Acad Sci U S A. 2014; 111(7):2638-2643.

30. Hondius DC, van Nierop P, Li KW, Hoozemans JJ, van der Schors RC, van Haastert ES, van der Vies SM, Rozemuller AJ and Smit AB. Profiling the human hippocampal proteome at all pathologic stages of Alzheimer's disease. Alzheimers Dement. 2016; 12(6):654-668.

31. Nagayama S, Homma R and Imamura F. Neuronal organization of olfactory bulb circuits. Front Neural Circuits. 2014; 8:98.

32. Lovatt D, Bell T and Eberwine J. Single-neuron isolation for RNA analysis using pipette capture and laser capture microdissection. Cold Spring Harb Protoc. 2015; 2015(1):pdb prot072439.

33. Fabregat A, Sidiropoulos K, Garapati P, Gillespie M, Hausmann K, Haw R, Jassal B, Jupe S, Korninger F, McKay S, Matthews L, May B, Milacic M, Rothfels K, Shamovsky V, Webber M, et al. The Reactome pathway Knowledgebase. Nucleic Acids Res. 2016; 44(D1):D481-487.

34. Zelaya MV, Perez-Valderrama E, de Morentin XM, Tunon T, Ferrer I, Luquin MR, Fernandez-Irigoyen J and Santamaria E. Olfactory bulb proteome dynamics during the progression of sporadic Alzheimer's disease: identification of common and distinct olfactory targets across Alzheimer-related co-pathologies. Oncotarget. 2015; 6(37):39437-39456.

35. Walton NM, de Koning A, Xie X, Shin R, Chen Q, Miyake S, Tajinda K, Gross AK, Kogan JH, Heusner CL, Tamura K and Matsumoto M. Gastrin-releasing peptide contributes to the regulation of adult hippocampal neurogenesis and neuronal development. Stem Cells. 2014; 32(9):2454-2466.

36. Horgusluoglu E, Nudelman K, Nho K and Saykin AJ. Adult neurogenesis and neurodegenerative diseases: A systems biology perspective. Am J Med Genet B Neuropsychiatr Genet. 2016; 174(1):93-112.

37. Narayan PJ, Lill C, Faull R, Curtis MA and Dragunow M. Increased acetyl and total histone levels in post-mortem Alzheimer's disease brain. Neurobiol Dis. 2015; 74:281-294.

38. Ansoleaga B, Garcia-Esparcia P, Llorens F, Moreno J, Aso E and Ferrer I. Dysregulation of brain olfactory and taste receptors in AD, PSP and CJD, and AD-related model. Neuroscience. 2013; 248:369-382.

39. Xu A, Li G, Yang D, Wu S, Ouyang H, Xu P and He F. Evolutionary Characteristics of Missing Proteins: Insights into the Evolution of Human Chromosomes Related to Missing-Protein-Encoding Genes. J Proteome Res. 2015; 14(12):4985-4994.

40. Choong WK, Chang HY, Chen CT, Tsai CF, Hsu WL, Chen YJ and Sung TY. Informatics View on the Challenges of Identifying Missing Proteins from Shotgun Proteomics. J Proteome Res. 2015; 14(12):5396-5407.

41. Schleinitz N, Chiche L, Guia S, Bouvier G, Vernier J, Morice A, Houssaint E, Harle JR, Kaplanski G, Montero-Julian FA and Vely F. Pattern of DAP12 expression in leukocytes from both healthy and systemic lupus erythematosus patients. PLoS One. 2009; 4(7):e6264.

42. Wagner B, Natarajan A, Grunaug S, Kroismayr R, Wagner EF and Sibilia M. Neuronal survival depends on EGFR signaling in cortical but not midbrain astrocytes. EMBO J. 2006; 25(4):752-762.

43. Rahn T, Leippe M, Roeder T and Fedders H. EGFR signaling in the brain is necessary for olfactory learning in Drosophila larvae. Learn Mem. 2013; 20(4):194-200.

44. Enwere E, Shingo T, Gregg C, Fujikawa H, Ohta S and Weiss S. Aging results in reduced epidermal growth factor receptor signaling, diminished olfactory neurogenesis, and deficits in fine olfactory discrimination. J Neurosci. 2004; 24(38):8354-8365.

45. Birecree E, Whetsell WO, Jr., Stoscheck C, King LE, Jr. and Nanney LB. Immunoreactive epidermal growth factor receptors in neuritic plaques from patients with Alzheimer's disease. J Neuropathol Exp Neurol. 1988; 47(5):549-560.

46. Hochstrasser T, Ehrlich D, Marksteiner J, Sperner-Unterweger B and Humpel C. Matrix metalloproteinase-2 and epidermal growth factor are decreased in platelets of Alzheimer patients. Curr Alzheimer Res. 2012; 9(8):982-989.

47. Sakamoto K, Karelina K and Obrietan K. CREB: a multifaceted regulator of neuronal plasticity and protection. J Neurochem. 2011; 116(1):1-9.

48. Tully T, Bourtchouladze R, Scott R and Tallman J. Targeting the CREB pathway for memory enhancers. Nat Rev Drug Discov. 2003; 2(4):267-277.

49. Teich AF, Nicholls RE, Puzzo D, Fiorito J, Purgatorio R, Fa M and Arancio O. Synaptic therapy in Alzheimer's disease: a CREB-centric approach. Neurotherapeutics. 2015; 12(1):29-41.

50. Saura CA. CREB-regulated transcription coactivator 1-dependent transcription in Alzheimer's disease mice. Neurodegener Dis. 2012; 10(1-4):250-252.

51. Saura CA and Valero J. The role of CREB signaling in Alzheimer's disease and other cognitive disorders. Rev Neurosci. 2011; 22(2):153-169.

52. Eufemi M, Cocchiola R, Romaniello D, Correani V, Di Francesco L, Fabrizi C, Maras B and Schinina ME. Acetylation and phosphorylation of STAT3 are involved in the responsiveness of microglia to beta amyloid. Neurochem Int. 2015; 81:48-56.

53. Ben Haim L, Ceyzeriat K, Carrillo-de Sauvage MA, Aubry F, Auregan G, Guillermier M, Ruiz M, Petit F, Houitte D, Faivre E, Vandesquille M, Aron-Badin R, Dhenain M, Deglon N, Hantraye P, Brouillet E, et al. The JAK/STAT3 pathway is a common inducer of astrocyte reactivity in Alzheimer's and Huntington's diseases. J Neurosci. 2015; 35(6):2817-2829.

54. Yu Y, Ren W and Ren B. Expression of signal transducers and activator of transcription 3 (STAT3) determines differentiation of olfactory bulb cells. Mol Cell Biochem. 2009; 320(1-2):101-108.

55. Luzzi S, Snowden JS, Neary D, Coccia M, Provinciali L and Lambon Ralph MA. Distinct patterns of olfactory impairment in Alzheimer's disease, semantic dementia, frontotemporal dementia, and corticobasal degeneration. Neuropsychologia. 2007; 45(8):1823-1831.

56. McLaughlin NC and Westervelt HJ. Odor identification deficits in frontotemporal dementia: a preliminary study. Arch Clin Neuropsychol. 2008; 23(1):119-123.

57. Doty RL. Olfactory dysfunction in Parkinson disease. Nat Rev Neurol. 2012; 8(6):329-339.

58. Hoyles K and Sharma JC. Olfactory loss as a supporting feature in the diagnosis of Parkinson's disease: a pragmatic approach. J Neurol. 2013; 260(12):2951-2958.

59. Alves J, Petrosyan A and Magalhaes R. Olfactory dysfunction in dementia. World J Clin Cases. 2014; 2(11):661-667.

60. Gray AJ, Staples V, Murren K, Dhariwal A and Bentham P. Olfactory identification is impaired in clinic-based patients with vascular dementia and senile dementia of Alzheimer type. Int J Geriatr Psychiatry. 2001; 16(5):513-517.

61. Anderson AJ, Su JH and Cotman CW. DNA damage and apoptosis in Alzheimer's disease: colocalization with c-Jun immunoreactivity, relationship to brain area, and effect of postmortem delay. J Neurosci. 1996; 16(5):1710-1719.

62. Marcus DL, Strafaci JA, Miller DC, Masia S, Thomas CG, Rosman J, Hussain S and Freedman ML. Quantitative neuronal c-fos and c-jun expression in Alzheimer's disease. Neurobiol Aging. 1998; 19(5):393-400.

63. Thakur A, Wang X, Siedlak SL, Perry G, Smith MA and Zhu X. c-Jun phosphorylation in Alzheimer disease. J Neurosci Res. 2007; 85(8):1668-1673.

64. Savage MJ, Lin YG, Ciallella JR, Flood DG and Scott RW. Activation of c-Jun N-terminal kinase and p38 in an Alzheimer's disease model is associated with amyloid deposition. J Neurosci. 2002; 22(9):3376-3385.

65. Ploia C, Antoniou X, Sclip A, Grande V, Cardinetti D, Colombo A, Canu N, Benussi L, Ghidoni R, Forloni G and Borsello T. JNK plays a key role in tau hyperphosphorylation in Alzheimer's disease models. J Alzheimers Dis. 2011; 26(2):315-329.

66. Sclip A, Tozzi A, Abaza A, Cardinetti D, Colombo I, Calabresi P, Salmona M, Welker E and Borsello T. c-Jun N-terminal kinase has a key role in Alzheimer disease synaptic dysfunction in vivo. Cell Death Dis. 2014; 5:e1019.

67. Bamji-Mirza M, Callaghan D, Najem D, Shen S, Hasim MS, Yang Z and Zhang W. Stimulation of insulin signaling and inhibition of JNK-AP1 activation protect cells from amyloid-beta-induced signaling dysregulation and inflammatory response. J Alzheimers Dis. 2014; 40(1):105-122.

68. Vukic V, Callaghan D, Walker D, Lue LF, Liu QY, Couraud PO, Romero IA, Weksler B, Stanimirovic DB and Zhang W. Expression of inflammatory genes induced by beta-amyloid peptides in human brain endothelial cells and in Alzheimer's brain is mediated by the JNK-AP1 signaling pathway. Neurobiol Dis. 2009; 34(1):95-106.

69. Braak H, Alafuzoff I, Arzberger T, Kretzschmar H and Del Tredici K. Staging of Alzheimer disease-associated neurofibrillary pathology using paraffin sections and immunocytochemistry. Acta Neuropathol. 2006; 112(4):389-404.

70. Alafuzoff I, Arzberger T, Al-Sarraj S, Bodi I, Bogdanovic N, Braak H, Bugiani O, Del-Tredici K, Ferrer I, Gelpi E, Giaccone G, Graeber MB, Ince P, Kamphorst W, King A, Korkolopoulou P, et al. Staging of neurofibrillary pathology in Alzheimer's disease: a study of the BrainNet Europe Consortium. Brain Pathol. 2008; 18(4):484-496.

71. Montine TJ, Phelps CH, Beach TG, Bigio EH, Cairns NJ, Dickson DW, Duyckaerts C, Frosch MP, Masliah E, Mirra SS, Nelson PT, Schneider JA, Thal DR, Trojanowski JQ, Vinters HV and Hyman BT. National Institute on Aging-Alzheimer's Association guidelines for the neuropathologic assessment of Alzheimer's disease: a practical approach. Acta Neuropathol. 2012; 123(1):1-11.

72. Thal DR, Rub U, Orantes M and Braak H. Phases of A beta-deposition in the human brain and its relevance for the development of AD. Neurology. 2002; 58(12):1791-1800.

73. Crary JF, Trojanowski JQ, Schneider JA, Abisambra JF, Abner EL, Alafuzoff I, Arnold SE, Attems J, Beach TG, Bigio EH, Cairns NJ, Dickson DW, Gearing M, Grinberg LT, Hof PR, Hyman BT, et al. Primary age-related tauopathy (PART): a common pathology associated with human aging. Acta Neuropathol. 2014; 128(6):755-766.

74. Mackenzie IR, Neumann M, Baborie A, Sampathu DM, Du Plessis D, Jaros E, Perry RH, Trojanowski JQ, Mann DM and Lee VM. A harmonized classification system for FTLD-TDP43 pathology. Acta Neuropathol. 2011; 122(1):111-113.

75. Roman GC, Tatemichi TK, Erkinjuntti T, Cummings JL, Masdeu JC, Garcia JH, Amaducci L, Orgogozo JM, Brun A, Hofman A and et al. Vascular dementia: diagnostic criteria for research studies. Report of the NINDS-AIREN International Workshop. Neurology. 1993; 43(2):250-260.

76. Litvan I, Hauw JJ, Bartko JJ, Lantos PL, Daniel SE, Horoupian DS, McKee A, Dickson D, Bancher C, Tabaton M, Jellinger K and Anderson DW. Validity and reliability of the preliminary NINDS neuropathologic criteria for progressive supranuclear palsy and related disorders. J Neuropathol Exp Neurol. 1996; 55(1):97-105.

77. Irizarry RA, Bolstad BM, Collin F, Cope LM, Hobbs B and Speed TP. Summaries of Affymetrix GeneChip probe level data. Nucleic Acids Res. 2003; 31(4):e15.

78. Cuadrado-Tejedor M, Garcia-Barroso C, Sanchez-Arias JA, Rabal O, Perez-Gonzalez M, Mederos S, Ugarte A, Franco R, Segura V, Perea G, Oyarzabal J and Garcia-Osta A. A First-in-Class Small-Molecule that Acts as a Dual Inhibitor of HDAC and PDE5 and that Rescues Hippocampal Synaptic Impairment in Alzheimer's Disease Mice. Neuropsychopharmacology. 2016; 42(2):524-539.

CHAPTER 3

Olfactory bulb neuroproteomics reveals a chronological perturbation of survival routes and a disruption of prohibitin complex during Alzheimer's disease progression

Mercedes Lachén-Montes[1], Andrea González-Morales[1], María Victoria Zelaya[1,2,3], Estela Pérez-Valderrama[4], Karina Ausín[4], Isidro Ferrer[5], Joaquín Fernández-Irigoyen[1,2,4]§, Enrique Santamaría[1,2,4]§

[1] *Clinical Neuroproteomics Group, Navarrabiomed, Departamento de Salud, Universidad Pública de Navarra, Pamplona, Spain*

[2] *IDISNA, Navarra Institute for Health Research, Pamplona, Spain*

[3] *Pathological Anatomy Department, Navarra Hospital Complex, Pamplona, Spain*

[4] *Proteored-ISCIII. Proteomics Unit, Navarrabiomed, Departamento de Salud, Universidad Pública de Navarra, Pamplona, Spain*

[5] *Institut de Neuropatologia, IDIBELL-Hospital Universitari de Bellvitge, Universitat de Barcelona, L'Hospitalet de Llobregat, CIBERNED (Centro de Investigación Biomédica en Red de Enfermedades Neurodegenerativas), Spain.*

Abstract

Olfactory dysfunction is among the earliest features of Alzheimer´s disease (AD). Although neuropathological abnormalities have been detected in the olfactory bulb (OB), little is known about its dynamic biology. Here, OB- proteome analysis showed a stage-dependent synaptic proteostasis impairment during AD evolution. In addition to progressive modulation of tau and amyloid precursor protein (APP) interactomes, network-driven proteomics revealed an early disruption of upstream and downstream p38 MAPK pathway and a subsequent impairment of Phosphoinositide-dependent protein kinase 1 (PDK1)/Protein kinase C (PKC) signaling axis in the OB from AD subjects. Moreover, a mitochondrial imbalance was evidenced by a depletion of Prohibitin-2 (Phb2) levels and a specific decrease in the phosphorylated isoforms of Phb1 in intermediate and advanced AD stages. Interestingly, olfactory Phb subunits were also deregulated across different types of dementia. Phb2 showed a specific up-regulation in mixed dementia, while Phb1 isoforms were down-regulated in frontotemporal lobar degeneration (FTLD). However, no differences were observed in the olfactory expression of Phb subunits in progressive supranuclear palsy (PSP). To sum up, our data reflect, in part, the missing links in the biochemical understanding of olfactory dysfunction in AD, unveiling Phb complex as a differential driver of neurodegeneration at olfactory level.

Introduction

Alzheimer's disease (AD) is the most common form of senile dementia [1]. In general, two subgroups are recognized, a familial early-onset form, and a sporadic late-onset form, albeit 95% of the patients develop sporadic AD [2]. Together with typical symptoms such as memory loss and behavioral disorders, AD patients present olfactory dysfunction in 90% of the cases [3]. Interestingly, this deficit occurs at early stages of the disease and it is considered a premotor sign of neurodegeneration [3, 4]. The olfactory bulb (OB) is the first central structure of the olfactory pathway in the brain [5]. Multiple reports have evidenced neuropathological changes, and molecular alterations in the OB derived from rodent AD models, and human AD brains [6],[7]. Interestingly, the accumulation of beta-amyloid (Aβ) and phospho-Tau protein in the anterior olfactory nucleus and OB correlates with the progression of olfactory deficits and the severity of the disease in other brain regions [3], suggesting the potential utility of olfactory tissue in the early diagnosis of AD.

Taking into account the cellular complexity and protein heterogeneity present in the OB [8],[9], proteome-wide analysis based on high-resolution MS [10] has become an attractive technology to characterize and quantify the OB proteome in different biological contexts [11]. Although this unbiased technology has greatly enhanced the ability to characterize novel pathways particularly in brain areas associated with AD [12,13], few studies have examined the proteome profiling of the early-affected OB region with the aim to investigate incipient neurodegenerative changes in AD phenotypes. Mass-spectrometric exploration of the OB derived from AD models has revealed a clear proteostasis impairment in this olfactory region. In the APP/PS1 (Amyloid precursor protein/Preselinin 1) mouse model of AD, an early dysregulation of FAK and MEK/ERK signaling pathways precedes the β-amyloid deposition in the OB [7]. Moreover, these early events are subsequently accompanied by multiple proteomic, phosphoproteomic, and glycoproteomic changes in the OB, leading to a disruption in signaling pathways related to

synaptic plasticity and cytoskeletal dynamics during the progression of AD-associated amyloid pathology in APP/PS1 mice [14]. However, the AD progression in APP/PS1 mice is reminiscent of, but not identical to human sporadic AD [15]. We consider that deciphering the progressive proteome-wide alterations that occurs in a stage-dependent manner in the human OB, might complement the integrated view of the biochemical pathways involved in the olfactory pathophysiology of AD. In this study, we used a discovery platform combining neuropathological diagnosis, label-free quantitative proteomics, physical and functional interaction data, and biochemical approaches in order to understand the means by which the molecular pathways harboured in the OB are chronologically regulated during AD progression. We have revealed an olfactory proteostasis impairment across neuropathological grading detecting: i) differential expression of 278 proteins between controls and AD phenotypes, ii) a progressive modulation of APP, and Tau interactome networks across AD stages, iii) alteration in MKK3-6/p38 MAPK, and PDK1/PKC signaling pathways, and iv) potential mitochondrial impairment due to the imbalance of Prohibitin (Phb) complex. Interestingly, a cross-disease study also pointed out that Phb subunits are differentially modulated in the OB across AD-related co-pathologies, providing mechanistic clues to the intriguing divergence of AD pathology across different types of dementias.

Results

Proteostasis impairment in the OB during AD progression

To determine the OB site-specific proteomic signature during AD progression, a label-free MS-based approach was performed on OB tissue derived from AD subjects with different grading and controls with no known neurological history (Table 1).

			Duration	Brain	PMI	Pathological diagnosis	IHQ: βA in OB		IHQ: TAU in OB	
Cases	age	sex	(years)	weight (g)	(hours)	(NIA-AA) criteria	MP	DP	Tangles	neurites
Advanced AD										
BCN349	70	M	4	1104	2.5	AD (A3B3C3)	++	+++	++	+++
BCN367	89	M	13	1015	3	AD (A2B3C3)	+	+++	+++	+++
BCN369	86	M	8	973	2.5	AD (A3B3C3)	+	-	+	++
BCN376	93	M	3	1050	2.4	AD (A3B3C3)	+	+++	+++	+++
Intermediate AD										
BCN0104	85	M	12	1115	3.3	AD (A2B2C2)	-	+	+++	+++
BCN0136	97	F	9	900	n.d	AD (A2B2C2)	n.d	n.d	n.d	n.d
BCN381	77	M	17	1103	1.5	AD (A2B2C1)	-	-	++	++
BCN222	86	F	9	1000	3	AD (A2B2C2)	-	+	++	++
Initial AD										
BCN342	88	M	1	1400	3.45	AD (A2B1C2)	++	+	++	++
BCN336	85	F	8	1130	2	AD (A2B1C1)	-	-	+	+
BCN358	80	M	5	1090	3	AD (A2B1C1)	++	++	++	+++
A12/0046	75	F	n.d	1125	6	AD (A1B1C1)	-	-	+	+
A12/0067	72	F	n.d	810	4	AD (A1B1C1)	-	-	+	+
Control										
BCN362	72	M		1407	9	Thal 1 Cerad 1 no tau deposit	-	-	-	+
BCN283	99	M		992	3	No protein deposit+vascular disease	-	-	-	+
BCN387	81	F		1176	3.3	PART (Braak I)+vascular disase	-	-	-	+

Table 1. Subjects included in the proteomic study. The neuropathological assessment was performed according to Thal phases, CERAD score, NIA-AA guidelines and PART criteria. Aβ immunopositivity was scored on a 4-tiered scale as: (-) negative, (+) 1-2 isolated Aβ depositions, (++) 3-4 Aβ depositions, and (+++) >4 Aβ depositions. Graduation of phospho-TAU deposit: (-) negative +: low; ++: intermediate; +++ high. PMI: post-mortem interval; n.d: not determined; MP: Mature plaques; DP: Diffuse plaques; v.d: vascular disease.

Among 1311 quantified proteins across all experimental groups, 278 proteins tend to be differentially expressed between controls and AD phenotypes (Figure 1a, Supplementary Table 1 and Supplementary Fig. 1 on line). Our analysis revealed that 110 olfactory proteins are differentially expressed in early AD stages, increasing the proteome alterations as the disease progresses (125, and 158 differential proteins in intermediate and advanced stages respectively)

(Figure 1b). The distribution between up-regulated and down-regulated proteins was very similar across AD grading (Figure 1b). Interestingly, 24 proteins overlapped between all stages (Figure 1c), suggesting a potential role during AD evolution (Table 2). This set of proteins mainly clustered in specific biological process like growth of neurites (CLASP2, CPNE1), long-term potentiation (PPP1R1B), protein degradation (USP7, PSMD12, PSMF1), neuritogenesis (TNIK, S100B, STMN1), morphology of the nervous system (MUT, YES1), and synaptic plasticity (AP2S1, AP3D1, STXBP1). In order to evaluate the impact of AD in the OB at synaptic level, we have compared the OB differential expressed proteomes across AD staging with the information stored in three repositories containing the largest number of synapse specific proteins (G2Cdb, Synaptome DB, and SynsysNet) [16,17,18]. The analysis revealed that 162 out of 278 differential proteins (58% of the differential protein set) tend to localize to synaptic terminal (63, 70, and 96 differentially expressed synaptic proteins in initial, intermediate, and advanced stages respectively) (Supplementary Fig. 2 on line). This meta-analysis verified a progressive synaptic degeneration at the level of OB during AD progression.

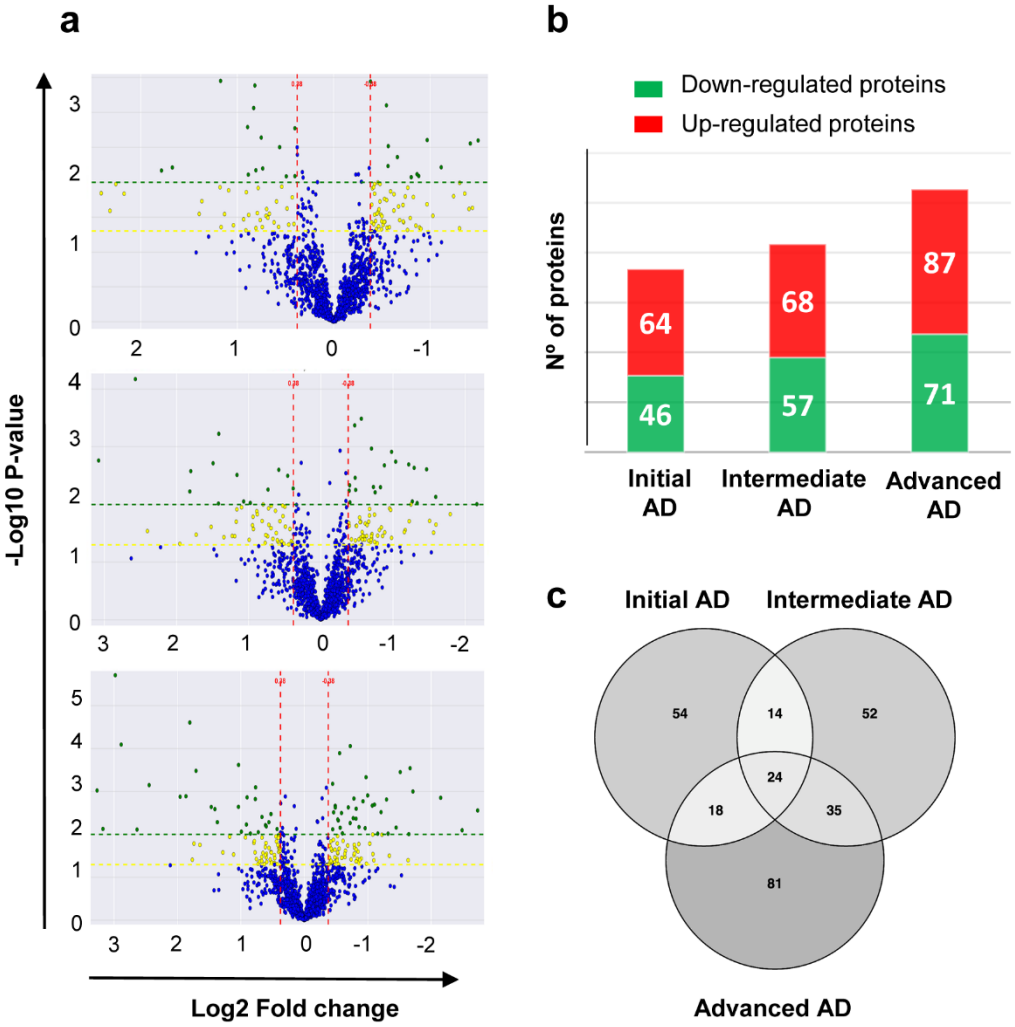

Figure 1. Differentially expressed proteins in the OB across AD-related phenotypes. A) Volcano plots representing the fold-change of identified proteins with associated P values from the pair-wise quantitative comparisons of control vs initial AD stage (upper panel), control vs intermediate AD stage (middle panel), and control vs advanced AD stage (lower panel). In green, very significantly changed proteins ($P < 0.01$), in yellow, significantly changed proteins ($P < 0.05$) and in blue, unchanged proteins between the pair-wise comparisons. B) Differential olfactory proteome distribution across AD stages.C) Venn diagram of common and unique differential proteins between AD stages. The distribution of common and distinct proteins in initial, intermediate, and advanced stages is shown.

Protein names	Gene	Uniprot code	Unique peptides	P-value Initial AD	P-value Int. AD	P-value Adv. AD	FC initial AD	FC Int. AD	FC Adv. AD	Functional interactor of APP	Functional interactor of Tau
Down-regulated proteins across AD staging											
TRAF2 and NCK-interacting protein kinase	*TNIK*	Q9UKE5	4	0.022	0.015	0.010	0.63	0.29	0.45		✓
CLIP-associating protein 2	*CLASP2*	O75122	3	0.002	0.001	0.002	0.51	0.51	0.48		
Copine-1 (Fragment)	*CPNE1*	F2Z2V0	5	0.026	0.009	0.010	0.65	0.76	0.40		
Protein S100-B	*S100B*	P04271	7	0.006	0.020	0.050	0.46	0.68	0.69	✓	✓
VPS10 domain-containing receptor SorCS2	*SORCS2*	B5MED8	3	0.010	0.002	0.029	0.40	0.41	0.47		
Importin subunit alpha-4	*KPNA3*	O00505	4	0.047	0.006	0.000	0.74	0.59	0.60		
Protein phosphatase 1 regulatory subunit 1B	*PPP1R1B*	Q9UD71	3	0.042	0.009	0.010	0.55	0.42	0.43		
Up/Down-regulated proteins across AD staging											
Stathmin	*STMN1*	P16949	3	0.002	0.005	0.001	1.32	0.56	0.73	✓	✓
Up-regulated proteins across AD staging											
Translationally-controlled tumor protein	*TPT1*	Q5W0H4	2	0.002	0.001	0.009	1.85	2.66	1.99	✓	✓
Cullin-3	*CUL3*	Q13618	5	0.000	0.049	0.006	1.76	1.31	1.53	✓	
AP-2 complex subunit sigma	*AP2S1*	P53680	4	0.007	0.025	0.000	3.44	2.87	3.49		
Fibrinogen beta chain	*FGB*	P02675	12	0.026	0.002	0.001	4.98	8.44	9.62		
Ubiquitin carboxyl-terminal hydrolase 7	*USP7*	Q93009	4	0.014	0.029	0.000	5.31	5.28	7.88		
26S proteasome non-ATPase regulatory subunit 12	*PSMD12*	O00232	5	0.002	0.036	0.039	1.68	1.67	3.40		
Proteasome inhibitor PI31 subunit	*PSMF1*	Q5QPM7	3	0.019	0.002	0.002	2.58	2.81	2.76		
Cytochrome c oxidase subunit 5A, mitochondrial	*COX5A*	P20674	3	0.014	0.020	0.001	1.87	1.48	1.87		
Eukaryotic translation initiation factor 3 subunit B	*EIF3B*	P55884	4	0.015	0.049	0.001	4.50	3.87	5.44		
AP-3 complex subunit delta-1	*AP3D1*	O14617	2	0.028	0.003	0.028	1.59	1.37	1.51		
Isoform 2 of Syntaxin-binding protein 1	*STXBP1*	P61764-2	2	0.012	0.010	0.000	2.26	1.74	3.26	✓	✓
Succinyl-CoA ligase [ADP/GDP-forming] subunit alpha	*SUCLG1*	P53597	7	0.046	0.012	0.034	1.75	1.65	1.51	✓	✓
L-xylulose reductase	*DCXR*	Q7Z4W1	6	0.035	0.016	0.038	1.69	1.92	1.69		
Methylmalonyl-CoA mutase, mitochondrial	*MUT*	P22033	4	0.029	0.006	0.016	2.63	3.52	3.34		
Delta-aminolevulinic acid dehydratase	*ALAD*	P13716	4	0.030	0.010	0.005	1.84	2.67	2.58		
Non-specific protein-tyrosine kinase	*YES1*	J3QRU1	6	0.044	0.003	0.027	2.24	2.23	1.57		

Table 2. Common differential expressed OB proteins across AD stages. The fold-change (FC) of differential proteins with associated p-values from the pair-wise comparisons of control vs each AD stage, together with Protein/gene names, protein code by Uniprot, and unique peptides used for quantitation are shown. The significant downward or upward trend is represented in green or red color respectively. Proteins that are functional interactors of APP and Tau proteins are also indicated.

Pathway-specific alterations during AD progression

In order to perform a proteome mapping analysis of the stage-dependent protein profiles across specific-neuronal processes, we used the IPA information of experimental and predictive origin regarding central nervous system, in order to be confident about the potential affected signaling pathways. As shown in Figure 2, neuronal processes such as neuritogenesis, growth and outgrowth of neurites, axonogenesis, and growth of axons are compromised across AD stages. Moreover, our results pointed out a stage-dependent deregulation of specific biological processes (Figure 2 and Supplementary Table 2 on line). Protein clusters involved in synaptic

transmission, and morphology of neuroglia were specifically mapped in initial stages while protein groups involved in formation of OB and cell death of oligodendrocytes were exclusively detected in intermediate stages. Interestingly, a de-regulation in protein clusters related to branching of neurites and axons, astrocytosis, vesicle trafficking, and myelination appears throughout initial and advanced stages (Figure 2).

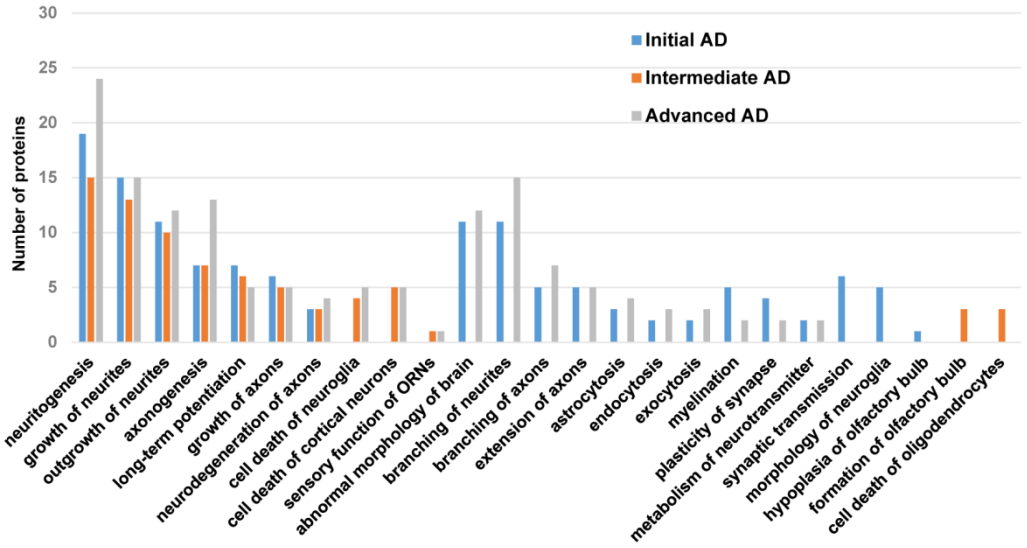

Figure 2. Functional metrics of the differential OB proteome across AD staging. Specific-neuronal pathway analysis for the differential OB proteomic expression profile detected in each AD stage is shown.

Network-driven proteomics reveals an imbalance in the olfactory MKK3-6/p38 MAPK and PDK1/PKC signaling across AD grading

To enhance the analytical outcome of proteomic experiments, we have performed proteome-scale interaction networks merging the olfactory proteins that tend to be de-regulated across stages of AD. To that end, a protein interactome map has been constructed for each stage using the IPA software (Figure 3). In initial stages, a deregulation of cross-linkers between plasma membrane and actin-based cytoskeleton such as the protein complex ezrin-moesin-radixin (EZR-

MSN-RDX) and regulators of the interaction between components of cell-cell junctions (L1CAM, CD9, CD81, CTTN, cadherin) suggested an imbalance in the cellular assembly and morphology at early AD stages (figure 3a). The functional clustering also suggested a central function of ERK1/2 mediating the structural stabilization at the level of OB (figure 3a). In accordance with these data, our group has previously demonstrated an early hyperactivation of ERK1/2 in the OB of AD subjects [7]. In intermediate stages, the proteome-scale interaction network reflected an impaired mitochondrial function and an imbalance in redox signaling, due to dysregulation of subunits of mitochondrial respiratory chain complexes I, and IV (COX5A, COX7A2, COX6B1, NDUFV2) and protein components involved in antioxidant defense mechanisms (HSPE1, GSTM1, TXN2) (Figure 3b). In advanced stages, the functional interactome network indicated an alteration in HNRNP complexes (FUS, HNRNPA1, HNRNPH1) and specific RNA binding proteins (EFTUD2, and MATR3), suggesting an impairment in RNA stability, and pre-mRNA splicing processes. Moreover, the alteration of COP9 signalosome complex subunit 1 (GPS1), and cullin-3 (CUL3) pointed out an alteration in the proteasomal degradation pathway in advanced stages of the disease (Figure 3c). Both p38 MAPK and PKC appeared as principal nodes in protein interactome maps (Figure 3b and 3c). Even though changes in their expression were not detected in our proteomic experiments, the alteration of some of their targets may be compatible with a dysregulation of their functionality during AD progression at the level of OB.

A

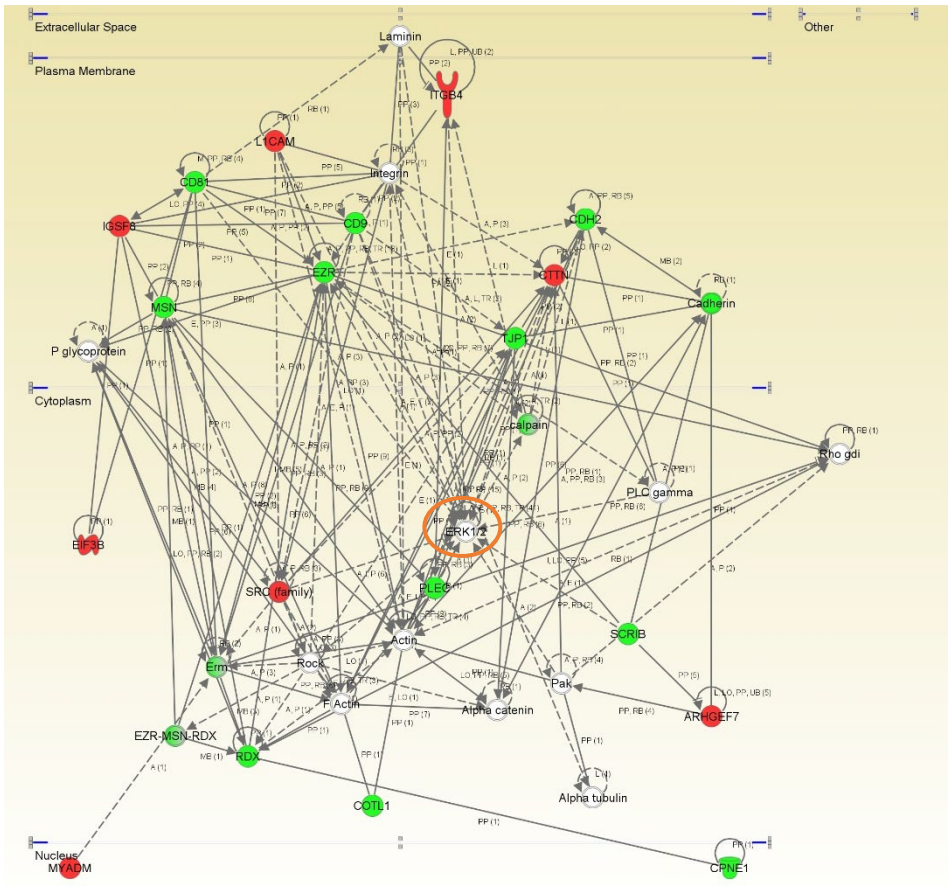

B

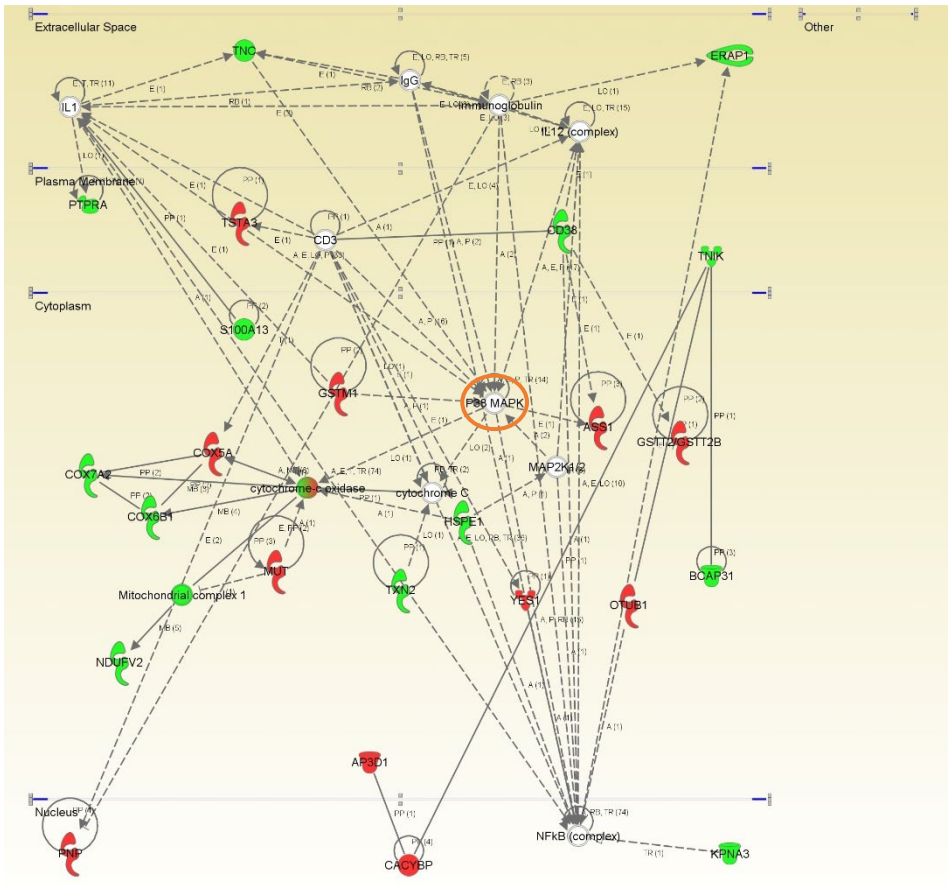

C

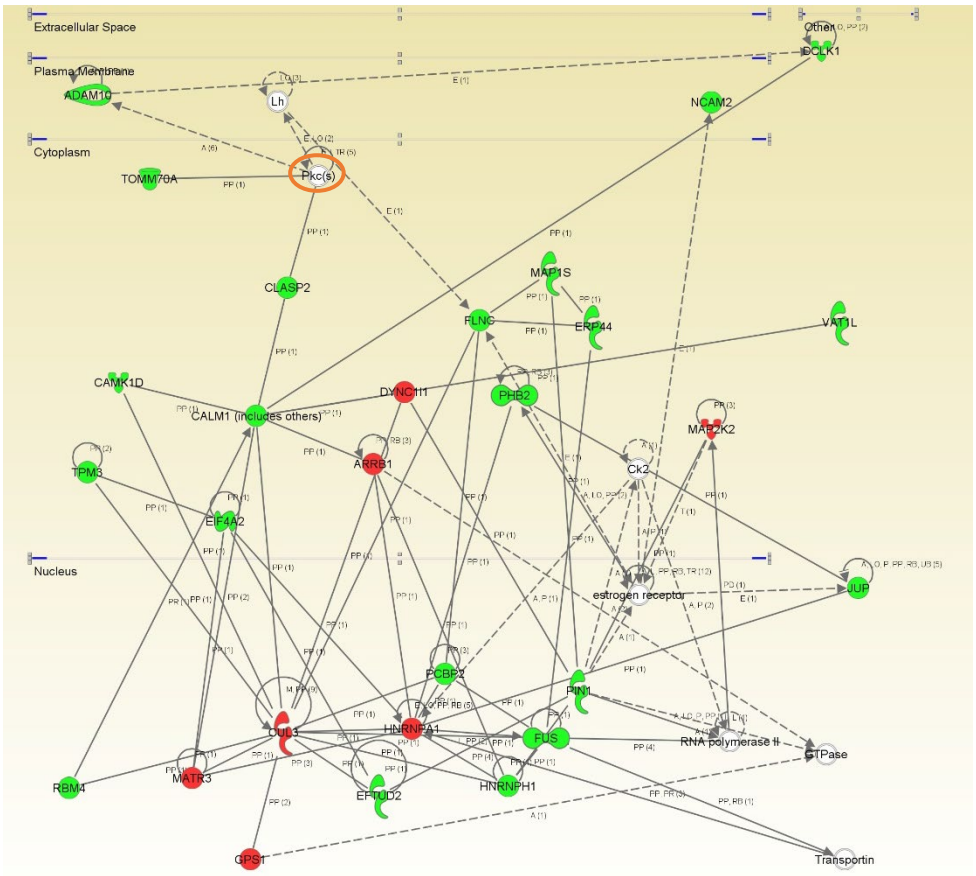

Figure 3. High-scoring protein interactome maps for differentially expressed proteins in the OB during AD progression. Visual representation of the relationships between differential expressed proteins and functional interactors in initial (A), intermediate (B), and advanced AD stages (C). Dysregulated proteins are highlighted in red (up-regulated) and green (down-regulated) for each stage. Continuous and discontinuous lines represent direct and indirect interactions respectively. The complete legend including main features, molecule shapes, and relationships is found in http://ingenuity.force.com/ipa/articles/Feature_Description/Legend.

Subsequent experiments were performed to monitor the activation state of p38 MAPK and PKC signaling pathways across AD stages. MKK3 and MKK6 are two closely related dual-specificity protein kinases that activate p38 MAPK [19]. Western-blot analysis revealed a decrease in the activation status of upstream MKK3 and MKK6 in initial AD stages (Figure 4a). This early down-regulation was accompanied by a fall in p38 MAPK levels and a paralleled decrease in ATF2 and HSP27 phosphorylation (Figure 4b), well-known downstream substrates of p38 MAPK [20] [21].

However, olfactory p38 MAPK activity tends to increase during AD progression, as demonstrated by the increment in the phosphorylation status of HSP27 and ATF2 in advanced stages (Figure 4b). PDK1 activity depends on the autophosphorylation on Ser241 and activates PKC signal transduction by phosphorylation on the activation loop [22,23]. Although, a significant up-regulation in total PDK1 and PKC levels was evidenced in early stages (figure 4c), PDK1 inactivation was accompanied by a decrease in the activation status of PKC isoforms in intermediate stages, as revealed by Western-blot using a specific antibody against phosphorylated PKC isoforms at a residue homologous to activated Thr514 of human PKCγ (figure 4c). Accompanying the PKC inactivation, Myristoylated alanine-rich C-kinase substrate (MARCKS), a substrate of PKC [24] was also down-regulated in intermediate stages (Supplementary Table 1 on line). However, the accumulation of PKC isoforms maintained PKC active in advanced stages, despite the PDK1 inactivation observed in these stages (figure 4c). Altogether, an early disruption in upstream p38 MAPK pathway and a subsequent impairment of PDK1/PKC signaling axis occurs in the OB from AD subjects. However, the tangled regulatory mechanisms that govern the PKC signaling needs further exploration, to elucidate the specific role of each PKC isoform during the AD neurodegeneration that occurs in the OB.

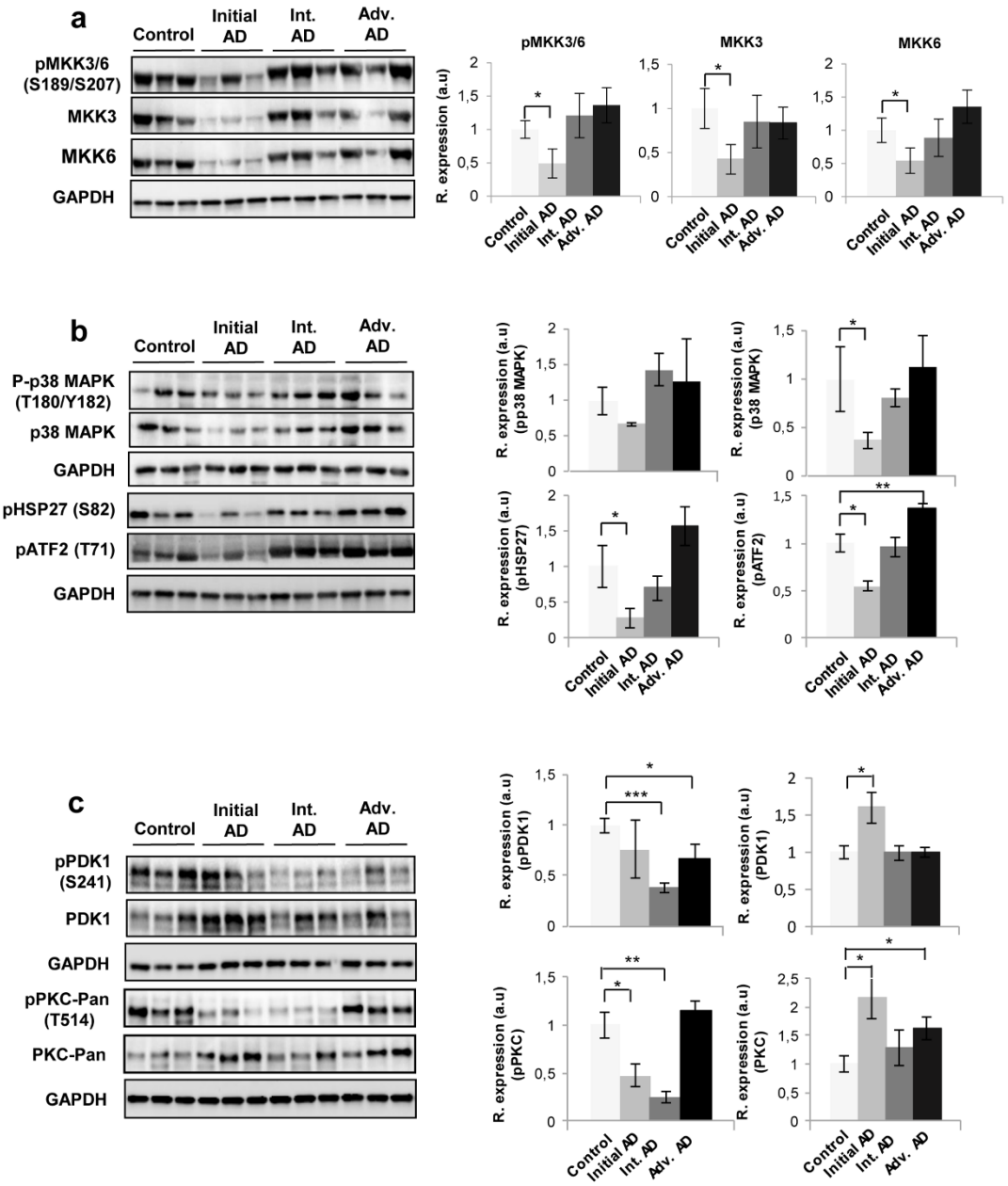

Figure 4. Signaling pathways disrupted in the OB across AD grading. Levels and residue-specific phosphorylation of MKK3/6 (A), p38 MAPK, ATF2, and HSP27 (B), PDK1, and PKC (C) in the OB across AD phenotypes. Equal loading of the gels was assessed by Ponceau staining and hybridization with a GAPDH specific antibody. Right panels show histograms of band densities. Data are presented as mean ± SEM from 5 independent OB samples per group. *P < 0.05 vs control group; **P < 0.01 vs control group. Representative Western blot gels (n = 3/experimental group) are shown. Full-length blots/gels are presented in Supplementary information.

Dysregulation of AD-related protein interactomes in the OB during the neurodegenerative process

We consider that the discovery of unexpected relationships between apparently unrelated proteins and AD-causing neuropathological substrates is a powerful strategy for the characterization of novel AD causative/susceptibility proteins with a central role during the neurodegenerative process that occurs in olfactory areas. We explored whether well-established AD-related proteins were indeed highly interconnected with the stage-dependent differential olfactory proteomes. As shown in figure 5, differential functional interactors for neuropathological substrates like APP and tau proteins were identified in the OB. With respect to OB controls, the APP interactome was composed by 12, 24, and 32 differential targets in initial, intermediate, and advanced AD stages respectively (Supplementary Fig. 3 on line). In the case of tau protein, 9 differential targets were detected in early AD stages, whereas 18 and 19 targets constituted the differential Tau interactome in intermediate and advanced AD stages respectively (Figure 5 and Supplementary Fig. 4 on line). Interestingly, 5 differential targets were shared between APP and Tau interactomes across AD grading. These proteins correspond to succinyl-CoA ligase [ADP/GDP-forming] subunit alpha (SUCLG1), Stathmin 1 (STMN1), translationally-controlled tumor protein (TPT1), protein S100-B (S100B), and syntaxin-binding protein 1 (STXBP1) (Supplementary Fig. 3 and 4 on line). Our analysis also revealed other functional interactomes that are modulated during AD progression in which the central nodes correspond to cAMP responsive element binding protein 1 (CREB1) and estrogen receptor 1 (ESR1) (Figure 5 and Supplementary Fig. 5 and 6 on line).

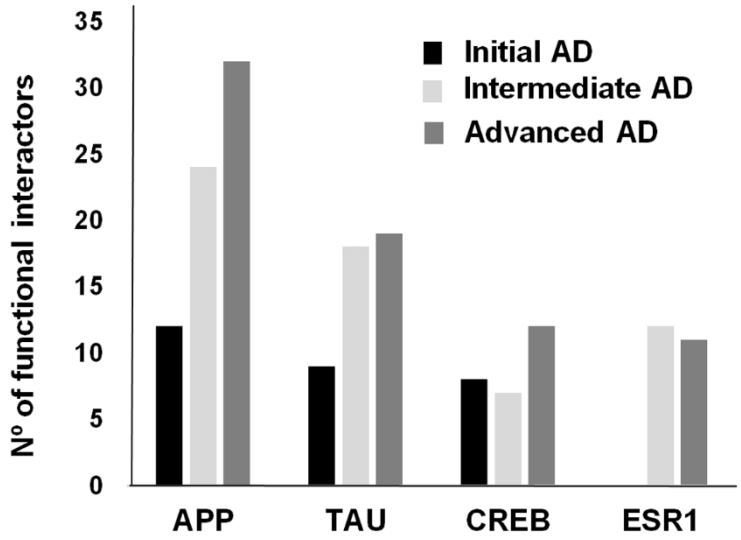

Figure 5. Functional interactome distribution across AD stages. The number of predicted functional interactors for hub proteins with impact in neurobiology is represented.

Validation of differential olfactory proteins across AD grading: Focus on Prohibitin complex

Previous studies identified a down-regulation of olfactory XRCC5, and FABP5 in initial AD stages, together with the overexpression of CD166 antigen, V-type proton ATPase subunit H, and histone H4 in advanced AD stages [6]. Our results confirm these previous observations (Supplementary Table 1 on line), partially validating the label free-based liquid chromatography tandem mass spectrometry (LC-MS/MS) approach. With the aim to complement and validate quantitative proteome measurements, subsequent experiments were performed to check the steady-state levels of a subset of differential proteins using downstream assays. We consider the selection of assessing Vimentin (Vim) and Prohibitin-2 (Phb2) proteins for validation. The absence of the intermediate filament protein Vim exacerbates the amyloid plaque load and the increase in dystrophic neurites in APP/PS1 mouse model of AD [25] and Phb2 deficiency leads to Tau hyperphosphorylation, and neurodegeneration in mice [26]. First, we performed immunohistochemical analysis to localize Vim and Phb subunits in the OB region during AD progression (Figure 6). Vim tends to be expressed in the glomerular layer and preferentially

distributed in the walls of the blood vessels (Figure 6). Both Phb subunits were detected at dendritic connections in glomerular layer and across the neuropil, being highly expressed in the cytoplasm of mitral cells and neurons of the anterior olfactory nucleus (AON) (Figure 6).

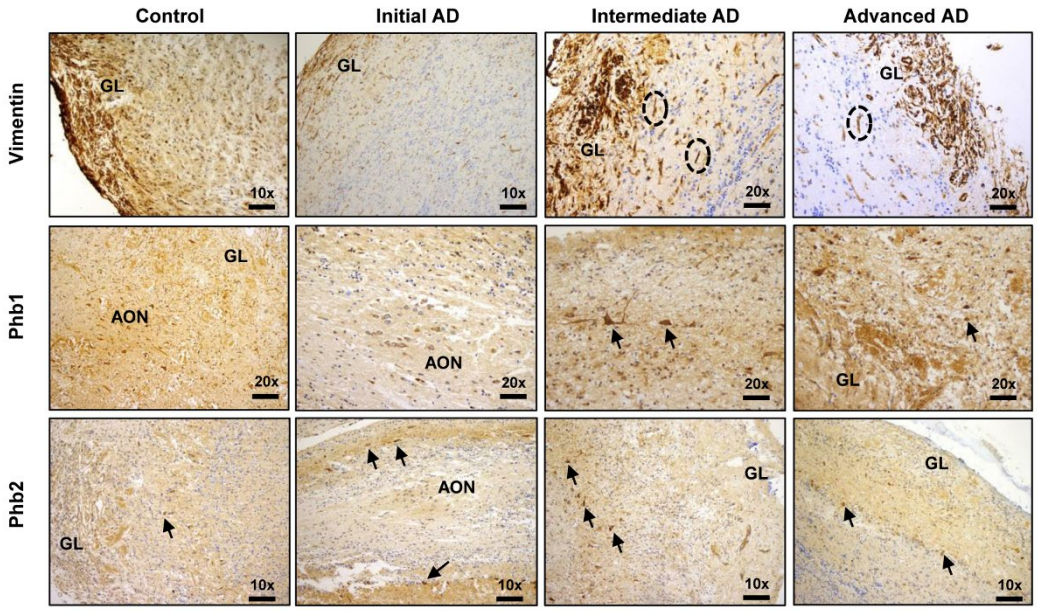

Figure 6. Immunohistochemical localization of OB Vim, Phb1 and Phb2 across AD grading. First line: Representative immunohistochemical staining pattern of Vim across AD grading. Positive staining in glomerular cell layer (GL) and wall of endothelial cells (ovals). Second line: Representative immunohistochemical staining pattern of Phb1 across AD grading. Positive staining in glomerular layer (GL), anterior olfactory nucleus (AON), and mitral cells (asterisks). Third line: Representative immunohistochemical staining pattern of Phb2 across AD grading. Positive staining in glomerular layer (GL), anterior olfactory nucleus (AON), and mitral cells (asterisks).

In order to evaluate the potential role of Vim and Phb subunits in the early-affected OB region in human AD phenotypes, protein expression levels were monitored by Western blotting across AD staging (Figure 7). In accordance with proteomic data (Supplementary Table 1 on line), immunoblotting analysis revealed a slight decrease in olfactory Vim protein levels in initial and advanced AD stages, and a down-regulation of Phb2 protein levels in intermediate and advanced

AD stages with respect to controls (figure 7a). Mitochondrial prohibitin complex (constituted by Phb1 and Phb2) modulates mitochondrial dynamics, participates in the mitochondrial respiratory complex assembly, and exerts beneficial effects on neurons by reducing free radical production [27]-[28]. Generally, repression of Phb2 is paralleled by a concomitant reduction of its assembly partner Phb1 and vice versa [26]-[29]. In agreement with our mass spectrometry (MS) data (Supplementary Table 1 on line), Phb1 levels were unchanged across AD stages (Figure 7a), pointing out that Phb subunits are not functionally interdependent in the OB during AD neurodegeneration. However, phosphorylated Phb1 isoforms at Thr258 and Y259 were down-expressed in intermediate and advanced AD stages (Figure 7b), suggesting potential fluctuations in the Phb1 interactome across AD stages.

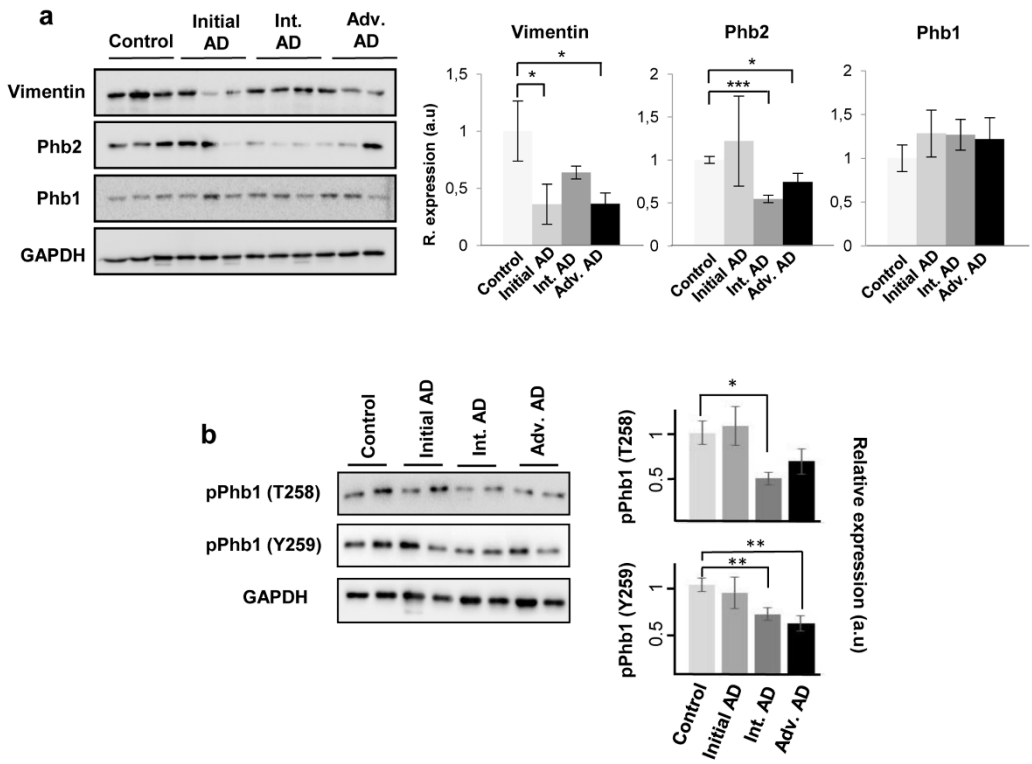

Figure 7: Olfactory expression of Vim and Phb subunits across AD stages. A) Protein levels of Vim, Phb2, and Phb1 were monitored by Western-blotting. Equal loading of the gels was assessed by Ponceau staining and hybridization with a GAPDH specific antibody. Representative Western blot gels (n = 3/experimental group) are shown (left). Right panels show histograms of band densities. Data are presented as mean ± SEM from 3 independent OB samples per group.

*P < 0.05 vs control group; ***P < 0.001 vs control group. B) OB phosphorylation profiling of PHb1 across AD staging. Representative Western blot gels (n = 2/experimental group) are shown (left). Right panel shows histograms of band densities. Data are presented as mean ± SEM from 3 independent OB samples per group. *P < 0.05 vs control group; **P < 0.01 vs control group. Full-length blots/gels are presented in Supplementary information.

OB protein expression of Prohibitin complex across Alzheimer-related co-pathologies

In contrast to the common separate investigation of neurological disorders, targeted cross-disease studies comparing shared molecular relationships may give new insights into possible olfactory perturbations common for all or some neurological backgrounds. To check the potential vulnerability of PHB complex across different Alzheimer-related co-pathologies at the level of OB, we have evaluated the OB protein expression of Phb2, Phb1, Thr258-, and Y259-phosphorylated Phb1 isoforms by Western-blot across AD-related diseases (n= 28 OB samples) (Supplementary Table 3 on line). We have included pathologies with common smell impairment like FTLD [3], PSP where olfactory loss occurs to a lesser extent or is absent [3,30], and mixed dementia (Mix AD VD). Mixed dementia is a condition in which AD and vascular dementia occur at the same time, and both separate disorders often display olfactory dysfunction [31]. As shown in Figure 8a, steady-state and phosphorylated levels of Phb1 remained unchanged in the OB from Mixed AD VD subjects respect to controls, while Phb2 protein expression is significantly increased. Moreover, a significant reduction in Phb1 expression (steady-state and phosphorylated levels) was detected in FTLD subjects, and no significant differences were observed with respect to Phb2 protein levels (Figure 8b). On the other hand, both Phb subunits were statistically unchanged in PSP subjects, albeit 50% of PSP subjects presented a slight tendency to down-regulation in the case of Phb1 (Figure 8c). Although equivalent olfactory deficits are observed between some AD-related co-pathologies, these data pointed out that the

olfactory pattern of Phb subunits is proteinopathy-dependent, suggesting different mechanistic clues to the neurodegenerative process that occurs in the OB.

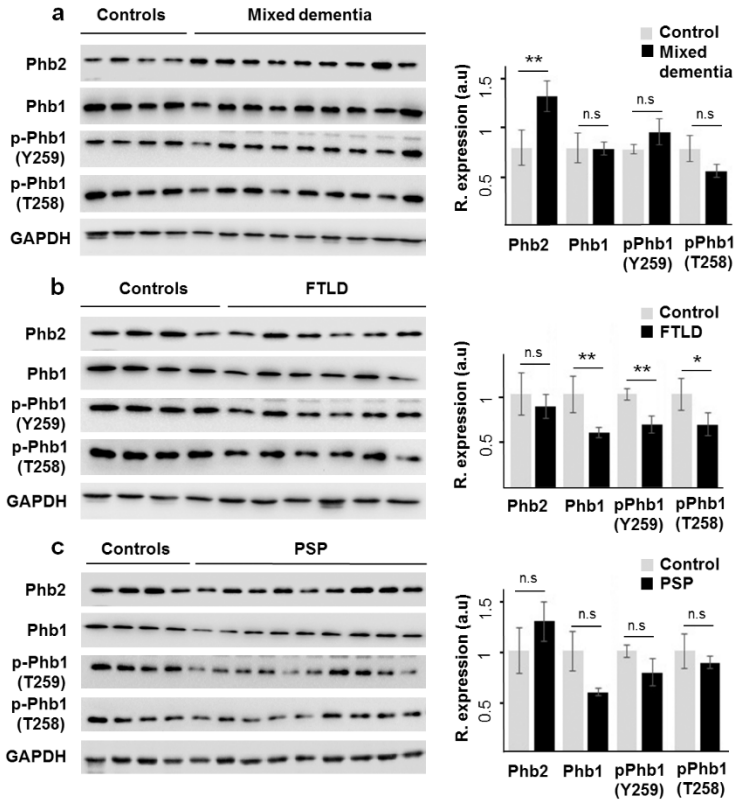

Figure 8. OB protein expression of Phb isoforms across AD-related proteinopathies. Olfactory expression of Phb2, Phb1, and Phb1 phosphorylated isoforms in Mix AD VD (A), FTLD (B), and PSP (C). Representative Western blot gels are shown for each Phb subunit. Histograms of band densities derived from 28 independent OB samples. Data are presented as mean ± SEM from: Controls (n = 4 cases), mixed dementia (mix AD VD) (n = 9 cases), FTLD (n = 6 cases), and PSP (n = 9 cases). *P < 0.05 vs control group; ** P < 0.01 vs control group. Full-length blots/gels are presented in Supplementary information.

Discussion

During the last years, proteomics has emerged as a large-scale comprehensive approach to characterize and quantify specific olfactory-related proteomes in ageing and neurodegeneration [11]. Due to the early involvement of the olfactory dysfunction in AD [4], we consider that the application of tissue proteomics in the OB is an ideal approach that allows zooming-in where pathophysiological changes are taking place. In the current work, we have used a discovery platform combining neuropathological diagnosis, label-free quantitative proteomics, physical and functional interaction data, and biochemical approaches in order to determine the chronologic regulation of the OB proteome during AD progression. Our group has previously identified common and distinct olfactory targets across tauopathies and synucleopathies using a labeling proteomic approach [6]. The use of labeling strategies usually results in the identification of more proteins, but label-free methods allow us to analyze and compare more samples individually, indicating that both workflows are complementary [32]. It is important to note that due to technical reasons, only the most abundant OB proteins were explored. Consequently, alterations other than those reported in this study might also participate in the AD neurodegeneration at the level of the OB. However, according to our integrative meta-analysis (Supplementary Table 4 on line), most of the differential OB proteins reported in this study has not been previously reported in differential proteomic studies performed in human AD brains.

In agreement with previous studies performed in the APP/PS1 mouse model of AD [14], our data revealed a stage-dependent synaptic proteostasis impairment in the OB during AD pathogenesis, where more than 50% of the differential proteome across AD phenotypes tends to localize to synaptic ending. Interestingly, 17% of the OB differential proteome (47 out of 278 proteins), is also deregulated in hippocampal tissue during AD progression [12], suggesting a coordinated regulation of specific protein modules across AD-related brain structures that might

turn out detrimental or potentially protective mechanisms during the disease evolution. The synaptic plasticity imbalance was accompanied by specific proteomic fingerprints that are dynamically modulated in a stage-dependent manner throughout the OB. Interestingly, 24 early-affected proteins involved in protein degradation, growth of neurites, long-term potentiation, and neuritogenesis were deregulated across all stages, highlighting their potential importance for targeting AD at an early stage. Assuming that causative and susceptibility proteins tend to be highly interconnected in AD [33], we have employed network-driven proteomics to yield novel insights into the signaling pathways that govern the evolution of AD at olfactory level. Our data point out that functional protein interactomes and specific pathways are dynamically modulated across AD staging in the OB, emphasizing the potential impact of stage-dependent analysis using high-throughput proteome screenings [12]. It has been proposed that the aberrant regulation of a subset of kinases may represent the triggering events leading to the spread of an aberrant signaling in AD [34]. In this context, the dysregulation of kinases regulating neuronal plasticity, learning, and memory have been proposed as the starting signal, which promotes neurotoxic outcomes [34,35]. Analyzing the upstream signaling interactions of the differentially expressed proteomes in the OB, we determined upstream regulators (ERK1/2, p38 MAPK, and PKC) that were highly interconnected with downstream regulated proteins. Despite ERK1/2 is a well-defined pro-survival factor, neuronal ERK has been reported to be involved in the induction of cell death, APP processing, and Tau phosphorylation [36,37,38]. Our data point out that olfactory ERK1/2 hyperactivation [7] may be involved in the improper cytoskeletal coupling that occurs in olfactory neurons at early stages, probably driving the synaptic impairment [39]. p38 MAPK is a multifunctional kinase in AD pathophysiology [40]. It has been shown that p38 MAPK is activated by Aβ in cultured neurons [41], mediates the inflammatory activation initiated by Aβ [42], and phosphorylates Tau protein [43,44]. In this regard, previous studies have demonstrated that p38 MAPK signaling cascade is overactivated in hippocampal and cortical regions at early stages of AD pathology [45,46,47], being considered as a potential

target to treat AD neurodegeneration [40]. In contrast, we detected a specific upstream and downstream disruption in p38 MAPK pathway in early stages at the level of the OB, recovering normal levels in intermediate and advanced stages. This early deregulation was further validated by paralleled decrease in ATF2 and HSP27 phosphorylation, well-known downstream substrates of p38 MAPK [20, 21]. In spite of detrimental effects of p38 MAPK activation during AD pathogenesis [40], recent studies have dissected the role of specific p38 MAPK isoforms identifying different functions. It has been characterized that the inhibition of neuronal p38alpha, but not p38beta MAPK, provides neuroprotection in different neurotoxic environments [48]. Interestingly, a depletion of neuronal p38alpha MAPK attenuates Aβ pathology in AD mouse and cell models [49]. In line with these findings, the early down-regulation of p38 MAPK in olfactory neurons might be part of the neuroprotective mechanisms induced in initial stages against Aβ. In addition, a subsequent impairment of PDK1/PKC signaling axis occurs in the OB from AD subjects. An increment in PDK1 activity has been reported in the brain from AD patients [50], however, its inhibition or silencing points out a beneficial effect in AD-like pathology. In vitro studies have demonstrated that inhibition of PDK1 blocks neuronal cell death induced by Aβ [51]. Interestingly, quenching PDK1 activity in three APP-transgenic mouse models of AD rescued TACE-mediated neuroprotective cleavage of APP, and decreased Aβ deposition, counteracting memory and cognitive deficits [50]. Thus, our data suggest that the significant reduction in PDK1 activation may be a signal to protect neuronal function in the OB. PDK1 is an upstream regulator of some PKC family members [52], critically involved in memory acquisition and maintenance [53]. Deficits in neuronal PKC signal cascades are one of the earliest abnormalities in AD brains [54]. Aβ can directly inhibit PKC isoforms, induces PKC degradation, and reduces PKC-mediated phosphorylation and membrane translocation [55,′56,′57]. In line with these findings, the PKC inactivation observed in the OB, could contribute to the Aβ-related toxicity across initial-intermediate phases of AD. Although PKC activation has been proposed for the treatment of dementias [58], the tangled regulatory mechanisms that

govern the PKC signaling needs further exploration at olfactory level, in order to clarify the specific role of each PKC isoform during the neurodegenerative process [53].

Our proteomic screening further suggested an impairment of mitochondrial function in the OB [6], revealing dysregulation of 29 mitochondrial proteins across intermediate and advanced AD stages. This impairment is a common finding in human AD brains, and also in rodent, and cellular AD models [59], where intracellular Aβ accumulation leads to a decrease electron transfer efficiency, reduce ATP production, and increase ROS production [60]. Interestingly, cross-validation by immunoblotting analysis revealed a down-regulation of Phb2 protein levels in intermediate and advanced stages. Phb complex (constituted by Phb1 and Phb2) is located in the mitochondrial inner membrane acting as a membrane-bound chaperone involved in the correct folding and assembly of some of the components of the mitochondrial respiratory chain [61]. According to this hypothesis, a deficiency in Phb2 may impair the native and functional organization of respiratory proteins, compromising mitochondrial functionality [28]. Interestingly, neuron-specific deletion of Phb2 induces an aberrant mitochondrial ultrastructure, and Tau hyperphosphorylation in mice, leading to behavioral impairments and cognitive deficiencies [26]. Therefore, Phb2 deficiency might suggest a direct link between mitochondrial defects and tau pathology in olfactory neurons. We have observed a reversed Phb2 pattern between mixed dementia (Mix AD VD) respect to the protein profile observed in AD. Transcriptional and translational events may explain the difference observed in Phb2 protein levels. A possible explanation is that the vascular damage may induce a decrease in the Phb2 degradation rate at mRNA and/or protein levels at the level of the OB in mix AD VD. However, we should consider that the activation/inhibition of the transcription factor machinery that regulates the transcription of *PHB2* gene may also be compromised (as a consequence of the vascular damage), leading to an increase in Phb2 mRNA and protein levels. However, additional validation studies should be conducted employing large cohorts to verify the protein expression changes observed in our sample set. Repression of Phb2 is usually paralleled by a concomitant

reduction of its assembly partner Phb1 and vice versa [26]. However, in agreement with previous studies performed in frontal cortex derived from AD subjects [62], steady-state levels of OB Phb1 was unchanged across AD grading, demonstrating that Phb subunits are not functionally interdependent in the OB during AD neurodegeneration. In addition, Phb1 and Phb2 are present in different subcellular localizations, presenting clear and distinctive functions [63]. While some associations at the plasma membrane and in the mitochondria require both Phb1 and Phb2, both proteins function independently in the nucleus, influencing the activity of multiple transcription factors [64]. However, based on our immunohistochemical analysis, most of Phb2 staining is not detected in the nucleus of olfactory neurons, suggesting that Phb2 may not be directly involved in transcriptional events. On the other hand, Phb subunits are post-translationally modified by O-linked N-acetylglucosamine, palmitoylation, transamidation, nytrosylation, and phosphorylation [65]. A decreased in phosphorylated Phb1 isoforms at T258 and Y259 was detected in the OB from AD subjects. Both residues are present in the C-terminal coiled-coil domain that is involved in protein-protein interactions, including the interaction between Phb1 and Phb2 as well as transcriptional regulation [66]. Although the kinase that phosphorylates the Y259 remains unknown, it is well documented that Akt phosphorylates Phb1 at T258 in non-neuronal contexts. Specifically, Akt may phosphorylate this residue in the cytoplasm, promoting Phb1 mitochondrial translocation [67] or in the lipid raft domain of the plasma membrane to activate the Ras-MAPK and PI3K/Akt pathways [68]. However, previous work in our laboratory demonstrated that the activation state of Akt remains unchanged, and ERK is hyper-activated in the OB from AD subjects [7], suggesting that OB Phb1 dephosphorylation may be due to a phosphatase action or the inactivation of a specific kinase different than Akt. Although our results serve as a foundation for new areas of investigation into the role of olfactory signaling in human AD-related co-pathologies, further work is necessary to clarify the regulatory mechanisms involved in post-translational modifications of Phb subunits,

in order to understand the final effect of olfactory Phb complex on cell survival and apoptosis across proteinopathies.

Methods

Materials - The following reagents and materials were used: anti-GAPDH (Calbiochem), anti-MKK3, anti-MKK6, anti-phospho MKK3 (Ser189)/MKK6 (Ser207), anti-p38 MAP kinase, anti-phospho p38 MAP kinase (Thr180/Tyr 182), anti-phospho HSP27 (Ser82), anti-phospho ATF2 (Thr71), anti-PDK1, anti-phospho PDK1 (S241), anti-PKC-Pan, anti-phospho PKC-pan (T514), anti-Prohibitin 1 (Phb1), anti-Prohibitin 2 (Phb2), (Cell signaling). Anti-vimentin antibody was purchased from Santa Cruz biotechnology. Anti-phospho Phb1 (T258), and anti-phospho Phb1 (Y259) were purchased from Signalway Antibody. Electrophoresis reagents were purchased from Biorad and trypsin from Promega.

Human samples - According to the Spanish Law 14/2007 of Biomedical Research, inform written consent forms of the Neurological Tissue Bank of Navarra Health Service, Brain Bank of IDIBELL, and Neurological Tissue Bank of IDIBAPS-Hospital Clinic (Barcelona, Spain) was obtained for research purposes from relatives of patients included in this study. The study was conducted in accordance with the Declaration of Helsinki and all assessments, post-mortem evaluations, and procedures were previously approved by the Clinical Ethics Committee of Navarra Health Service. For the proteomic phase, fourteen AD cases were distributed into different groups according to specific consensus diagnostic criteria [69, 70,71]: initial, intermediate, and advanced AD stages (n = 4-5/group). Three cases from elderly subjects with no history or histological findings of any neurological disease were used as a control group. All human brains considered in the proteomic study had a post-mortem interval (PMI) lower than 10 hours (Table 1). Brain processing and the neuropathological study for protein deposits aggregates Aβ and phospho-Tau were performed as previously described [6]. For the discovery phase, neuropathological assessment was performed according to standardized neuropathological scoring/grading systems, including Thal phases of Beta-amyloid deposition, Braak staging of neurofibrillary lesions, Consortium to Established a Registry for Alzheimer's Disease, National

Institute on Aging-Alzheimer's Association (NIA-AA) guidelines, and primary age-related tauopathy (PART) criteria [69,70,71,72,73]. For the validation phase, OB tissue from additional controls and AD subjects were included (n=4-5/group) (Supplementary Table 3 on line). This material was obtained from the Neurological Tissue Banks of IDIBELL and IDIBAPS-Hospital Clinic, Barcelona, Spain. For the specificity analysis, different NDs were considered: Progressive supranuclear palsy (PSP) (n = 9 cases; 4F/5M; median age: 74 years), frontotemporal lobar degeneration (FTLD) (n = 6; 3F/3M; median age: 81 years), mixed dementia (mix AD VD) (n = 9 cases; 4F/5M; median age: 85 years), and controls (n = 4; 1F/3M; median age: 79 years). In these cases, neuropathological assessment was performed according to standardized neuropathological guidelines: Mackenzie criteria for FTLD pathology[74], NINDS-AIREN criteria for vascular dementia[75], and NINDS criteria for PSP[76]. 80% of the OB samples included in this phase had a PMI lower than 10 hours (Supplementary Table 3 on line).

Sample preparation for proteomic analysis - OB specimens derived from control and AD cases were homogenized in lysis buffer containing 7 M urea, 2 M thiourea, 4% (w/v) CHAPS, 50 mM DTT. The homogenates were spinned down at 100.000 x g for 1 h at 15°C. Prior to proteomic analysis, protein extracts were precipitated with methanol/choloroform, and pellets dissolved in 6M Urea, Tris 100mM pH 7.8. Protein quantitation was performed with the Bradford assay kit (Bio-Rad).

Label free LC-MS/MS – The protein extract for each sample was diluted in Laemmli sample buffer and loaded into a 0.75 mm thick polyacrylamide gel with a 4% stacking gel casted over a 12.5% resolving gel. The run was stopped as soon as the front entered 3 mm into the resolving gel so that the whole proteome became concentrated in the stacking/resolving gel interface. Bands were stained with Coomassie Brilliant Blue and excised from the gel. Protein enzymatic cleavage (10ug) was carried out with trypsin (Promega; 1:20, w/w) at 37°C for 16 h as previously described [77]. Purification and concentration of peptides was performed using C18 Zip Tip Solid Phase

Extraction (Millipore). Peptides mixtures were separated by reverse phase chromatography using an Eksigent nanoLC ultra 2D pump fitted with a 75 µm ID column (Eksigent 0.075 x 250). Samples were first loaded for desalting and concentration into a 0.5 cm length 100 µm ID precolumn packed with the same chemistry as the separating column. Mobile phases were 100% water 0.1% formic acid (FA) (buffer A) and 100% Acetonitrile 0.1% FA (buffer B). Column gradient was developed in a 240 min two step gradient from 5% B to 25% B in 210 min and 25%B to 40% B in 30 min. Column was equilibrated in 95% B for 9 min and 5% B for 14 min. During all process, precolumn was in line with column and flow maintained all along the gradient at 300 nl/min. Eluting peptides from the column were analyzed using an Sciex 5600 Triple-TOF system. Information data acquisition was acquired upon a survey scan performed in a mass range from 350 m/z up to 1250 m/z in a scan time of 250 ms. Top 35 peaks were selected for fragmentation. Minimum accumulation time for MS/MS was set to 100 ms giving a total cycle time of 3.8 s. Product ions were scanned in a mass range from 230 m/z up to 1500 m/z and excluded for further fragmentation during 15 s.

Peptide Identification and Quantification – MS/MS data acquisition was performed using Analyst 1.7.1 (AB Sciex) and spectra files were processed through Protein Pilot Software (v.5.0-ABSciex) using Paragon™ algorithm (v.4.0.0.0) for database search [78], Progroup™ for data grouping, and searched against the concatenated target-decoy UniProt proteome reference Human database (Proteome ID: UP000005640, 70902 proteins, December 2015). False discovery rate was performed using a non lineal fitting method [79] and displayed results were those reporting a 1% Global false discovery rate or better. The peptide quantification was performed using the Progenesis LC−MS software (ver. 2.0.5556.29015, Nonlinear Dynamics). Using the accurate mass measurements from full survey scans in the TOF detector and the observed retention times, runs were aligned to compensate for between-run variations in our nanoLC separation system. To this end, all runs were aligned to a reference run automatically chosen by the software, and a master list of features considering m/z values and retention times was generated. The quality

of these alignments was manually supervised with the help of quality scores provided by the software. The peptide identifications were exported from Protein Pilot software and imported in Progenesis LC– MS software where they were matched to the respective features. Output data files were managed using R scripts for subsequent statistical analyses and representation. Proteins identified by site (identification based only on a modification), reverse proteins (identified by decoy database) and potential contaminants were filtered out. Proteins quantified with at least two unique peptides, an ANOVA p-value lower than 0.05, and an absolute fold change of <0.77 (down-regulation) or >1.3 (up-regulation) in linear scale were considered to be significantly differentially expressed. MS raw data and search results files have been deposited to the ProteomeXchange Consortium (http://proteomecentral.proteomexchange.org) via the PRIDE partner repository [80] with the dataset identifiers PXD005319.

Bioinformatics –The proteomic data were analyzed through the use of QIAGEN's Ingenuity® Pathway Analysis (IPA) (QIAGEN Redwood City, www.qiagen.com/ingenuity), in order to detect and infer differentially activated/deactivated pathways as a result of AD phenotypes. This software comprises curated information from databases of experimental and predictive origin, enabling discovery of highly represented functions, pathways, and interactome networks.

Immunohistochemistry - For the immunohistochemical study, formalin fixed sections (3-5 mm-thick) were mounted on slides and deparaffinized. Tissue sections were labelled with the following primary antibodies: anti-vimentin (dilution 1/200), anti-Prohibitin-1 (Phb1) (dilution 1/120), and anti-Prohibitin-2 (Phb2) (dilution 1/50). The reaction product was visualized using an automated slide immunostainer (Leica Bond Max) with Bond Polymer Refine Detection (Leica Biosystems Newcastle Ltd).

Immunoblotting analysis - Equal amounts of protein (10 µg) were resolved in 12.5% SDS-PAGE gels. OB proteins derived from human samples were electrophoretically transferred onto nitrocellulose membranes using a Trans-blot Turbo transfer system (up to 25V, 7min) (Bio-rad).

Equal loading of the gels was assessed by Ponceau staining. Membranes were probed with primary antibodies at 1:1000 dilution in 5% nonfat milk or BSA. After incubation with the appropriate horseradish peroxidase-conjugated secondary antibody (1:5000), the immunoreactivity was visualized by enhanced chemiluminiscence (Perkin Elmer) and detected by a Chemidoc MP Imaging System (Bio-Rad). After densitometric analyses (Image Lab Software Version 5.2; Bio-Rad), optical density values were expressed as arbitrary units and normalized to GAPDH.

References

[1] Qiu, C., De Ronchi, D., Fratiglioni, L., The epidemiology of the dementias: an update. *Curr Opin Psychiatry* 2007, *20*, 380-385.

[2] Bettens, K., Sleegers, K., Van Broeckhoven, C., Current status on Alzheimer disease molecular genetics: from past, to present, to future. *Hum Mol Genet* 2010, *19*, R4-R11.

[3] Attems, J., Walker, L., Jellinger, K. A., Olfactory bulb involvement in neurodegenerative diseases. *Acta Neuropathol* 2014, *127*, 459-475.

[4] Roberts, R. O., Christianson, T. J., Kremers, W. K., Mielke, M. M.*, et al.*, Association Between Olfactory Dysfunction and Amnestic Mild Cognitive Impairment and Alzheimer Disease Dementia. *JAMA Neurol* 2016, *73*, 93-101.

[5] Doty, R. L., The olfactory vector hypothesis of neurodegenerative disease: is it viable? *Ann Neurol* 2008, *63*, 7-15.

[6] Zelaya, M. V., Perez-Valderrama, E., de Morentin, X. M., Tunon, T.*, et al.*, Olfactory bulb proteome dynamics during the progression of sporadic Alzheimer's disease: identification of common and distinct olfactory targets across Alzheimer-related co-pathologies. *Oncotarget* 2015, *6*, 39437-39456.

[7] Lachen-Montes, M., Gonzalez-Morales, A., de Morentin, X. M., Perez-Valderrama, E.*, et al.*, An early dysregulation of FAK and MEK/ERK signaling pathways precedes the beta-amyloid deposition in the olfactory bulb of APP/PS1 mouse model of Alzheimer's disease. *J Proteomics* 2016, *148*, 149-158.

[8] Fernandez-Irigoyen, J., Corrales, F. J., Santamaria, E., Proteomic atlas of the human olfactory bulb. *J Proteomics* 2012, *75*, 4005-4016.

[9] Nagayama, S., Homma, R., Imamura, F., Neuronal organization of olfactory bulb circuits. *Front Neural Circuits* 2014, *8*, 98.

[10] Aebersold, R., Mann, M., Mass-spectrometric exploration of proteome structure and function. *Nature* 2016, *537*, 347-355.

[11] Lachen-Montes, M., Fernandez-Irigoyen, J., Santamaria, E., Deconstructing the molecular architecture of olfactory areas using proteomics. *Proteomics Clin Appl* 2016.

[12] Hondius, D. C., van Nierop, P., Li, K. W., Hoozemans, J. J.*, et al.*, Profiling the human hippocampal proteome at all pathologic stages of Alzheimer's disease. *Alzheimers Dement* 2016, *12*, 654-668.

[13] Krzyzanowska, A., Garcia-Consuegra, I., Pascual, C., Antequera, D.*, et al.*, Expression of regulatory proteins in choroid plexus changes in early stages of Alzheimer disease. *J Neuropathol Exp Neurol* 2015, *74*, 359-369.

[14] Kempf, S. J., Metaxas, A., Ibanez-Vea, M., Darvesh, S.*, et al.*, An integrated proteomics approach shows synaptic plasticity changes in an APP/PS1 Alzheimer's mouse model. *Oncotarget* 2016, *7*, 33627-33648.

[15] Lopez-Gonzalez, I., Schluter, A., Aso, E., Garcia-Esparcia, P.*, et al.*, Neuroinflammatory signals in Alzheimer disease and APP/PS1 transgenic mice: correlations with plaques, tangles, and oligomeric species. *J Neuropathol Exp Neurol* 2015, *74*, 319-344.

[16] von Eichborn, J., Dunkel, M., Gohlke, B. O., Preissner, S. C.*, et al.*, SynSysNet: integration of experimental data on synaptic protein-protein interactions with drug-target relations. *Nucleic Acids Res* 2013, *41*, D834-840.

[17] Croning, M. D., Marshall, M. C., McLaren, P., Armstrong, J. D., Grant, S. G., G2Cdb: the Genes to Cognition database. *Nucleic Acids Res* 2009, *37*, D846-851.

[18] Pirooznia, M., Wang, T., Avramopoulos, D., Valle, D.*, et al.*, SynaptomeDB: an ontology-based knowledgebase for synaptic genes. *Bioinformatics* 2012, *28*, 897-899.

[19] Derijard, B., Raingeaud, J., Barrett, T., Wu, I. H.*, et al.*, Independent human MAP-kinase signal transduction pathways defined by MEK and MKK isoforms. *Science* 1995, *267*, 682-685.

[20] Puig, B., Vinals, F., Ferrer, I., Active stress kinase p38 enhances and perpetuates abnormal tau phosphorylation and deposition in Pick's disease. *Acta Neuropathol* 2004, *107*, 185-189.

[21] Song, C., Perides, G., Wang, D., Liu, Y. F., beta-Amyloid peptide induces formation of actin stress fibers through p38 mitogen-activated protein kinase. *J Neurochem* 2002, *83*, 828-836.

[22] Casamayor, A., Morrice, N. A., Alessi, D. R., Phosphorylation of Ser-241 is essential for the activity of 3-phosphoinositide-dependent protein kinase-1: identification of five sites of phosphorylation in vivo. *Biochem J* 1999, *342 (Pt 2)*, 287-292.

[23] Mora, A., Komander, D., van Aalten, D. M., Alessi, D. R., PDK1, the master regulator of AGC kinase signal transduction. *Semin Cell Dev Biol* 2004, *15*, 161-170.

[24] Kimura, T., Yamamoto, H., Takamatsu, J., Yuzuriha, T.*, et al.*, Phosphorylation of MARCKS in Alzheimer disease brains. *Neuroreport* 2000, *11*, 869-873.

[25] Kraft, A. W., Hu, X., Yoon, H., Yan, P.*, et al.*, Attenuating astrocyte activation accelerates plaque pathogenesis in APP/PS1 mice. *FASEB J* 2013, *27*, 187-198.

[26] Merkwirth, C., Martinelli, P., Korwitz, A., Morbin, M.*, et al.*, Loss of prohibitin membrane scaffolds impairs mitochondrial architecture and leads to tau hyperphosphorylation and neurodegeneration. *PLoS Genet* 2012, *8*, e1003021.

[27] Zhou, P., Qian, L., D'Aurelio, M., Cho, S.*, et al.*, Prohibitin reduces mitochondrial free radical production and protects brain cells from different injury modalities. *J Neurosci* 2012, *32*, 583-592.

[28] Artal-Sanz, M., Tavernarakis, N., Prohibitin and mitochondrial biology. *Trends Endocrinol Metab* 2009, *20*, 394-401.

[29] Sanchez-Quiles, V., Santamaria, E., Segura, V., Sesma, L.*, et al.*, Prohibitin deficiency blocks proliferation and induces apoptosis in human hepatoma cells: molecular mechanisms and functional implications. *Proteomics* 2010, *10*, 1609-1620.

[30] Doty, R. L., Olfactory dysfunction in Parkinson disease. *Nat Rev Neurol* 2012, *8*, 329-339.

[31] Gray, A. J., Staples, V., Murren, K., Dhariwal, A., Bentham, P., Olfactory identification is impaired in clinic-based patients with vascular dementia and senile dementia of Alzheimer type. *Int J Geriatr Psychiatry* 2001, *16*, 513-517.
[32] Filiou, M. D., Martins-de-Souza, D., Guest, P. C., Bahn, S., Turck, C. W., To label or not to label: applications of quantitative proteomics in neuroscience research. *Proteomics* 2012, *12*, 736-747.

[33] Soler-Lopez, M., Zanzoni, A., Lluis, R., Stelzl, U., Aloy, P., Interactome mapping suggests new mechanistic details underlying Alzheimer's disease. *Genome Res* 2011, *21*, 364-376.

[34] Perluigi, M., Barone, E., Di Domenico, F., Butterfield, D. A., Aberrant protein phosphorylation in Alzheimer disease brain disturbs pro-survival and cell death pathways. *Biochim Biophys Acta* 2016, *1862*, 1871-1882.

[35] Koleske, A. J., Molecular mechanisms of dendrite stability. *Nat Rev Neurosci* 2013, *14*, 536-550.

[36] Dehvari, N., Isacsson, O., Winblad, B., Cedazo-Minguez, A., Cowburn, R. F., Presenilin regulates extracellular regulated kinase (Erk) activity by a protein kinase C alpha dependent mechanism. *Neurosci Lett* 2008, *436*, 77-80.

[37] Subramaniam, S., Zirrgiebel, U., von Bohlen Und Halbach, O., Strelau, J.*, et al.*, ERK activation promotes neuronal degeneration predominantly through plasma membrane damage and independently of caspase-3. *J Cell Biol* 2004, *165*, 357-369.

[38] Cheung, E. C., Slack, R. S., Emerging role for ERK as a key regulator of neuronal apoptosis. *Sci STKE* 2004, *2004*, PE45.

[39] Origlia, N., Arancio, O., Domenici, L., Yan, S. S., MAPK, beta-amyloid and synaptic dysfunction: the role of RAGE. *Expert Rev Neurother* 2009, *9*, 1635-1645.

[40] Munoz, L., Ammit, A. J., Targeting p38 MAPK pathway for the treatment of Alzheimer's disease. *Neuropharmacology* 2010, *58*, 561-568.
[41] Criscuolo, C., Fabiani, C., Bonadonna, C., Origlia, N., Domenici, L., BDNF prevents amyloid-dependent impairment of LTP in the entorhinal cortex by attenuating p38 MAPK phosphorylation. *Neurobiol Aging* 2015, *36*, 1303-1309.

[42] Bachstetter, A. D., Xing, B., de Almeida, L., Dimayuga, E. R., *et al.*, Microglial p38alpha MAPK is a key regulator of proinflammatory cytokine up-regulation induced by toll-like receptor (TLR) ligands or beta-amyloid (Abeta). *J Neuroinflammation* 2011, *8*, 79.

[43] Li, Y., Liu, L., Barger, S. W., Griffin, W. S., Interleukin-1 mediates pathological effects of microglia on tau phosphorylation and on synaptophysin synthesis in cortical neurons through a p38-MAPK pathway. *J Neurosci* 2003, *23*, 1605-1611.

[44] Ferrer, I., Gomez-Isla, T., Puig, B., Freixes, M., *et al.*, Current advances on different kinases involved in tau phosphorylation, and implications in Alzheimer's disease and tauopathies. *Curr Alzheimer Res* 2005, *2*, 3-18.

[45] Sun, A., Liu, M., Nguyen, X. V., Bing, G., P38 MAP kinase is activated at early stages in Alzheimer's disease brain. *Exp Neurol* 2003, *183*, 394-405.

[46] Pei, J. J., Braak, E., Braak, H., Grundke-Iqbal, I., *et al.*, Localization of active forms of C-jun kinase (JNK) and p38 kinase in Alzheimer's disease brains at different stages of neurofibrillary degeneration. *J Alzheimers Dis* 2001, *3*, 41-48.

[47] Hensley, K., Floyd, R. A., Zheng, N. Y., Nael, R., *et al.*, p38 kinase is activated in the Alzheimer's disease brain. *J Neurochem* 1999, *72*, 2053-2058.

[48] Xing, B., Bachstetter, A. D., Van Eldik, L. J., Inhibition of neuronal p38alpha, but not p38beta MAPK, provides neuroprotection against three different neurotoxic insults. *J Mol Neurosci* 2015, *55*, 509-518.

[49] Schnoder, L., Hao, W., Qin, Y., Liu, S., *et al.*, Deficiency of Neuronal p38alpha MAPK Attenuates Amyloid Pathology in Alzheimer Disease Mouse and Cell Models through Facilitating Lysosomal Degradation of BACE1. *J Biol Chem* 2016, *291*, 2067-2079.

[50] Pietri, M., Dakowski, C., Hannaoui, S., Alleaume-Butaux, A., *et al.*, PDK1 decreases TACE-mediated alpha-secretase activity and promotes disease progression in prion and Alzheimer's diseases. *Nat Med* 2013, *19*, 1124-1131.
[51] Manterola, L., Hernando-Rodriguez, M., Ruiz, A., Apraiz, A., *et al.*, 1-42 beta-amyloid peptide requires PDK1/nPKC/Rac 1 pathway to induce neuronal death. *Transl Psychiatry* 2013, *3*, e219.

[52] Le Good, J. A., Ziegler, W. H., Parekh, D. B., Alessi, D. R., *et al.*, Protein kinase C isotypes controlled by phosphoinositide 3-kinase through the protein kinase PDK1. *Science* 1998, *281*, 2042-2045.

[53] Sun, M. K., Alkon, D. L., The "memory kinases": roles of PKC isoforms in signal processing and memory formation. *Prog Mol Biol Transl Sci* 2014, *122*, 31-59.

[54] Alkon, D. L., Sun, M. K., Nelson, T. J., PKC signaling deficits: a mechanistic hypothesis for the origins of Alzheimer's disease. *Trends Pharmacol Sci* 2007, *28*, 51-60.

[55] Desdouits, F., Buxbaum, J. D., Desdouits-Magnen, J., Nairn, A. C., Greengard, P., Amyloid beta peptide formation in cell-free preparations. Regulation by protein kinase C, calmodulin, and calcineurin. *J Biol Chem* 1996, *271*, 24670-24674.
[56] Lee, W., Boo, J. H., Jung, M. W., Park, S. D., *et al.*, Amyloid beta peptide directly inhibits PKC activation. *Mol Cell Neurosci* 2004, *26*, 222-231.

[57] Liang, W. S., Dunckley, T., Beach, T. G., Grover, A., *et al.*, Altered neuronal gene expression in brain regions differentially affected by Alzheimer's disease: a reference data set. *Physiol Genomics* 2008, *33*, 240-256.

[58] Sun, M. K., Alkon, D. L., Activation of protein kinase C isozymes for the treatment of dementias. *Adv Pharmacol* 2012, *64*, 273-302.

[59] Friedland-Leuner, K., Stockburger, C., Denzer, I., Eckert, G. P., Muller, W. E., Mitochondrial dysfunction: cause and consequence of Alzheimer's disease. *Prog Mol Biol Transl Sci* 2014, *127*, 183-210.

[60] Tillement, L., Lecanu, L., Papadopoulos, V., Alzheimer's disease: effects of beta-amyloid on mitochondria. *Mitochondrion* 2011, *11*, 13-21.
[61] Nijtmans, L. G., de Jong, L., Artal Sanz, M., Coates, P. J., *et al.*, Prohibitins act as a membrane-bound chaperone for the stabilization of mitochondrial proteins. *EMBO J* 2000, *19*, 2444-2451.

[62] Perez-Gracia, E., Torrejon-Escribano, B., Ferrer, I., Dystrophic neurites of senile plaques in Alzheimer's disease are deficient in cytochrome c oxidase. *Acta Neuropathol* 2008, *116*, 261-268.

[63] Thuaud, F., Ribeiro, N., Nebigil, C. G., Desaubry, L., Prohibitin ligands in cell death and survival: mode of action and therapeutic potential. *Chem Biol* 2013, *20*, 316-331.

[64] Bavelloni, A., Piazzi, M., Raffini, M., Faenza, I., Blalock, W. L., Prohibitin 2: At a communications crossroads. *IUBMB Life* 2015, *67*, 239-254.

[65] Mishra, S., Ande, S. R., Nyomba, B. L., The role of prohibitin in cell signaling. *FEBS J* 2010, *277*, 3937-3946.

[66] Peng, Y. T., Chen, P., Ouyang, R. Y., Song, L., Multifaceted role of prohibitin in cell survival and apoptosis. *Apoptosis* 2015, *20*, 1135-1149.

[67] Jiang, L., Dong, P., Zhang, Z., Li, C*., et al.*, Akt phosphorylates Prohibitin 1 to mediate its mitochondrial localization and promote proliferation of bladder cancer cells. *Cell Death Dis* 2015, *6*, e1660.

[68] Chiu, C. F., Ho, M. Y., Peng, J. M., Hung, S. W*., et al.*, Raf activation by Ras and promotion of cellular metastasis require phosphorylation of prohibitin in the raft domain of the plasma membrane. *Oncogene* 2013, *32*, 777-787.

[69] Braak, H., Alafuzoff, I., Arzberger, T., Kretzschmar, H., Del Tredici, K., Staging of Alzheimer disease-associated neurofibrillary pathology using paraffin sections and immunocytochemistry. *Acta Neuropathol* 2006, *112*, 389-404.

[70] Alafuzoff, I., Arzberger, T., Al-Sarraj, S., Bodi, I*., et al.*, Staging of neurofibrillary pathology in Alzheimer's disease: a study of the BrainNet Europe Consortium. *Brain Pathol* 2008, *18*, 484-496.

[71] Montine, T. J., Phelps, C. H., Beach, T. G., Bigio, E. H*., et al.*, National Institute on Aging-Alzheimer's Association guidelines for the neuropathologic assessment of Alzheimer's disease: a practical approach. *Acta Neuropathol* 2012, *123*, 1-11.

[72] Thal, D. R., Rub, U., Orantes, M., Braak, H., Phases of A beta-deposition in the human brain and its relevance for the development of AD. *Neurology* 2002, *58*, 1791-1800.

[73] Crary, J. F., Trojanowski, J. Q., Schneider, J. A., Abisambra, J. F*., et al.*, Primary age-related tauopathy (PART): a common pathology associated with human aging. *Acta Neuropathol* 2014, *128*, 755-766.

[74] Mackenzie, I. R., Neumann, M., Baborie, A., Sampathu, D. M*., et al.*, A harmonized classification system for FTLD-TDP43 pathology. *Acta Neuropathol* 2011, *122*, 111-113.

[75] Roman, G. C., Tatemichi, T. K., Erkinjuntti, T., Cummings, J. L*., et al.*, Vascular dementia: diagnostic criteria for research studies. Report of the NINDS-AIREN International Workshop. *Neurology* 1993, *43*, 250-260.

[76] Litvan, I., Hauw, J. J., Bartko, J. J., Lantos, P. L*., et al.*, Validity and reliability of the preliminary NINDS neuropathologic criteria for progressive supranuclear palsy and related disorders. *J Neuropathol Exp Neurol* 1996, *55*, 97-105.

[77] Shevchenko, A., Tomas, H., Havlis, J., Olsen, J. V., Mann, M., In-gel digestion for mass spectrometric characterization of proteins and proteomes. *Nat Protoc* 2006, *1*, 2856-2860.

[78] Shilov, I. V., Seymour, S. L., Patel, A. A., Loboda, A*., et al.*, The Paragon Algorithm, a next generation search engine that uses sequence temperature values and feature probabilities to identify peptides from tandem mass spectra. *Mol Cell Proteomics* 2007, *6*, 1638-1655.

[79] Tang, W. H., Shilov, I. V., Seymour, S. L., Nonlinear fitting method for determining local false discovery rates from decoy database searches. *J Proteome Res* 2008, *7*, 3661-3667.

[80] Vizcaino, J. A., Deutsch, E. W., Wang, R., Csordas, A*., et al.*, ProteomeXchange provides globally coordinated proteomics data submission and dissemination. *Nat Biotechnol* 2014, *32*, 223-226.

CHAPTER 4

Network-driven proteogenomics unveils an aging-related imbalance in the olfactory IκB alpha-NFκB p65 complex functionality in Tg2576 Alzheimer´s disease mouse model

Maialen Palomino[1], **Mercedes Lachén-Montes**[1,2,3], Andrea González-Morales[1,2,3], Karina Ausín[2,3], Alberto Pérez-Mediavilla[3,4], Joaquín Fernández-Irigoyen[1,2,3] §, Enrique Santamaría[1,2,3] §

1 Clinical Neuroproteomics Group, Navarrabiomed, Departamento de Salud, Universidad Pública de Navarra, Pamplona, Spain;

2 Proteored-ISCIII. Proteomics Unit, Navarrabiomed, Departamento de Salud, Universidad Pública de Navarra, Pamplona, Spain;

3 IDISNA, Navarra Institute for Health Research, Pamplona, Spain

4 Neurobiology of Alzheimer's disease, Neurosciences Division, Center for Applied Medical Research (CIMA), Department of Biochemistry, University of Navarra, Pamplona, Spain;

Abstract

Olfaction is often deregulated in Alzheimer´s disease (AD) patients, being also impaired in transgenic Tg2576 AD mouse model, which overexpress the Swedish mutated form of human amyloid precursor protein (APP). However, little is known about the molecular mechanisms that accompany the neurodegeneration of olfactory structures in aged Tg2576 mice. For that, we have applied proteome- and transcriptome-wide approaches to probe molecular disturbances in the olfactory bulb (OB) dissected from aged Tg2576 mice (18 months of age) respect to age matched wild-type (WT) littermates. Some over-represented biological functions were directly relevant to neuronal homeostasis, and processes of learning, cognition, and behavior. In addition to the modulation of CREB1 and APP interactomes, an imbalance in the functionality of the IκB alpha-NFκB p65 complex was observed during the aging process in the OB of Tg2576 mice. At two months of age, the phosphorylated isoforms of olfactory IκB alpha and NFκB p65 were inversely regulated in transgenic mice. However, both phosphorylated proteins were increased at 6 months of age, while a specific drop in IκB alpha levels was detected in 18-month-old Tg2576 mice, suggesting a transient activation of NFκB in the OB of Tg2576 mice. Taken together, our data provide a metabolic map of olfactory alterations in aged Tg2576 mice, reflecting the progressive effect of APP overproduction and Aβ accumulation on the OB homeostasis in aged stages.

1. Introduction

Although olfactory involvement may also appear in healthy non-demented elderly subjects [1], olfactory dysfunction is present in up to 90% of AD patients [2]. Some studies suggest that olfactory dysfunction is an early event of AD, preceding the appearance of typical AD symptoms, such as memory loss, and dementia. The Tg2576 AD mouse model expresses the human APP695 isoform with double mutation K670 N, M671 L also known as hAPPSw, via the hamster prion promoter [3]. These mice displayed an increase of APP production with consequent overproduction of Aβ40 and Aβ42 and plaques formation in the frontal, temporal, and entorhinal cortices, hippocampus, presubiculum, and cerebellum at about 11–13 months of age [4]. There is strong evidence that accumulation of Aβ peptide, derived via APP proteolysis, is responsible for age-related memory decline in this model [5] [6] [7]. Other than the increase in Aβ production, these mice can also display hyperphosphorylated tau at old age. Synaptic deficits, and mitochondrial imbalance have been reported for this late-plaque model [8] [9]. Metabolic and posttranslational modification alterations occur long before the onset of behavioral impairment [10] [11,12]. However, Tg2576 mice did not present a profound cognitive impairment, even at old ages [13].

The olfactory bulb (OB) is the first central structure of the olfactory pathway in the brain [14]. APP processing products have been observed in the OB of 1-month-old Tg2576 mice, detecting Aβ deposition at 13.5 months of age [15]. Moreover, Tg2576 mice (between ages of 6.5 and 8 months) present a reduced rate of OB neurogenesis, a reduction in the volume of the granular cell layer of the OB [16], and some olfactory memory deficits [16,17]. A detailed analysis of olfaction in Tg2576 AD model also revealed behavioral deficits included perseveration of initial odor investigation, impaired short term odor habituation, and impaired odor discrimination [18,19]. Interestingly, the emergence of these specific behavioral impairments corresponds with a progressive Aβ burden in specific olfactory regions [18]. In view of these data, an in depth

biochemical characterization of the OB is necessary to reveal the missing links in the biochemical understanding of smell impairments in Tg2576 AD model.

In this study, we used transcriptome-wide analyses, and mass-spectrometry based quantitative proteomics as a discovery platform to increase our knowledge about the pathophysiological mechanisms that are disturbed in the OB from aged Tg2576 mice (18 months of age) respect to age matched background strain control mice. 107 differential genes, and 25 differential expressed proteins were detected, pinpointing specific pathways, protein interaction networks, and potential novel therapeutic targets.

2. Results and discussion

Although it is widely believed that OB perturbations are responsible for olfactory dysfunction in neurological syndromes [2], few studies have examined this area using high throughput molecular technologies [27-30]. Focusing on the transgenic Tg2576 mouse AD model, different proteomic and transcriptomic studies have been attempted to discover novel molecular mediators associated with AD pathogenesis in brain areas differentially affected by the disease [9,31-37]. However, to our knowledge, this is the first study to characterize AD-associated molecular changes in the OB derived from this late-plaque model using omic technologies.

2.1 Molecular alterations detected in the OB of 18-month-old Tg2576 mice

Tg2576 transgenic mice suffer from memory deficits accompanied by β-amyloid plaques that increase with disease progression [5-7]. We have applied a dual-omic approach to analyze the molecular imbalance induced by hAPPSw isoform at olfactory level, with the final goal to reveal novel information about the OB site-specific molecular signature at late AD stages in 18-month-old Tg2576 mice. To screen the potential differences in OB molecular expression profiles, OB specimens for each experimental group (Tg2576 and WT mice) were separately subjected into isobaric tags (iTRAQ) coupled to 2D nano-liquid chromatography tandem mass spectrometry (3 mice/condition) and into RNA microarray platform (3 mice/condition) (Figure 1).

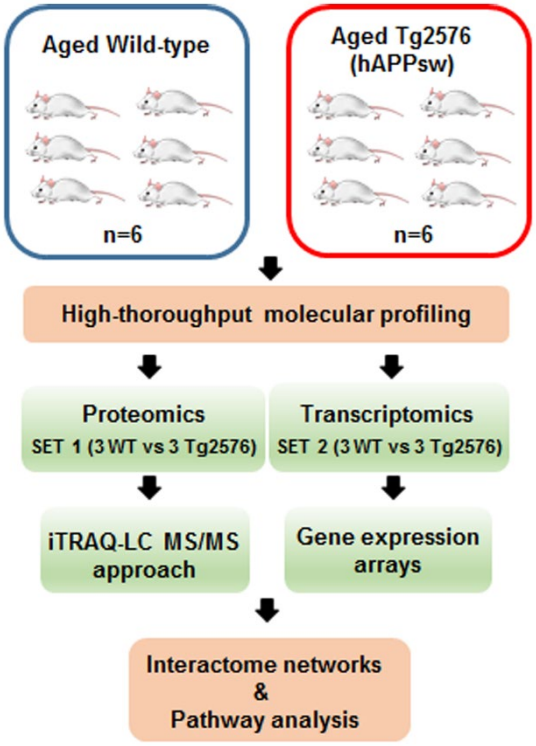

Figure 1. An overview of the workflow used for the molecular characterization of the OB derived from aged Tg2576 mice.

Among 2466 quantified proteins (Supplementary Table 1), differential analysis revealed 25 de-regulated proteins in Tg2576 OBs with respect to WT OBs (11 down- and 14 up-regulated in aged Tg2576 mice) (Figure 2A-B, and Supplementary table 2). The up-regulation of our intrinsic positive control (APP) was verified by Western-blotting (Figure 2A). According to STRING Database [26], this subproteome are mainly involved in membrane organization (FDR: 1.21E-05; e.g: *SYNE2*, *NOL3*, *AP1G1*), protein transport (FDR: 0.047; e.g: *RAB5B*, *RPL28*, *SRPR*, *RPL18*, *CHMP3*, *COPE*), and negative regulation of neuron differentiation (FDR: 0.041; e.g: *APP*, *APOE*, *GFAP*, *MT3*). In the transcriptomic phase, 107 protein-coding genes were differentially regulated in the OB of aged Tg2576 mice (16 down- and 91 up-regulated genes with respect to WTs) (Supplementary Table 3). Gene interactome networks suggested an alteration in the response to cAMP (down regulation of *EGR1*, *EGR2*, *NR4A1*, *JUNB*, and *FOSB* genes), and in the olfactory

transduction signaling, due to the up-regulation of *ADCY3*, and *GNAL* genes, together with the overexpression of some olfactory receptors (OR) like *OLFR553*, *OLFR1312*, and *OLFR597* genes (Figure 2C).

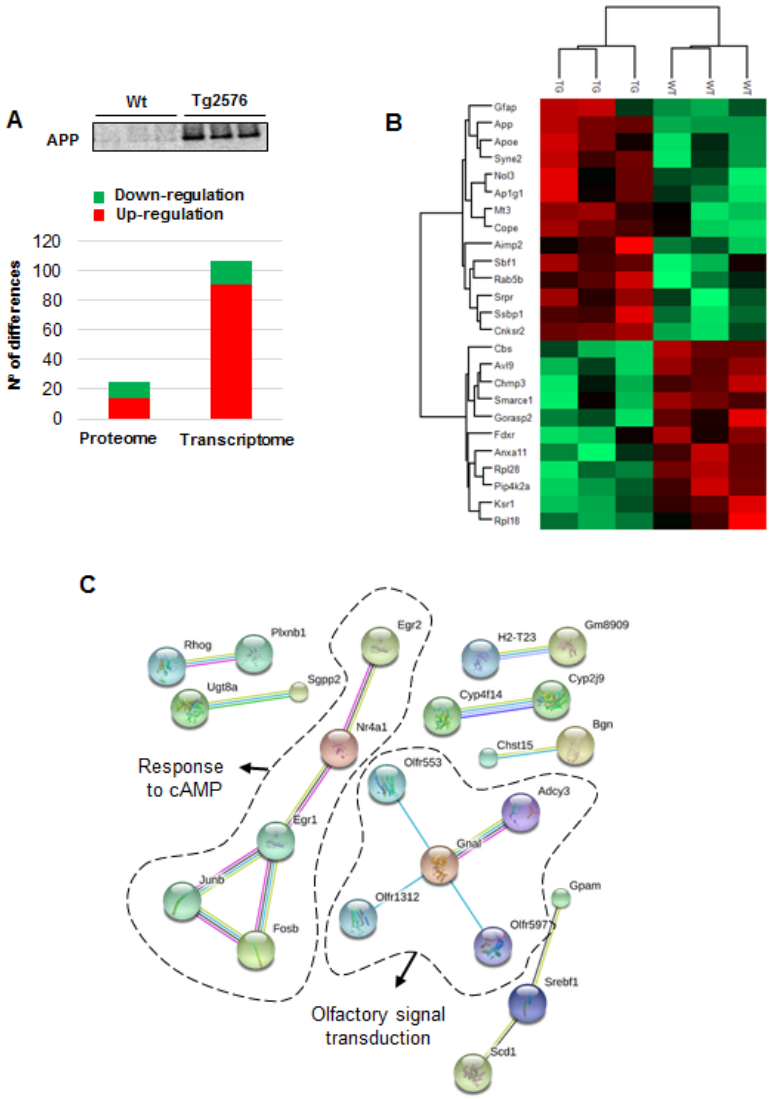

Figure 2. Multi-omic approach to decipher the OB site-specific molecular signature in aged Tg2576 mice. A) Differential molecular profiling detected by the dual-omic approach in Tg2576 OBs. The olfactory protein expression levels of APP at late AD stages in 18-month-old Tg2576 mice is shown. B) Heat map representing the degree of change for the differentially expressed proteins (Supplementary table 2) between 18-month-old WT and Tg2576 mice. Red and green, up- and down-regulated proteins, respectively. C) Gene interactome networks for the differentially expressed genes detected in aged Tg2576 mice. Network analysis was performed submitting the corresponding gene IDs to the STRING (Search Tool for the Retrieval of Interacting Genes) software (v.10.5) (http://stringdb.org/). This is a large database of known and

predicted protein/gene interactions. Genes were represented with nodes and the functional interactions with edges. All the edges were supported by at least a reference from the literature or from canonical information stored in the STRING database (e.g: by text mining, co-expression, co-occurrence, databases, etc). To minimize false positives as well as false negatives, only interactions tagged as "high confidence" (>0.7) in STRING database were considered.

Moreover, *RTP2* was also up-regulated in the OB of Tg2576 mice. RTP2 (Receptor-transporter-protein 2) promotes OR cell-surface expression and activation in response to odorant stimulation [38]. A deregulation of sensory perception of smell has been previously proposed from transcriptomic information extracted from prefrontal cortex derived from AD subjects [39]. According with our data, OR gene dysregulation has been also demonstrated in OB, entorhinal and frontal cortex in human AD subjects [40, 41]. On the other hand, there was not an evident RNA-protein correlation derived from the differential datasets obtained from Tg2576 OBs. This may be due to the use of different set of animals for each technological platform. Moreover, other reasons may also explain the observed discrepancy such as the spatial and temporal delayed synthesis between mRNA and protein [42], post-transcriptional events, and the different hydrophobicity and solubility of the "missing proteome" during the proteomic phase, hampering its characterization and quantitation by mass-spectrometry (e.g: ORs) [43].

2.2 Biological functions and neuronal-specific processes altered in the OB of aged Tg2576

To obtain a more detailed description of the proteogenomic modulation in the Tg2576 OBs, differential datasets were analyzed for higher-level organization of genes and proteins into common biological pathways. For that, differential proteomic and transcriptomic datasets were merged, and functionally analyzed across specific biological functions using the IPA software. Some statistically over-represented processes were directly relevant to cell movement (p-val: 0,0003), cell survival (p-val:0,00015), and cell death (p-val: 1.08E-6) (Figure 3A and

Supplementary Table 4). Moreover, molecular clusters involved in learning (p-val: 0,004), cognition (p-val: 0,0007), behavior (p-val: 0.003), and dementia (p-val: 0,003) were also enriched (Figure 3B and Supplementary Table 4).

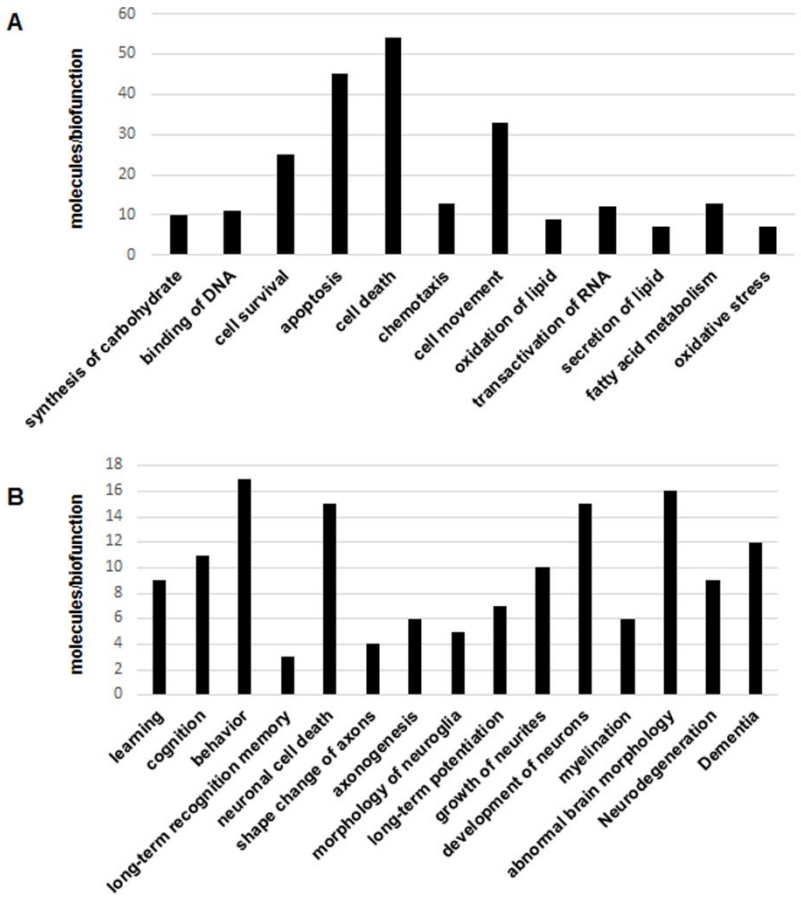

Figure 3. Significantly enriched biofunctions in the OB of aged Tg2576 mice. Canonical (A) and neuronal-specific (B) over-represented biofunctions in omic datasets derived from 18-month-old Tg2576.

Athough the role of β-amyloid in olfactory deficits detected in Tg2576 mice has been extensively studied [18, 19], there is no information about the survival potential of OB neurons in aged Tg2576 mice. To complement our proteogenomic workflow, survival and apoptotic pathways were mapped to monitor the effect of β-amyloid burden on neuronal viability in the OB of aged Tg2576 mice. For that, steady-state levels of survival proteins like Bcl-xL and activated forms of caspase-3, -9, and -12 were measured in protein extracts from Tg2576 OBs at 18 months. The stepwise characterization of constitutive pro- and anti-apoptotic factors revealed no activation of endoplasmic reticulum or mitochondrial apoptotic pathways in aged Tg2576 at the level of OB (data not shown). Subsequent experiments were performed to monitor specific survival pathways at the level of OB. Total and residue-specific phosphorylation of FAK, Akt, MEK/ERK, PDK1, PKC, p38 MAPK, and SEK1/MKK4 were measured in Tg2576 and WT OBs. As shown in figure 4, no changes in the activation state of this survival panel were observed between transgenic and WT mice at 18 months of age, except a slight increase in the activation state of SEK1/MKK4 kinase (Figure 4).

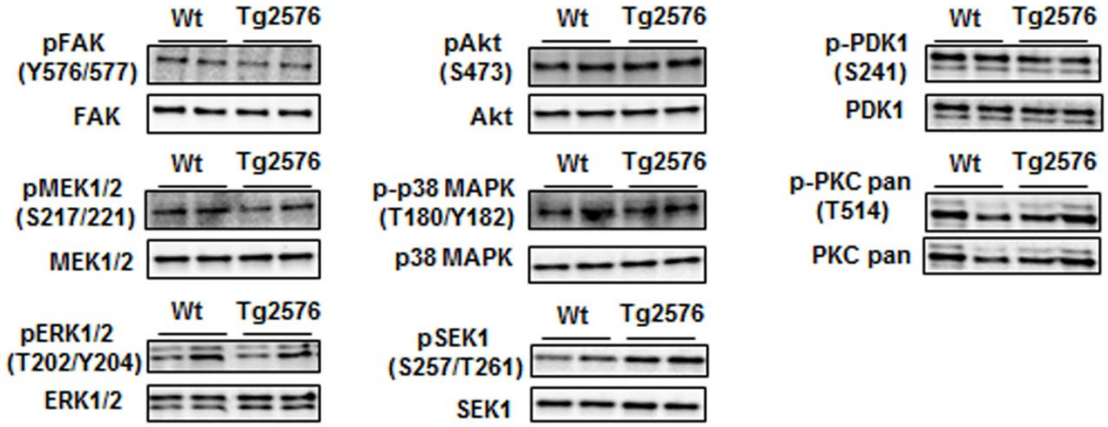

Figure 4. Activation state of specific survival pathways in the OB of aged Tg2576 mice. Levels and residue-specific phosphorylation of FAK, MEK/ERK, Akt, PDK1, PKC, p38 MAPK, and SEK1/MKK4, in the OB of aged Tg2576 mice. Equal loading of the gels was assessed by stain free digitalization.

However, deregulation of MAP kinases (MEK, ERK), and PDK1/PKC axis has been observed in human OB at advanced AD stages [29, 30]. This is not an unexpected observation, because the AD progression in Tg2576 mice is reminiscent of, but not identical to sporadic human AD. This may be explained, in part, by specie- and stage-dependent responses [30], and differences in molecular mechanisms associated to β-amyloidogenesis.

2.3 Functional interactome of hAPPSw isoform at olfactory level: Characterization of potential hubs by network-driven proteogenomics

To explore the cooperative action among differentially expressed OB genes/proteins in aged Tg2576 mice, we performed molecular interaction networks merging the olfactory targets that tend to be de-regulated in this model. We consider that the discovery of unexpected relationships between apparently unrelated proteins and AD-causing neuropathological substrates is a powerful strategy for the characterization of novel AD causative/susceptibility targets with a central role during olfactory neurodegeneration. Using IPA software, functional interactome maps were generated (Figures 5, and 6). We explored whether hAPPSw isoform highly expressed in Tg2576 mice, may potentially be interconnected with differential molecular targets detected by our dual-omic approach. As shown in figure 5, differential functional interactors for APP protein were identified in the OB from aged transgenic mice. The functional APP interactome was composed by targets potentially distributed in different cellular compartments: i) APOE, SERPINH1, and BGN in the extracellular space, ii) VAPA at plasma membrane level, iii) Irgm1, GFAP, MT3, ARC, GAB1, ZDHHC23, and GORASP2 in the cytoplasm, and iv) FOSB, JUNB, ZFP36L1, NR4A2, HEY2, EGR1, TP63, and Mmp in the nuclear compartment (Figure 5).

A

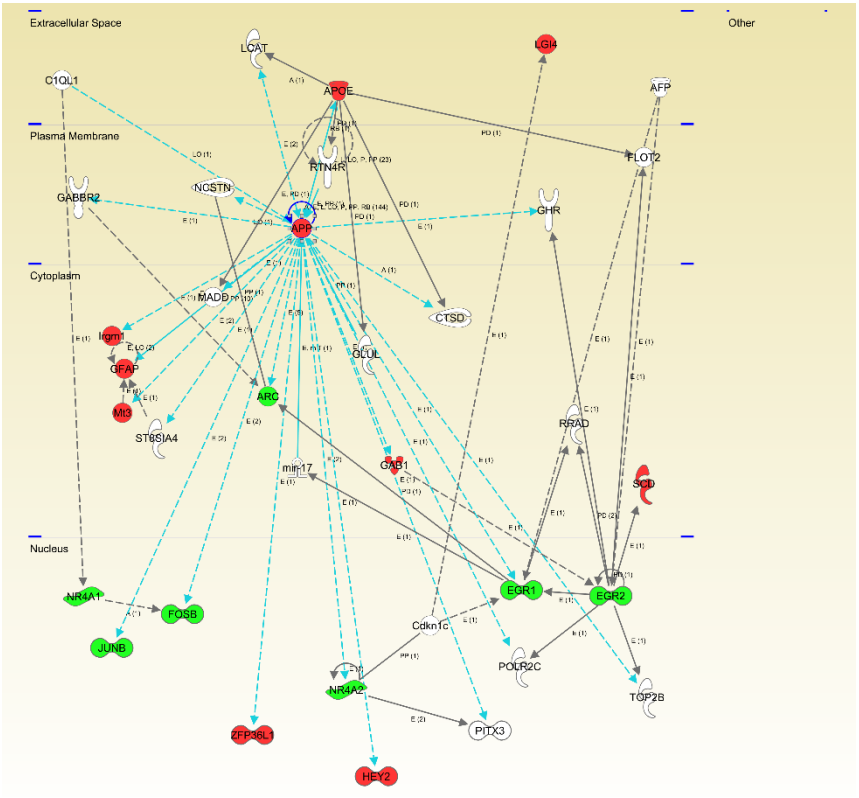

B

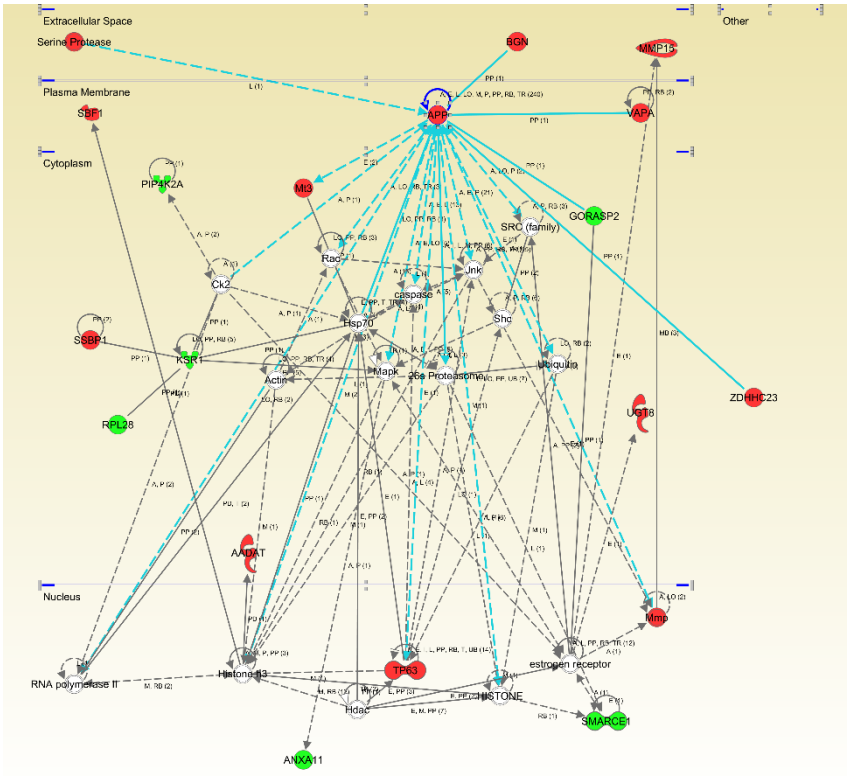

Figure 5. Modulation of APP molecular interaction network in the OB of aged Tg2576 mice. A and B) Visual representation of the relationships between differential expressed genes/proteins

and APP functional interactors (blue lines) are shown in both potentially deregulated networks in Tg2576 OBs. Dysregulated molecules are highlighted in red (up-regulated) and green (down-regulated). Continuous and discontinuous lines represent direct and indirect interactions respectively. The complete legend including main features, molecule shapes, and relationships is found in http://ingenuity.force.com/ipa/articles/Feature_Description/Legend.

Moreover, integrative network analysis also allowed us to establish a framework to map interaction between differentially expressed targets and network hubs. According to IPA analysis, CREB1, NFKBIA (IκB alpha), and NFκB were postulated as potential upstream regulators of part of the differential targets detected in our study (Table 1).

Upstream Regulator	Molecule Type	p-value	Target molecules IN OB omics dataset
CREB1	transcription regulator	0,00000209	APOE,ARC,EGR1,EGR2,FOSB,GNAL,HLA-A,JUNB,NR4A1,NR4A2,NR4A3,RBP4,SCD,ZDHHC23
NFKBIA	transcription regulator	0,00916	BCL2A1,CD82,HLA-A,JUNB,MMP15,NID1,NR4A1
NFKB1	transcription regulator	0,0000748	APOE,APP,BCL2A1,CD82,EGR1,HLA-DMB,NR4A1,TBX21
NFkB (complex)	complex	0,00174	APOE,APP,BCL2A1,CD82,EGR1,GFAP,HLA-A,HLA-DMB,JUNB,KLF3

Table 1. Potential upstream regulators of differential targets detected in our study.

Even though changes in their expression was not detected in our system-wide approaches, the alteration of some of their targets may be compatible with a dysregulation of their functionality in the OB of aged Tg2576 mice. For that, subsequent experiments were performed to monitor the protein expression of CREB1 as well as the activation state of IκB alpha- NFκB p65 complex in the OB of aged Tg2576 mice. CREB1 is at a central converging point of activated pathways during the processes of synaptic strengthening and memory formation [44-46]. Protein expression levels of transcription factor CREB1 were significantly reduced in the OB of TG2576 mice (figure 6), in parallel with the down-regulation of well-known activity-dependent CREB target genes such as *FOSB*, *NR4A2*, and *EGR1* [47] (Figure 6 and Supplementary Table 3). Our data obtained in aged Tg2576 mice reinforce the direct relationship between a reduction of CREB1 activation and AD pathology [47,48].

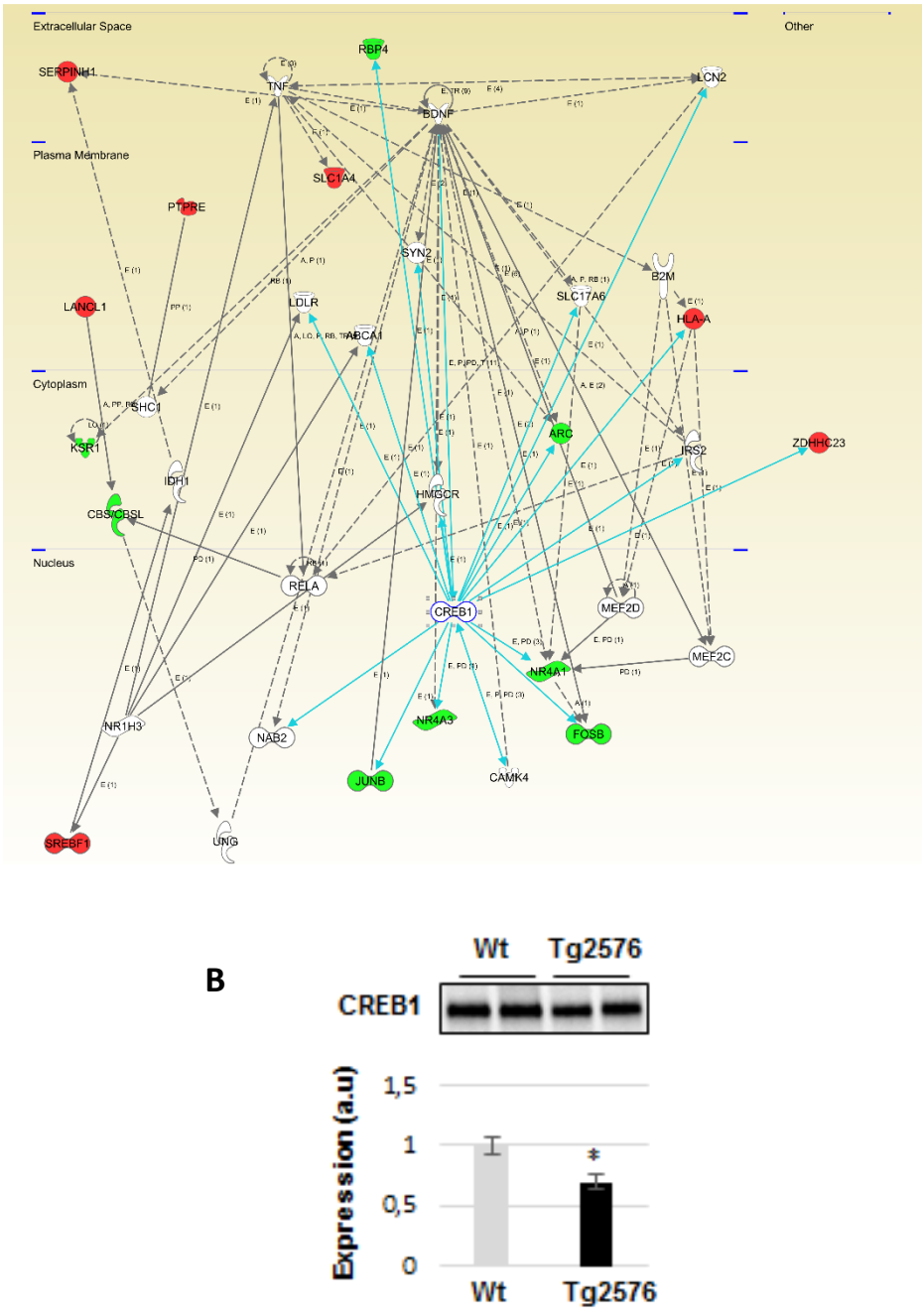

Figure 6. Modulation of CREB1 molecular interactome in the OB of aged Tg2576 mice. Visual representation of the relationships between differential expressed genes/proteins and CREB1 functional interactors (blue lines) are shown in the deregulated network in Tg2576 OBs (A). Dysregulated molecules are highlighted in red (up-regulated) and green (down-regulated). Continuous and discontinuous lines represent direct and indirect interactions respectively. The complete legend including main features, molecule shapes, and relationships is found in

http://ingenuity.force.com/ipa/articles/Feature_Description/Legend. CREB1 protein levels were down-regulated in the OB of aged Tg2576 mice (B).

2.4 An impairment in the olfactory IκB alpha-NFκB p65 complex functionality during the progression of AD in Tg2576 mice

The nuclear factor NFκB controls the transcription of a wide variety of genes include pro-apoptotic and pro-survival genes, proinflammatory cytokines, antioxidant enzymes, pro-oxidant enzymes and many others [49]. In general, the formation of a complex of NFκB dimer with a typical member of IkB family prevents the nuclear translocation and gene activation function of NF-κB [50]. The phosphorylation of serine 32 of IκBα leads to ubiquitination and proteasomal degradation of IκBα, allowing the phosphorylation of NFκB p65 subunit and the enhancement of p65 transactivation potential [50]. In our study, we have monitored the functionality of IκB alpha-NFκB p65 complex at three stages of AD: long before (2 months of age), immediately before (6 months) and after (18 months) the appearance of Aβ plaques [9]. At two months of age, the phosphorylated isoforms of IκB alpha and NFκB p65 were inversely regulated in Tg2576 transgenic mice (Figure 7A-B). However, both phosphorylated proteins were increased at 6 months of age, whereas a specific drop in IκB alpha levels was detected in 18-month-old Tg2576 mice (Figure 7A-B). Based on these data, it may be hypothesized that APP overproduction induces a transient activation of NFκB in the OB of Tg2576 mice respect to WT mice. It has been previously observed an increased NFκB activity in different hippocampal and cortical structures in post-mortem AD brains [51-53], probably due to an increased oxidative stress, inflammatory reactions and toxicity of accumulated Aβ peptides [49]. To deep our understanding of the functional dynamics of olfactory IκB alpha-NFκB p65 complex during the aging process, steady-state levels and phosphorylated isoforms were independently evaluated in WT and Tg2576 mice during aging. For that, protein profiles were quantified in a time-dependent manner. Respect to data obtained at 2 months of age, a specific drop in NFκB p65 protein levels and a progressive decrease in the phosphorylated NFκB p65 subunit were observed in WT mice, whereas an

increment in NFκB p65 activity at 6 months was exclusively observed in Tg2576 mice (figure 7C). In addition, the increment in total and phosphorylated levels of IkB alpha observed in 18-month-old WT mice, was blocked in aged Tg2576 mice (figure 7C). Previous reports have shown that NFκB inhibitors prevent Aβ-induced toxicity *in vivo* and *in vitro* AD experimental models [54]. To our knowledge, the early impairment in NFκB functionality observed in Tg2576 mice at the level of OB, might open new avenues of targeting the NF-κB signaling cascade at olfactory level, gaining new insight into disease pathogenesis and identifying potential disease modifying agents. However, it is important to note that the phosphoproteome of IκB alpha-NFκB complexes is highly complicated [50], and many post-translational modifications (PTMs) have been characterized (see http://www.uniprot.org/uniprot/Q04206, and http://www.uniprot.org/uniprot/P25963) being still unclear how the tangled crosstalk between all PTMs regulates the ability of NF-κB proteins to induce or to repress defined target genes. Due to the early olfactory imbalance detected in the IκB alpha-NFκB p65 complex in Tg2576 mice, additional studies will be necessary to decipher the effects of APP-dependent NFκB dysregulation on the OB molecular landscape at early stages of AD pathology, in order to understand the abnormal olfactory-driven behaviors and olfactory sensory impairment that appear during the AD progression in Tg2576 mice.

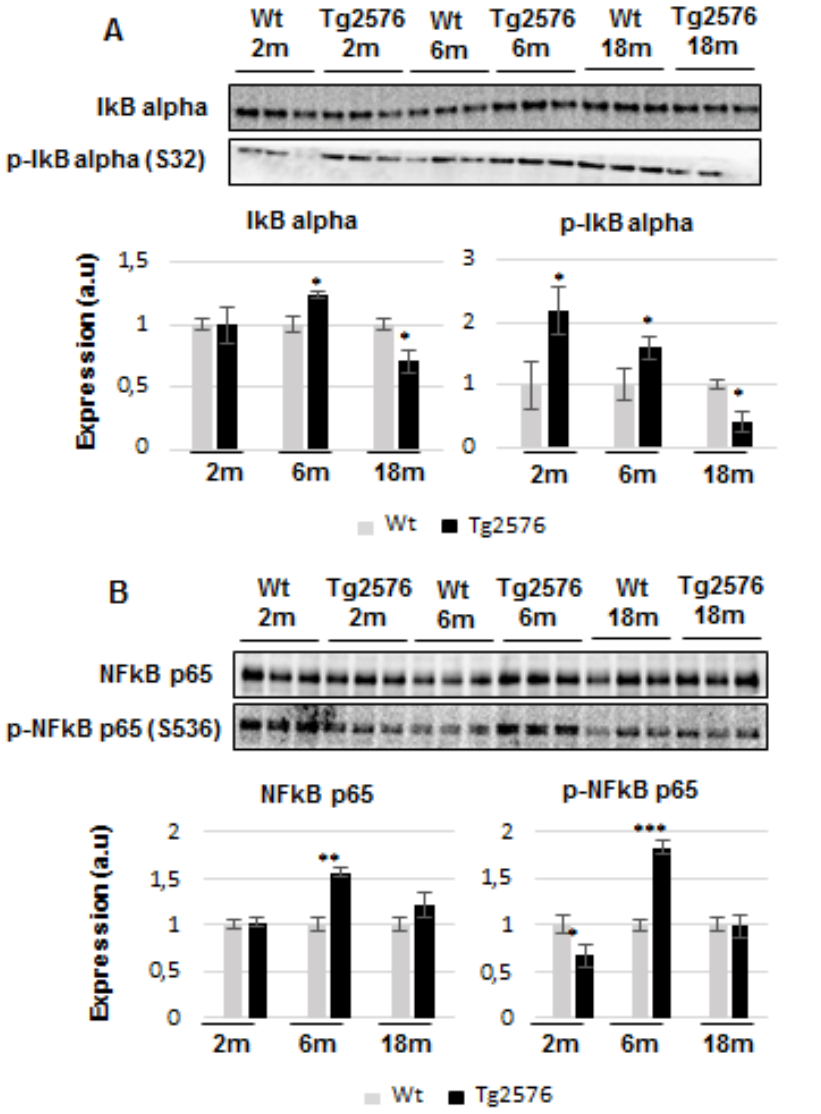

Figure 7. Time-dependent functionality of the OB IκB alpha-NFκB p65 complex in Tg2576 mice. Levels and residue-specific phosphorylation of IκB alpha (A), levels and residue-specific phosphorylation of NFκB p65 subunit (B). Equal loading of the gels was assessed by stain-free digitalization. Panels show histograms of band densities. Data are presented as mean ± SEM from 3 independent OB samples per group. *P < 0.05 vs control group; **P < 0.01 vs control group; *** P<0.001 vs control group. The expression of IκB alpha-NFκB p65 complex was also evaluated during the aging process in WT and Tg2576 mice (C).

Although the accumulation of Aβ oligomers in specific OB regions results in impaired neural integrity in specific OB cell layers in Tg2576 mice during AD progression [55], our results indicate that: i) 1% of the 2.466 quantified proteins are differentially expressed, and ii) 0,5% of the 20.900 protein-coding genes are differentially modulated in the OB of 18-month-old Tg2576 mice. These data pointed out that AD-related effects on the OB transcriptome and proteome composition at the bulk level are not massive at RNA and protein levels at old stages. It is important to note that due to technical reasons, only the most abundant OB proteins corresponding to approximately 10% of the mouse proteome were explored. Consequently, alterations other than those reported in this study might also participate in the AD neurodegeneration at the level of the OB in aged Tg2576 mice. Although the analysis of the OB proteogenome provides a unique window into their biochemistry and dysfunction in aged Tg2576 mice, there are additional limitations of our study that warrant discussion. We have processed all cellular layers present in the bulk OB. However, the OB is composed by intermixed multiple cell types with intricate architecture and connectivity [56], and information about specific-cell types where mRNAs and proteins originated from is lost in our workflow. The implementation of novel approaches that allow the exploration of olfactory cell-type specific molecular profiling would complement the output of our nonbiased exploration of the OB transcriptome/proteome, minimizing the effect of multiple neuronal microenvironments, and deciphering the specific role of each olfactory neuronal population in the aged Tg2576 OBs.

3. Conclusions

The largely similar OB proteogenome of aged WT and Tg2576 mice suggests that abnormal protein-protein interactions or post-translational modifications, defective intracellular trafficking or misfolding of proteins could play a pivotal part in driving the neurodegeneration that occur at olfactory level in aged Tg2576 mice. Moreover, omics sciences have partially revealed the potential interactome of hAPPSw isoform at olfactory level as well as the disruption of IκB alpha-NFκB p65 complex during the neurodegenerative process, providing molecular features that may be used as novel olfactory drug target candidates to treat AD.

4. Materials and methods

Materials - The following reagents and materials were used: anti-APP, anti-FAK, anti-phospho-FAK (Y576/577), anti-Akt, anti-phospho-Akt (S473), anti-PDK1, anti-phospho-PDK1 (S241), anti-PKC-pan, anti-phospho-PKC pan (T514), anti-p38 MAPK, anti-phospho-p38 MAPK (T180/Y182), anti-MEK1/2, anti-phospho-MEK1/2 (S217/221), anti-ERK1/2, anti-phospho-ERK1/2 (T202/y204), anti-CREB, anti-IκB alpha, anti-phospho-IκB alpha (S32), anti-NFκB p65, and anti-phospho-NFκB p65, anti-SEK1, anti-phospho-SEK1 (S257/T261) were from Cell Siganling Technology. Electrophoresis reagents were purchased from Bio-rad and trypsin from Promega.

Sample preparation for proteomic analysis – Murine OB specimens were homogenized in lysis buffer containing 7 M urea, 2 M thiourea, 50 mM DTT. The homogenates were spinned down at 100.000 x g for 1 h at 15ºC. Protein concentration was measured in the supernatants with the Bradford assay kit (Bio-rad).

Protein Digestion and Peptide iTRAQ Labeling - A shotgun comparative proteomic analysis of OB proteomes using iTRAQ (isobaric Tags for Relative and Absolute Quantitation) was performed. Protein extracts were precipitated with Clean-up kit (Bio-Rad), and pellets dissolved in 7M urea, 2 M thiourea. Protein quantitation was performed with the Bradford assay kit (Bio-Rad). iTRAQ labeling of each sample was performed according to the manufacturer's protocol (Sciex). Briefly, equal amounts of OB proteins (50 µg) from each sample were reduced with 50 mM tris (2-carboxyethyl) phosphine (TCEP) at 60 °C for 1 h. Cysteine residues were alkylated with 200 mM methylmethanethiosulfonate (MMTS) at room temperature for 15 min. Protein enzymatic cleavage was carried out with trypsin (Promega; 1:20, w/w) at 37 °C for 16 h. Each tryptic digest was labelled according to the manufacturer's instructions with one isobaric amine-reactive tags as follows: Tag113, WT-1; Tag114, WT-2; Tag115, WT-3; Tag116, Tg2576-1; Tag117, Tg2576-2; Tag118, tg2576-3. After 2h incubation, the set of labelled samples were pooled and evaporated in a vacuum centrifuge.

Liquid Chromatography tandem mass Spectrometry and data Analysis - To increase the proteome coverage, the peptide pool was submitted to cation exchange chromatography using spin Columns (Pierce). 12 fractions were collected (from 10mM to 150 mM KCl), evaporated under vacuum and reconstituted into10 µl of 2% acetonitrile, 0.1% formic acid, 98% MilliQ-H_20 prior to mass spectrometric analysis. Peptide mixtures were separated by reverse phase chromatography using an Eksigent nanoLC ultra 2D pump fitted with a 75 µm ID column (Eksigent 0.075 x 250). Samples were first loaded for desalting and concentration into a 0.5 cm length 100 µm ID precolumn packed with the same chemistry as the separating column. Mobile phases were 100% water 0.1% formic acid (FA) (buffer A) and 100% Acetonitrile 0.1% FA (buffer B). Column gradient was developed in a 146 min two step gradient from 5% B to 25% B in 120 min and 25%B to 70% B in 15 min. Column was equilibrated in 95% B for 9 min and 5% B for 14 min. During all process, precolumn was in line with column and flow maintained all along the gradient at 300 nl/min. Eluting peptides from the column were analyzed using an Sciex 5600 Triple-TOF system. Information data acquisition was acquired upon a survey scan performed in a mass range from 350 m/z up to 1250 m/z in a scan time of 250 ms. Top 25 peaks were selected for fragmentation. Minimum accumulation time for MS/MS was set to 100 ms giving a total cycle time of 2.75 s. Product ions were scanned in a mass range from 100 m/z up to 1500 m/z and excluded for further fragmentation during 15 s. The raw MS/MS spectra search were processed using the freely available MaxQuant software (v.1.5.8.3) [20]. Initial maximum precursor and fragment mass deviations were set to 25 ppm and 0.5 Da, respectively. Variable modification (methionine oxidation and N-terminal acetylation) and fixed modification (MMTS) were set for the search and trypsin with a maximum of 1 missed cleavages was chosen for searching. The minimum peptide length was set to 7 amino acids and the false discovery rate (FDR) for PSM and protein identification was set to 1%. Matching against the protein sequence database was carried out after improving the precursor ion mass accuracy using the mass-dependent recalibration option of the software. The false-discovery rate was controlled at various levels by

using a target-decoy search strategy, which integrates multiple peptide parameters such as length, charge, number of modifications and the identification score into a single quality that acts as the statistical evidence on the quality of each single peptide spectrum match. The frequently observed laboratory contaminants were removed and the protein identification was considered valid only when at least one unique or "razor" peptide was present. Following protein identification, the intensity for each identified protein was calculated using ion reporter intensities. The protein quantification was calculated using at least 2 razor + unique peptides, and calculation of statistical significance was carried out using two-way Student-t test ($p < 0.05$). A 1.3-fold change cutoff for all iTRAQ ratios (ratio ≤0.77 or ≥1.3) was selected to classify proteins as up- or down-regulated. Proteins with iTRAQ ratios below the low range (0.77) were considered to be underexpressed, whereas those above the high range (1.3) were considered to be overexpressed. The freely available software Perseus (version 1.5.6.0) [21] was used for statistical analysis and data visualization. MS raw data and search results files have been deposited to the ProteomeXchange Consortium (http://proteomecentral.proteomexchange.org) via the PRIDE partner repository [22] with the dataset identifiers PXD007795.

Microarray hybridization and data analysis - For OB mRNA extraction, the Maxwell® 16 simplyRNA Kit (Promega) was used. The sense cDNA was prepared from 1 ng of total RNA and then fragmented and biotinylated using Affymetrix Clarion S Pico assay (902932). Labeled sense cDNA was hybridized to the Affymetrix mouse Clarion S chip according to the manufacturer protocols and using GeneChip® Hybridization, Wash and Stain Kit. Gene chips were scanned with the Affymetrix GeneChip® Scanner 3000. For microarray data analysis, both background correction and normalization were done using RMA (Robust Multichip Average) algorithm [23]. R/Bioconductor was used for preprocessing and statistical analysis. For analysis of genes related to pathological changes, aged Tg2576 mice were compared to WT littermates. LIMMA (Linear Models for Microarray Data) was used to find out the probe sets that showed significant

differential expression between tg2576 and WTs. We first used a threshold criteria of False Discovery Rate (FDR) < 5% to select differentially expressed genes. As in other transcriptomic studies performed in AD brains [24,25], we did not achieve significant results using this criterion, so we worked with a p-value < 0.01 (without using any method for multiple testing correction). Microarray data files were submitted to the GEO (Gene Expression Omnibus) database and are available under accession number GSE103835.

Bioinformatics - The identification of specifically dysregulated regulatory/metabolic networks was analysed through the use of QIAGEN's Ingenuity® Pathway Analysis (IPA) (QIAGEN Redwood City, www.qiagen.com/ingenuity) and STRING software [26]. Both softwares comprises curated information from databases of experimental and predictive origin, enabling discovery of highly represented functions, pathways, and interactome networks. The IPA comparison analysis considers the signalling pathway/biofunctions rank according to the calculated p-value and reports it hierarchically. The software generates significance values (p-values) between each biological or molecular event and the imported molecules based on the Fisher´s exact test ($p \leq 0.05$).

Immunoblotting analysis - Equal amounts of OB protein (5 µg) were resolved in 4-15% TGX stain-Free gels (Bio-Rad). OB proteins derived from murine samples were electrophoretically transferred onto nitrocellulose membranes using a Trans-blot Turbo transfer system (up to 25V, 7min) (Bio-rad). Equal loading of the gels was assessed by stain free digitalization and by Ponceau staining. Membranes were probed with primary antibodies at 1:1000 dilution in 5% nonfat milk or BSA. After incubation with the appropriate horseradish peroxidase-conjugated secondary antibody (1:5000), antibody binding was detected by a Chemidoc MP Imaging System (Bio-Rad) after incubation with an enhanced chemiluminescence substrate (Perkin Elmer). After densitometric analyses (Image Lab Software Version 5.2; Bio-Rad), optical density values were expressed as arbitrary units and normalized to total stain in each gel lane.

References

1. Bahar-Fuchs, A.; Chetelat, G.; Villemagne, V.L.; Moss, S.; Pike, K.; Masters, C.L.; Rowe, C.; Savage, G. Olfactory deficits and amyloid-beta burden in alzheimer's disease, mild cognitive impairment, and healthy aging: A pib pet study. *J Alzheimers Dis* 2010, *22*, 1081-1087.

2. Attems, J.; Walker, L.; Jellinger, K.A. Olfactory bulb involvement in neurodegenerative diseases. *Acta Neuropathol* 2014, *127*, 459-475.

3. Hsiao, K.; Chapman, P.; Nilsen, S.; Eckman, C.; Harigaya, Y.; Younkin, S.; Yang, F.; Cole, G. Correlative memory deficits, abeta elevation, and amyloid plaques in transgenic mice. *Science* 1996, *274*, 99-102.

4. Puzzo, D.; Gulisano, W.; Palmeri, A.; Arancio, O. Rodent models for alzheimer's disease drug discovery. *Expert Opin Drug Discov* 2015, *10*, 703-711.

5. Westerman, M.A.; Cooper-Blacketer, D.; Mariash, A.; Kotilinek, L.; Kawarabayashi, T.; Younkin, L.H.; Carlson, G.A.; Younkin, S.G.; Ashe, K.H. The relationship between abeta and memory in the tg2576 mouse model of alzheimer's disease. *J Neurosci* 2002, *22*, 1858-1867.

6. Janus, C.; Pearson, J.; McLaurin, J.; Mathews, P.M.; Jiang, Y.; Schmidt, S.D.; Chishti, M.A.; Horne, P.; Heslin, D.; French, J.*, et al.* A beta peptide immunization reduces behavioural impairment and plaques in a model of alzheimer's disease. *Nature* 2000, *408*, 979-982.

7. Chen, G.; Chen, K.S.; Knox, J.; Inglis, J.; Bernard, A.; Martin, S.J.; Justice, A.; McConlogue, L.; Games, D.; Freedman, S.B.*, et al.* A learning deficit related to age and beta-amyloid plaques in a mouse model of alzheimer's disease. *Nature* 2000, *408*, 975-979.

8.Jacobsen, J.S.; Wu, C.C.; Redwine, J.M.; Comery, T.A.; Arias, R.; Bowlby, M.; Martone, R.; Morrison, J.H.; Pangalos, M.N.; Reinhart, P.H.*, et al.* Early-onset behavioral and synaptic deficits in a mouse model of alzheimer's disease. *Proc Natl Acad Sci U S A* 2006, *103*, 5161-5166.

9. Reddy, P.H.; McWeeney, S.; Park, B.S.; Manczak, M.; Gutala, R.V.; Partovi, D.; Jung, Y.; Yau, V.; Searles, R.; Mori, M.*, et al.* Gene expression profiles of transcripts in amyloid precursor protein transgenic mice: Up-regulation of mitochondrial metabolism and apoptotic genes is an early cellular change in alzheimer's disease. *Hum Mol Genet* 2004, *13*, 1225-1240.

10. Lalande, J.; Halley, H.; Balayssac, S.; Gilard, V.; Dejean, S.; Martino, R.; Frances, B.; Lassalle, J.M.; Malet-Martino, M. 1h nmr metabolomic signatures in five brain regions of the abetappswe tg2576 mouse model of alzheimer's disease at four ages. *J Alzheimers Dis* 2014, *39*, 121-143.

11.Nistico, R.; Ferraina, C.; Marconi, V.; Blandini, F.; Negri, L.; Egebjerg, J.; Feligioni, M. Age-related changes of protein sumoylation balance in the abetapp tg2576 mouse model of alzheimer's disease. *Front Pharmacol* 2014, *5*, 63.

12. Fodero, L.R.; Saez-Valero, J.; McLean, C.A.; Martins, R.N.; Beyreuther, K.; Masters, C.L.; Robertson, T.A.; Small, D.H. Altered glycosylation of acetylcholinesterase in app (sw) tg2576 transgenic mice occurs prior to amyloid plaque deposition. *J Neurochem* 2002, *81*, 441-448.

13. King, D.L.; Arendash, G.W. Behavioral characterization of the tg2576 transgenic model of alzheimer's disease through 19 months. *Physiol Behav* 2002, *75*, 627-642.

14. Doty, R.L. The olfactory vector hypothesis of neurodegenerative disease: Is it viable? *Ann Neurol* 2008, *63*, 7-15.

15. Lehman, E.J.; Kulnane, L.S.; Lamb, B.T. Alterations in beta-amyloid production and deposition in brain regions of two transgenic models. *Neurobiol Aging* 2003, *24*, 645-653.

16. Guerin, D.; Sacquet, J.; Mandairon, N.; Jourdan, F.; Didier, A. Early locus coeruleus degeneration and olfactory dysfunctions in tg2576 mice. *Neurobiol Aging* 2009, *30*, 272-283.

17. Young, J.W.; Sharkey, J.; Finlayson, K. Progressive impairment in olfactory working memory in a mouse model of mild cognitive impairment. *Neurobiol Aging* 2009, *30*, 1430-1443.

18. Wesson, D.W.; Levy, E.; Nixon, R.A.; Wilson, D.A. Olfactory dysfunction correlates with amyloid-beta burden in an alzheimer's disease mouse model. *J Neurosci* 2010, *30*, 505-514.

19. Wesson, D.W.; Borkowski, A.H.; Landreth, G.E.; Nixon, R.A.; Levy, E.; Wilson, D.A. Sensory network dysfunction, behavioral impairments, and their reversibility in an alzheimer's beta-amyloidosis mouse model. *J Neurosci* 2011, *31*, 15962-15971.

20. Tyanova, S.; Temu, T.; Cox, J. The maxquant computational platform for mass spectrometry-based shotgun proteomics. *Nat Protoc* 2016, *11*, 2301-2319.

21. Tyanova, S.; Temu, T.; Sinitcyn, P.; Carlson, A.; Hein, M.Y.; Geiger, T.; Mann, M.; Cox, J. The perseus computational platform for comprehensive analysis of (prote)omics data. *Nat Methods* 2016, *13*, 731-740.

22. Vizcaino, J.A.; Deutsch, E.W.; Wang, R.; Csordas, A.; Reisinger, F.; Rios, D.; Dianes, J.A.; Sun, Z.; Farrah, T.; Bandeira, N.*, et al.* Proteomexchange provides globally coordinated proteomics data submission and dissemination. *Nat Biotechnol* 2014, *32*, 223-226.

23. Irizarry, R.A.; Bolstad, B.M.; Collin, F.; Cope, L.M.; Hobbs, B.; Speed, T.P. Summaries of affymetrix genechip probe level data. *Nucleic Acids Res* 2003, *31*, e15.

24. Silva, A.R.; Grinberg, L.T.; Farfel, J.M.; Diniz, B.S.; Lima, L.A.; Silva, P.J.; Ferretti, R.E.; Rocha, R.M.; Filho, W.J.; Carraro, D.M.*, et al.* Transcriptional alterations related to neuropathology and clinical manifestation of alzheimer's disease. *PLoS One* 2012, *7*, e48751.

25. Cuadrado-Tejedor, M.; Garcia-Barroso, C.; Sanchez-Arias, J.A.; Rabal, O.; Perez-Gonzalez, M.; Mederos, S.; Ugarte, A.; Franco, R.; Segura, V.; Perea, G.*, et al.* A first-in-class small-molecule that acts as a dual inhibitor of hdac and pde5 and that rescues hippocampal synaptic impairment in alzheimer's disease mice. *Neuropsychopharmacology* 2016, *42*, 524-539.

26. Szklarczyk, D.; Morris, J.H.; Cook, H.; Kuhn, M.; Wyder, S.; Simonovic, M.; Santos, A.; Doncheva, N.T.; Roth, A.; Bork, P.*, et al.* The string database in 2017: Quality-controlled protein-protein association networks, made broadly accessible. *Nucleic Acids Res* 2017, *45*, D362-D368.

27. Fernandez-Irigoyen, J.; Corrales, F.J.; Santamaria, E. Proteomic atlas of the human olfactory bulb. *J Proteomics* 2012, *75*, 4005-4016.

28. Zelaya, M.V.; Perez-Valderrama, E.; de Morentin, X.M.; Tunon, T.; Ferrer, I.; Luquin, M.R.; Fernandez-Irigoyen, J.; Santamaria, E. Olfactory bulb proteome dynamics during the progression of sporadic alzheimer's disease: Identification of common and distinct olfactory targets across alzheimer-related co-pathologies. *Oncotarget* 2015, *6*, 39437-39456.

29. Lachen-Montes, M.; Gonzalez-Morales, A.; Zelaya, M.V.; Perez-Valderrama, E.; Ausin, K.; Ferrer, I.; Fernandez-Irigoyen, J.; Santamaria, E. Olfactory bulb neuroproteomics reveals a chronological perturbation of survival routes and a disruption of prohibitin complex during alzheimer's disease progression. *Sci Rep* 2017, *7*, 9115.

30. Lachen-Montes, M.; Gonzalez-Morales, A.; de Morentin, X.M.; Perez-Valderrama, E.; Ausin, K.; Zelaya, M.V.; Serna, A.; Aso, E.; Ferrer, I.; Fernandez-Irigoyen, J.*, et al.* An early dysregulation of fak and mek/erk signaling pathways

precedes the beta-amyloid deposition in the olfactory bulb of app/ps1 mouse model of alzheimer's disease. *J Proteomics* 2016, *148*, 149-158.

31. Stein, T.D.; Johnson, J.A. Lack of neurodegeneration in transgenic mice overexpressing mutant amyloid precursor protein is associated with increased levels of transthyretin and the activation of cell survival pathways. *J Neurosci* 2002, *22*, 7380-7388.

32. George, A.J.; Gordon, L.; Beissbarth, T.; Koukoulas, I.; Holsinger, R.M.; Perreau, V.; Cappai, R.; Tan, S.S.; Masters, C.L.; Scott, H.S.*, et al.* A serial analysis of gene expression profile of the alzheimer's disease tg2576 mouse model. *Neurotox Res* 2010, *17*, 360-379.

33. Tan, L.; Wang, X.; Ni, Z.F.; Zhu, X.; Wu, W.; Zhu, L.Q.; Liu, D. A systematic analysis of genomic changes in tg2576 mice. *Mol Neurobiol* 2013, *47*, 883-891.

34. Shin, S.J.; Lee, S.E.; Boo, J.H.; Kim, M.; Yoon, Y.D.; Kim, S.I.; Mook-Jung, I. Profiling proteins related to amyloid deposited brain of tg2576 mice. *Proteomics* 2004, *4*, 3359-3368.

35. Gillardon, F.; Rist, W.; Kussmaul, L.; Vogel, J.; Berg, M.; Danzer, K.; Kraut, N.; Hengerer, B. Proteomic and functional alterations in brain mitochondria from tg2576 mice occur before amyloid plaque deposition. *Proteomics* 2007, *7*, 605-616.

36. Shevchenko, G.; Wetterhall, M.; Bergquist, J.; Hoglund, K.; Andersson, L.I.; Kultima, K. Longitudinal characterization of the brain proteomes for the tg2576 amyloid mouse model using shotgun based mass spectrometry. *J Proteome Res* 2012, *11*, 6159-6174.

37. Cuadrado-Tejedor, M.; Cabodevilla, J.F.; Zamarbide, M.; Gomez-Isla, T.; Franco, R.; Perez-Mediavilla, A. Age-related mitochondrial alterations without neuronal loss in the hippocampus of a transgenic model of alzheimer's disease. *Curr Alzheimer Res* 2013, *10*, 390-405.

38. Saito, H.; Kubota, M.; Roberts, R.W.; Chi, Q.; Matsunami, H. Rtp family members induce functional expression of mammalian odorant receptors. *Cell* 2004, *119*, 679-691.

39. Zhang, B.; Gaiteri, C.; Bodea, L.G.; Wang, Z.; McElwee, J.; Podtelezhnikov, A.A.; Zhang, C.; Xie, T.; Tran, L.; Dobrin, R.*, et al.* Integrated systems approach identifies genetic nodes and networks in late-onset alzheimer's disease. *Cell* 2013, *153*, 707-720.

40.Ansoleaga, B.; Garcia-Esparcia, P.; Llorens, F.; Moreno, J.; Aso, E.; Ferrer, I. Dysregulation of brain olfactory and taste receptors in ad, psp and cjd, and ad-related model. *Neuroscience* 2013, *248*, 369-382.

41. Lachen-Montes, M.; Zelaya, M.; Segura, V.; Fernández-Irigoyen, J.; Santamaría, E. Progressive modulation of the human olfactory bulb transcriptome during alzheimer´s disease evolution: Novel insights into the olfactory signaling across proteinopathies. *Oncotarget* 2017.

42. Liu, Y.; Beyer, A.; Aebersold, R. On the dependency of cellular protein levels on mrna abundance. *Cell* 2016, *165*, 535-550.

43. Baker, M.S.; Ahn, S.B.; Mohamedali, A.; Islam, M.T.; Cantor, D.; Verhaert, P.D.; Fanayan, S.; Sharma, S.; Nice, E.C.; Connor, M.*, et al.* Accelerating the search for the missing proteins in the human proteome. *Nat Commun* 2017, *8*, 14271.

44. Sakamoto, K.; Karelina, K.; Obrietan, K. Creb: A multifaceted regulator of neuronal plasticity and protection. *J Neurochem* 2011, *116*, 1-9.

45. Tully, T.; Bourtchouladze, R.; Scott, R.; Tallman, J. Targeting the creb pathway for memory enhancers. *Nat Rev Drug Discov* 2003, *2*, 267-277.

46. Teich, A.F.; Nicholls, R.E.; Puzzo, D.; Fiorito, J.; Purgatorio, R.; Fa, M.; Arancio, O. Synaptic therapy in alzheimer's disease: A creb-centric approach. *Neurotherapeutics* 2015, *12*, 29-41.

47. Saura, C.A. Creb-regulated transcription coactivator 1-dependent transcription in alzheimer's disease mice. *Neurodegener Dis* 2012, *10*, 250-252.

48. Saura, C.A.; Valero, J. The role of creb signaling in alzheimer's disease and other cognitive disorders. *Rev Neurosci* 2011, *22*, 153-169.

49 .Kaur, U.; Banerjee, P.; Bir, A.; Sinha, M.; Biswas, A.; Chakrabarti, S. Reactive oxygen species, redox signaling and neuroinflammation in alzheimer's disease: The nf-kappab connection. *Curr Top Med Chem* 2015, *15*, 446-457.

50. Viatour, P.; Merville, M.P.; Bours, V.; Chariot, A. Phosphorylation of nf-kappab and ikappab proteins: Implications in cancer and inflammation. *Trends Biochem Sci* 2005, *30*, 43-52.

51. Kaltschmidt, B.; Uherek, M.; Volk, B.; Baeuerle, P.A.; Kaltschmidt, C. Transcription factor nf-kappab is activated in primary neurons by amyloid beta peptides and in neurons surrounding early plaques from patients with alzheimer disease. *Proc Natl Acad Sci U S A* 1997, *94*, 2642-2647.

52. Terai, K.; Matsuo, A.; McGeer, P.L. Enhancement of immunoreactivity for nf-kappa b in the hippocampal formation and cerebral cortex of alzheimer's disease. *Brain Res* 1996, *735*, 159-168.

53.Ferrer, I.; Marti, E.; Lopez, E.; Tortosa, A. Nf-kb immunoreactivity is observed in association with beta a4 diffuse plaques in patients with alzheimer's disease. *Neuropathol Appl Neurobiol* 1998, *24*, 271-277.

54. Paris, D.; Patel, N.; Quadros, A.; Linan, M.; Bakshi, P.; Ait-Ghezala, G.; Mullan, M. Inhibition of abeta production by nf-kappab inhibitors. *Neurosci Lett* 2007, *415*, 11-16.

55. Yoo, S.J.; Lee, J.H.; Kim, S.Y.; Son, G.; Kim, J.Y.; Cho, B.; Yu, S.W.; Chang, K.A.; Suh, Y.H.; Moon, C. Differential spatial expression of peripheral olfactory neuron-derived bace1 induces olfactory impairment by region-specific accumulation of beta-amyloid oligomer. *Cell Death Dis* 2017, *8*, e2977.

56. Nagayama, S.; Homma, R.; Imamura, F. Neuronal organization of olfactory bulb circuits. *Front Neural Circuits* 2014, *8*, 98.

CHAPTER 5

Unveiling the olfactory proteostatic disarrangement in Parkinson's disease by proteome-wide profiling

Mercedes Lachén-Montes,[1,2] Andrea González-Morales,[1,2] Ibon Iloro,[3] Felix Elortza,[3] Isidre Ferrer,[4] Djordje Gveric,[5] Joaquín Fernández-Irigoyen,[1,2]§, Enrique Santamaría,[1,2]§

[1] *Clinical Neuroproteomics Group, Navarrabiomed, Complejo Hospitalario de Navarra (CHN), Universidad Pública de Navarra (UPNA), IdiSNA. Irunlarrea, 3 31008 Pamplona, Spain;*

[2] *Proteored-ISCIII. Proteomics Unit, Navarrabiomed, Complejo Hospitalario de Navarra (CHN), Universidad Pública de Navarra (UPNA), IdiSNA. Irunlarrea, 3 31008 Pamplona, Spain;*

[3] *Proteomics Platform, CIC bioGUNE, CIBERehd, ProteoRed-ISCIII, Bizkaia Science and Technology Park, Derio, Spain;*

[4] *Institut de Neuropatologia, IDIBELL-Hospital Universitari de Bellvitge, Universitat de Barcelona, L'Hospitalet de Llobregat, CIBERNED, Spain;*

[5] *Centre for Brain Sciences, Imperial College London, London, UK*

Abstract

Olfactory dysfunction is one of the earliest features in Lewy-type alpha-synucleinopathies (LTS) such as Parkinson´s disease (PD). However, the underlying molecular mechanisms associated to smell impairment are poorly understood. Applying mass spectrometry-based quantitative proteomics in postmortem olfactory bulbs (OB) across limbic, early-neocortical, and neocortical LTS stages of parkinsonian subjects, a proteostasis impairment was observed, identifying 268 differentially expressed proteins between controls and PD phenotypes. In addition, network-driven proteomics revealed a modulation in ERK1/2, MKK3/6, and PDK1/PKC signalling axis. Moreover, a cross-disease study of selected olfactory molecules in sporadic Alzheimer's disease (AD) cases, revealed different protein derangements in the modulation of Secretagogin (SCGN), Calcyclin binding protein (CACYBP), and Glucosamine 6 phosphate isomerase 2 (GNPDA2) between PD and AD. An inverse correlation between GNPDA2 and α-synuclein protein levels was also reflected in PD cerebrospinal fluid (CSF). Interestingly, PD patients exhibited significantly lower serum GNPDA2 levels than controls (n=82/group). Our study provides important avenues for understanding the OB proteostasis imbalance in PD, deciphering mechanistic clues to the equivalent smell deficits observed in AD and PD pathologies.

1. Introduction

Olfactory dysfunction is present in up to 95% of PD patients (Attems et al., 2014; Doty, 2012b). In Lewy body diseases (LBDs), including PD, the olfactory deficit is an early prodromal event being considered as a premotor sign of neurodegeneration (Baba et al., 2012; Beach et al., 2009; Doty, 2008, 2012b). The initial induction of α-synuclein misfolding and subsequent deposition, probably occurs in the olfactory bulb (OB) and/or the enteric nervous system (Klingelhoefer and Reichmann, 2015; Rey et al., 2016). Clinical features of olfactory dysfunction have been correlated with the presence of Lewy-type alpha-synucleopathy (LTS) in different olfactory areas (Attems et al., 2014; Beach et al., 2009; Saito et al., 2016; Ubeda-Banon et al., 2010a; Ubeda-Banon et al., 2012; Ubeda-Banon et al., 2010b). Furthermore, microstructural white matter reductions in the olfactory system, the reduction of the cholinergic centrifugal inputs to the OB, and the increased number of the dopaminergic cells observed in the OB, have also been suggested as potential origins of smell loss (Ibarretxe-Bilbao et al., 2010; Mundinano et al., 2011; Mundinano et al., 2013).

PD and Dementia with Lewy bodies (DLB) are Lewy body diseases (LBD) because of the presence of typical intracytoplasmic neuronal inclusions named Lewy bodies (LB) together with Lewy neurites containing abnormal α-synuclein. Systematic study of cases with LB pathology has prompted a staging classification of PD (and LBDs) from the medulla oblongata and OB to the midbrain, diencephalic nuclei, and neocortex (Braak et al., 2002; Braak et al., 2003; Braak et al., 2004). Stages 1, 2, 3 reflect, respectively, LB pathology in the medulla oblongata, pons and midbrain; stage 4 includes, in addition, the basal prosencephalon and mesocortex; stage 5 extends to sensory association areas of the neocortex and prefrontal neocortex; and stage 6 includes, in addition, lesions in first order sensory association areas of the neocortex and pre-motor areas (Braak et al., 2002; Braak et al., 2003; Braak et al., 2004). Similar categorization of LB pathology was used to classify DLB (McKeith et al., 2017; McKeith et al., 2005; McKeith et al.,

1996). The later classification covers three stages: brain stem, limbic and neocortical. Atypical cases not following a clear gradient of LB pathology from the lower brain stem and olfactory regions to the neocortex constitute about ten percent of total LBDs (Braak et al., 2006; Jellinger, 2008, 2009). The most frequent atypical LBD is the amygdala-predominant which was added as a peculiar form to the former LBD-brain stem, LBD-limbic and LBD-neocortical classification (Leverenz et al., 2008). All these classifications are based on the putative progression with time of LB pathology in the brain from the medulla oblongata and OB to the neocortex. Neuropathological studies have pointed out that the presence and severity of α-synuclein pathology in the OB reflects the presence and severity of synucleinopathy in other brain regions (Attems et al., 2014; Beach et al., 2009). Some studies have demonstrated that the presence of LTS in the OB predicts with 90% sensitivity and specificity the existence of neuropathologically confirmed PD (Beach et al., 2009). Moreover, the sensitivity and specificity of clinical olfactory testing in differentiating PD from non-PD ranges from 80% to 100% (Doty, 2012a). In addition, an OB atrophy and a significant reduction in olfactory performance have been detected in PD respect to control subjects (Brodoehl et al., 2012; Li et al., 2016). In view of these clinical and neuropathological data, an in depth molecular characterization of the OB neurodegeneration is necessary to reveal the missing links in the biochemical understanding of the early smell impairment in PD.

In this work, we applied mass-spectrometry based quantitative proteomics as a discovery platform to explore the magnitude and chronology of the OB proteome modulation across limbic, early-neocortical, and neocortical LTS stages in PD cases, also named LBD-limbic stage, LBD-early neocortical stage, and LBD neocortical stage. First, we have used a novel technique, called MALDI-IMS, or MALDI - Imaging. The use of MALDI-IMS offers the great advantage to investigate the physiopathological changes taking place directly in tissue while retaining the histopathological context, enabling the so-called “Molecular Histology” (Caprioli et al., 1997; Chaurand et al., 2004). Second, we have applied a label-free shotgun proteomic approach

getting more than 250 differential expressed proteins between controls and PD-related phenotypes, pinpointing specific pathways, protein interaction networks, and potential novel therapeutic targets.

2. Materials and methods

2.1 Materials - The following reagents and materials were used: anti-GAPDH (Calbiochem), anti-MKK3, anti-MKK6, anti-phospho MKK3 (Ser189)/MKK6 (Ser207), anti-p38 MAP kinase, anti-phospho p38 MAP kinase (Thr180/Tyr 182), anti-p38 MAPK alpha, anti-p38 MAPK beta, anti-PDK1, anti-phospho PDK1 (S241), anti-PKC-Pan, anti-phospho PKC-pan (T514), anti-pAkt (Ser473), anti-Akt, anti-pERK1/2 (Thr202/Tyr204), anti-ERK1/2 and anti-CACYBP (Cell Signaling), anti-CPNE6 (Thermo), anti-GNPDA2, anti-NEGR1, anti-RACK1, anti-SCGN (Abcam), anti-α-synuclein (Santa Cruz Biotech), and anti-DPP6 (Sigma). Electrophoresis reagents were purchased from Bio-rad and trypsin from Promega.

2.2 Human samples – According to the Spanish Law 14/2007 of Biomedical Research, inform written consent forms were obtained for research purposes from relatives of patients included in this study. The study was conducted in accordance with the Declaration of Helsinki and all assessments, post-mortem evaluations, and procedures were previously approved by the Clinical Ethics Committee of Navarra Health Service. OB specimens (Table 1), CSF samples (additional file 7) and associated clinical and neuropathological data from PD subjects were supplied by the Parkinson's UK Brain Bank, funded by Parkinson's UK, a charity registered in England and Wales (258197) and in Scotland (SC037554), and the Neurological Tissue Bank from Navarrabiomed (Pamplona, Spain). Neuropathological assessment was performed according to standardized neuropathological scoring/grading systems (Alafuzoff et al., 2009). Twenty-one PD cases were distributed into: LBD-limbic stage (LBDL) (n=7), LBD-early neocortical stage (LBDE) (n=6), and LBD-neocortical stage (LBDN) (n=8). Eight cases from elderly subjects with no history or histological findings of any neurological disease were used as a control group. For validation and specificity analysis, OB specimens and associated neuropathological data from AD subjects (n=14), were supplied by the Neurological Tissue Bank of the Biobank from the Hospital Clinic-Institut d'Investigacions Biomèdiques August Pi i Sunyer (IDIBAPS), and the Neurological Tissue

Bank of HUB-ICO-IDIBELL (Barcelona, Spain). All human brains considered in this study (n=43) had a post-mortem interval (PMI) lower than 26 hours (Table 1). Serum samples and data from patients included in the study were provided by the Biobank of the University of Navarra and were processed following standard operating procedures approved by the Ethical and Scientific Committees (Additional file 1).

2.3 MALDI imaging mass spectrometry (IMS) - OBs from three different conditions were washed with PBS and immediately frozen and stored at − 80 °C until analyzed in order to preserve the native tissue morphology and minimize protein degradation. Sample tissues were sectioned at 14 µm using a Leica RM2235 cryostat (Leica, Wetzlar, DE) and thaw-mounted on ITO-coated glass slides (Bruker Daltonics, Bremen, DE) for mass spectrometry (MS) analysis, following previously published protocols (Lloro et al., 2017; Mourino-Alvarez et al., 2016).

2.4 Sample preparation for shotgun proteomics - OB specimens derived from control and PD cases were homogenized in lysis buffer containing 7 M urea, 2 M thiourea, 4% (w/v) CHAPS, 50 mM DTT. The homogenates were spinned down at 100.000 x g for 1 h at 15°C. Prior to proteomic analysis, protein extracts were precipitated with methanol/choloroform, and pellets dissolved in 6M Urea, Tris 100mM pH 7.8. Protein quantitation was performed with the Bradford assay kit (Bio-Rad).

2.5 Label free LC-MS/MS –Protein enzymatic cleavage (10ug) was carried out with trypsin (Promega; 1:20, w/w) at 37°C for 16 h as previously described (Shevchenko et al., 2006). Peptides mixtures were separated by reverse phase chromatography using an Eksigent nanoLC ultra 2D pump fitted with a 75 µm ID column (Eksigent 0.075 x 250). Samples were first loaded for desalting and concentration into a 0.5 cm length 100 µm ID precolumn packed with the same chemistry as the separating column. Mobile phases were 100% water 0.1% formic acid (FA) (buffer A) and 100% Acetonitrile 0.1% FA (buffer B). Column gradient was developed in a 240 min two step gradient from 5% B to 25% B in 210 min and 25%B to 40% B in 30 min. Eluting

peptides were analyzed using a 5600 Triple-TOF system, as previously described (Lachen-Montes et al., 2017).

2.6 Peptide Identification and Quantification – MS/MS data acquisition, searching, peptide quantitation, and statistical analysis were performed as previously described (Lachen-Montes et al., 2017). MS raw data and search results files have been deposited to the ProteomeXchange Consortium (http://proteomecentral.proteomexchange.org) via the PRIDE partner repository (Vizcaino et al., 2014) with the dataset identifiers PXD008036.

2.7 Statistical analysis - The statistical analysis used for the identification of differentially expressed proteins was performed using the Progenesis software and R scripts. Before applying any statistical test, data were submitted to several mathematical algorithms to remove the background, to align and compensate the ''between-run variation'', and to choose the same peaks in all samples in the peak picking phase. Then, peptides were identified with the information obtained using Protein Pilot software. Output files with the identified proteins were then managed with R scripts for subsequent statistical analysis. One-way ANOVA test was applied to compare the results between all groups and unpaired Student's t-test was used for direct comparisons between two groups of samples. Statistical significance was set at $p<0.05$ in all cases and 1% peptide FDR (False discovery rate) threshold was considered (calculated based on the search results against a decoy database). Additionally, an absolute fold change of <0.77 (down-regulation) or >1.3 (up-regulation) in linear scale was considered to be significantly differentially expressed. Concerning the immunoassays, the comparison made between the neuropathological groups and the neurological intact control group was performed using the unpaired T test for independent samples. A p value <0.05 was considered significant. Results are represented as mean ± SE and errors bars show the standard error of the mean from the samples used in each group.

2.8 Bioinformatics –The proteomic information was analyzed using Reactome (Fabregat et al., 2018) in order to detect and infer differentially activated/deactivated pathways as a result of PD phenotypes. The identification of specifically dysregulated regulatory/metabolic networks across PD stages was analysed through the use of QIAGEN's Ingenuity® Pathway Analysis (IPA) (QIAGEN Redwood City, www.qiagen.com/ingenuity).

2.9 Immunoblotting analysis - In the case of CSF samples, 100-150µl were precipitated with four volumes of acetone o/n at -20ºC. Then, samples were centrifuged during 15 minutes at 14000rpm to obtain the protein pellet. Equal amounts of OB protein (10 µg) or CSF protein (8 µg) were resolved in 4-15% TGX stain-Free gels (Bio-Rad). Western-blot analysis were performed as previously described (Lachen-Montes et al., 2017). After densitometric analyses (Image Lab Software Version 5.2; Bio-Rad), optical density values were expressed as arbitrary units and normalized to GAPDH (tissue analysis) or to total stain in each gel lane (CSF analysis) (Moritz, 2017).

2.10 Enzyme-Linked Immunosorbent Assay. Serum GNPDA2 concentrations were measured using enzyme-linked immunosorbent assay (ELISA) kits according to the manufacturer's instructions (MBS93411798; MyBiosource). The detection range was 0.62 ng/ml – 20 ng/ml. Data were analyzed using Graphpad Prism software. Mann–Whitney U test was used for between-group comparisons. We considered p-value less than 0.05 to be statistically significant.

3. Results

3.1 Proteostasis impairment in the OB across Lewy-type alpha-synucleinopathy (LTS) staging

In this work, we combined two complementary mass spectrometry-based proteomic approaches such as MALDI-IMS and label-free quantitative proteomics to probe additional molecular disturbances in post-mortem OBs dissected from clinically confirmed PD cases respect to neurologically intact controls. First, MALDI-IMS was applied for the first time in OB region to visualize in situ additional molecular disturbances between control and LB neuropathological stages (Figure 1). Several masses with differential spatial distribution between control and LB stages have been found with ROC (Receiving Operating Characteristic) curves with statistical significance (Area Under the Curve (AUC) >0.8).

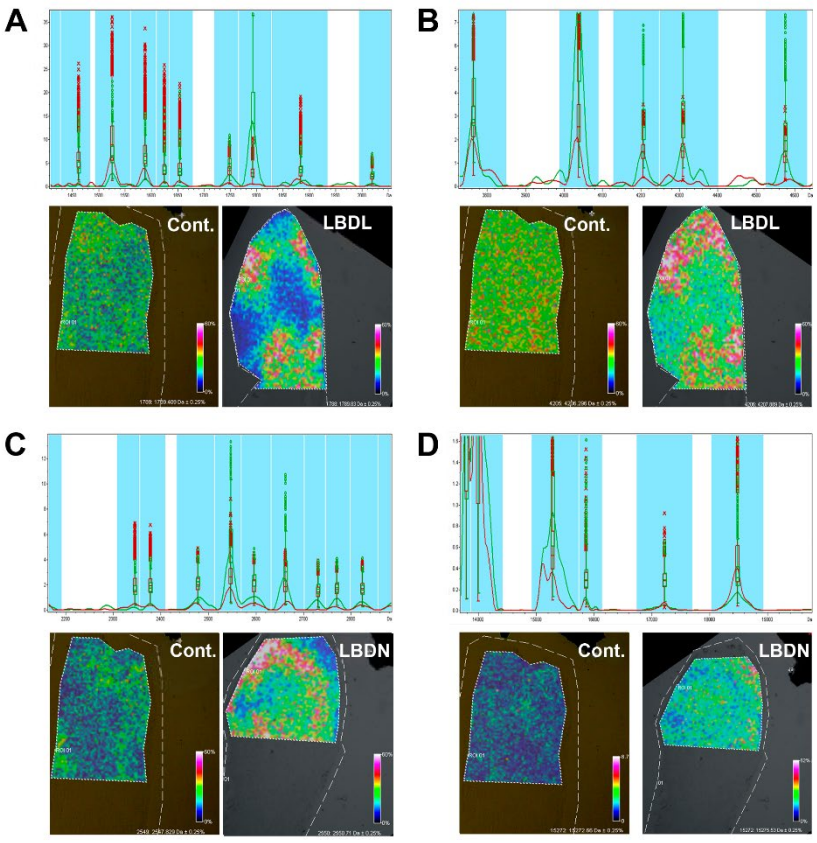

Figure 1. MALDI imaging mass spectrometry of human OB. Mean spectra of the whole section of control OB (red) and each LTS stages (green), and the corresponding spatial distribution of

the selected peaks. A) band at 1789 Th. B) band at 4205 Th. C) band at 2549 Th, and D) band at 15272 Th. This pattern can also be shown in the corresponding whisker-plots.

To determine and characterize the progression and complexity of LTS-associated changes in this olfactory structure, the OB site-specific proteomic signature was monitored across LTS staging using a complementary label-free MS-based approach. Among 1629 quantified proteins across all experimental groups, 268 proteins tend to be differentially expressed between controls and PD phenotypes (Fig.2A and additional file 2). A progressive increment in OB monomeric α-synuclein protein levels was also evidenced across LTS stages by Western-blot (Fig.2B). Our analysis revealed that 148, 139, and 197 OB proteins are differentially expressed in LBDL, LBDE, and LBDN stages, respectively. The distribution between up-regulated and down-regulated proteins was very similar across LTS grading (35-40% down-regulated, and 60-65% up-regulated proteins) (Fig. 2C). Interestingly, 65 OB proteins overlapped between all stages (Fig. 2D), suggesting a potential role during LTS progression in PD subjects. Most of these proteins mainly clustered in specific biological process like transport and RNA processing with specific molecular functions such as nucleotide binding and hydrolase activities (Additional file 3).

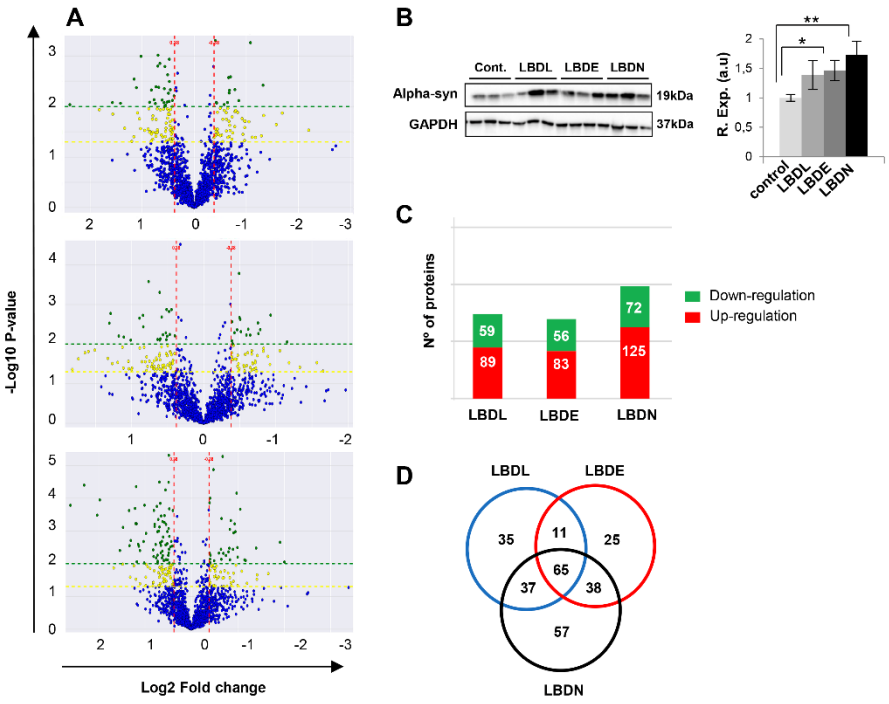

Figure 2. OB Differentially proteins across PD-related phenotypes. A) Volcano plots from the pair-wise comparisons: control vs LBDL stage (upper panel), LBDE stage (middle panel), and LBDN stage (lower panel). Differential proteins: P < 0.01 in green, and P < 0.05 in yellow. B) OB monomeric α-synuclein expression. C) Differential olfactory proteome distributions. D) Common and unique differential proteins between LTS stages.

3.2 Olfactory dysregulated pathways across LTS grading

To extract biological knowledge, the differential OB proteome detected in each LTS stage, was functionally categorized (Additional file 4). Immune system, metabolism of lipids, aminoacids, and carbohydrates, signaling by growth factors and specific survival pathways, together with vesicle-mediated transport and axon guidance were the common over-represented dysregulated processes across LTS grading (Additional file 5A). To gain a more detailed description of the molecular mechanisms involved in the OB during LB pathology, subsequent analyses were performed to explore the differential olfactory proteome distributions across specific neuronal functionalities. As shown in additional file 5B, our results point out a deregulation of specific protein clusters related to cell death, basal ganglia dysfunction, and

movement disorders. Specifically, proteins involved in dyskinesia and tremor were exclusively mapped in LBDN stage (Additional file 6). To characterize, in detail, the potential dysregulation of LTS-related protein interactomes in the OB during the neurodegenerative process, we have performed proteome-scale interaction networks merging the olfactory proteins that tend to be deregulated in each LTS stage. Using IPA software, protein interactome maps has been constructed for each LTS stage (Figure 3). In LBDL stage, the functional interaction network indicated an alteration in HNRNP complexes (HNRNPA2B1, HNRNPM, HNRNPC, HNRNPH3, HNRNPR), RNA binding proteins (ILF2, MATR3, DDX6), as well as transcriptional and translational repressors (XRCC5, RACK1, RUVBL1) suggesting an impairment in RNA stability and pre-mRNA splicing processes (Figure 3A). In LBDE stage, the proteome-scale interaction network reflected an alteration in multiple interactors of nucleophosmin (NPM1), reinforcing the transcriptional derangements that occur at the level of the OB (Figure 3B). The functional clustering also suggested an imbalance in signaling molecules involved in cell survival and differentiation such as CSNK2B, LIMS1, and PP2A (Figure 3B). In LBDN stage, functional interactors of specific survival routes were compromised, suggesting an imbalance in the survival potential of olfactory neurons (Figure 3C).

A

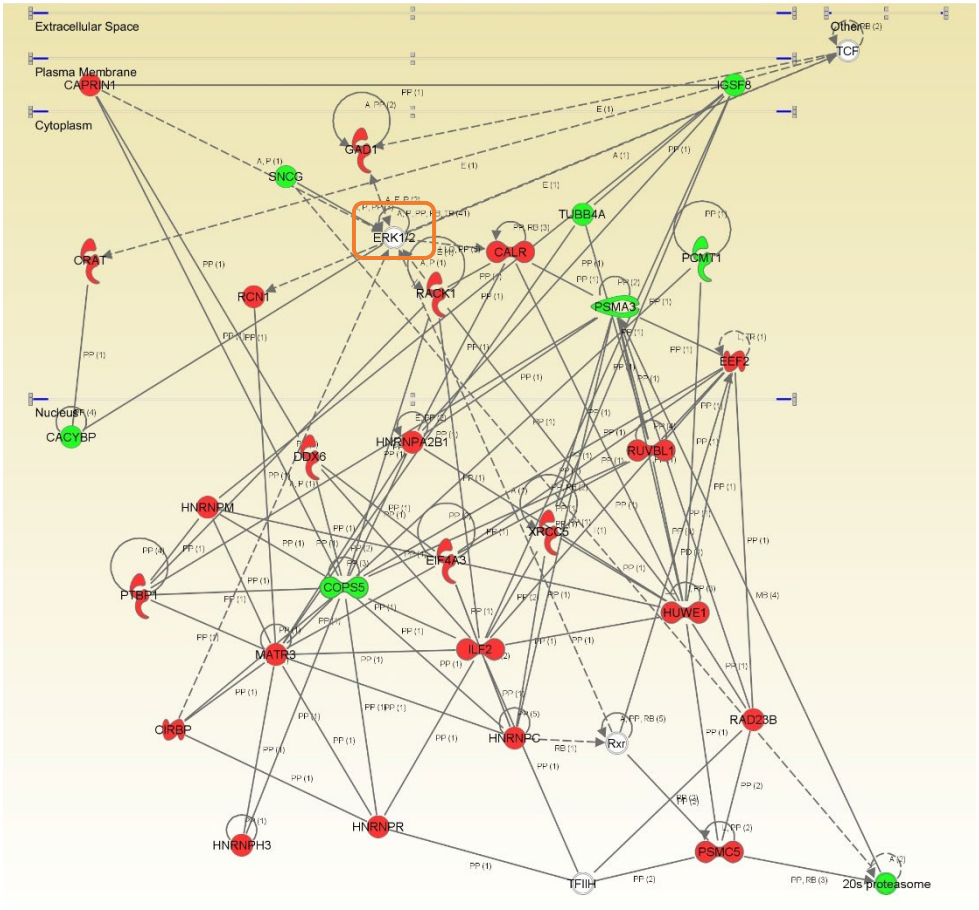

B

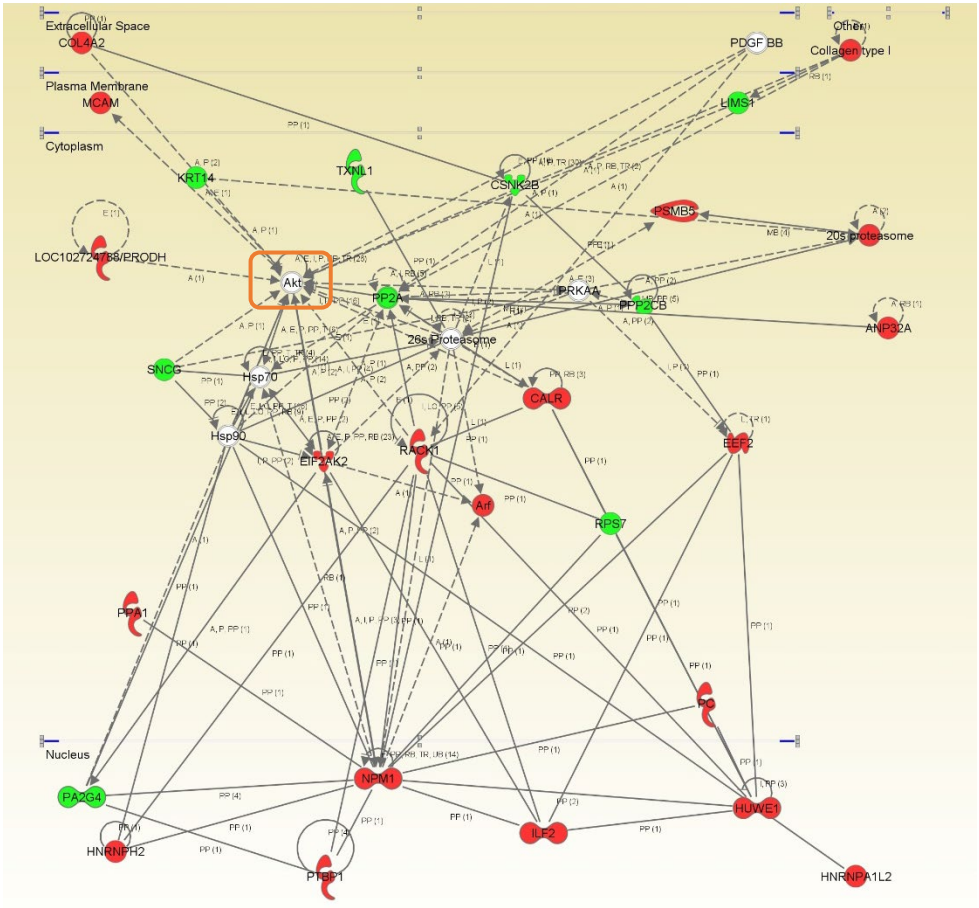

C

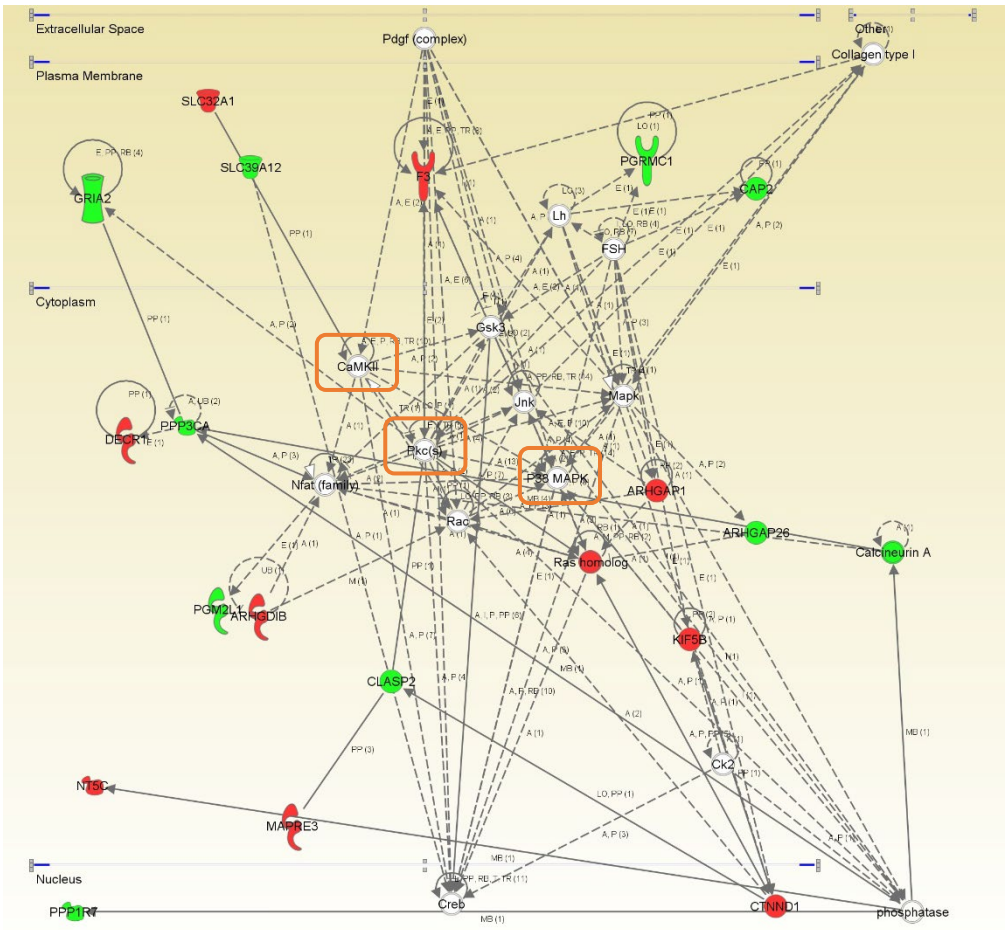

Figure 3. Protein interactome maps for differentially expressed proteins in the OB during LTS progression. Visual representation of the relationships detected in LBDL (A), LBDE (B), and LBDN (C). Up-regulated proteins in red, and down-regulated proteins in green. Complete legend in http://ingenuity.force.com/ipa/articles/Feature_Description/Legend.

3.3 Network-driven proteomics reveals olfactory derangements in survival pathways in Parkinson´s disease

Signaling modulators like ERK, Akt, CaMKII, PKC and p38 MAPK appeared as principal nodes in protein interactome maps (figure 3). Subsequent experiments were performed to monitor the activation state of this kinase panel across LTS staging. Respect to MAPK pathway, a significant increment in the steady-state levels of MEK was observed in LBDN stage. On the contrary, a progressive down-regulation of ERK levels was evidenced across LTS staging (figure 4A).

Phosphoinositide-dependent protein kinase 1 (PDK1) activity depends on the autophosphorylation on Ser241, activating PKC signal transduction (Mora et al., 2004). Despite the up-regulation in total PDK1 levels observed in LBDL stage, PDK1 was inactivated across LBDE and LBDN stages (figure 4B). Moreover, PDK1 inactivation was accompanied by a decrease in the activation status of PKC isoforms in LBDE stage, as revealed by Western-blot using a specific pan-antibody against phosphorylated PKC isoforms (Figure 4B). MKK3 and MKK6 are dual-specificity protein kinases that activate p38 MAPK (Derijard et al., 1995). We evaluated the activation state of olfactory MKK3-6/p38 MAPK axis across LTS staging. As shown in figure 4C, MKK3/6 were significantly inactivated across all stages, mainly due to a drop in total MKK6 levels. On the other hand, no significant changes were observed in the activation state of p38 MAPK, detecting an over-expression of p38-alpha and -beta subunits in LBDL stage, and a specific increment of p38-alpha protein in LBDN stage (Figure 4C). These data suggest the existence of upstream disruption of olfactory MAPK, PDK1/PKC, and MKK3-6/p38 MAPK axis among neuropathological stages. On the other hand, a slightly increment in the activation state of Akt and CaMKII was observed in LBDL stage, although these changes were not statistically significant (Figure 4D).

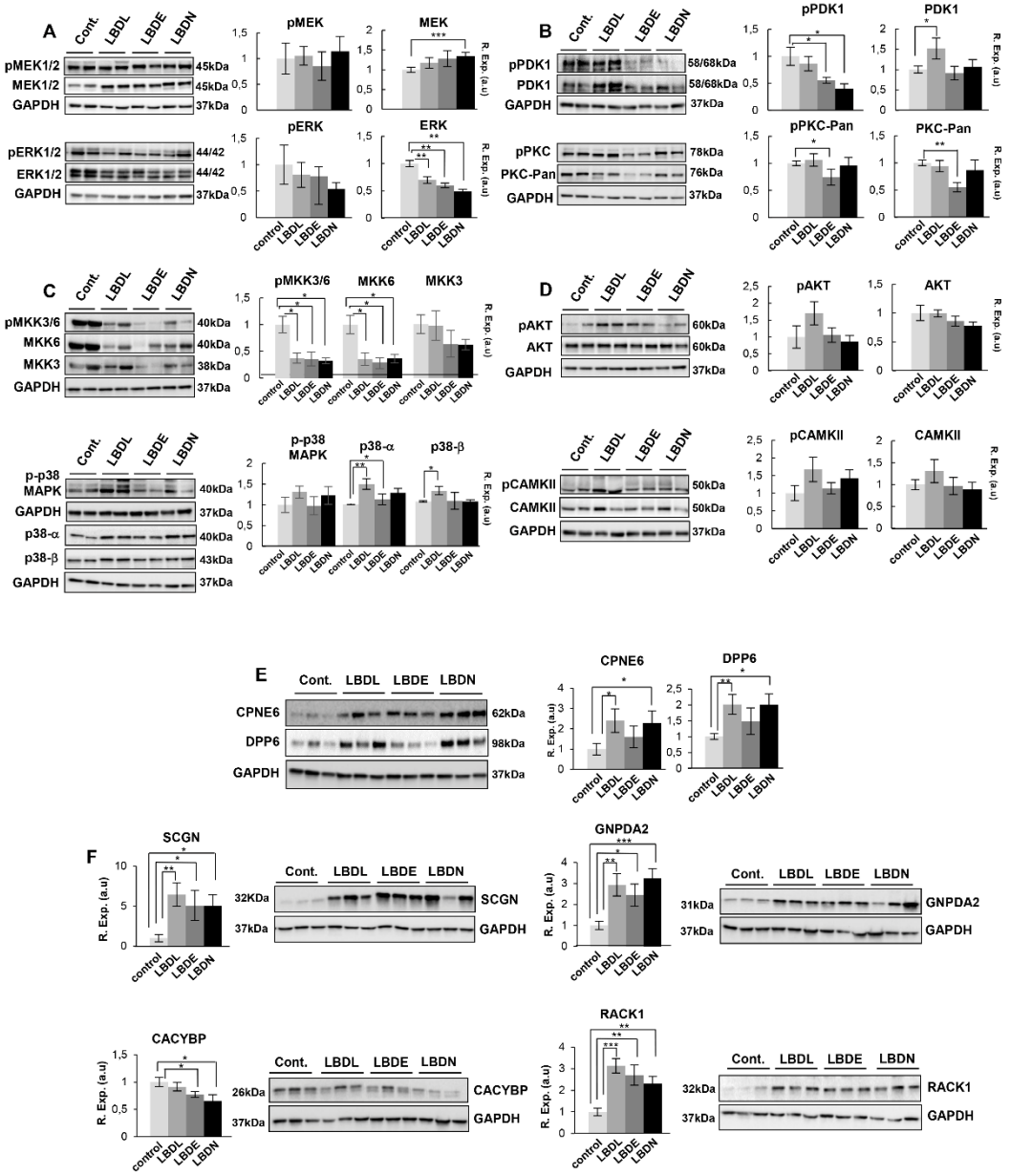

Figure 4. Monitoring of OB survival routes and specific protein intermediates across LTS grading. Levels and phosphorylation of MAP kinases (A), PDK1/PKC (B), MKK3-6/p38 MAPK (C), and AKT and CaMKII kinases (D) in the OB across PD phenotypes. CPNE6 and DPP6 protein expression levels across LTS stages (E). Protein variation in SCGN, CACYBP, GNPDA2, and RACK1 levels across PD phenotypes (F). *P < 0.05 vs control group; ** P < 0.01 vs control group; *** P < 0.01 vs control group. Statistical analysis between LTS stages is shown in additional file 9A.

3.4 Searching common pathological olfactory substrates in AD and PD phenotypes

It has been recently proposed the potential existence of common olfactory pathological substrates in AD and PD, mainly due to the equivalent severe olfactory deficits present at earliest stages of both neurological syndromes (Doty, 2012b, 2017). With the aim to identify common olfactory protein intermediates deregulated in both neurodegenerative backgrounds, a cross-disease study of selected olfactory molecules was performed in sporadic AD cases. For that, OB samples derived from low (Braak I-II), intermediate (Braak III-IV), and high AD (Braak V-VI) were included in the cross-disease study (Table 1). The selection of assessing the protein panel for verification was based primarily on: i) differential expression across LTS stages and novelty in human PD pathophysiology (SCGN, CACYBP, GNPDA2, RACK1) and ii) differential expression in the OB from different neurological disorders (CPNE6, and DPP6) (Zelaya et al., 2015). Our group has previously identified CPNE6 (Copine-6) and DPP6 (Dipeptidyl aminopeptidase-like protein 6) as olfactory protein mediators deregulated in specific neurological syndromes (Zelaya et al., 2015). As shown in figure 4E, olfactory CPNE6 and DPP6 protein levels were significantly increased in LBDL and LBDN stages. SCGN (Secretagogin) is a calcium binding protein considered marker of periglomerular and deep-layer olfactory interneurons (Attems et al., 2012). CACYBP (Calcyclin binding protein) is involved in cytoskeletal dynamics and in the regulation of transcriptional responses in neurons (Filipek et al., 2008; Kilanczyk et al., 2015). GNPDA2 (Glucosamine 6 phosphate isomerase 2) participates in the glucose metabolism, converting D-glucosamine-6-phosphate into D-fructose-6-phosphate and ammonium (Arreola et al., 2003). RACK1 (Receptor of activated protein C kinase 1) protects neurons from oxidative-stress-induced apoptosis (Ma et al., 2014). First, and with the aim to complement and partially validate our proteomic workflow, the steady-state levels of our protein panel were checked across LTS staging by Western blotting. In accordance with our proteomic findings, the immunoblots confirmed the olfactory over-expression of SCGN, GNPDA2, and RACK1 across LTS stages (Figure 4F). In addition, a significant down-regulation of CACYBP was observed in LBDE, and LBDN stages

(Figure 4F). The monitorization of the expression of our protein panel in the OB from AD cases (Figure 5A) revealed that: i) SCGN protein levels were down-regulated in the OB derived from high AD cases, ii) CACYBP was specifically over-expressed in low AD cases, iii) a significant increment in OB GNPDA2 protein levels across low and intermediate AD, iv) no significant changes in OB RACK1 were observed across AD staging. This cross-disease analysis revealed the existence of common protein intermediates that are differentially deregulated during PD and AD progression at the level of the OB.

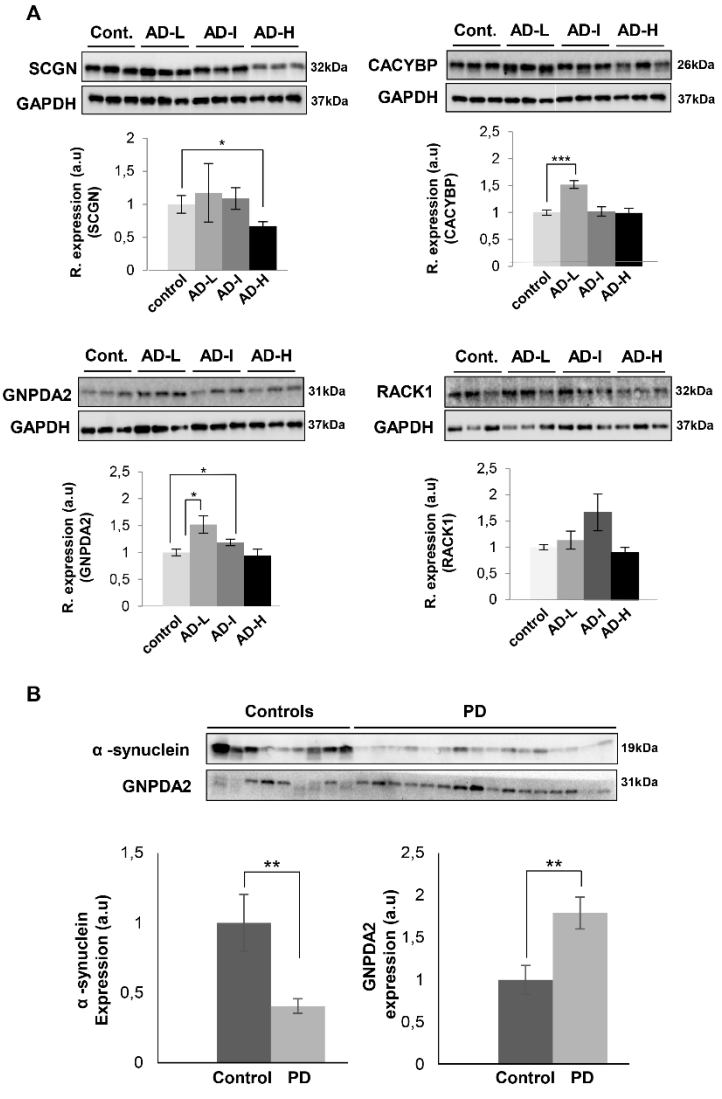

Figure 5. Monitoring of specific olfactory proteins during AD progression. GNPDA2 and α-synuclein levels in the CSF of PD subjects. A) Protein levels of SCGN, CACYBP, GNPDA2, and RACK1 were monitored by Western-blotting across AD stages**.** Statistical analysis between AD stages is shown in additional file 9B. B) Inverse correlation between GNPDA2 and α-synuclein

protein expression in CSF from PD subjects. *P < 0.05 vs control group; ** P < 0.01 vs control group; *** P < 0.01 vs control group**.**

3.5 GNPDA2 protein biofluid profile differs between controls and PD subjects

We further examined whether our protein panel could be detected in the CSF of PD subjects and ultimately serves as potential novel PD biomarkers. Interestingly, GNPDA2 was previously characterized by mass-spectrometry in CSF (Guldbrandsen et al., 2014). Subsequent experiments were performed to check the GNPDA2 expression in the CSF of PD patients (n=16) and healthy control subjects (n=9) (Additional file 7) by Western-blot analysis. As shown in figure 5B, GNPDA2 protein levels were significantly increased in CSF from PD patients respect to controls, showing an inverse correlation between GNPDA2 and α -synuclein protein levels detected in CSF. However, serum GNPDA2 levels were decreased in PD population (Figure 6) (Additional file 1), suggesting that the GNPDA2 profiles observed in both biofluids may be a consequence of the damaged blood-brain barrier (BBB) previously observed in PD (Sweeney et al., 2018).

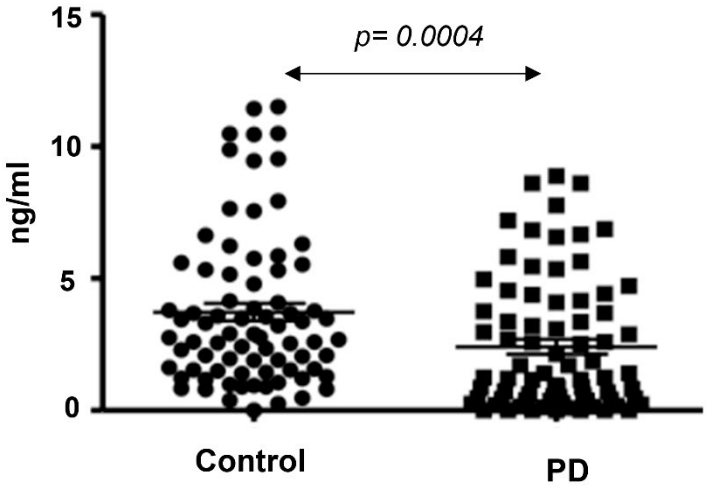

Figure 6. Serum GNPDA2 levels in PD population. GNPDA2 levels were measured in the sera derived from 164 individuals (82 controls; mean age: 69 years; 51M/31F and 82 PD subjects: mean age: 67 years; 41M/41F) by ELISA (Mann–Whitney U test; p-value: 0.0004).

4. Discussion

In view of the general recognition that olfactory dysfunction is an early feature of PD, we consider that the elucidation of the progressive proteome-wide alterations that occurs in the OB, might provide novel candidate proteins for a druggability assessment in PD. Neuroproteomics has been successfully applied to discover novel protein mediators associated with PD pathogenesis, diagnosis and evolution (Jin et al., 2006; Lehnert et al., 2012; Licker et al., 2012; Licker et al., 2014; Liu et al., 2015). To our knowledge, this is the first study to characterize potential PD-associated molecular changes in the human OB combining imaging mass-spectrometry and quantitative proteomics. In a first approach, using MALDI-IMS as a molecular histology technique, we have observed that there are obvious molecular changes between control and LB stages, at protein level, with several distinctive masses (ROC curves with AUC values >0.8) adopting marked positional domains in LB stages. Our data suggest that MALDI-IMS is a suitable approach that complements current neuropathological classifications. Some of the differential expressed OB proteins detected across LTS stages have been proposed as α-synuclein interactors or protein components of Lewy body inclusions (Betzer et al., 2015; Leverenz et al., 2007): IGSF8 (in LBDL stage), GNAO1, OMG, ARPC5, and NIPSNAP1 (in LBDE stage), HSD17B10, ATP6V1D, PGRMC1, ACADS, and TUBB2 (in LBDN stage), VPS53 (common to LBDL and LBDE stages), ATP1A2, EHD1, EEF1A2, and BANF1 (common to LBDE and LBDN stages), and TUBB4A, TPPP, and TUBA4A (common to all stages). To establish a functional relationship between the OB and other PD-affected regions at proteome level, a traceability analysis was performed comparing the differential OB protein set with respect to deregulated proteins previously detected in functionally related structures such as SN, striatum, and cortex derived from PD subjects (Licker et al., 2014; Riley et al., 2014). In accordance with down-regulated OB proteome, the expression of five nigral proteins, three cortical proteins, and striatal protein OMG were also down-modulated in PD. In contrast, nigral protein MYO6, fourteen striatal

proteins, and eighteen cortical proteins present an opposite expression pattern (up-regulation) in PD subjects (Additional file 8). With respect to the up-regulated OB proteome, four nigral proteins, twenty striatal proteins, and seventeen cortical proteins were also up-regulated in PD phenotypes (Additional file 8). This information suggests that the coordinated deregulation of specific protein modules shared among brain areas might explain, in part, the existence of conserved transcriptional programs that may be activated/deactivated across structures during PD pathogenesis.

The aberrant regulation of a subset of kinases may represent the triggering events leading to the spread of an abnormal signaling in PD (Wang et al., 2012). In this context, cell survival mechanisms have been proposed as targets for neuroprotective strategies in delay onset, or slow progression of PD (Goswami et al., 2017). Analyzing the signaling interactions predicted by our network-system biology approach, we determine potential upstream regulators highly interconnected with deregulated olfactory proteins. An increment in phospho-ERK levels has been previously reported in midbrain dopaminergic neurons in PD brains (Zhu et al., 2003; Zhu et al., 2002). However, in leukocytes, ERK1/2 activity does not significantly differ between controls and PD subjects (White et al., 2007). In our case, the activation of the pro-survival factor ERK1/2 tends to be compromised across LTS stages. Interestingly, a hyperactivation of upstream MEK1/2 and ERK1/2 was evidenced in the OB derived from AD subjects (Lachen-Montes et al., 2016), suggesting that MAPK signalling clearly differs between PD and AD phenotypes at olfactory level. It has been shown that p38 MAPK is activated by α-synuclein (Rannikko et al., 2015), being localized in neurons of PD brain stem bearing LBs or α-synuclein deposits (Ferrer et al., 2001). An early inactivation of MKK3/6-p38 MAPK axis has been observed in initial AD stages at OB level, recovering normal levels in intermediate and advanced AD stages (Lachen-Montes et al., 2017). However, a distinct profile was observed in PD phenotypes. The inactivation of MKK3/6 across LTS stages suggests the involvement of other kinase-based route in the apparent maintenance of olfactory p38 MAPK activity in the OB from PD. To our knowledge, our data

represent the first molecular link between PDK1 dysregulation and PD. An impairment of olfactory PDK1/PKC signaling axis was observed in LBDL and LBDE stages. Interestingly, and in line with these findings, this pathway is also modified in the OB of AD subjects (Lachen-Montes et al., 2017). As α-synuclein specifically downregulates PKCδ isoform in dopaminergic cells (Jin et al., 2011), further work will be necessary to clarify the specific role of each PKC isoform in olfactory neurons during PD progression.

Although the activation state of specific olfactory survival pathways differs between PD and AD, this study has allowed the identification of a subset of common protein intermediates in the OB from PD and AD subjects respect to non-demented controls, suggesting that these shared proteins might participate as common pathological substrates during the olfactory neurodegenerative process in both neurological disorders (Doty, 2012b, 2017). However, it is important to note that 14 out of 21 (67%) PD subjects included in our study, present concomitant AD-type Tau pathology (Braak stage I-II) (data not shown). Said that, we cannot exclude the possibility that the shared differential OB proteome observed between AD and PD may be due to the AD concomitant pathology present in PD subjects. In the present study, novel common mediators have emerged but with different expression profiling between PD and AD phenotypes, emphasizing the importance of neuropathological stage-dependent analysis in the search of potential olfactory therapeutic targets. CPN6, and DPP6 tend to be up-regulated in the OB from PD subjects, indicating specific differences in spine plasticity and synaptic function (Lin et al., 2013; Reinhard et al., 2016) respect to AD (Zelaya et al., 2015). Moreover, the different expression profile observed between AD and LTS stages for SCGN, CACYBP, and RACK1 proteins also points out subtle differences in calcium fluxes, cytoskeletal dynamics, and oxidative response in the OB from AD and PD subjects. Interestingly, the metabolic enzyme GNPDA2 was over-expressed in most PD and AD cases (see also additional file 9B), showing an inverse correlation between GNPDA2 and α-synuclein protein levels in the CSF from PD subjects. However, serum GNPDA2 levels were significantly decreased in PD population. The different

protein profile across fluids has been also observed for other proteins in the context of PD such as Complement C4, serotransferrin, apolipoprotein AI, haptoglobin, zinc-alpha-2-glycoprotein, Apolipoprotein E, beta-2-glycoprotein, ceruloplasmin, complement C3 and serum albumin (Halbgebauer et al., 2016). The lack of standardization between laboratories in CSF collection and preparation procedures may be a reason for this type of observation. However, from a biological point of view, these molecular events may be due to the damage of the blood-brain barrier (BBB) observed in PD subjects Checking the Human Protein Atlas (Uhlen et al., 2010)(www.proteinatlas.org), GNPDA2 is highly expressed by the brain (https://www.proteinatlas.org/ENSG00000163281-GNPDA2/tissue), so additional experiments are needed to explain the GNPDA2 efflux, rates, and transportation (both the brain-to-blood and the blood-to-brain directions) in the PD pathophysiology. Being aware of the small number of cases assessed in this study, the novel relation of secreted GNPDA2, and α-synuclein should be further evaluated in combination with other biochemical markers in order to improve the current diagnostic assays (Eusebi et al., 2017; Forland et al., 2018).

5. Conclusion

Overall, the current study provides new insights regarding the molecular mechanisms governing the olfactory dysfunction occurring during PD progression. Besides the pathological depositions of α-synuclein occurring at the level of the OB, we have demonstrated a clear disarrangement in the olfactory proteostasis, affecting cell survival routes and showing potential common pathological substrates between PD and AD. Moreover, the application of high-throughput proteomic approaches again proves to be a useful tool to decipher the proteome expression profiles in olfactory structures and more importantly, to define potential fluid biomarkers for the diagnosis of neurodegenerative processes.

References

Alafuzoff, I., Ince, P.G., Arzberger, T., Al-Sarraj, S., Bell, J., Bodi, I., Bogdanovic, N., Bugiani, O., Ferrer, I., Gelpi, E., Gentleman, S., Giaccone, G., Ironside, J.W., Kavantzas, N., King, A., Korkolopoulou, P., Kovacs, G.G., Meyronet, D., Monoranu, C., Parchi, P., Parkkinen, L., Patsouris, E., Roggendorf, W., Rozemuller, A., Stadelmann-Nessler, C., Streichenberger, N., Thal, D.R., Kretzschmar, H., 2009. Staging/typing of Lewy body related alpha-synuclein pathology: a study of the BrainNet Europe Consortium. Acta Neuropathol 117(6), 635-652.

Alexander, G.M., Schwartzman, R.J., Grothusen, J.R., Gordon, S.W., 1994. Effect of plasma levels of large neutral amino acids and degree of parkinsonism on the blood-to-brain transport of levodopa in naive and MPTP parkinsonian monkeys. Neurology 44(8), 1491-1499.

Arreola, R., Valderrama, B., Morante, M.L., Horjales, E., 2003. Two mammalian glucosamine-6-phosphate deaminases: a structural and genetic study. FEBS Lett 551(1-3), 63-70.

Attems, J., Alpar, A., Spence, L., McParland, S., Heikenwalder, M., Uhlen, M., Tanila, H., Hokfelt, T.G., Harkany, T., 2012. Clusters of secretagogin-expressing neurons in the aged human olfactory tract lack terminal differentiation. Proc Natl Acad Sci U S A 109(16), 6259-6264.

Attems, J., Walker, L., Jellinger, K.A., 2014. Olfactory bulb involvement in neurodegenerative diseases. Acta Neuropathol 127(4), 459-475.

Baba, T., Kikuchi, A., Hirayama, K., Nishio, Y., Hosokai, Y., Kanno, S., Hasegawa, T., Sugeno, N., Konno, M., Suzuki, K., Takahashi, S., Fukuda, H., Aoki, M., Itoyama, Y., Mori, E., Takeda, A., 2012. Severe olfactory dysfunction is a prodromal symptom of dementia associated with Parkinson's disease: a 3 year longitudinal study. Brain 135(Pt 1), 161-169.

Beach, T.G., White, C.L., 3rd, Hladik, C.L., Sabbagh, M.N., Connor, D.J., Shill, H.A., Sue, L.I., Sasse, J., Bachalakuri, J., Henry-Watson, J., Akiyama, H., Adler, C.H., 2009. Olfactory bulb alpha-synucleinopathy has high specificity and sensitivity for Lewy body disorders. Acta Neuropathol 117(2), 169-174.

Betzer, C., Movius, A.J., Shi, M., Gai, W.P., Zhang, J., Jensen, P.H., 2015. Identification of synaptosomal proteins binding to monomeric and oligomeric alpha-synuclein. PLoS One 10(2), e0116473.

Braak, H., Del Tredici, K., Bratzke, H., Hamm-Clement, J., Sandmann-Keil, D., Rub, U., 2002. Staging of the intracerebral inclusion body pathology associated with idiopathic Parkinson's disease (preclinical and clinical stages). J Neurol 249 Suppl 3, III/1-5.

Braak, H., Del Tredici, K., Rub, U., de Vos, R.A., Jansen Steur, E.N., Braak, E., 2003. Staging of brain pathology related to sporadic Parkinson's disease. Neurobiol Aging 24(2), 197-211.

Braak, H., Ghebremedhin, E., Rub, U., Bratzke, H., Del Tredici, K., 2004. Stages in the development of Parkinson's disease-related pathology. Cell Tissue Res 318(1), 121-134.

Braak, H., Muller, C.M., Rub, U., Ackermann, H., Bratzke, H., de Vos, R.A., Del Tredici, K., 2006. Pathology associated with sporadic Parkinson's disease--where does it end? J Neural Transm Suppl(70), 89-97.

Brodoehl, S., Klingner, C., Volk, G.F., Bitter, T., Witte, O.W., Redecker, C., 2012. Decreased olfactory bulb volume in idiopathic Parkinson's disease detected by 3.0-tesla magnetic resonance imaging. Mov Disord 27(8), 1019-1025.

Caprioli, R.M., Farmer, T.B., Gile, J., 1997. Molecular imaging of biological samples: localization of peptides and proteins using MALDI-TOF MS. Anal Chem 69(23), 4751-4760.

Chaurand, P., Schwartz, S.A., Billheimer, D., Xu, B.J., Crecelius, A., Caprioli, R.M., 2004. Integrating histology and imaging mass spectrometry. Anal Chem 76(4), 1145-1155.

Derijard, B., Raingeaud, J., Barrett, T., Wu, I.H., Han, J., Ulevitch, R.J., Davis, R.J., 1995. Independent human MAP-kinase signal transduction pathways defined by MEK and MKK isoforms. Science 267(5198), 682-685.

Doty, R.L., 2008. The olfactory vector hypothesis of neurodegenerative disease: is it viable? Ann Neurol 63(1), 7-15.

Doty, R.L., 2012a. Olfaction in Parkinson's disease and related disorders. Neurobiol Dis 46(3), 527-552.

Doty, R.L., 2012b. Olfactory dysfunction in Parkinson disease. Nat Rev Neurol 8(6), 329-339.

Doty, R.L., 2017. Olfactory dysfunction in neurodegenerative diseases: is there a common pathological substrate? Lancet Neurol 16(6), 478-488.

Eusebi, P., Giannandrea, D., Biscetti, L., Abraha, I., Chiasserini, D., Orso, M., Calabresi, P., Parnetti, L., 2017. Diagnostic utility of cerebrospinal fluid alpha-synuclein in Parkinson's disease: A systematic review and meta-analysis. Mov Disord 32(10), 1389-1400.

Fabregat, A., Jupe, S., Matthews, L., Sidiropoulos, K., Gillespie, M., Garapati, P., Haw, R., Jassal, B., Korninger, F., May, B., Milacic, M., Roca, C.D., Rothfels, K., Sevilla, C., Shamovsky, V., Shorser, S., Varusai, T., Viteri, G., Weiser, J., Wu, G., Stein, L., Hermjakob, H., D'Eustachio, P., 2018. The Reactome Pathway Knowledgebase. Nucleic Acids Res 46(D1), D649-D655.

Ferrer, I., Blanco, R., Carmona, M., Puig, B., Barrachina, M., Gomez, C., Ambrosio, S., 2001. Active, phosphorylation-dependent mitogen-activated protein kinase (MAPK/ERK), stress-activated protein kinase/c-Jun N-terminal kinase (SAPK/JNK), and p38 kinase expression in Parkinson's disease and Dementia with Lewy bodies. J Neural Transm (Vienna) 108(12), 1383-1396.

Filipek, A., Schneider, G., Mietelska, A., Figiel, I., Niewiadomska, G., 2008. Age-dependent changes in neuronal distribution of CacyBP/SIP: comparison to tubulin and the tau protein. J Neural Transm (Vienna) 115(9), 1257-1264.

Forland, M.G., Ohrfelt, A., Dalen, I., Tysnes, O.B., Blennow, K., Zetterberg, H., Pedersen, K.F., Alves, G., Lange, J., 2018. Evolution of cerebrospinal fluid total alpha-synuclein in Parkinson's disease. Parkinsonism Relat Disord 49, 4-8.

Goswami, P., Joshi, N., Singh, S., 2017. Neurodegenerative signaling factors and mechanisms in Parkinson's pathology. Toxicol In Vitro 43, 104-112.

Guldbrandsen, A., Vethe, H., Farag, Y., Oveland, E., Garberg, H., Berle, M., Myhr, K.M., Opsahl, J.A., Barsnes, H., Berven, F.S., 2014. In-depth characterization of the cerebrospinal fluid (CSF) proteome displayed through the CSF proteome resource (CSF-PR). Mol Cell Proteomics 13(11), 3152-3163.

Halbgebauer, S., Ockl, P., Wirth, K., Steinacker, P., Otto, M., 2016. Protein biomarkers in Parkinson's disease: Focus on cerebrospinal fluid markers and synaptic proteins. Mov Disord 31(6), 848-860.

Ibarretxe-Bilbao, N., Junque, C., Marti, M.J., Valldeoriola, F., Vendrell, P., Bargallo, N., Zarei, M., Tolosa, E., 2010. Olfactory impairment in Parkinson's disease and white matter abnormalities in central olfactory areas: A voxel-based diffusion tensor imaging study. Mov Disord 25(12), 1888-1894.

Jellinger, K.A., 2008. A critical reappraisal of current staging of Lewy-related pathology in human brain. Acta Neuropathol 116(1), 1-16.

Jellinger, K.A., 2009. A critical evaluation of current staging of alpha-synuclein pathology in Lewy body disorders. Biochim Biophys Acta 1792(7), 730-740.

Jin, H., Kanthasamy, A., Ghosh, A., Yang, Y., Anantharam, V., Kanthasamy, A.G., 2011. alpha-Synuclein negatively regulates protein kinase Cdelta expression to suppress apoptosis in dopaminergic neurons by reducing p300 histone acetyltransferase activity. J Neurosci 31(6), 2035-2051.

Jin, J., Hulette, C., Wang, Y., Zhang, T., Pan, C., Wadhwa, R., Zhang, J., 2006. Proteomic identification of a stress protein, mortalin/mthsp70/GRP75: relevance to Parkinson disease. Mol Cell Proteomics 5(7), 1193-1204.

Kilanczyk, E., Filipek, A., Hetman, M., 2015. Calcyclin-binding protein/Siah-1-interacting protein as a regulator of transcriptional responses in brain cells. J Neurosci Res 93(1), 75-81.

Klingelhoefer, L., Reichmann, H., 2015. Pathogenesis of Parkinson disease--the gut-brain axis and environmental factors. Nat Rev Neurol 11(11), 625-636.

Kortekaas, R., Leenders, K.L., van Oostrom, J.C., Vaalburg, W., Bart, J., Willemsen, A.T., Hendrikse, N.H., 2005. Blood-brain barrier dysfunction in parkinsonian midbrain in vivo. Ann Neurol 57(2), 176-179.

Lachen-Montes, M., Gonzalez-Morales, A., de Morentin, X.M., Perez-Valderrama, E., Ausin, K., Zelaya, M.V., Serna, A., Aso, E., Ferrer, I., Fernandez-Irigoyen, J., Santamaria, E., 2016. An early dysregulation of FAK and MEK/ERK signaling pathways precedes the beta-amyloid deposition in the olfactory bulb of APP/PS1 mouse model of Alzheimer's disease. J Proteomics 148, 149-158.

Lachen-Montes, M., Gonzalez-Morales, A., Zelaya, M.V., Perez-Valderrama, E., Ausin, K., Ferrer, I., Fernandez-Irigoyen, J., Santamaria, E., 2017. Olfactory bulb neuroproteomics reveals a chronological perturbation of survival routes and a disruption of prohibitin complex during Alzheimer's disease progression. Sci Rep 7(1), 9115.

Lehnert, S., Jesse, S., Rist, W., Steinacker, P., Soininen, H., Herukka, S.K., Tumani, H., Lenter, M., Oeckl, P., Ferger, B., Hengerer, B., Otto, M., 2012. iTRAQ and multiple reaction monitoring as proteomic tools for biomarker search in cerebrospinal fluid of patients with Parkinson's disease dementia. Exp Neurol 234(2), 499-505.

Leverenz, J.B., Hamilton, R., Tsuang, D.W., Schantz, A., Vavrek, D., Larson, E.B., Kukull, W.A., Lopez, O., Galasko, D., Masliah, E., Kaye, J., Woltjer, R., Clark, C., Trojanowski, J.Q., Montine, T.J., 2008. Empiric refinement of the pathologic assessment of Lewy-related pathology in the dementia patient. Brain Pathol 18(2), 220-224.

Leverenz, J.B., Umar, I., Wang, Q., Montine, T.J., McMillan, P.J., Tsuang, D.W., Jin, J., Pan, C., Shin, J., Zhu, D., Zhang, J., 2007. Proteomic identification of novel proteins in cortical lewy bodies. Brain Pathol 17(2), 139-145.

Li, J., Gu, C.Z., Su, J.B., Zhu, L.H., Zhou, Y., Huang, H.Y., Liu, C.F., 2016. Changes in Olfactory Bulb Volume in Parkinson's Disease: A Systematic Review and Meta-Analysis. PLoS One 11(2), e0149286.

Licker, V., Cote, M., Lobrinus, J.A., Rodrigo, N., Kovari, E., Hochstrasser, D.F., Turck, N., Sanchez, J.C., Burkhard, P.R., 2012. Proteomic profiling of the substantia nigra demonstrates CNDP2 overexpression in Parkinson's disease. J Proteomics 75(15), 4656-4667.

Licker, V., Turck, N., Kovari, E., Burkhardt, K., Cote, M., Surini-Demiri, M., Lobrinus, J.A., Sanchez, J.C., Burkhard, P.R., 2014. Proteomic analysis of human substantia nigra identifies novel candidates involved in Parkinson's disease pathogenesis. Proteomics 14(6), 784-794.

Lin, L., Sun, W., Throesch, B., Kung, F., Decoster, J.T., Berner, C.J., Cheney, R.E., Rudy, B., Hoffman, D.A., 2013. DPP6 regulation of dendritic morphogenesis impacts hippocampal synaptic development. Nat Commun 4, 2270.

Liu, Y., Zhou, Q., Tang, M., Fu, N., Shao, W., Zhang, S., Yin, Y., Zeng, R., Wang, X., Hu, G., Zhou, J., 2015. Upregulation of alphaB-crystallin expression in the substantia nigra of patients with Parkinson's disease. Neurobiol Aging 36(4), 1686-1691.

Lloro, I., Fernandez-Irigoyen, J., Escobes, I., Azkargorta, M., Santamaria, E., Elortza, F., 2017. Methods for human olfactory bulb tissue studies using peptide/protein MALDI-TOF imaging mass spectrometry, in: Santamaria, E., Fernandez-Irigoyen, J. (Eds.), Neuromethods. Humana Press, New York, NY, pp. 91-106.

Ma, J., Wu, R., Zhang, Q., Wu, J.B., Lou, J., Zheng, Z., Ding, J.Q., Yuan, Z., 2014. DJ-1 interacts with RACK1 and protects neurons from oxidative-stress-induced apoptosis. Biochem J 462(3), 489-497.

McKeith, I.G., Boeve, B.F., Dickson, D.W., Halliday, G., Taylor, J.P., Weintraub, D., Aarsland, D., Galvin, J., Attems, J., Ballard, C.G., Bayston, A., Beach, T.G., Blanc, F., Bohnen, N., Bonanni, L., Bras, J., Brundin, P., Burn, D., Chen-Plotkin, A., Duda, J.E., El-Agnaf, O., Feldman, H., Ferman, T.J., Ffytche, D., Fujishiro, H., Galasko, D., Goldman, J.G., Gomperts, S.N., Graff-Radford, N.R., Honig, L.S., Iranzo, A., Kantarci, K., Kaufer, D., Kukull, W., Lee, V.M.Y., Leverenz, J.B., Lewis, S., Lippa, C., Lunde, A., Masellis, M., Masliah, E., McLean, P., Mollenhauer, B., Montine, T.J., Moreno, E., Mori, E., Murray, M., O'Brien, J.T., Orimo, S., Postuma, R.B., Ramaswamy, S., Ross, O.A., Salmon, D.P., Singleton, A., Taylor, A., Thomas, A., Tiraboschi, P., Toledo, J.B., Trojanowski, J.Q., Tsuang, D., Walker, Z., Yamada, M., Kosaka, K., 2017. Diagnosis and management of dementia with Lewy bodies: Fourth consensus report of the DLB Consortium. Neurology 89(1), 88-100.

McKeith, I.G., Dickson, D.W., Lowe, J., Emre, M., O'Brien, J.T., Feldman, H., Cummings, J., Duda, J.E., Lippa, C., Perry, E.K., Aarsland, D., Arai, H., Ballard, C.G., Boeve, B., Burn, D.J., Costa, D., Del Ser, T., Dubois, B., Galasko, D., Gauthier, S., Goetz, C.G., Gomez-Tortosa, E., Halliday, G., Hansen, L.A., Hardy, J., Iwatsubo, T., Kalaria, R.N., Kaufer, D., Kenny, R.A., Korczyn, A., Kosaka, K., Lee, V.M., Lees, A., Litvan, I., Londos, E., Lopez, O.L., Minoshima, S., Mizuno, Y., Molina, J.A., Mukaetova-Ladinska, E.B., Pasquier, F., Perry, R.H., Schulz, J.B., Trojanowski, J.Q., Yamada, M., 2005. Diagnosis and management of dementia with Lewy bodies: third report of the DLB Consortium. Neurology 65(12), 1863-1872.

McKeith, I.G., Galasko, D., Kosaka, K., Perry, E.K., Dickson, D.W., Hansen, L.A., Salmon, D.P., Lowe, J., Mirra, S.S., Byrne, E.J., Lennox, G., Quinn, N.P., Edwardson, J.A., Ince, P.G., Bergeron, C., Burns, A., Miller, B.L., Lovestone, S., Collerton, D., Jansen, E.N., Ballard, C., de Vos, R.A., Wilcock, G.K., Jellinger, K.A., Perry, R.H., 1996. Consensus guidelines for the clinical and pathologic diagnosis of dementia with Lewy bodies (DLB): report of the consortium on DLB international workshop. Neurology 47(5), 1113-1124.

Mora, A., Komander, D., van Aalten, D.M., Alessi, D.R., 2004. PDK1, the master regulator of AGC kinase signal transduction. Semin Cell Dev Biol 15(2), 161-170.

Moritz, C.P., 2017. Tubulin or Not Tubulin: Heading Toward Total Protein Staining as Loading Control in Western Blots. Proteomics 17(20).

Mourino-Alvarez, L., Iloro, I., de la Cuesta, F., Azkargorta, M., Sastre-Oliva, T., Escobes, I., Lopez-Almodovar, L.F., Sanchez, P.L., Urreta, H., Fernandez-Aviles, F., Pinto, A., Padial, L.R., Akerstrom, F., Elortza, F., Barderas, M.G., 2016. MALDI-Imaging Mass Spectrometry: a step forward in the anatomopathological characterization of stenotic aortic valve tissue. Sci Rep 6, 27106.

Mundinano, I.C., Caballero, M.C., Ordonez, C., Hernandez, M., DiCaudo, C., Marcilla, I., Erro, M.E., Tunon, M.T., Luquin, M.R., 2011. Increased dopaminergic cells and protein aggregates in the olfactory bulb of patients with neurodegenerative disorders. Acta Neuropathol 122(1), 61-74.

Mundinano, I.C., Hernandez, M., Dicaudo, C., Ordonez, C., Marcilla, I., Tunon, M.T., Luquin, M.R., 2013. Reduced cholinergic olfactory centrifugal inputs in patients with neurodegenerative disorders and MPTP-treated monkeys. Acta Neuropathol 126(3), 411-425.

Rannikko, E.H., Weber, S.S., Kahle, P.J., 2015. Exogenous alpha-synuclein induces toll-like receptor 4 dependent inflammatory responses in astrocytes. BMC Neurosci 16, 57.

Reinhard, J.R., Kriz, A., Galic, M., Angliker, N., Rajalu, M., Vogt, K.E., Ruegg, M.A., 2016. The calcium sensor Copine-6 regulates spine structural plasticity and learning and memory. Nat Commun 7, 11613.

Rey, N.L., Steiner, J.A., Maroof, N., Luk, K.C., Madaj, Z., Trojanowski, J.Q., Lee, V.M., Brundin, P., 2016. Widespread transneuronal propagation of alpha-synucleinopathy triggered in olfactory bulb mimics prodromal Parkinson's disease. J Exp Med 213(9), 1759-1778.

Riley, B.E., Gardai, S.J., Emig-Agius, D., Bessarabova, M., Ivliev, A.E., Schule, B., Alexander, J., Wallace, W., Halliday, G.M., Langston, J.W., Braxton, S., Yednock, T., Shaler, T., Johnston, J.A., 2014. Systems-based analyses of brain regions functionally impacted in Parkinson's disease reveals underlying causal mechanisms. PLoS One 9(8), e102909.

Saito, Y., Shioya, A., Sano, T., Sumikura, H., Murata, M., Murayama, S., 2016. Lewy body pathology involves the olfactory cells in Parkinson's disease and related disorders. Mov Disord 31(1), 135-138.

Shevchenko, A., Tomas, H., Havlis, J., Olsen, J.V., Mann, M., 2006. In-gel digestion for mass spectrometric characterization of proteins and proteomes. Nat Protoc 1(6), 2856-2860.

Sweeney, M.D., Sagare, A.P., Zlokovic, B.V., 2018. Blood-brain barrier breakdown in Alzheimer disease and other neurodegenerative disorders. Nat Rev Neurol 14(3), 133-150.

Ubeda-Banon, I., Saiz-Sanchez, D., de la Rosa-Prieto, C., Argandona-Palacios, L., Garcia-Munozguren, S., Martinez-Marcos, A., 2010a. alpha-Synucleinopathy in the human olfactory system in Parkinson's disease: involvement of calcium-binding protein- and substance P-positive cells. Acta Neuropathol 119(6), 723-735.

Ubeda-Banon, I., Saiz-Sanchez, D., de la Rosa-Prieto, C., Martinez-Marcos, A., 2012. alpha-Synuclein in the olfactory system of a mouse model of Parkinson's disease: correlation with olfactory projections. Brain Struct Funct 217(2), 447-458.

Ubeda-Banon, I., Saiz-Sanchez, D., de la Rosa-Prieto, C., Mohedano-Moriano, A., Fradejas, N., Calvo, S., Argandona-Palacios, L., Garcia-Munozguren, S., Martinez-Marcos, A., 2010b. Staging of alpha-synuclein in the olfactory bulb in a model of Parkinson's disease: cell types involved. Mov Disord 25(11), 1701-1707.

Uhlen, M., Oksvold, P., Fagerberg, L., Lundberg, E., Jonasson, K., Forsberg, M., Zwahlen, M., Kampf, C., Wester, K., Hober, S., Wernerus, H., Bjorling, L., Ponten, F., 2010. Towards a knowledge-based Human Protein Atlas. Nat Biotechnol 28(12), 1248-1250.

Vizcaino, J.A., Deutsch, E.W., Wang, R., Csordas, A., Reisinger, F., Rios, D., Dianes, J.A., Sun, Z., Farrah, T., Bandeira, N., Binz, P.A., Xenarios, I., Eisenacher, M., Mayer, G., Gatto, L., Campos, A., Chalkley, R.J., Kraus, H.J., Albar, J.P., Martinez-Bartolome, S., Apweiler, R., Omenn, G.S., Martens, L., Jones, A.R., Hermjakob, H., 2014. ProteomeXchange provides globally coordinated proteomics data submission and dissemination. Nat Biotechnol 32(3), 223-226.

Wang, G., Pan, J., Chen, S.D., 2012. Kinases and kinase signaling pathways: potential therapeutic targets in Parkinson's disease. Prog Neurobiol 98(2), 207-221.

White, L.R., Toft, M., Kvam, S.N., Farrer, M.J., Aasly, J.O., 2007. MAPK-pathway activity, Lrrk2 G2019S, and Parkinson's disease. J Neurosci Res 85(6), 1288-1294.

Zelaya, M.V., Perez-Valderrama, E., de Morentin, X.M., Tunon, T., Ferrer, I., Luquin, M.R., Fernandez-Irigoyen, J., Santamaria, E., 2015. Olfactory bulb proteome dynamics during the progression of sporadic Alzheimer's disease: identification of common and distinct olfactory targets across Alzheimer-related co-pathologies. Oncotarget 6(37), 39437-39456.

Zhu, J.H., Guo, F., Shelburne, J., Watkins, S., Chu, C.T., 2003. Localization of phosphorylated ERK/MAP kinases to mitochondria and autophagosomes in Lewy body diseases. Brain Pathol 13(4), 473-481.

Zhu, J.H., Kulich, S.M., Oury, T.D., Chu, C.T., 2002. Cytoplasmic aggregates of phosphorylated extracellular signal-regulated protein kinases in Lewy body diseases. Am J Pathol 161(6), 2087-2098

CHAPTER 6

Early-onset molecular Derangements in the Olfactory Bulb of the Alzheimer´s disease Tg2576 mice: novel insights into stress-responsive olfactory kinase dynamics in Alzheimer's disease

Mercedes Lachén-Montes[1,2,3]**,** Andrea González-Morales[1,2,3], Maialen Palomino-Alonso[1], Karina Ausin[2,3], Marta Gómez-Ochoa[4], María Victoria Zelaya[1,3,4], Isidro Ferrer[5], Alberto Pérez-Mediavilla[3,6], Joaquín Fernández-Irigoyen[1,2,3§], Enrique Santamaría[1,2,3§*]

1 Clinical Neuroproteomics Group, Navarrabiomed, Complejo Hospitalario de Navarra (CHN), Universidad Pública de Navarra (UPNA). Irunlarrea, 3 31008 Pamplona, Spain;

2 Proteored-ISCIII. Proteomics Unit, Navarrabiomed, Complejo Hospitalario de Navarra (CHN), Universidad Pública de Navarra (UPNA), Irunlarrea 3, 31008, Pamplona, Spain.

3 IDISNA, Navarra Institute for Health Research, Pamplona, Spain,

4 Department of Pathology, Complejo Hospitalario de Navarra, 31008, Pamplona, Navarra, Spain.

5 Institut de Neuropatologia, IDIBELL-Hospital Universitari de Bellvitge, Universitat de Barcelona, L'Hospitalet de Llobregat, CIBERNED (Centro de Investigación Biomédica en Red de Enfermedades Neurodegenerativas), Spain.

6 Neurobiology of Alzheimer's disease, Neurosciences Division, Center for Applied Medical Research (CIMA), Department of Biochemistry, University of Navarra, Pamplona, Spain.

Abstract

The olfactory bulb (OB) is the first processing station in the olfactory pathway. Despite smell impairment is considered an early event in Alzheimer´s disease (AD), little is known about the initial molecular disturbances that accompany the AD development at olfactory level. We have interrogated the time-dependent OB molecular landscape in Tg2576 AD mice prior to the appearance of neuropathological amyloid plaques (2-, and 6-month-old), using combinatorial omics analysis. The metabolic modulation induced by human mutated amyloid precursor protein (APP) overproduction clearly differs between both time points. Besides the progressive perturbation of the APP interactome, network-driven systems biology approach unveiled an inverse regulation of downstream extracellular signal-regulated kinase (ERK1/2), and p38 mitogen-activated protein kinase (MAPK) routes in 2-month-old Tg2576 mice respect to wild-type (WT) mice. In contrast, Akt and mitogen-activated protein kinase Kinase 4 (SEK1/MKK4)/ stress-activated protein kinase/Jun-amino terminal kinase (SAPK/JNK) axis were parallel activated in the OB of 6-months-old-Tg2576 mice. Furthermore, a survival kinome profiling performed during the aging process (2-, 6-, and 18-month-old) revealed that olfactory APP overexpression leads to changes in the activation dynamics of protein kinase A (PKA), and SEK1/MKK4-SAPK/JNK between 6 and 18 months of age, when memory deficits appear and AD pathology is well established in transgenic mice. Interestingly, both olfactory pathways were differentially activated in a stage-dependent manner in human AD subjects with different neuropathological grading. Taken together, our data reflect the early impact of mutated APP on the OB molecular homeostasis, highlighting the progressive modulation of specific signaling pathways during the olfactory amyloidogenic pathology.

1. Introduction

Together with typical symptoms such as memory loss and behavioral disorders, AD patients present olfactory dysfunction in 90% of the cases (1, 2). However, the etiology of this smell impairment is complex and remains mostly unknown. Neuropathological studies support the hypothesis that hyperphosphorylated Tau and Aβ aggregation present in the olfactory bulb (OB) are early and important events in the AD pathophysiology (3). It has been demonstrated that these protein deposits reflect the presence and severity of AD pathology in other brain structures (1).

Although no animal model recapitulates the entirety of human AD pathology (4), some AD transgenic mouse models also present olfactory deficits. Tg2576 transgenic mice express an isoform of human APP with double mutation K670N, M671L (hAPPSw) (5). Production of Aβ40 and Aβ42 and plaques formation are observed in cortical and hippocampal areas of these mice at the age of 11-13 months (6). Previous reports have pointed out that the accumulation of Aβ peptide is related to age-related memory decline in these mice (7-9), inducing synaptic deficits and mitochondrial imbalance (10, 11). The presence of APP processing products has been characterized in the OB of 1-month-old Tg2576 mice, detecting Aβ deposition at 13.5 months of age (12). This progressive Aβ deposition in specific olfactory structures is accompanied by behavioural deficits in odour habituation, and discrimination, diminished rate of OB neurogenesis, and an altered volume of the OB granular cell layer in Tg2576 mice (13-16).

Several studies using human AD brains and AD mouse models have demonstrated that the deposition of amyloid plaques is accompanied by an alteration in the OB´s molecular homeostasis (17-21). However, it is still unclear how the progressive amyloidogenic pathology affects the OB functionality in the absence of plaques. In this study, we used a high-throughput technological pipeline applying mass-spectrometry based quantitative proteomics, and transcriptome-wide analyses, to ascertain the magnitude and chronology of the OB molecular

remodeling in Tg2576 mice at two stages of AD: long before (2 months of age), and immediately before (6 months of age) the appearance of Aβ plaques, respect to age matched background strain wild-type (WT) mice. Our system-wide approach revealed stage-dependent molecular pathways and kinase activation dynamics that are disturbed during the initial phase of the amyloid pathology, providing basic information for understanding how olfactory molecular networks evolve as the AD pathology progresses at early stages. Further mining of this molecular resource may provide potential therapeutic agents for disease modification as well as candidate biomarkers for early AD diagnosis and evolution.

2. Materials and methods

2.1 Human samples - According to the Spanish Law 14/2007 of Biomedical Research, inform written consent forms of Brain Bank of IDIBELL, and Neurological Tissue Bank of IDIBAPS-Hospital Clinic (Barcelona, Spain) was obtained for research purposes from relatives of patients included in this study. The study was conducted in accordance with the Declaration of Helsinki and all assessments, post-mortem evaluations, and procedures were previously approved by the Clinical Ethics Committee of Navarra Health Service. For the validation phase, fourteen AD cases were distributed into different groups according to specific consensus diagnostic criteria (22, 23): initial (Braak I-II), intermediate (Braak III-IV), and advanced AD stages (Braak V-VI) (n = 4-5/group). Five cases from elderly subjects with no history or histological findings of any neurological disease were used as a control group. 85% of human brains considered in this study had a post-mortem interval (PMI) lower than 15 hours (Table 1).

Case	Sex	Age	PMI (hours)	Pathological diagnosis
Controls				
BK-0300	F	75	20	ARP I-II
BK-1378	M	78	6	vascular encephalopathy
BK-1078	F	84	6	vascular encephalopathy, NFT I
BK-1195	F	82	8	acute ictus, cerebellar hematoma
BK-1563	M	79	15	acute ictus, AgD II
Initial AD				
A13/70	F	79	10	AD II/A
A14/29	F	78	3.5	AD II/A
A14/33	M	62	9.5	AD II/0
A14/52	M	70	3	AD II/0
Intermediate AD				
A12/42	F	82	17	AD IV/A
A12/47	M	81	5	AD III/A
A12/48	M	84	12	AD IV/A
A12/54	M	89	3	AD IV/A
A15/17	M	84	20	AD III/A
Advanced AD				
CS-1445	F	73	3.5	AD VI/C + moderate CAA
CS-0662	M	75	4	AD VI/C
CS-0535	F	81	4.5	AD VI/C
CS-0673	M	75	4.25	AD VI/C
CS-1232	M	84	5	AD VI C + CAA

Table 1. Subjects included in this study. PMI: post-mortem interval.

2.2 Materials - The following reagents and materials were used. From Cell Signaling technology: anti-APP (ref. 2450), anti-MEK1/2 (ref. 9126), anti-phospho-MEK1/2 (S217/221) (ref. 9154), anti-ERK1/2 (ref. 9102), anti-phospho-ERK1/2 (T202/y204) (ref. 4370), anti-Akt (ref. 4685), anti-phospho-Akt (S473) (ref. 4060), anti-p38 MAPK (ref. 9212), anti-phospho-p38 MAPK (T180/Y182) (ref. 9211), anti-phospho-ATF2 (T71) (ref. 5112), anti-SAPK/JNK (ref. 9252), anti-phospho-SAPK/JNK (T183/Y185) (ref. 9255), anti-SEK1 (ref. 9152), anti-phospho-SEK1 (S257/T261) (Ref. 9156), anti-PKA C-alpha (ref. 4782), anti-phospho-PKA C (T197) (ref. 5661), anti-PP5 (ref. 2289), anti-PDK1 (ref. 3062), anti-phospho-PDK1 (S241) (ref. 3061), anti-phospho-PKC pan (T514) (ref. 9379), anti-phospho-FAK (Y576/577) (ref. 3281), anti-Phb1 (ref. 2426), and anti-Phb2 (ref. 14085). Anti-PKC-pan was from Sigma Aldrich (ref. SAB4502356). Electrophoresis reagents were purchased from Bio-rad and trypsin from Promega.

2.3 Animals - Transgenic mice (Tg2576) overexpressing hAPP carrying the Swedish (K670N/M671L) familial AD mutation under control of the prion promoter (5) were used. Mice were on an inbred C57BL/6/SJL genetic background. Animals were housed 4–5 per cage with free access to food and water, and maintained in a temperature-controlled environment on a 12 h light–dark cycle. Animal care procedures were conducted in accordance with the European Community Council Directive (2010/63/EU) and approved by the local ethics committee. Twenty-four animals, divided into two sets, were used for proteomics and transcriptomics analysis (12 mice/approach), with at least 3 wild-type and 3 Tg2576 transgenic mice per stage (2 and 6-month-old). The progressive development of AD signs in our colony has been previously described (24). We have previously observed that behavior (Morris Water Maze test; MWM) is completely normal and amyloid levels are equal to wild type at 2 months of age. At 6 months of age, mice show impaired cognitive functions in the contextual fear conditioning test, coinciding with the increased cortical and hippocampal soluble beta amyloid levels. At 12 months, the impairment in MWM is present in most of mice, but few are normal and with less plaques (but

they are present); and finally, in aged mice (17-18 months) the pathology is robust and 100% of mice shows plaques and MWM impairment.

2.4 Sample preparation for proteomic analysis - Murine OB specimens were homogenized in lysis buffer containing 7 M urea, 2 M thiourea, 50 mM DTT. The homogenates were spinned down at 100.000 x g for 1 h at 15ºC. Protein concentration was measured in the supernatants with the Bradford assay kit (Bio-rad).

2.5 Olfactory bulb proteomics - Sample preparation, Protein Digestion and Peptide iTRAQ Labeling was performed as previously described (17, 19). Briefly, each tryptic digest was labelled according to the manufacturer's instructions with one isobaric amine-reactive tags as follows: Set 1 (experiment with 2-months-old mice): Tag113, WT-1; Tag114, WT-2; Tag115, WT-3; Tag116, Tg2576-1; Tag117, Tg2576-2; Tag118, tg2576-3, and Set 2 (experiment with 6-months-old mice): Tag113, WT-1; Tag114, WT-2; Tag115, WT-3; Tag116, Tg2576-1; Tag117, Tg2576-2; Tag118, Tg2576-3. After 2h incubation, the set of labelled samples were pooled and evaporated in a vacuum centrifuge. To increase the proteome coverage, the peptide pool was submitted to cation exchange chromatography using spin Columns (Pierce). 12 fractions were collected (from 5mM to 250 mM KCl), concentrated using C18 zip tip solid phase extraction (Millipore), evaporated under vacuum and reconstituted into 10 µl of 2% acetonitrile, 0.1% formic acid, 98% MilliQ-H20 prior to mass spectrometric analysis. Peptide mixtures were separated by reverse phase chromatography and analysed by mass-spectrometry as previously described (21). The raw MS/MS spectra search were processed using the MaxQuant software (v.1.5.8.3) (25) and searched against the Uniprot proteome reference for Mus musculus (Proteome ID: UP000000589, May 2017). The parameters used were as follows: Initial maximum precursor (25ppm), fragment mass deviations (40ppm); variable modification (methionine oxidation and N-terminal acetylation) and fixed modification (MMTS); enzyme (trypsin) with a maximum of 1 missed cleavages; minimum peptide length (7 amino acids); false discovery rate (FDR) for PSM

and protein identification (1%). Frequently observed laboratory contaminants were removed. Protein identification was considered valid with at least one unique or "razor" peptide. The protein quantification was calculated using at least 2 razor + unique peptides, and statistical significance was calculated by a two-way Student-t test ($p < 0.05$). A 1.3-fold change cut-off was used. Proteins with iTRAQ ratios below the low range (0.77) were considered to be down-regulated, whereas those above the high range (1.3) were considered to be upregulated. The Perseus software (version 1.5.6.0) (26) was used for statistical analysis and data visualization. Search results files and MS raw data were deposited to the ProteomeXchange Consortium (http://proteomecentral.proteomexchange.org) via the PRIDE partner repository (27) with the dataset identifiers PXD007813 (username: reviewer31643@ebi.ac.uk; password: gMcgfWzD).

2.6 Olfactory bulb transcriptomics - Transcriptomics-Maxwell® 16 simplyRNA Kit (Promega) was used to extract the OB mRNAs from Tg2576 mice and WT littermates. The sense cDNA was fragmented and biotinylated using the Affymetrix Clarion S Pico assay (902932). Affymetrix mouse Clarion S chips were used according to the manufacturer protocols. Hybridization, washing, staining, scanning, and data analysis (28) was performed as previously described (20). As in other transcriptomic studies performed in AD brains (29, 30), we worked with a p-value < 0.01 (without using any method for multiple testing correction). Microarray data files were submitted to the GEO (Gene Expression Omnibus) database and are available under accession number GSE106643.

2.7 Bioinformatics - The identification of specifically dysregulated regulatory/metabolic networks in Tg2576 OBs was analysed using QIAGEN's Ingenuity® Pathway Analysis (IPA) (QIAGEN Redwood City, www.qiagen.com/ingenuity). The software generates significance values (p-values) between each biological or molecular event and the imported molecules based on the Fisheŕs exact test ($p \leq 0.05$). The IPA comparison analysis considers the signalling pathway rank according to the calculated p-value and reports it hierarchically.

2.8 Immunoblotting analysis - Equal amounts of OB protein (5 µg) were resolved in 4-15% TGX stain-Free gels (Bio-Rad). OB proteins derived from murine and human samples were electrophoretically transferred onto nitrocellulose membranes using a Trans-blot Turbo transfer system (up to 25V, 7min) (Bio-rad). Equal loading of the gels was assessed by stain free digitalization and by Ponceau staining. Western-blotting was performed as previously described (19). After densitometric analyses (Image Lab Software Version 5.2; Bio-Rad), optical density values were expressed as arbitrary units and normalized to total stain in each gel lane.

2.9 Immunohistochemistry - Under xylazine/ketamine anesthesia, animals were perfused transcardially with saline for 3 min at a 11 ml/min flow, and 4% paraformaldehyde in phosphate buffered saline (PBS) for 2 min at a 9 ml/min flow. After perfusion, brains were removed, post-fixed in 4% paraformaldehyde for 1 h at room temperature and cryoprotected in 30% sucrose solution in PBS overnight at 4 °C. Brains were sliced into 40-µm-thick coronal sections along the rostral axis with a freezing microtome (Leica, Germany) and collected in 0.125 M PBS containing 2 % dimethylsulphoxide (Sigma), 20 % glycerin (Panreac) and 0.05 % sodium azide and stored at −20ºC until their subsequent analysis. Five free floating tissue sections comprising the olfactory bulb of four animals per age group (2-, 6- and 14-month old) were processed for immunohistochemistry. Sections were washed (3 × 10 min) with a solution buffer containing PBS 0.125 M (pH 7.4), 0.5% Triton X-100 and 0.1% BSA. After washing, sections were treated with methanol and H2O2 to inhibit endogenous peroxidase activity and incubated in 70% formic acid for 5 min to expose the epitope. Subsequently, the sections were incubated overnight with a primary mouse antibody (6E10) raised against human beta amyloid (amino acids 1 to 16) (BioLegend, San Diego, CA) diluted 1:1000 in PBS 0.125 M (pH 7.4), 0.5% Triton X-100, 0.1% BSA and 5% normal goat sera. After washing (3 x 5 min) in PBS sections were incubated for 30 min with biotinylated goat anti-mouse secondary antibody (DakoCytomation, Glostrup, Denmark) diluted 1:500 in PBS. The sections were then processed using the avidin–biotin-peroxidase complex (Vectastain kit, Vector laboratories, Burlingame, CA) and reacted with 0.05% 3,3'-

diaminobenzidine tetrahydrochloride (DAB) and 0.015% H2O2 in 50 mM Tris HCl, pH 7.2. After washing in deionized water, sections were mounted on gelatinized slides, counterstained with Thionine at 60 °C (Panreac Quimica, Barcelona, Spain) and coverslipped with DPX (VWR, Dublin, Ireland). Respect to human OB samples, formalin-fixed, paraffin-embedded tissue sections from OB (derived from controls and AD cases) were sectioned at 5µm and counterstained with haematoxylin for immnuhistochemistry analysis with anti-SEK1 (ref. 9152) (1:50), anti-phospho-SEK1 (S257/T261) (Ref. 9156) (1:250), anti-PKA C-alpha (ref. 4782) (1:50), anti-phospho-PKA C (T197) (ref. 5661) (1:250). Visualization was performed by an automated slide immunostainer (Leica Bond Max) with BondPolymer Refine Detection (Leica Biosystems Newcastle Ltd

3. Results

3.1 APP overproduction induces early, and time-dependent molecular derangements in the olfactory bulb of Tg2576 mice

First, we analyzed the olfactory β-Amyloid pathology in TG2576 mice. As shown in figure 1, intraneuronal Aβ immunoreactivity was observed in 2-month-old transgenic mice, detecting Aβ deposition in form of diffuse plaques and mature plaques at the age of 6 and 14 months respectively. As the primary aim of our study was to analyze early-onset molecular derangements in the OB of Tg2576 mice, we deeply monitored OB molecular disturbances at two time-points (2 and 6 months) using high-throughput molecular technologies (Fig. 2A). At both time-points, Tg2576 mice displayed abundant full-length human APP expression in the OB (Fig. 2B). To examine the consequences of initial incremental accumulation of APP on OB molecular homeostasis, we applied proteomics and transcriptomics with the final goal to decipher novel information about the OB site-specific molecular signature at early AD stages in 2-month and 6-month-old Tg2576 mice. To analyze the potential differences in olfactory molecular expression profiles, OB specimens for each experimental group (Tg2576 and WT mice) were subjected into chemical tags (iTRAQ) coupled to tandem mass spectrometry and into RNA microarray platform. Respect to transcriptome-wide analysis, 187 protein-coding genes were differentially regulated in the OB of 2-month-old Tg2576 mice (46 down- and 141 up-regulated genes with respect to WT mice), whereas 287 differentially expressed genes were found in 6-month-old Tg2576 OBs (107 down- and 180 up-regulated genes with respect to WT mice) (Fig. 2B, and supplementary table 1). In the proteomic phase, 1605, and 1752 proteins were quantified at 2 and 6 months respectively. The expression levels of 31 proteins were found to be significantly different between 2-month-old WT and Tg2576 mice (12 down- and 19 up-regulated proteins with respect to WT mice), and 61 differentially expressed proteins were detected at 6 months of age (26 down- and 35 up-regulated proteins with respect to WT

animals) (Fig. 2B-C, and supplementary table 2). To partially validate our quantitative LC-MS/MS approach, the increment in Serine/threonine-protein phosphatase 5 (PP5), a phosphatase that protects neurons against Aβ toxicity (31), was verified by Western-blotting in 6-month-old Tg2576 OB (Supplementary Figure 1A). Interestingly, the genes and proteins affected between both stages varied widely, with only 1 protein (APP) and 9 genes common to the two time-points (Fig. 2D). Of these nine genes, four were co-downregulated (FOS, ARC, NPAS4, RGSL1) and five were co-upregulated (STMN4, STMN2, F3, HIF3a, EMB).

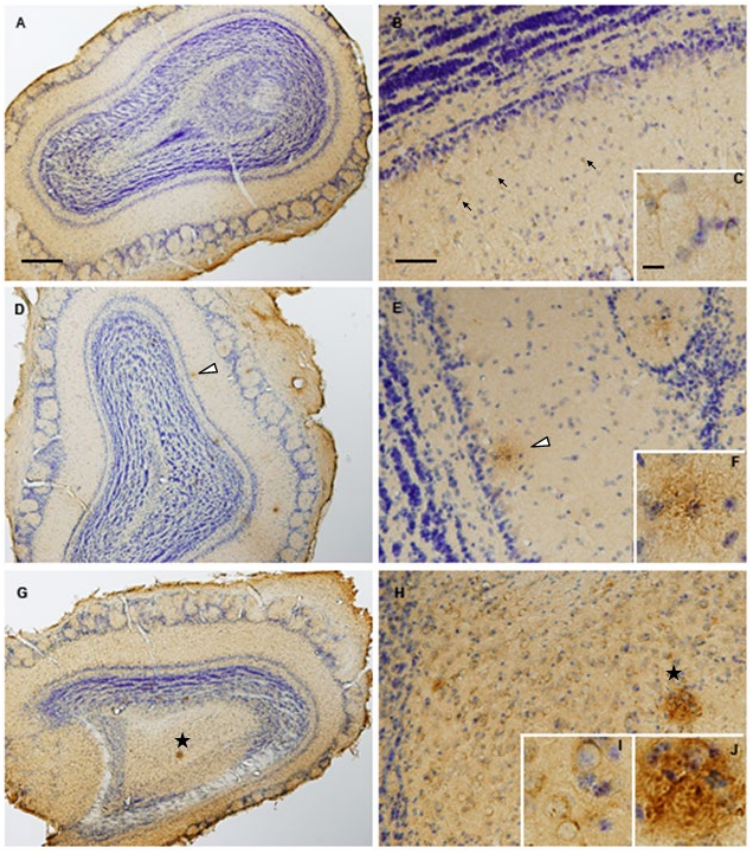

Figure 1. Olfactory β-Amyloid pathology increases with the disease progression in TG2576 mice. OBs were harvested from 2 (A-C), 6 (D-F) and 14 (G-J) month-old Tg2576 mice. Intraneuronal Aβ immunoreactivity can be observed in 2 month-old mice (arrow heads) (panel B and more detailed in panel C). OB samples from 6 month-old animals (panels D, E and F) shows moderate Aβ deposition in form of diffuse plaques (asterisk). By contrast, mature plaques

(asterisk in panel G, H and insert J) and vascular Aβ (insert I) is evident in 14 month-old Tg2576. Scale bars 500 µm for panels A, D, G, 100 µm for panels B, E, H) or 10 µm (C, F, I, J).

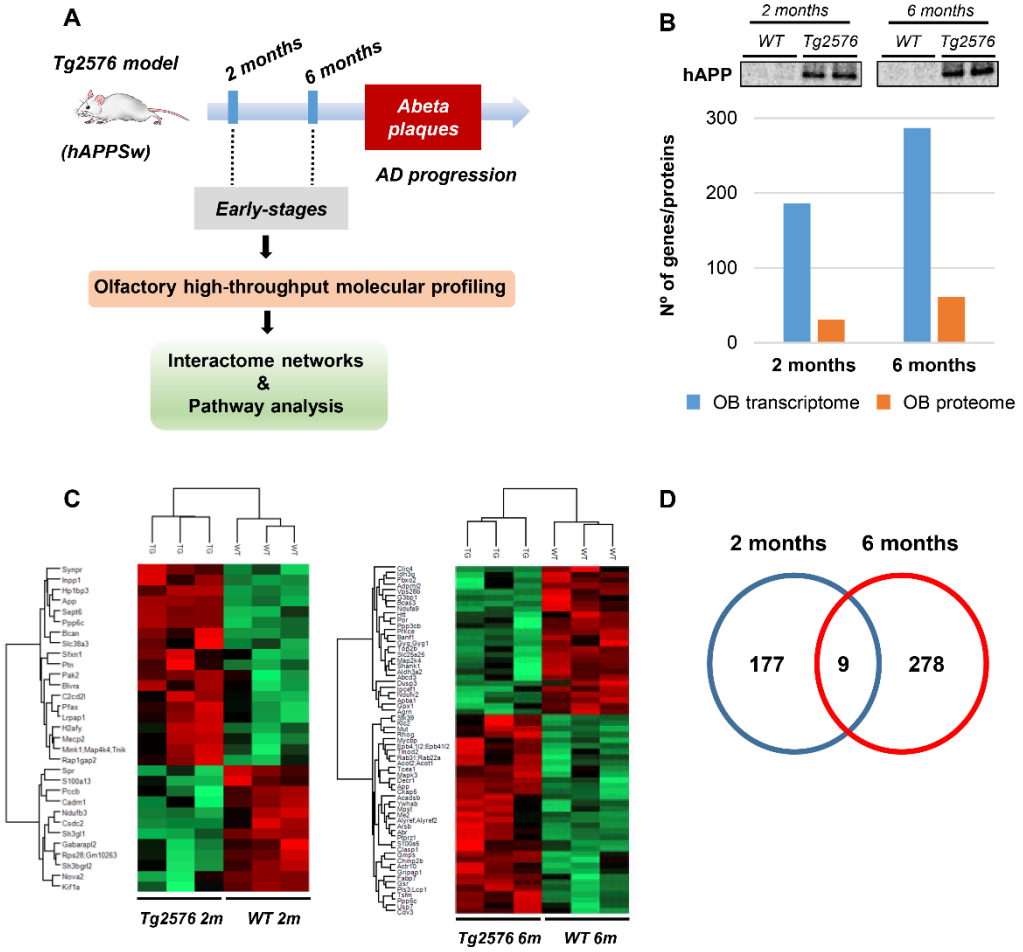

Figure 2. Dual-omic approach to characterize the OB molecular homeostasis between 2-month-old and 6-month-old Tg2576 mice. A) An overview of the experimental workflow used in this study. B) Differential molecular profiling detected by -omics in Tg2576 OBs (2 and 6 months of age). The OB protein expression levels of APP at early AD stages in Tg2576 mice is shown. C) Heat maps representing the degree of change for the differentially expressed proteins (Supplementary Table 2) between 2 and 6-month-old Tg2576 mice respect to WT littermates. Red and green, up- and down-regulated proteins, respectively. D) Venn diagram for the differentially expressed genes detected in Tg2576 mice at both time points (Supplementary Table 1).

3.2 Functional modules progressively disrupted by human mutated APP in the olfactory bulb of Tg2576 mice

To characterize in detail the proteogenomic modulation induced by the presence of human mutated APP at pre-plaque stages in the OB, differential proteomic and transcriptomic datasets were merged, and functionally analyzed across specific biological functions (See Supplementary Table 3). Functional bioinformatic analysis revealed that the accumulation of APP resulted in disturbances of statistically over-represented molecular processes directly relevant to adhesion (p-val: 0.0001), viability (p-val: 0.01), and interaction of neuroglia (p-val: 0.0001), quantity (p-val: 0.003), development (p-val: 0.04), and plasticity of synapse (p-val: 0.001), long-term potentiation (p-val: 0.006), growth of neurites (p-val: 0.03), and neuronal proliferation (p-val: 0.04) in 2-month-old Tg2576 mice (Figure 3). In 6-month-old Tg2576 mice, the olfactory amyloid pathology resulted predominantly in the significant alteration of microtubule dynamics (p-val: 0.0001), neuritogenesis (p-val: 0.0005), axonogenesis (p-val: 0.007), synaptic transmission (p-val: 0.01), transmembrane potential of mitochondria (p-val: 0.00001), metabolism of ROS (p-val: 0.02), and neurodegeneration of sensory neurons (p-val: 0.02) between others (Figure 3). However, functional commonalities focused on synthesis, and concentration of lipids/fatty acids, cell death, astrocytosis, and accumulation of vesicles were also detected in 2- and 6-month-old Tg2576 OBs (Figure 3, and Supplementary Table 3).

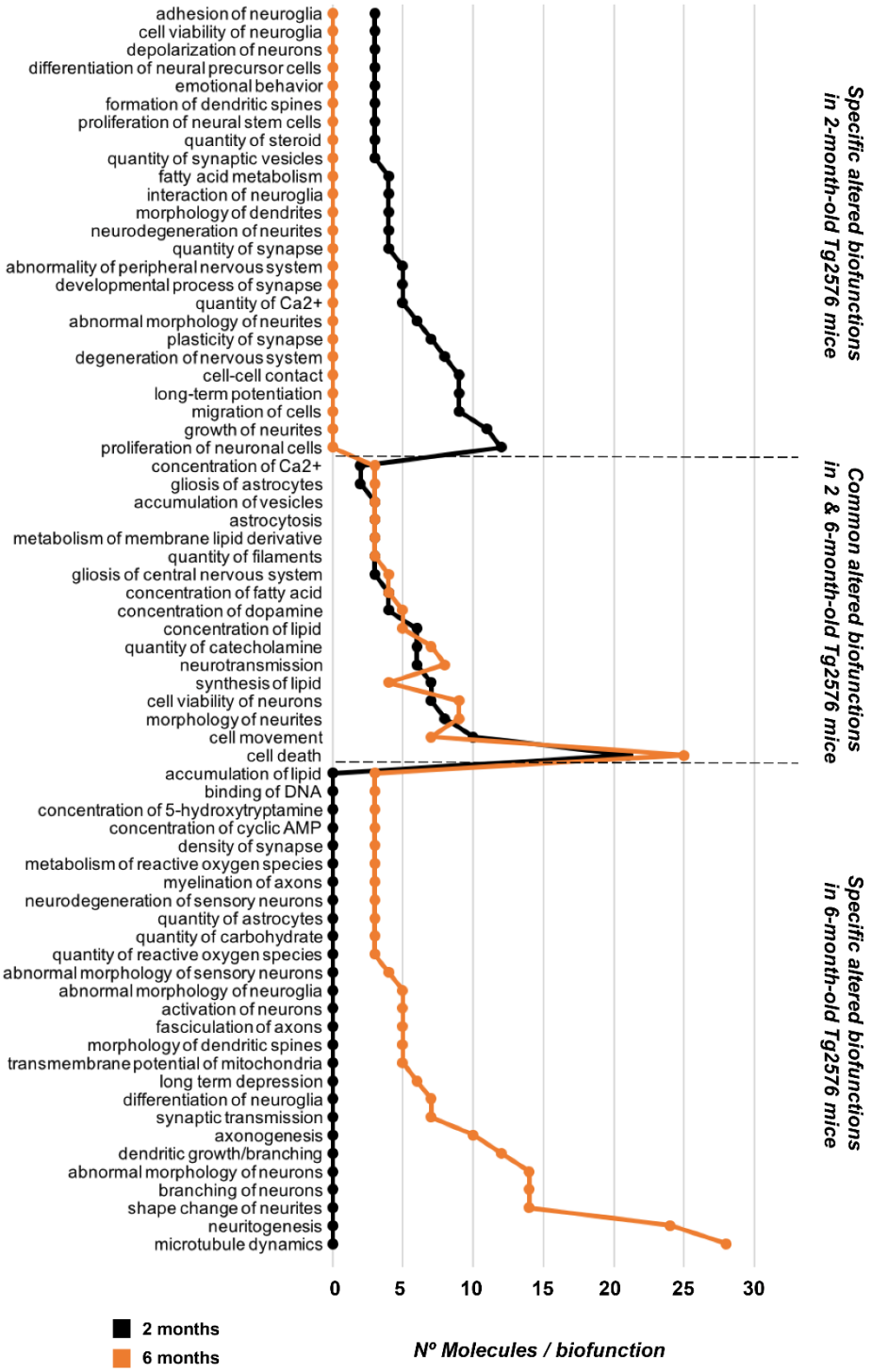

Figure 3. Profiling of molecular biofunctions potentially altered in the OB of Tg2576 mice. Functional analysis was performed with IPA software using exclusively the database information of experimental and predictive origin regarding central nervous system to be confident about the potential affected signalling pathways (See Supplementary Table 3 for details).

Considering that the discovery of unexpected connections between seemingly unrelated molecules and human mutated APP is a straightforward approach for the identification of novel AD causative targets involved in early olfactory neurodegeneration, we explored whether highly expressed APP isoform was potentially interconnected with differential molecular mediators identified in our proteogenomic approach. For that, functional interactomes were generated using IPA software. Interestingly, 35 differential functional interactors for APP were identified in the OB of Tg2576 mice at pre-plaque stages, suggesting the involvement in related biological functions. (Figure 4). Specifically, at 2 months of age, olfactory APP is central to an interconnected molecular network composed by targets with specific subcellular distribution: i) IGF2, OGN, TIMP3 at extracellular level, ii) LRPAP1, NNAT, STMN2 in the plasma membrane, iii) cytoplasmic GSTM3, MT-ND3, MAPK10, ACTG1, PRDX6, RNF24, NDUFA8, ARC, and S100B, and iv) MECP2, FOSB, EGR1, FOS, EGR2 in the nucleus (Figure 4A). At 6 months of age, the olfactory APP interactome completely varied at extracellular (MBP, and CSF1), plasma membrane (GNG2, GAP43, STMN2, MERTK), cytoplasmic (APBA1, PVALB, MAPK3, GSR, CRYM, MAP2K4, ABCD3, KLC2, FBXO2, ARC), and nuclear (FOS, TOP2B) levels (Figure 4B).

A

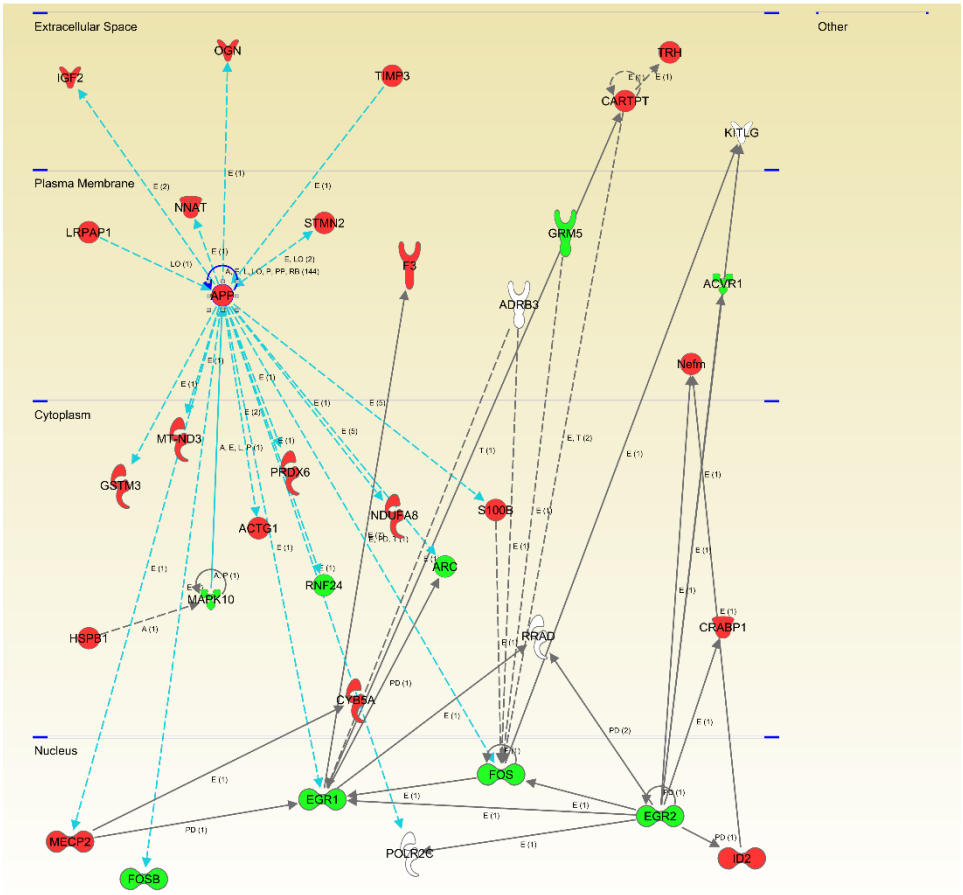

B

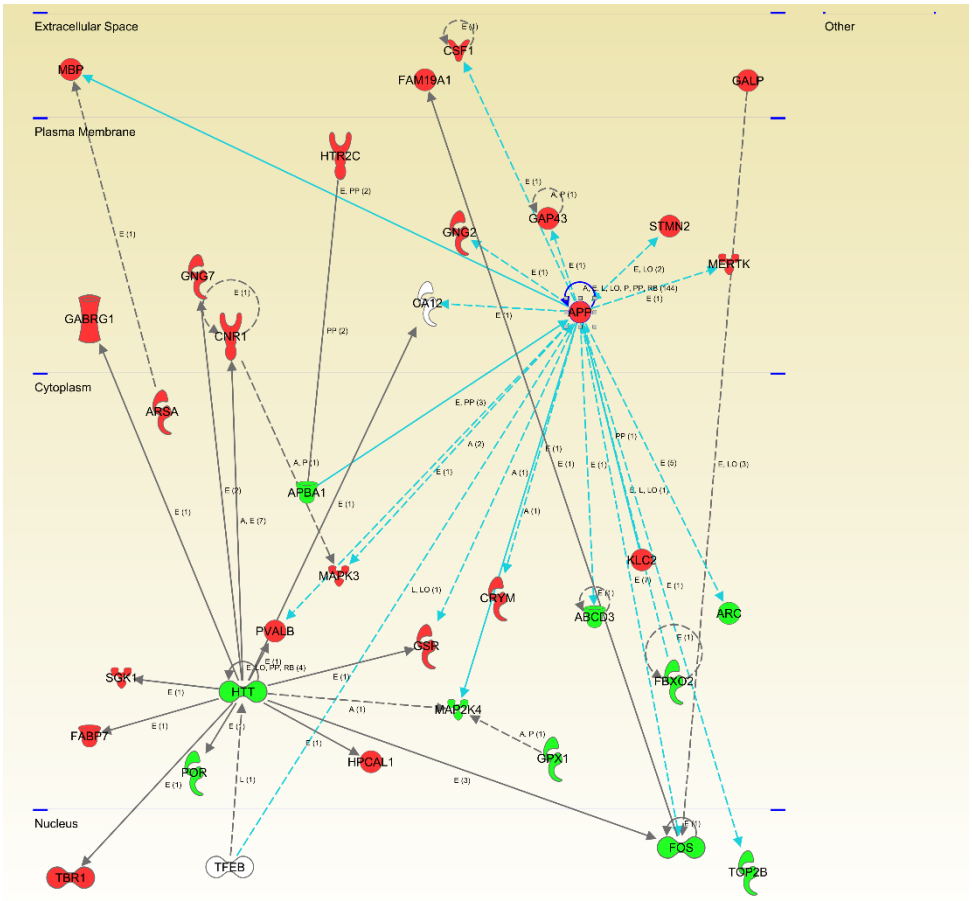

Figure 4. Modulation of the APP functional interactome in Tg2576 mice at the level of OB. Adaptation of APP functional network in Tg2576 OBs at 2 months of age (A), and 6 months of age (B). Relationships between differential expressed genes/proteins and APP functional interactors are represented with blue lines. Continuous lines represent direct interactions, while discontinuous lines correspond to indirect functional interactions. Up-regulated molecules in red, and down-regulated molecules in green. (See complete legend at: http://ingenuity.force.com/ipa/articles/Feature_Description/Legend).

Additional integrative networks unveiled an early disruption of EIF2 signaling based on the up-regulation of a subset of ribosomal proteins (Figure 5A), suggesting that olfactory protein synthesis is compromised in 2-month-old Tg2576 mice. Furthermore, a dysregulation of specific subunits corresponding to the mitochondrial complexes I, and VI was evidenced in the OB of 2-month-old Tg2576 mice, suggesting an olfactory mitochondrial impairment (Figure 5B). It is well-known that prohibitin complex (constituted by Phb1 and Phb2) is a mitochondrial inner membrane-bound chaperone that participates in the mitochondrial respiratory complex assembly, modulates mitochondrial dynamics, and exerts beneficial effects on neurons by reducing free radical production (32, 33). Subsequent experiments were performed to monitor the expression of both Phb subunits in the OB from Tg2576 mice. As shown in figure 5C, a significant drop in Phb1 levels was evidenced in 2-month-old Tg2576 OBs, increasing its levels at 6 months of age respect to WT littermates. Interestingly, similar trend was also observed for Phb2 protein in Tg2576 mice (Figure 5C). OB Phb complex was also independently evaluated in WT and Tg2576 mice during aging. Respect to data obtained at 2 months of age, Phb1 and Phb2 protein levels are decreased at 6 and 18 months in WT animals, maintaining constant levels in Tg2576 mice during the aging process (Figure 5C). These data indicate that Phb complex is an early target of human mutated APP, suggesting that the stable maintenance of Phb levels may help to counteract the oxidative stress present in olfactory neurons during AD progression in Tg2576 mice.

A

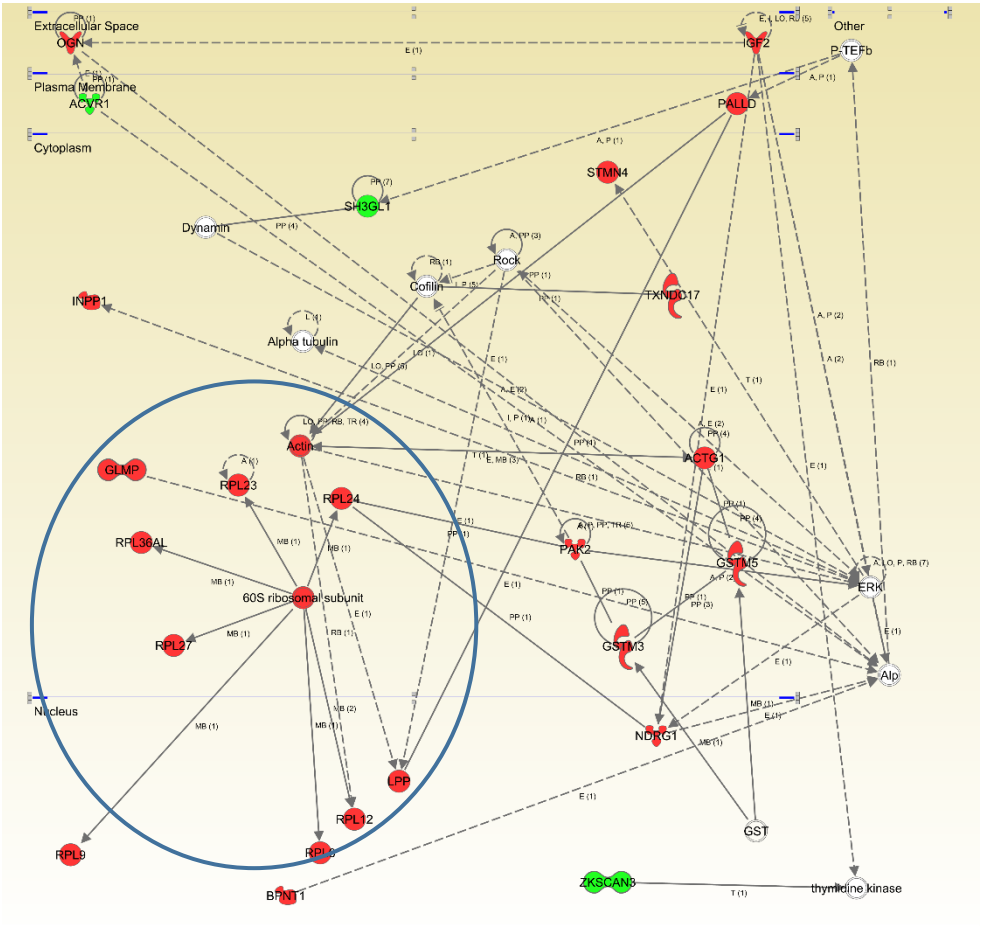

B

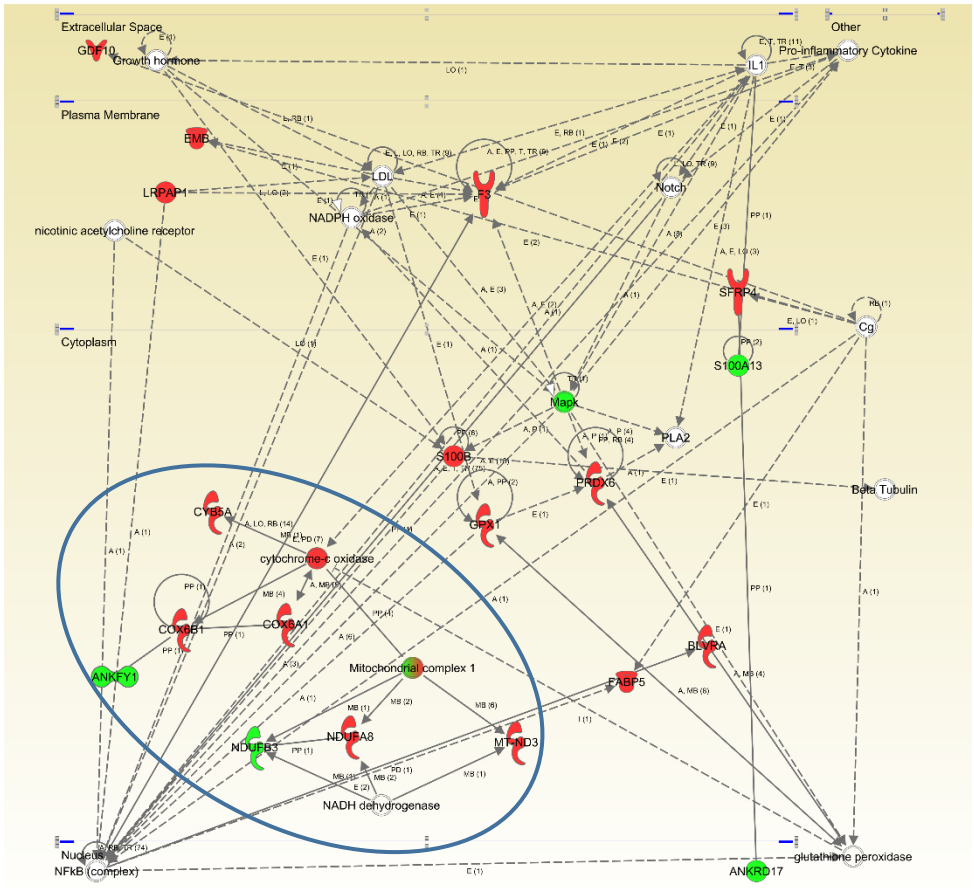

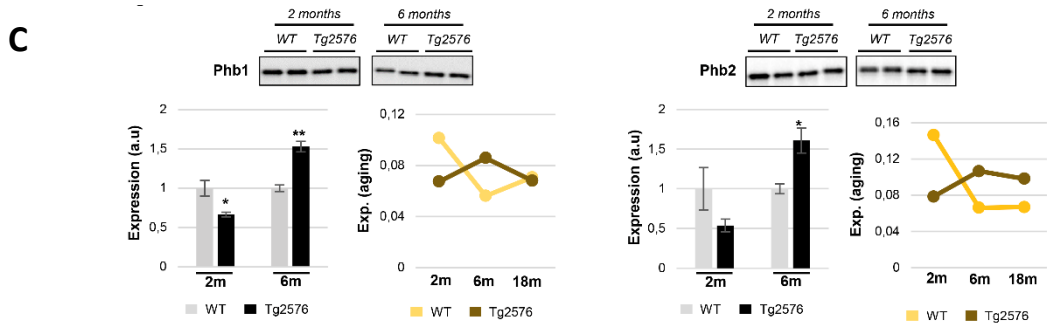

Figure 5. Protein synthesis, and mitochondrial homeostasis are early compromised in Tg2576 at olfactory level. A) Molecular network representing the up-regulation of ribosomal proteins (blue circles) in the OB of 2-month-old Tg2576. B) molecular network highlighting the dysregulation of specific components of the mitochondrial respiratory chain (Complex I, and Complex VI subunits) in the OB of 2-month-old Tg2576. C) Time-dependent disruption of the olfactory Phb1-Phb2 complex in Tg2576 mice. Phb expression was monitored by Western-blotting. Equal loading of the gels was assessed by stain-free digitalization. Panels show histograms of band densities. Data are presented as mean ± SEM from 3 independent OB samples per group (*P < 0.05 vs control group; **P < 0.01 vs control group). Right graphs represent the expression of both Phb subunits during the aging process in WT and Tg2576 mice (2, 6, and 18-month-old).

3.3 Human mutated APP modifies the olfactory signaling routes in a stage-dependent manner

The molecular network analysis also pointed out functional links between APP and a cluster of survival kinases such as ERK, p38 MAPK, and Akt (Figure 6A). Subsequent experiments were performed to analyze the activation state of MAPKs, Akt, and p38 MAPK at pre-plaque stages in the OB of Tg2576 mice. A downstream inactivation in the MAPK pathway at the level of ERK was specifically observed in 2-month-old Tg2576 mice (Figure 6C), being the activation state of upstream MEK unaffected (Figure 6B). Moreover, olfactory Akt was specifically activated in 6-month-old transgenic mice (Figure 6D). In addition, Western-blot analysis revealed an increase in the activation status of OB p38 MAPK in 2-month-old transgenic mice (Figure 6E). This early activation was accompanied by a paralleled increment in the phosphorylation status of ATF2

(Figure 6E), a well-known downstream substrate of p38 MAPK (34). To complement our signaling mapping, other stress-responsive kinases were checked. The signal transduction of the SEK1-SAPK/JNK axis was specifically activated in 6-month-old Tg2576 OBs (Figure 7A-B) while no appreciable changes were detected in the activation status of PKA (Figure 7C) and other survival kinases such as FAK, and PDK1/PKC axis respect to WT animals (Supplementary figure 1).To deepen our understanding of the APP-dependent regulatory effects on kinase dynamics during the aging process in the OB of Tg2576 mice, steady-state levels and phosphorylated isoforms were independently evaluated in WT and Tg2576 mice during aging. For that, protein profiles were quantified in a time-dependent manner at 2-, 6-, and 18-months old (Figure 8). With respect to data obtained at 2 months of age, the activation of downstream ERK, and PDK1/PKC axis were constant in Tg2576 OBs, whereas a drop in the activation status of OB p38 MAPK was observed in 18-month-old Tg2576 mice, when AD pathology is well stablished. No changes were observed in the activation state of olfactory SEK1/MKK4 during the aging process in Tg2576 mice, in contrast with the inactivation observed in 6-, and 18-month-old WT animals (Figure 8). Conversely, a progressive inactivation was detected in its kinase downstream cascade as evidenced by SAPK/JNK dephosphorylation in Tg2576 mice (6-, and 18-month old). In addition, a significant variation was also observed in OB PKA levels in 6-month-old Tg2576.

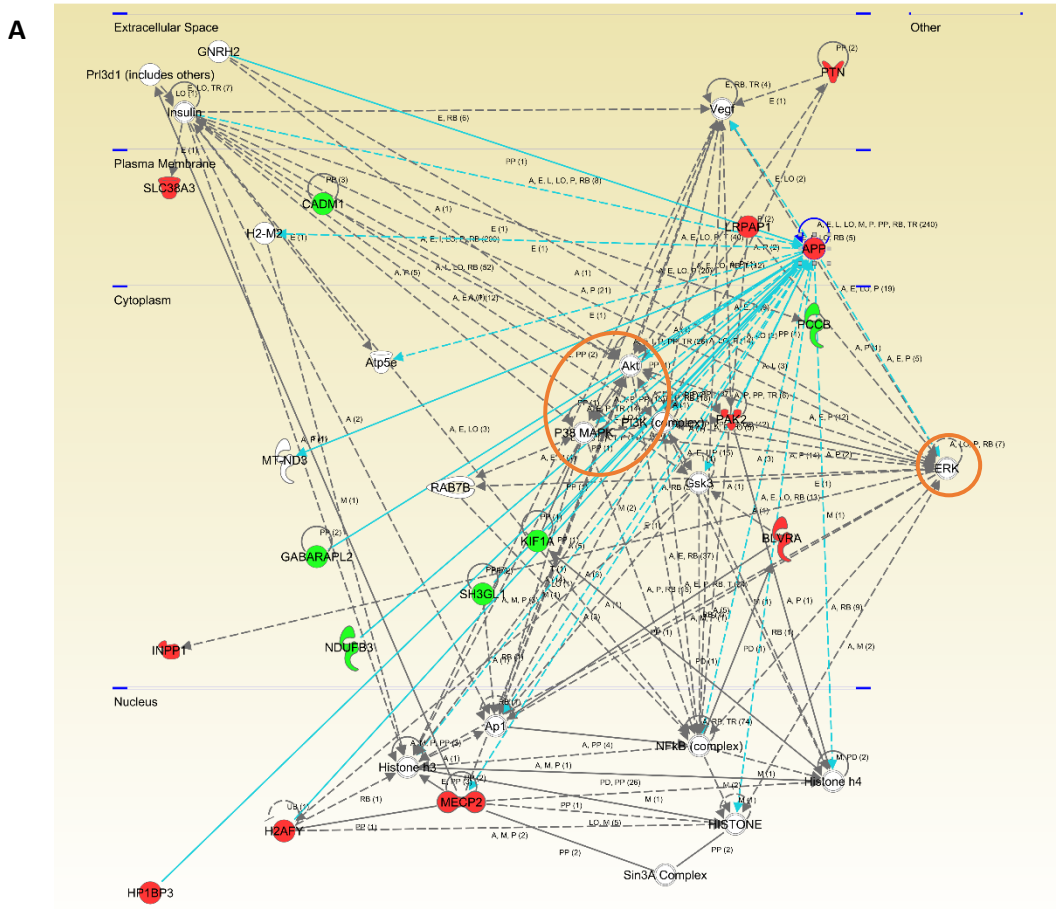

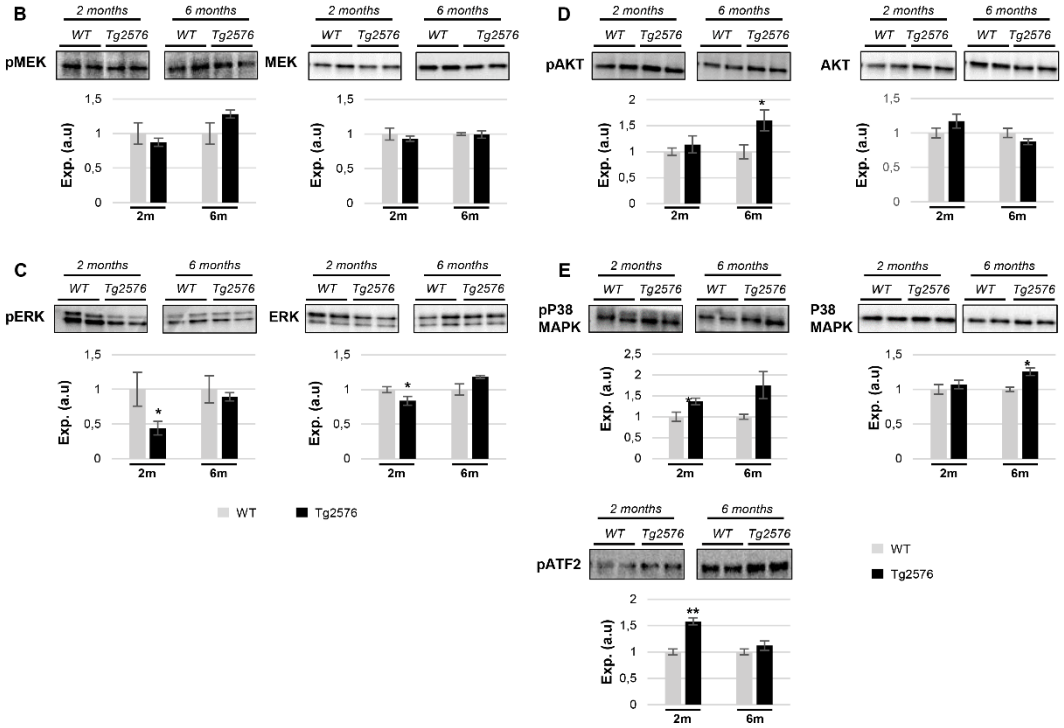

Figure 6. APP overproduction affects the activation state of olfactory ERK1/2, Akt, and p38 MAPK at early AD stages in Tg2576 mice. A) Visualization of predictive interactions between APP and survival kinases (orange circles) based on differential datasets derived from 2-month-old Tg2576 mice. Levels and residue-specific phosphorylation of MEK1/2 (B), ERK1/2 (C), Akt (D), and p38 MAPK-ATF2 axis (E). Equal loading of the gels was assessed by stain-free digitalization. Panels show histograms of band densities. Data are presented as mean ± SEM from 3 independent OB samples per group. *P < 0.05 vs control group; **P < 0.01 vs control group.

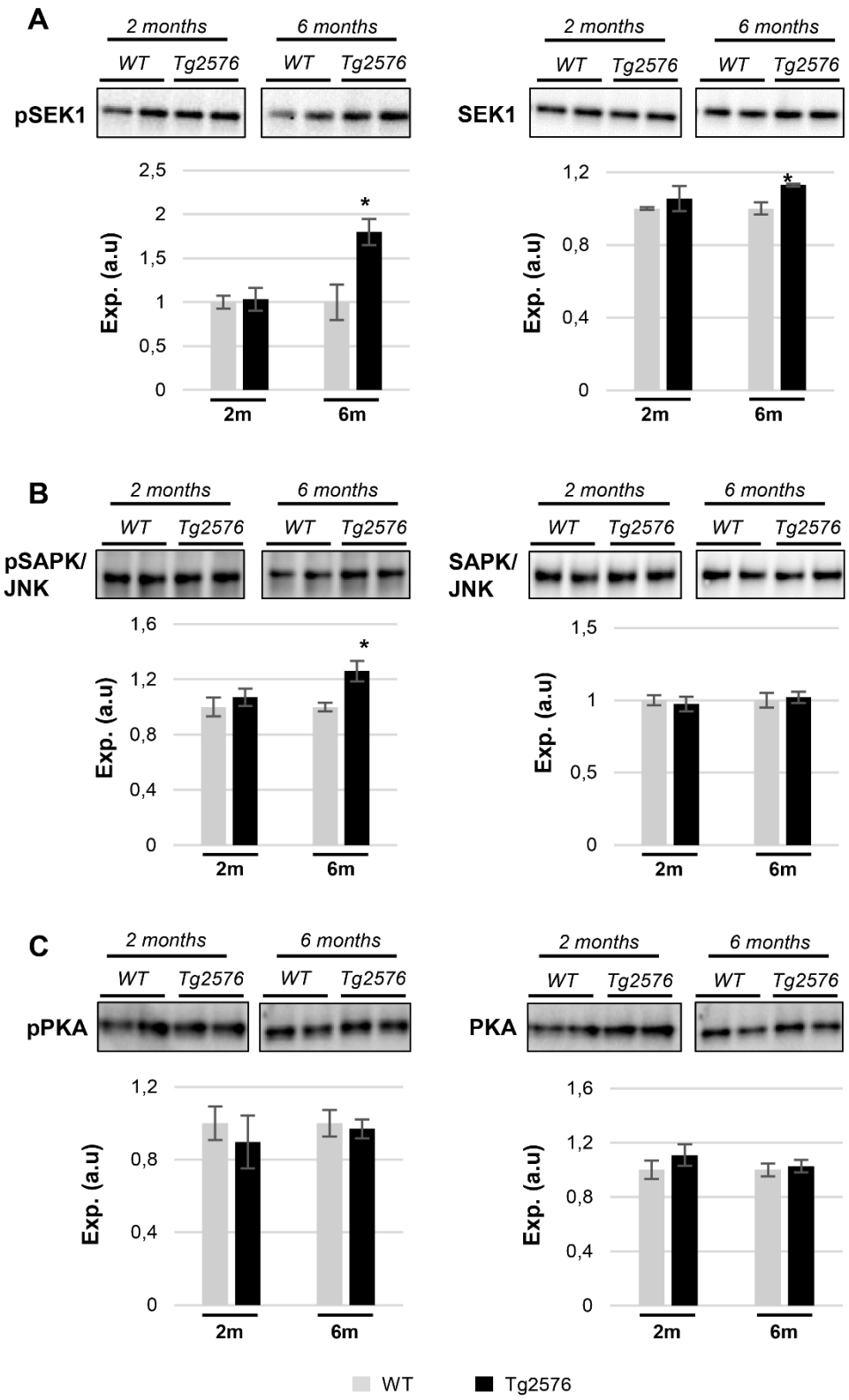

Figure 7. APP overproduction specifically modulates the activation of the SEK1/MKK4-SAPK/JNK axis in 6-month-old Tg2576 mice. Time-dependent expression of total and

phosphorylated levels of SEK1 (A), SAPK/JNK (B), and PKA (C). Equal loading of the gels was assessed by stain-free digitalization. Panels show histograms of band densities. Data are presented as mean ± SEM from 3 independent OB samples per group. *P < 0.05 vs control group.

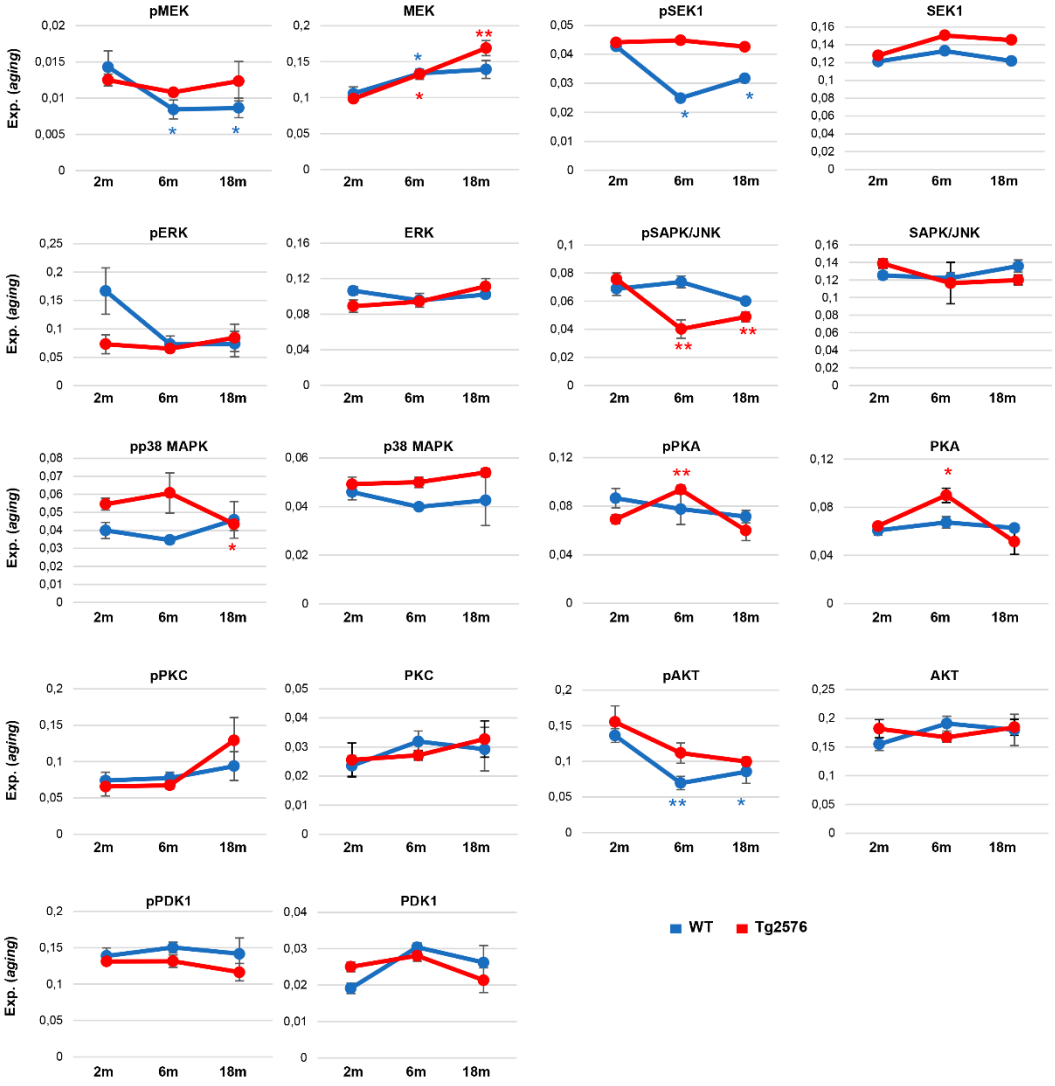

Figure 8. Monitorization of survival kinases during the aging process in WT and Tg2576 OBs. Western-blotting were performed for the kinase panel (total and phosphorylated levels) in the OB from WT and Tg2576 mice of 2, 6, and 18 months of age. Quantitation data were referred to the observed levels in 2-month-old mice for each condition. *P < 0.05 vs 2-month-old mice; **P < 0.01 vs 2-month-old mice.

3.4 Olfactory SEK1/MKK4 and PKA signaling are de-regulated across human AD grading

Much effort has been spent on studying the role of β-amyloid in sporadic Alzheimer's disease (sAD) pathogenesis but the available information is insufficient to fully understand the disease progression at the level of olfactory signaling (19). To investigate whether SEK1/MKK4 and PKA signaling pathways perturbed in the OB of Tg2576 mice were also associated with human sAD, the activation state of the corresponding survival pathways was measured by Western blotting in OBs from sAD subjects with different neuropathological grading (Table 1). First, we performed immunohistochemical analysis to localize SEK1/MKK4 and PKA in human OB. As shown in Figure 9A-B, positive staining for the activated form of SEK1 was observed in the OB astrocytes and neurons. However, a specific mild staining for non-phosphorylated SEK1 was observed in neurons (Figure 9C-D). Respect to activated form of PKA, a diffuse staining of neuropil and all OB cellular components was observed (Figure 9E-F), even in glial cells from granular layer (Figure 9F), while a mild staining in neuropil was observed for the non-phosphorylated PKA (Figure 9G-H). As shown in figure 10, the activation of SEK1 was specifically increased in advanced AD stages (Braak V-VI) (Figure 10A). However, PKA activity was significantly increased in initial (Braak I-II) AD stage respect to subjects with normal neuropathological examination (Figure 10B). In intermediate AD stage (Braak III-IV), a significant increment was also observed in total and activated PKA levels (Figure 10B).

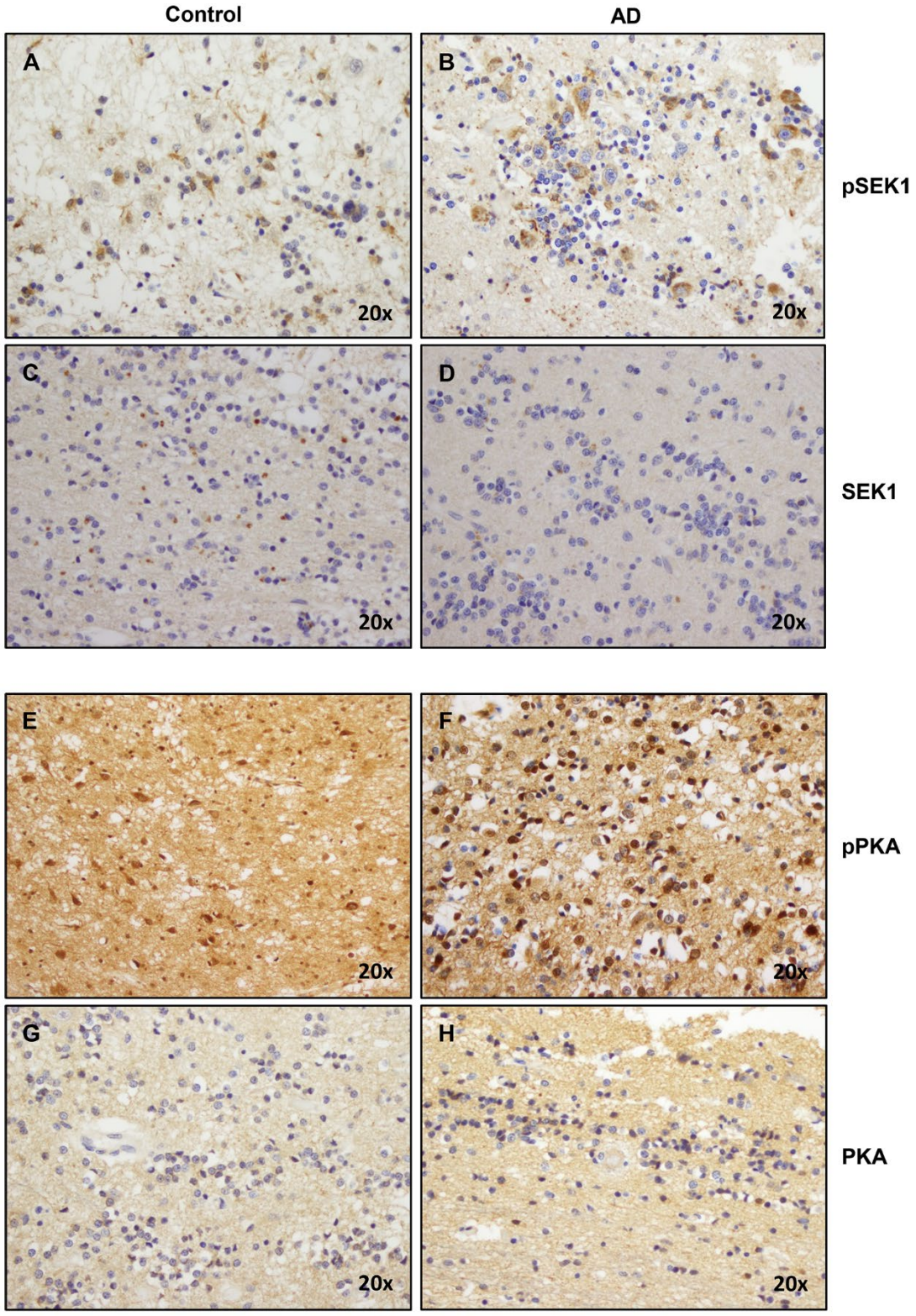

Figure 9. Immunohistochemical localization of OB SEK1 and PKA (phosphorylated and non-phosphorylated forms). Representative immunohistochemical staining pattern of pSEK1 (A,B), SEK1 (C, D), pPKA (E, F) and PKA (G, H) in control and AD cases.

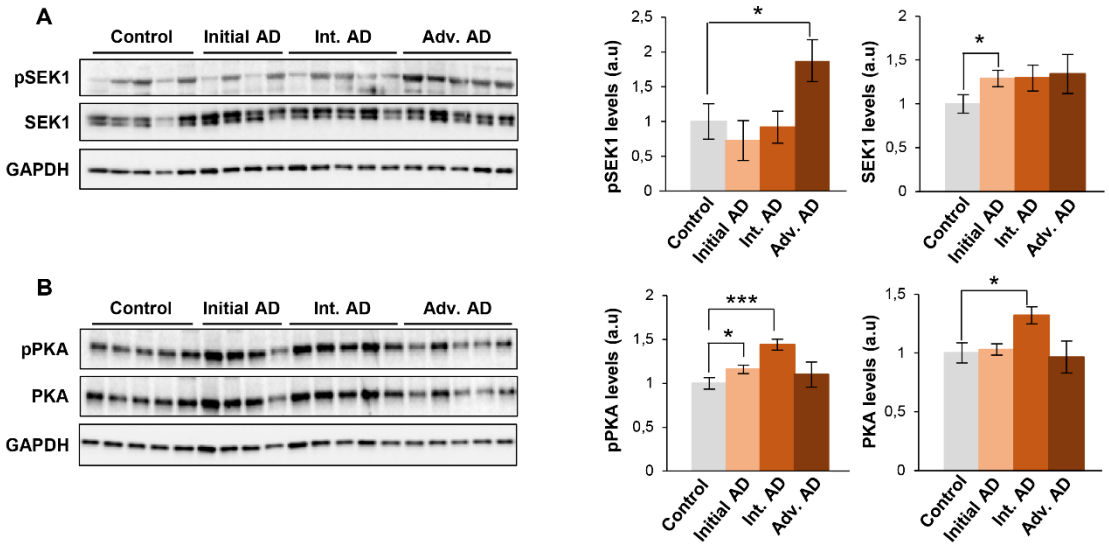

Figure 10. Olfactory SEK1/MKK4 and PKA are differentially activated across Braak stages in human AD. Levels and residue-specific phosphorylation of SEK1/MKK4 (A), and PKA (B) in the OB across AD phenotypes. Equal loading of the gels was assessed by Ponceau staining and hybridization with a GAPDH specific antibody. Right panels show histograms of band densities. Data are presented as mean ± SEM from 5 independent OB samples per group. *P < 0.05 vs control group; ***P < 0.001 vs control group. Representative Western blot gels are shown.

4. Discussion

We consider that a better understanding of the molecular events affected by the progressive accumulation of amyloid pathology might offer new olfactory targets for earlier diagnosis and therapeutic intervention. In particular, we report that: i) multiple OB proteotranscriptomic variations appear at pre-plaque stages in Tg2576 mice, ii) the functional interactome of the hAPPSw isoform at olfactory level is progressively modulated in these mice, iii) the mitochondrial PHB complex was compromised at early stages in Tg2576 OBs, iv) specific olfactory signaling routes (Akt, p38 MAPK, SEK1/MKK4, and SAPK/JNK) were modulated in a time-dependent manner respect to WT animals, v) APP overproduction induced specific regulatory effects on kinase dynamics (SEK1/SAPK, PKA) during the aging process in Tg2576 mice, and vi) the SEK1/MKK4, and PKA pathways were differentially activated during human AD grading at the level of the OB. All these findings at the very early pre-plaque stage provided mechanistic clues on the olfactory mechanisms involved in progression of cognitive deficits previously reported in these mice (24).

To systematically assess the global effect of olfactory APP production on gene expression at the transcript and protein level, we used a combinatorial omics analysis. The minimal overlap observed in transcriptome and proteome remodelings between 2-, and 6-month-old Tg2576 mice, supports the hypothesis that distinctive pathophysiological processes are involved in the OB during the initial progression of AD-like amyloid pathology. For example, functional clustering suggested that changes in the growth of neurites (in 2-month-old transgenic mice), and microtubule dynamics in the OB (in 6-month-old Tg2576 mice) occur in the absence of neuropathological amyloid plaques, supporting the notion that cytoskeletal remodeling is an early AD pathological hallmark (35). Despite the experimental and technical noise in both mRNA and protein measurements may contribute to an underestimation of true correlations, RNA-protein correlation was missing in our study. Buffering of mRNA variation against protein levels

can occur at multiple levels, including intra- and inter-individual genomic variation (36, 37). The discrepancy we observed may be due to: i) the use of different set of animals for each technological platform, ii) the spatial and temporal delayed synthesis between mRNA and protein (36), iii) post-transcriptional events, and iv) the different hydrophobicity and solubility of specific proteome subsets (e.g: olfactory receptors) that hampers their characterization and quantitation by mass-spectrometry.

Prohibitin deficiencies have been previously associated with neurodegenerative phenotypes (38, 39). During aging, our data indicated that Phb levels are stable while mutated APP is overproduced, probably to counteract the disease-aggravating oxidative stress during AD progression in Tg2576 mice. Generally, repression/induction of Phb1 is paralleled by a concomitant decrease/increase of its assembly partner Phb2 (38, 40). Accordingly, OB Phb subunits are functionally interdependent in Tg2576 mice. In contrast, Phb subunits are not interdependent in the OB during AD neurodegeneration in humans (19), indicating that the tangled regulatory mechanisms that govern the mitochondrial homeostasis in olfactory cells significantly differ between transgenic mice and sporadic human AD. Aberrant regulation of a subset of kinases may represent the triggering events leading to the spread of a perturbed signaling in AD (41). p38 MAPK is a multifunctional kinase that is activated by Aβ in cultured neurons (42), phosphorylates Tau protein (43, 44), and mediates the Aβ-induced inflammatory activation (45). Different alterations of p38 MAPK pathway have been observed in the OB, hippocampus, and cortical areas at early stages in human AD (19, 41, 46, 47). In Tg2576 mice, we observed an early activation of p38 MAPK (validated by paralleled increase in ATF2 phosphorylation levels), suggesting detrimental effects such as neuroinflammation, and excitotoxicity at the level of the OB (48). Despite Akt has been recently proposed as a therapeutic target for AD-associated memory impairments (49), different results have been obtained about the Akt activation across brain structures of human AD (18, 50, 51). The specific activation of olfactory Akt observed in 6-month-old Tg2576 mice indicates potential protective mechanisms

against memory impairments and synaptic deficits (49). In an effort to delineate the oxidative stress signalling events in the OB of Tg2576 mice, we observed an increment in the activation of SAPK/JNK pathway in 6-month-old Tg2576 OBs. This activation precedes the beta-amyloid deposition, although beta-amyloid may enhance its activation a later time (52). In human brain, phospho-JNK/SAPK is significantly increased in AD over control cases, overlapping with Tau-positive neurofibrillary pathology (44, 53). In this study, we have detected an increment in the expression of phosphorylated SEK1/MKK4 (an upstream activator of the SAPK/JNK route) exclusively in subjects with advanced AD stage (Braak V-VI). Previous reports suggest that this activation may play a role in the tau phosphorylation and consequently the formation of NFTs in late AD stages (52). PKA is a tau-kinase which expression/activity tends to be reduced in different contexts of AD pathology (54). In humans, a decrease in PKA activity was observed in temporal cortex from AD subjects with a Braak stage V-VI (55). However, we report a PKA overactivation that occurs in the OB derived from AD subjects with initial stages (Braak I-II), indicating that cAMP signalling appears to be stage-, and brain region specific.

Although our study has uncovered many intricacies in OB molecular homeostasis during early stages of AD-related amyloidogenic pathology, there are potential limitations of our study that warrant discussion. First, due to technological issues, we failed to accurately quantify many proteins expressed at low levels that might also participate in the olfactory AD progression in Tg2576 mice. Second, our results are limited by transcript/protein abundance averaging among the multiple cell layers present in the OB, hampering the exploration of olfactory cell-type specific molecular alterations. Third, Aβ, APP, and its derived species may co-exist inside neurons (56), and based on our experimental workflow, we cannot pinpoint which APP-derived species are responsible of the observed molecular disturbances.

5. Conclusion

Our dual-omic approach revealed the disruption of multiple molecular pathways at early stages of the OB amyloid pathology, leading to the identification of differential olfactory targets linked to APP metabolism. These findings point out the potential utility of alternative olfactory pathways for disease modification, in a stage-dependent manner, through intranasal therapies (57) based on enzyme replacement or specific drug delivery (58, 59).

References

1.Attems J, Walker L, Jellinger KA. Olfactory bulb involvement in neurodegenerative diseases. Acta Neuropathol. 2014 Apr;127(4):459-75.

2.Daulatzai MA. Olfactory dysfunction: its early temporal relationship and neural correlates in the pathogenesis of Alzheimer's disease. J Neural Transm (Vienna). Oct;122(10):1475-97.

3.Rey NL, Wesson DW, Brundin P. The olfactory bulb as the entry site for prion-like propagation in neurodegenerative diseases. Neurobiol Dis. Jan;109(Pt B):226-48.

4.Sasaguri H, Nilsson P, Hashimoto S, Nagata K, Saito T, De Strooper B, et al. APP mouse models for Alzheimer's disease preclinical studies. EMBO J. Sep 1;36(17):2473-87.

5.Hsiao K, Chapman P, Nilsen S, Eckman C, Harigaya Y, Younkin S, et al. Correlative memory deficits, Abeta elevation, and amyloid plaques in transgenic mice. Science. 1996 Oct 04;274(5284):99-102.

6.Puzzo D, Gulisano W, Palmeri A, Arancio O. Rodent models for Alzheimer's disease drug discovery. Expert Opin Drug Discov. 2015 Jul;10(7):703-11.

7.Westerman MA, Cooper-Blacketer D, Mariash A, Kotilinek L, Kawarabayashi T, Younkin LH, et al. The relationship between Abeta and memory in the Tg2576 mouse model of Alzheimer's disease. J Neurosci. 2002 Mar 01;22(5):1858-67.

8.Janus C, Pearson J, McLaurin J, Mathews PM, Jiang Y, Schmidt SD, et al. A beta peptide immunization reduces behavioural impairment and plaques in a model of Alzheimer's disease. Nature. 2000 Dec 21-28;408(6815):979-82.

9.Chen G, Chen KS, Knox J, Inglis J, Bernard A, Martin SJ, et al. A learning deficit related to age and beta-amyloid plaques in a mouse model of Alzheimer's disease. Nature. 2000 Dec 21-28;408(6815):975-9.

10.Jacobsen JS, Wu CC, Redwine JM, Comery TA, Arias R, Bowlby M, et al. Early-onset behavioral and synaptic deficits in a mouse model of Alzheimer's disease. Proc Natl Acad Sci U S A. 2006 Mar 28;103(13):5161-6.

11.Reddy PH, McWeeney S, Park BS, Manczak M, Gutala RV, Partovi D, et al. Gene expression profiles of transcripts in amyloid precursor protein transgenic mice: up-regulation of mitochondrial metabolism and apoptotic genes is an early cellular change in Alzheimer's disease. Hum Mol Genet. 2004 Jun 15;13(12):1225-40.

12.Lehman EJ, Kulnane LS, Lamb BT. Alterations in beta-amyloid production and deposition in brain regions of two transgenic models. Neurobiol Aging. 2003 Sep;24(5):645-53.

13.Guerin D, Sacquet J, Mandairon N, Jourdan F, Didier A. Early locus coeruleus degeneration and olfactory dysfunctions in Tg2576 mice. Neurobiol Aging. 2009 Feb;30(2):272-83.

14.Young JW, Sharkey J, Finlayson K. Progressive impairment in olfactory working memory in a mouse model of Mild Cognitive Impairment. Neurobiol Aging. 2009 Sep;30(9):1430-43.

15.Wesson DW, Levy E, Nixon RA, Wilson DA. Olfactory dysfunction correlates with amyloid-beta burden in an Alzheimer's disease mouse model. J Neurosci. 2010 Jan 13;30(2):505-14.

16.Wesson DW, Borkowski AH, Landreth GE, Nixon RA, Levy E, Wilson DA. Sensory network dysfunction, behavioral impairments, and their reversibility in an Alzheimer's beta-amyloidosis mouse model. J Neurosci. 2011 Nov 02;31(44):15962-71.

17.Zelaya MV, Perez-Valderrama E, de Morentin XM, Tunon T, Ferrer I, Luquin MR, et al. Olfactory bulb proteome dynamics during the progression of sporadic Alzheimer's disease: identification of common and distinct olfactory targets across Alzheimer-related co-pathologies. Oncotarget. 2015 Nov 24;6(37):39437-56.

18.Lachen-Montes M, Gonzalez-Morales A, de Morentin XM, Perez-Valderrama E, Ausin K, Zelaya MV, et al. An early dysregulation of FAK and MEK/ERK signaling pathways precedes the beta-amyloid deposition in the olfactory bulb of APP/PS1 mouse model of Alzheimer's disease. J Proteomics. 2016 Oct 4;148:149-58.

19.Lachen-Montes M, Gonzalez-Morales A, Zelaya MV, Perez-Valderrama E, Ausin K, Ferrer I, et al. Olfactory bulb neuroproteomics reveals a chronological perturbation of survival routes and a disruption of prohibitin complex during Alzheimer's disease progression. Sci Rep. 2017 Aug 22;7(1):9115.

20.Lachen-Montes M, Zelaya M, Segura V, Fernández-Irigoyen J, Santamaría E. Progressive modulation of the human olfactory bulb transcriptome during Alzheimer´s disease evolution: novel insights into the olfactory signaling across proteinopathies. Oncotarget. 2017.

21.Palomino-Alonso M, Lachen-Montes M, Gonzalez-Morales A, Ausin K, Perez-Mediavilla A, Fernandez-Irigoyen J, et al. Network-Driven Proteogenomics Unveils an Aging-Related Imbalance in the Olfactory IkappaBalpha-NFkappaB p65 Complex Functionality in Tg2576 Alzheimer's Disease Mouse Model. Int J Mol Sci. Oct 27;18(11).

22.Braak H, Alafuzoff I, Arzberger T, Kretzschmar H, Del Tredici K. Staging of Alzheimer disease-associated neurofibrillary pathology using paraffin sections and immunocytochemistry. Acta Neuropathol. 2006 Oct;112(4):389-404.

23.Alafuzoff I, Arzberger T, Al-Sarraj S, Bodi I, Bogdanovic N, Braak H, et al. Staging of neurofibrillary pathology in Alzheimer's disease: a study of the BrainNet Europe Consortium. Brain Pathol. 2008 Oct;18(4):484-96.

24.Cuadrado-Tejedor M, Garcia-Osta A. Current animal models of Alzheimer's disease: challenges in translational research. Front Neurol.5:182.

25.Tyanova S, Temu T, Cox J. The MaxQuant computational platform for mass spectrometry-based shotgun proteomics. Nat Protoc. 2016 Dec;11(12):2301-19.

26.Tyanova S, Temu T, Sinitcyn P, Carlson A, Hein MY, Geiger T, et al. The Perseus computational platform for comprehensive analysis of (prote)omics data. Nat Methods. 2016 Sep;13(9):731-40.

27.Vizcaino JA, Deutsch EW, Wang R, Csordas A, Reisinger F, Rios D, et al. ProteomeXchange provides globally coordinated proteomics data submission and dissemination. Nat Biotechnol. 2014 Mar;32(3):223-6.

28.Irizarry RA, Bolstad BM, Collin F, Cope LM, Hobbs B, Speed TP. Summaries of Affymetrix GeneChip probe level data. Nucleic Acids Res. 2003 Feb 15;31(4):e15.

29.Silva AR, Grinberg LT, Farfel JM, Diniz BS, Lima LA, Silva PJ, et al. Transcriptional alterations related to neuropathology and clinical manifestation of Alzheimer's disease. PLoS One. 2012;7(11):e48751.

30.Cuadrado-Tejedor M, Garcia-Barroso C, Sanchez-Arias JA, Rabal O, Perez-Gonzalez M, Mederos S, et al. A First-in-Class Small-Molecule that Acts as a Dual Inhibitor of HDAC and PDE5 and that Rescues Hippocampal Synaptic Impairment in Alzheimer's Disease Mice. Neuropsychopharmacology. 2016 Jan;42(2):524-39.

31.Sanchez-Ortiz E, Hahm BK, Armstrong DL, Rossie S. Protein phosphatase 5 protects neurons against amyloid-beta toxicity. J Neurochem. 2009 Oct;111(2):391-402.

32.Zhou P, Qian L, D'Aurelio M, Cho S, Wang G, Manfredi G, et al. Prohibitin reduces mitochondrial free radical production and protects brain cells from different injury modalities. J Neurosci. Jan 11;32(2):583-92.

33.Artal-Sanz M, Tavernarakis N. Prohibitin and mitochondrial biology. Trends Endocrinol Metab. 2009 Oct;20(8):394-401.

34.Puig B, Vinals F, Ferrer I. Active stress kinase p38 enhances and perpetuates abnormal tau phosphorylation and deposition in Pick's disease. Acta Neuropathol. 2004 Mar;107(3):185-9.

35.Do Carmo S, Crynen G, Paradis T, Reed J, Iulita MF, Ducatenzeiler A, et al. Hippocampal Proteomic Analysis Reveals Distinct Pathway Deregulation Profiles at Early and Late Stages in a Rat Model of Alzheimer's-Like Amyloid Pathology. Mol Neurobiol. Apr;55(4):3451-76.

36.Liu Y, Beyer A, Aebersold R. On the Dependency of Cellular Protein Levels on mRNA Abundance. Cell. 2016 Apr 21;165(3):535-50.

37.Battle A, Khan Z, Wang SH, Mitrano A, Ford MJ, Pritchard JK, et al. Genomic variation. Impact of regulatory variation from RNA to protein. Science. Feb 6;347(6222):664-7.

38.Merkwirth C, Martinelli P, Korwitz A, Morbin M, Bronneke HS, Jordan SD, et al. Loss of prohibitin membrane scaffolds impairs mitochondrial architecture and leads to tau hyperphosphorylation and neurodegeneration. PLoS Genet. 2012;8(11):e1003021.

39.Dutta D, Ali N, Banerjee E, Singh R, Naskar A, Paidi RK, et al. Low Levels of Prohibitin in Substantia Nigra Makes Dopaminergic Neurons Vulnerable in Parkinson's Disease. Mol Neurobiol. Jan;55(1):804-21.

40.Sanchez-Quiles V, Santamaria E, Segura V, Sesma L, Prieto J, Corrales FJ. Prohibitin deficiency blocks proliferation and induces apoptosis in human hepatoma cells: molecular mechanisms and functional implications. Proteomics. 2010 Apr;10(8):1609-20.

41.Perluigi M, Barone E, Di Domenico F, Butterfield DA. Aberrant protein phosphorylation in Alzheimer disease brain disturbs pro-survival and cell death pathways. Biochim Biophys Acta. Oct;1862(10):1871-82.

42.Criscuolo C, Fabiani C, Bonadonna C, Origlia N, Domenici L. BDNF prevents amyloid-dependent impairment of LTP in the entorhinal cortex by attenuating p38 MAPK phosphorylation. Neurobiol Aging. 2015 Mar;36(3):1303-9.

43.Li Y, Liu L, Barger SW, Griffin WS. Interleukin-1 mediates pathological effects of microglia on tau phosphorylation and on synaptophysin synthesis in cortical neurons through a p38-MAPK pathway. J Neurosci. 2003 Mar 1;23(5):1605-11.

44.Ferrer I, Gomez-Isla T, Puig B, Freixes M, Ribe E, Dalfo E, et al. Current advances on different kinases involved in tau phosphorylation, and implications in Alzheimer's disease and tauopathies. Curr Alzheimer Res. 2005 Jan;2(1):3-18.

45.Bachstetter AD, Xing B, de Almeida L, Dimayuga ER, Watterson DM, Van Eldik LJ. Microglial p38alpha MAPK is a key regulator of proinflammatory cytokine up-regulation induced by toll-like receptor (TLR) ligands or beta-amyloid (Abeta). J Neuroinflammation. 2011 Jul 06;8:79.

46.Sun A, Liu M, Nguyen XV, Bing G. P38 MAP kinase is activated at early stages in Alzheimer's disease brain. Exp Neurol. 2003 Oct;183(2):394-405.

47.Hensley K, Floyd RA, Zheng NY, Nael R, Robinson KA, Nguyen X, et al. p38 kinase is activated in the Alzheimer's disease brain. J Neurochem. 1999 May;72(5):2053-8.

48.Munoz L, Ammit AJ. Targeting p38 MAPK pathway for the treatment of Alzheimer's disease. Neuropharmacology. 2010 Mar;58(3):561-8.

49.Yi JH, Baek SJ, Heo S, Park HJ, Kwon H, Lee S, et al. Direct pharmacological Akt activation rescues Alzheimer's disease like memory impairments and aberrant synaptic plasticity. Neuropharmacology. Jan;128:282-92.

50.Griffin RJ, Moloney A, Kelliher M, Johnston JA, Ravid R, Dockery P, et al. Activation of Akt/PKB, increased phosphorylation of Akt substrates and loss and altered distribution of Akt and PTEN are features of Alzheimer's disease pathology. J Neurochem. 2005 Apr;93(1):105-17.

51.Rickle A, Bogdanovic N, Volkman I, Winblad B, Ravid R, Cowburn RF. Akt activity in Alzheimer's disease and other neurodegenerative disorders. Neuroreport. 2004 Apr 29;15(6):955-9.

52.Petersen RB, Nunomura A, Lee HG, Casadesus G, Perry G, Smith MA, et al. Signal transduction cascades associated with oxidative stress in Alzheimer's disease. J Alzheimers Dis. 2007 May;11(2):143-52.

53.Zhu X, Raina AK, Rottkamp CA, Aliev G, Perry G, Boux H, et al. Activation and redistribution of c-jun N-terminal kinase/stress activated protein kinase in degenerating neurons in Alzheimer's disease. J Neurochem. 2001 Jan;76(2):435-41.

54.Kelly MP. Cyclic nucleotide signaling changes associated with normal aging and age-related diseases of the brain. Cell Signal. Jan;42:281-91.

55.Liang Z, Liu F, Grundke-Iqbal I, Iqbal K, Gong CX. Down-regulation of cAMP-dependent protein kinase by over-activated calpain in Alzheimer disease brain. J Neurochem. 2007 Dec;103(6):2462-70.

56.Iulita MF, Allard S, Richter L, Munter LM, Ducatenzeiler A, Weise C, et al. Intracellular Abeta pathology and early cognitive impairments in a transgenic rat overexpressing human amyloid precursor protein: a multidimensional study. Acta Neuropathol Commun. Jun 5;2:61.

57.Crowe TP, Greenlee MHW, Kanthasamy AG, Hsu WH. Mechanism of intranasal drug delivery directly to the brain. Life Sci. Feb 15;195:44-52.

58.Cheng YS, Chen ZT, Liao TY, Lin C, Shen HC, Wang YH, et al. An intranasally delivered peptide drug ameliorates cognitive decline in Alzheimer transgenic mice. EMBO Mol Med. May;9(5):703-15.

59.Agrawal M, Saraf S, Antimisiaris SG, Chougule MB, Shoyele SA, Alexander A. Nose-to-brain drug delivery: An update on clinical challenges and progress towards approval of anti-Alzheimer drugs. J Control Release. Jul 10;281:139-77.

CHAPTER 7

The olfactory bulb proteotype differs across frontotemporal dementia spectrum: Focus on Progressive supranuclear palsy and Frontotemporal lobar degeneration TDP43 proteinopathy

Mercedes Lachén-Montes[1,2,3], Andrea González-Morales[1,2,3], Domitille Schvartz[4], María Victoria Zelaya[1,3,5], Karina Ausin[2,3], Joaquín Fernández-Irigoyen[1,2,3], Jean Charles Sánchez[4], Enrique Santamaría[1,2,3]

[1] *Clinical Neuroproteomics Group, Navarrabiomed, Complejo Hospitalario de Navarra (CHN), Universidad Pública de Navarra (UPNA), Irunlarrea, 3 31008 Pamplona, Spain*

[2] *Proteored-ISCIII. Proteomics Unit, Navarrabiomed, Complejo Hospitalario de Navarra (CHN), Universidad Pública de Navarra (UPNA), Irunlarrea 3, 31008 Pamplona, Spain*

[3] *IdiSNA. Navarra Institute for Health Research, Pamplona, Spain Irunlarrea 3, 31008 Pamplona, Spain, IdiSNA. Irunlarrea, 3 31008 Pamplona, Spain.*

[4] *Translational Biomarker Group, Department of Human Protein Sciences, University of Geneva, Rue Michel Servet 1, 1211 Geneve 4, Switzerland.*

[5] *Pathological Anatomy Department, Complejo Hospitalario de Navarra (CHN), Pamplona, Spain.*

Abstract

A mild olfactory dysfunction has been observed in frontotemporal dementias (FTD). However, the underlying molecular mechanisms associated to this deficit are poorly understood. Here, we applied mass spectrometry-based quantitative proteomics to analyse pathological effects on the olfactory bulb (OB) from progressive supranuclear palsy (PSP) and frontotemporal lobar degeneration TDP43 proteinopathy (FTLD-TDP43) subjects. 1% of the quantified OB proteome showed statistically significant differences in PSP and FTLD-TDP43 respect to elderly controls, revealing: i) a potential mitochondrial and calcium homeostasis impairment in PSP, ii) a disruption of protein synthesis and vesicle trafficking in FTLD-TDP43, and iii) an overproduction of specific cytoskeletal protein subsets in each pathology. Although differential OB proteomes clearly differ between both FTD phenotypes, functional analyses pointed out an imbalance in olfactory survival routes in both pathologies. Interestingly, a common inactivation of olfactory mitogen-activated protein kinases (MAPKs), calcium/calmodulin dependent protein kinase II (CAMKII), and protein kinase C (PKC) signalling pathways was observed in PSP and FTLD subjects. In contrast, a specific shut off in mitogen-activated protein kinase kinase 4 (SEK1/MKK4)/stress-activated protein kinase (SAPK) axis was exclusively observed in PSP, whereas a specific phosphoinositide-dependent protein kinase 1 (PDK1) inactivation was observed in FTLD. In summary, our data contribute to a better understanding of the molecular mechanisms that are modulated in PSP and FTLD-TDP43 at olfactory level, highlighting cross-disease similarities and differences in the regulation of survival pathways across FTD spectrum.

Introduction

Olfactory impairment is a common occurrence during aging, getting particularly aggravated in neurodegenerative disorders [1]. Despite the great attention that has caught in the last decade, this symptom still receives little attention in the clinical diagnosis, and clinicians rarely test this deficit in patients with suspicion of neurological disease. Olfactory dysfunction has been clearly associated with neurodegenerative disorders such as Alzheimer's disease [2,3] and Parkinson's disease [4,5], where the percentage of patients undergoing complete anosmia reaches 80 and 90%, respectively. Interestingly, it has also been demonstrated that patients suffering from other less frequent dementias, such as frontotemporal dementias (FTD), exhibit mild olfactory dysfunction [6-9]. Nevertheless, few studies have been published linking the specific subtypes of frontotemporal dementias and olfactory dysfunction and none of them delve into the molecular mechanisms governing this deficit.

Frontotemporal lobar degeneration (FTLD) is a macroscopic alteration observed in some cortical neurodegenerative disorders, causing a heterogeneous clinical syndrome characterized by progressive changes in behavior, personality or language. This group of disorders affects mainly the frontal and temporal lobes of the brain [10,11] and patients are often diagnosed with FTD. Thanks to immunohistochemistry analysis, it is now possible to classify FTLD in three different disease forms according to the neuropathological protein that accumulates in neurons and glia [12]. The microtubule associated protein, tau, is the main component of the neuronal intracytoplasmic inclusions in 45% of the cases, causing FTLD-TAU [13]. This group includes patients diagnosed with progressive supranuclear palsy (PSP) that, importantly, carry mild hyposmia. In about 50% of the cases, the TAR-DNA-binding protein 43 (TDP43) is present (FTLD-TDP43) [14]. Finally, 5% of the cases accumulate fused in sarcoma (FUS) protein (FTLD-FUS) [15].

Although the role of olfactory abnormalities in FTLD spectrum has not been elucidated, previous research has proved that odor identification is impaired in the frontal variant of FTD [7,16-18].

In addition, Doty (2017) published the results of a wide study in which distinct neurological disorders were ordered in terms of the relative differences obtained in University of Pennsylvania Smell Identification Test (UPSIT) scores [6]. Hence, the results revealed moderate and mild olfactory dysfunction in clinically diagnosed FTD and PSP patients, showing disparities in two clinically similar diseases. However, the relationship between the clinic and the pathophysiological role of neuropathological aggregates in these disorders is still unknown.

The olfactory bulb (OB) is the first brain region responsible for the processing of the olfactory information [1]. In this sense, neuropathological studies have revealed the presence of pathological proteins typically constituting the hallmarks of AD or PD, such as Aβ peptide or α-synuclein [19-21]. In contrast, little attention has been paid to the potential presence of tau and TDP43 in FTLD subjects at the level of OB [22] and few studies correlate this presence with frontotemporal dementias [3]. Thus, being aware of the scarce information regarding the relationship between olfactory deficits and FTLD pathogenesis, and taking into account that recent research is proposing the OB as the entry site for prion-like propagation in neurodegenerative diseases [25], the aim of this study was to perform a depth characterization of the OB proteome that could help to better understand the breakdown occurring in this region during the neurodegenerative process, in particular in two forms of FTD disorders. For that, we have applied a shotgun mass spectrometry approach to quantitate the OB proteome derived from PSP and FTLD-TDP43 subjects, revealing disease-specific changes in the olfactory proteostasis accompanied by an alteration in the survival signaling dynamics at the level of the OB.

Materials and methods

Materials - The following reagents and materials were used: anti-caspase 9 (ref. 9508), anti-cleaved-caspase3 (ref. 9661), anti-Bcl2 (ref. 3498), anti-Bcl-xL (ref. 2764), anti-pAkt (Ser473) (ref. 4060), anti-Akt (ref. 4685), anti-pMEK1/2 (Ser217/221) (ref. 9154), anti-MEK1/2 (ref. 9126), anti-pERK1/2 (Thr202/Tyr204) (ref. 4370), anti-ERK1/2 (ref. 9102), anti-pPKA (Thr197) (ref. 5661), anti-PKA (ref. 4782), anti-pCAMKII (Thr286) (ref. 12716), anti-CAMKII (ref.11945), anti-PARP cleaved (ref. 5625), anti-pSEK1/MKK4 (Ser257/Thr261) (ref. 9156), anti-SEK1/MKK4 (ref. 9152), anti pSAPK/JNK (Thr183/Tyr185) (ref. 9255), anti-pSAPK/JNK (ref. 9252S), anti pMKK3-6 (Thr183/Tyr185) (ref. 9231), anti-MKK3 (ref. 5674), anti-p-P38 MAPK (Thr180/Tyr182) (ref. 4511), anti-p38 MAPK (ref. 9212), anti-pPDK1 (ser241) (ref. 3061), anti-PDK1 (ref. 3062), anti-pPKC-pan (ref. 9379), and anti-TDP-43 (ref. 3449) were purchased from Cell signaling. Anti PKC-pan (ref. SAB4502356), and anti-Tau (ref. T9450) were from Sigma Aldrich. Anti-phospho-Tau (Thr212/Ser214) (ref. AT100) from Thermofisher Scientific). Anti-phospho-TDP43 (S409/S410) (ref. 22309-1-AP) from ProteinTech. Electrophoresis reagents were purchased from Biorad and trypsin from Promega.

Human samples - According to the Spanish Law 14/2007 of Biomedical Research, inform written consent forms of the Neurological Tissue Bank of Navarra Health Service, Brain Bank of IDIBELL, and Neurological Tissue Bank of IDIBAPS-Hospital Clinic (Barcelona, Spain) was obtained for research purposes from relatives of patients included in this study. The study was conducted in accordance with the Declaration of Helsinki and all assessments, post-mortem evaluations, and procedures were previously approved by the Clinical Ethics Committee of Navarra Health Service. For the proteomic phase, 4 FTLD-TDP43 and 4 PSP cases were analyzed. Four cases from elderly subjects with no history or histological findings of any neurological disease were used as a control group. All human brains considered in the proteomic study had a post-mortem interval (PMI) lower than 16 hours (Table 1). For the validation phase, OB tissue from additional PSP and

FTLD-TDP43 subjects were included (n=9 and 3, respectively). In all cases, neuropathological assessment was performed according to standardized neuropathological guidelines: Mackenzie criteria for FTLD pathology [23], and NINDS criteria for PSP [24].

	CASE (code)	AGE (years)	SEX	PMI	DEFINITIVE DX
Control	BK-0300	75	F	-	ARP I-II
	BK-1378	78	M	6h	multi-infarct
	BK-1078	84	F	6h	Vascular encephalopathy, NFT I
	BK-1195	82	F	8h	Acute stroke left cerebral artery + cerebellar hematoma
	BK-1563	79	M	5h	Acute stroke left cerebral artery + AgD II + diffuses amyloid plaques
PSP	CS-0595	71	F	4h	PSP, onset 66y
	CS-0950	76	F	4'25h	PSP
	CS-1306	67	M	5h	PSP, onset 62y
	CS-1268	66	M	6'5h	PSP, onset 58y
	133	88	F	5h	PSP+CAA+Thal1
	347	81	M	6h	PSP +CAA+Thal 1
	370	80	M	3h	PSP + Thal 4
	396	71	F	4h	PSP
	419	70	M	3'5h	PSP
	330	67	F	16h	PSP
	323	78	M	16h	PSP+AD A2B3C3
	421	85	F	2'5h	PSP +AD A1B2C2+CAA
	389	49	M	6h	PSP
FTLD-TDP43	CS-1370	66	M	5,15h	FTLD-TDP43 type A, onset 64y
	CS-0866	88	F	6,5h	FTLD-U-TDP43 type A + hipocampal esclerosis, onset 77y
	CS-1309	78	M	7,15h	FTLD-TDP43 type C, CAA mod, onset n.a
	CS-0679	77	F	7,6h	FTLD-U-TDP43 type A, onset 73y
	318	85	M	15h	FTD-MND (TDP 43Type B)+ A2B1C1
	418	78	M	4'5h	FTD TDP 43 (Type B) +PART
	452	89	F	5h	FTD-TDP43(Type B)+A1B1C1

Table 1. Clinicopathological data of PSP and FTLD-TDP43 subjects included in this study

Sample preparation for proteomic analysis - OB specimens derived from control, FTLD-TDP43 and PSP cases were homogenized using ''mini potters'' in lysis buffer containing 8 M urea, 0,1 M TEAB. The homogenates were spanned down at 14.000 x g for 15min at 4°C. Protein quantitation was performed with the Bradford assay kit (Bio-Rad).

Reduction, alkylation, digestion and TMT labeling – For the proteomic analysis, 25 µg of protein from each sample were used. Protein were first reduced with 10mM TCEP for 1h at 30ºC. Then, alkylation was performed for 30 min at room temperature using 40mM IAA. Samples were diluted 5 times to reduce the Urea concentration <1M and protein enzymatic cleavage was carried out overnight with trypsin (Promega; 1:50, w/w) at 37°C. Subsequently, each of the samples was labeled with one of the TMT reagents according to the manufacturer's instructions

(Thermo Scientific). Two TMT experiments were performed, one for each disease analyzed. Thereby, control cases were labeled with 127N, 127C, 128N, and 128C and disease cases were labeled with 129N, 129C, 130N and 130C. Labels 126 and 131 were used to label two pools of all samples as intern quality control of the procedure. After leaving the labeling reaction for 60min, all samples were pooled and dried in a speed-vacuum.

Off-gel electrophoresis – samples previously purified with C18 Macro Spin Columns (Harvard Apparatus) were fractionated using Off-gel electrophoresis (OGE) separation using Agilent 3100 off-gel fractionator, according to the manufacturer's instructions. Dried samples were reconstituted using OGE solution and focused using an immovilized pH gradient dry strip (13cm, pH 3-10). Samples were then desalted and purified using MicroSpins C18 columns, dried in a speed-vacuum and stored at -20ºC until analysis.

LC-MS/MS – A LTQ Orbitrap Q-exactive Plus mass spectrometer (Thermo Fisher) coupled with nanoflow high-pressure liquid chromatography (HPLC) was used to analyzed the OGE fractions, as previously described [25]. Peptides were reconstituted using 5%ACN 0,1%FA were trapped on 2 cm x 75 µm ID, 3 µm pre-column and separated on an Easy-spray column, 50 cm x 75 µm ID, PepMap C18, 2 µm (Thermo Scientific). The analytical separation was run for 60 min using a gradient of H2O/FA 99.9%/0.1% (solvent A) and CH3CN/FA 99.9%/0.1% (solvent B) at a flow rate of 300 nL/min. For MS survey scans, the OT resolution was set to 140'000 and the ion population was set to 3×10^6 with an m/z window from 350 to 2000. Twenty precursor ions were selected for higher-energy collisional dissociation (HCD) with a resolution of 35'000, an ion population set to 1 × 105 (isolation window of 0.5 m/z) and a normalized collision energy set to 30%.

Protein identification – MS data were processed using EasyProt. Peak list were obtained using the 12 OGE fractions and the combination of HCD-CID raw data peak list were generated. These data were submitted to the EasyProt software platform (version 2.3, build 718) that uses Phenyx software (GeneBio, Geneva, Switzerland) for the protein identification. The search was

performed using Uniprot/Swiss-Prot database (2014-10, 66903) (ref EasyProt--an easy-to-use graphical platform for proteomics data analysis). The following criteria were used: Homo Sapiens taxonomy, oxidized methionine as variable modification, and cysteine carbamethylation, TMT10 lysine and TMT10 amino-terminus as fixed modifications. One missed cleavage was selected and parent-ion tolerance was set to 10ppm and the accuracy of fragment ions to 0.6Da. Only proteins with a less than 1% false discovery rate (FDR) and at least two different unique peptides were selected for further analysis. A minimum peptide length of 6 amino acids was used.

Protein quantification- Isobaric quantification was performed using the Isobar R package (General statistical modeling of data from protein relative expression isobaric tags.) The manufacturer's isotopic distribution data was used to correct the isotopic impurities of TMT10 reporter-ion intensities. The equal median intensity method was used to normalize the reporter intensities. Peptides which did not present reporter intensities were not quantified. To test the ratio's accuracy and biological significance, technical and biological variability were calculated for each protein ratio. A ratio p value and sample p value were calculated for each variable. Furthermore, only proteins with a cut-off threshold value higher than 1.33 or lower than 0.77 were considered. MS raw data and search results files have been deposited to the ProteomeXchange Consortium (http://proteomecentral.proteomexchange.org) via the PRIDE partner repository [26] with the dataset identifiers PXD011446.

Western-Blotting - Equal amounts of protein (10 µg) were resolved in 4-15% stain free SDS-PAGE gels (Bio-rad). OB proteins derived from control, PSP and FTLD-TDP43 subjects were electrophoretically transferred onto nitrocellulose membranes using a Trans-blot Turbo transfer system (up to 25V, 7min) (Bio-rad). Membranes were probed with primary antibodies at 1:1000 dilution in 5% nonfat milk or BSA according to manufacturer instructions. After incubation with the appropriate horseradish peroxidase-conjugated secondary antibody (1:5000), the immunoreactivity was visualized by enhanced chemiluminiscence (Perkin Elmer) and detected

by a Chemidoc MP Imaging System (Bio-Rad). Equal loading of the gels was assessed by Ponceau staining and hybridization with a GAPDH specific antibody (Calbiochem). After densitometric analyses (Image Lab Software Version 5.2; Bio-Rad), optical density values were expressed as arbitrary units and normalized to GAPDH.

Results and discussion

Although it is widely known that patients suffering from neurological diseases experience loss of olfactory functionality including patients with FTD [1,6], few studies have examined the consequence of this deficit at molecular level. In fact, smell impairment and its relationship with Tau and TDP43 deposits in patients with PSP and FTLD-TDP43 has not been studied thoroughly. During the last years, neuroproteomic improvements have allowed a deeper understanding of the huge complexity of the olfactory system [27]. In this sense, we have considered olfactory proteomics as a reliable tool to characterize the potential molecular disarrangements that occur at the level of the OB in subjects with PSP or FTLD-TDP43 post-mortem diagnosis. The experimental workflow followed in this study is sum up in Figure 1.

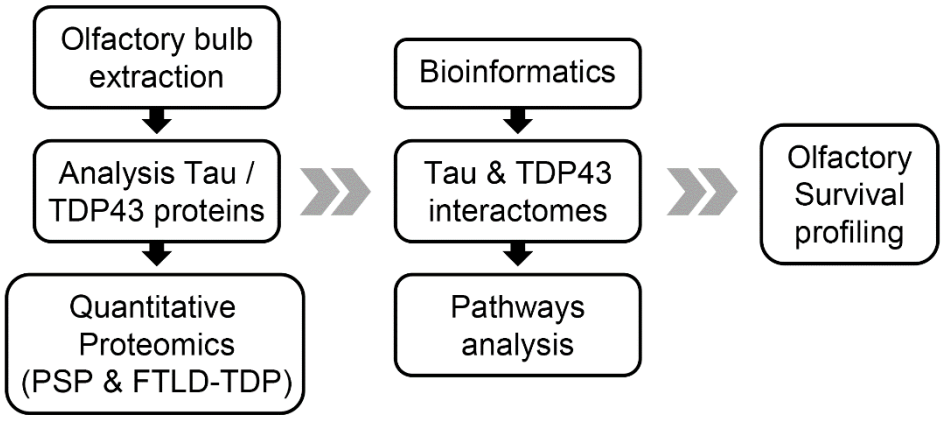

Figure 1. **An overview of the workflow used for the molecular characterization of the OB derived from PSP and FTLD-TDP43 subjects.**

Tau and TDP43 protein expression in OB from patients with PSP and FTLD-TDP43

First, we wanted to check the expression of the neuropathological substrates Tau and TDP43 in the OB derived from PSP and FTLD-TDP43 subjects. Phosphorylated and total levels of both proteins were monitored by Western Blotting. As shown in figure 2A, p-Tau levels tend to increase in the OB from FTLD-TDP43 subjects. According with previous reports [28,3], OB Tau

pathology is absent in PSP (figure 2A). However, an increment in p-TDP43 levels was observed in PSP and FTLD-TDP OBs (figure 2B). Although previous studies pointed out that PSP subjects lack abnormal TDP-43 accumulation [29], pathological TDP-43 has been detected in limbic structures from 25% PSP cases [30]. Although, the presence of both neuropathological inclusions has been previously studied at the level of the OB in different tauopathies and synucleinopathies [1,28], the significance of a TDP43 related neuropathological phenotype in the OB remains elusive [22,3]. Hence, we consider that the application of OB proteomics is an ideal approach to characterize in detail the molecular disturbances that accompany the presence of neuropathological substrates across FTD spectrum.

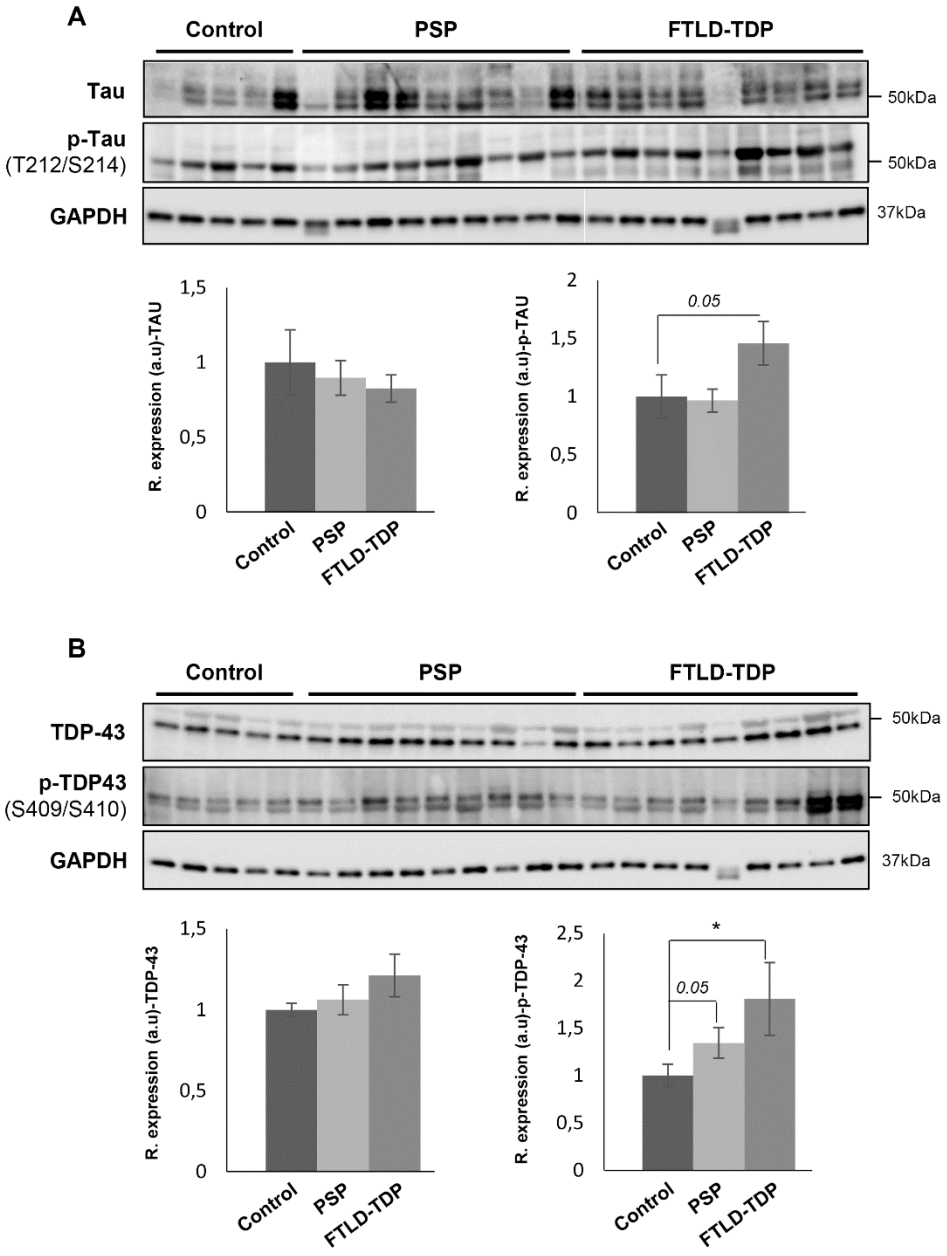

Figure 2. OB protein expression of Tau and TDP43 in PSP and FTLD-TDP43. A) Protein levels of olfactory Tau and phosphorylated Tau (T212/S214). B) Protein levels of olfactory TDP-43 and phosphorylated TDP-43 (S409/S410). Data are presented as mean ± SEM. *P < 0.05 vs control group.

OB proteome-wide analysis in PSP and FTLD-TDP43

To deep into the olfactory molecular alterations present in both FTD phenotypes, we have performed a differential OB proteome analysis using isobaric tags (TMT) coupled to 2D-liquid chromatography tandem mass spectrometry (4 subjects/disease compared to 4 neurological intact controls). Among the 2745 and 2911 identified proteins in PSP and FTLD-TDP43 subjects respectively (Supplementary table 1), only 25 and 28 proteins, were aberrantly expressed, either by overexpression or under expression (corresponding to 1% of the quantitated proteome) (Table 2). None of these protein-coding genes are deregulated at the level of medial temporal lobe across FTD phenotypes [31]. Our group has previously showed a strong disarrangement in the OB proteostasis during AD and PD progression [32, 33] showing that approximately 20% of the quantified proteins were deregulated across AD and PD phenotypes. As mentioned before, AD and PD patients suffer from great loss of olfactory functionality and above 90% of the patients lose their sense of smell in early stages of both diseases [1, 6]. Our molecular findings in PSP and FTLD-TDP43 are in agreement with the clinically mild olfactory deficit described for these two neurological disorders [6]. Among the deregulated proteins in PSP and FTLD-TDP43, only Protein phosphatase 1 regulatory subunit 1B (PPP1R1B) was commonly up-regulated in both phenotypes, suggesting a potential alteration in dopamine D1 receptor-mediated signaling cascades [34, 35]. Analyzing both differential datasets, the alteration of GLS, LARS2, OGDHL, LRPPRC, SLC25A22, ATP5L and ATP5J2 suggested an imbalance in mitochondrial functionality in PSP [36]. On the other hand, changes in the expression levels of RAB3C, CAPS, RPS11, RPL22, RPL13A indicated minor disruption of vesicle trafficking and protein synthesis. Moreover, each FTD phenotype induces an overproduction of specific cytoskeletal protein subsets in each pathology (SPTBN4, PLXNB3, PDLIM3, PLEKHA7 in PSP; COL6A3, COL6A1, COL6A2 in FTLD-TDP43) indicating differences at the level of cell motility and axon guidance. It is important to note that due to technical reasons, only the most abundant proteins were analyzed. Thus, other alterations may be present at the level of the OB in PSP and FTLD-TDP43 subjects. Moreover,

our study characterizes the whole OB, not distinguishing between the numerous cell types coexisting in this region, so we cannot attribute any protein dysfunction to a concrete cell type [37].

Protein names	Gene	Uniprot code	Peptide count	Ratio	P-value ratio	P-value sample
Down-regulated proteins across PSP disease						
Glutaminase kidney isoform, mitochondrial	GLS	O94925	5	**0.6461**	0.00088	7.75E-09
THO complex subunit 4	ALYREF	Q86V81	2	**0.691**	0.04446	1.05E-07
Probable leucine--tRNA ligase, mitochondrial	LARS2	Q15031	2	**0.6948**	0.02529	6.76E-09
Sorting and assembly machinery component 50 homolog	SAMM50	Q9Y512	4	**0.7122**	0.04277	1.30E-07
2-oxoglutarate dehydrogenase-like, mitochondrial	OGDHL	Q9ULD0	7	**0.7196**	0.04815	1.10E-07
von Willebrand factor A domain-containing protein 8	VWA8	A3KMH1	2	**0.7213**	0.00389	5.88E-08
PC4 and SFRS1-interacting protein	PSIP1	O75475	7	**0.7268**	0.02935	1.16E-07
Leucine-rich PPR motif-containing protein, mitochondrial	LRPPRC	P42704	14	**0.7415**	0.03542	2.74E-07
Mitochondrial glutamate carrier 1	SLC25A22	Q9H936	3	**0.7457**	0.0311	2.50E-07
ATP synthase subunit g, mitochondrial	ATP5L	O75964	3	**0.748**	0.02184	3.51E-07
Interleukin enhancer-binding factor 3	ILF3	Q12906	7	**0.752**	0.03514	2.40E-06
Transmembrane protein 35A	TMEM35A	Q53FP2	2	**0.7528**	0.03456	3.58E-07
Plasma membrane calcium-transporting ATPase 2	ATP2B2	Q01814	8	**0.7588**	0.00435	1.30E-06
Pre-mRNA-splicing factor ATP-dependent RNA helicase DHX15	DHX15	O43143	3	**0.7669**	0.04599	7.28E-05
Voltage-dependent R-type calcium channel subunit alpha-1E	CACNA1E	Q15878	2	**0.767**	0.01534	5.30E-07
ATP synthase subunit f, mitochondrial	ATP5J2	P56134	2	**0.7686**	0.00067	2.96E-07
Up/Down-regulated proteins across PSP disease						
Inositol-tetrakisphosphate 1-kinase	ITPK1	Q13572	3	**1.359**	0.01402	8.96E-05
Claudin-11	CLDN11	O75508	4	**1.3697**	0.04379	1.85E-06
Protein phosphatase 1 regulatory subunit 1B	PPP1R1B	Q9UD71	3	**1.401**	0.02547	1.63E-07
NAD-dependent protein deacetylase sirtuin-2	SIRT2	Q8IXJ6	8	**1.4426**	0.03192	2.80E-05
Heat shock protein beta-6	HSPB6	O14558	2	**1.4786**	0.00224	1.97E-09
Pleckstrin homology domain-containing family A member 7	PLEKHA7	Q6IQ23	2	**1.4834**	0.03796	3.34E-09
PDZ and LIM domain protein 3	PDLIM3	Q53GG5	2	**1.6116**	0.00542	4.70E-10
Plexin-B3	PLXNB3	Q9ULL4	2	**1.6405**	0.00076	1.36E-10
Spectrin beta chain, non-erythrocytic 4	SPTBN4	Q9H254	1	**1.8043**	0.0077	7.19E-10
Down-regulated proteins across FTLD-TDP43						
40S ribosomal protein S11	RPS11	P62280	2	**0.6723**	0.04317	3.65E-10
Amyloid-like protein 1	APLP1	P51693	3	**0.7056**	0.00232	8.70E-09
60S ribosomal protein L22	RPL22	P35268	2	**0.7083**	0.01674	1.12E-09
LYR motif-containing protein 9	LYRM9	A8MSI8	2	**0.7135**	0.00805	3.13E-09
High mobility group nucleosome-binding domain-containing protein 3	HMGN3	Q15651	2	**0.7194**	0.02965	9.40E-08
Breast carcinoma-amplified sequence 1	BCAS1	O75363	6	**0.7216**	0.03249	1.37E-08
Immunoglobulin lambda-like polypeptide 5	IGLL5	B9A064	3	**0.7216**	0.01993	9.82E-08
60S ribosomal protein L13a	RPL13A	P40429	2	**0.7239**	0.03597	2.61E-09
Neurofilament medium polypeptide	NEFM	P07197	25	**0.7492**	0.03147	4.29E-07
Protein kinase C beta type	PRKCB	P05771	4	**0.7505**	0.0034	3.44E-07
Ras-related protein Rab-3C	RAB3C	Q96E17	5	**0.7623**	0.00453	7.17E-07
Glycogen synthase kinase-3 alpha	GSK3A	P49840	2	**0.7669**	0.04257	1.01E-07
Sodium/calcium exchanger 2	SLC8A2	Q9UPR5	2	**0.7675**	0.00182	2.56E-08
DNA-dependent protein kinase catalytic subunit	PRKDC	P78527	8	**0.7682**	0.0152	6.95E-08
Neurosecretory protein VGF [Cleaved into: Neuroendocrine regulator	VGF	O15240	9	**0.7689**	0.00079	1.06E-07
Up-regulated proteins across FTLD-TDP43						
Diphosphoinositol polyphosphate phosphohydrolase 2	NUDT4	Q9NZJ9	3	**1.3341**	0.01967	3.59E-08
High mobility group nucleosome-binding domain-containing protein 5	HMGN5	P82970	2	**1.3784**	0.03317	4.79E-05
Peptidase inhibitor 16	PI16	Q6UXB8	3	**1.4051**	0.01628	4.85E-08
Peroxiredoxin-6	PRDX6	P30041	15	**1.4312**	0.02977	8.54E-10
Glycerol-3-phosphate dehydrogenase [NAD(+)], cytoplasmic	GPD1	P21695	3	**1.4313**	0.03162	2.69E-08
Chloride intracellular channel protein 1	CLIC1	O00299	4	**1.4321**	0.01196	1.09E-08
Ras-related protein R-Ras	RRAS	P10301	2	**1.4348**	0.01918	2.49E-09
Adipogenesis regulatory factor	ADIRF	Q15847	3	**1.4387**	0.01262	8.52E-12
Protein phosphatase 1 regulatory subunit 1B	PPP1R1B	Q9UD71	6	**1.4551**	0.0032	3.54E-08
Calcyphosin	CAPS	Q13938	6	**1.6676**	0.00208	1.60E-11
Collagen alpha-3(VI) chain	COL6A3	P12111	25	**1.771**	0.02416	4.55E-13
Collagen alpha-1(VI) chain	COL6A1	P12109	12	**1.9249**	0.03556	1.04E-13
Collagen alpha-2(VI) chain	COL6A2	P12110	6	**1.9442**	0.01452	7.43E-14

Table 2. Significantly deregulated proteins in PSP and FTLD-TDP43 OB samples

ATP2B2, a functional interactor of tau, is down-regulated in PSP OBs

As patients suffering from PSP and FTLD-TDP43 tend to accumulate Tau and TDP43 inclusions respectively [10], we have used the FpClass tool (http://dcv.uhnres. utoronto.ca/FPCLASS/) [38] as a data mining-based method to generate the potential interactome from human Tau and TDP-43 proteins, to obtain additional information about the role of the differentially expressed olfactory proteins in the field of PSP and FTLD-TDP43. We consider that the deployment of predictive bioinformatics tools is useful to improve the understanding of the large number of data obtained when using high-throughput approaches. Interestingly, we have observed some OB differentially expressed proteins as potential Tau/TDP-43 interactors. Five common interactors were found in case of PSP and only one regarding FTLD-TDP43 (figure 3A). Given the score offered by FPClass tool, the most significant match was the protein Plasma membrane calcium-transporting ATPase 2 (ATP2B2; PMCA2). PMCA2 is a transmembrane protein that catalyzes the hydrolysis of ATP coupled to the transport of calcium outside the cell, including neurons [39, 40]. From the four isoforms named from 1 to 4, PMCA2 is the one predominantly expressed in the brain [41]. It has been recently postulated that calcium homeostasis impairment is a primary cause of loss of neuroprotection and neural cell damage in FTD [42]. Our proteomic approach revealed that OB PMCA2 protein levels are decreased in PSP subjects (Table 2). This finding was further confirmed by Western blotting as shown in figure 3B. The alteration in calcium homeostasis at the level of OB is also supported by the down-regulation of the voltage-dependent R-type calcium channel subunit alpha-1E (CACNA1E) (Table 2), involved in the entry of calcium ions during firing patterns of neurons [43]. CaMKII is sensitive to the frequency of calcium oscillations [44], and its total and phosphorylated OB levels are decreased

across PSP and FTLD-TDP43 (Figure 3C), reinforcing the imbalance not only in the OB calcium homeostasis, but also in the olfactory synaptic transmission [45, 46] in both FTD phenotypes.

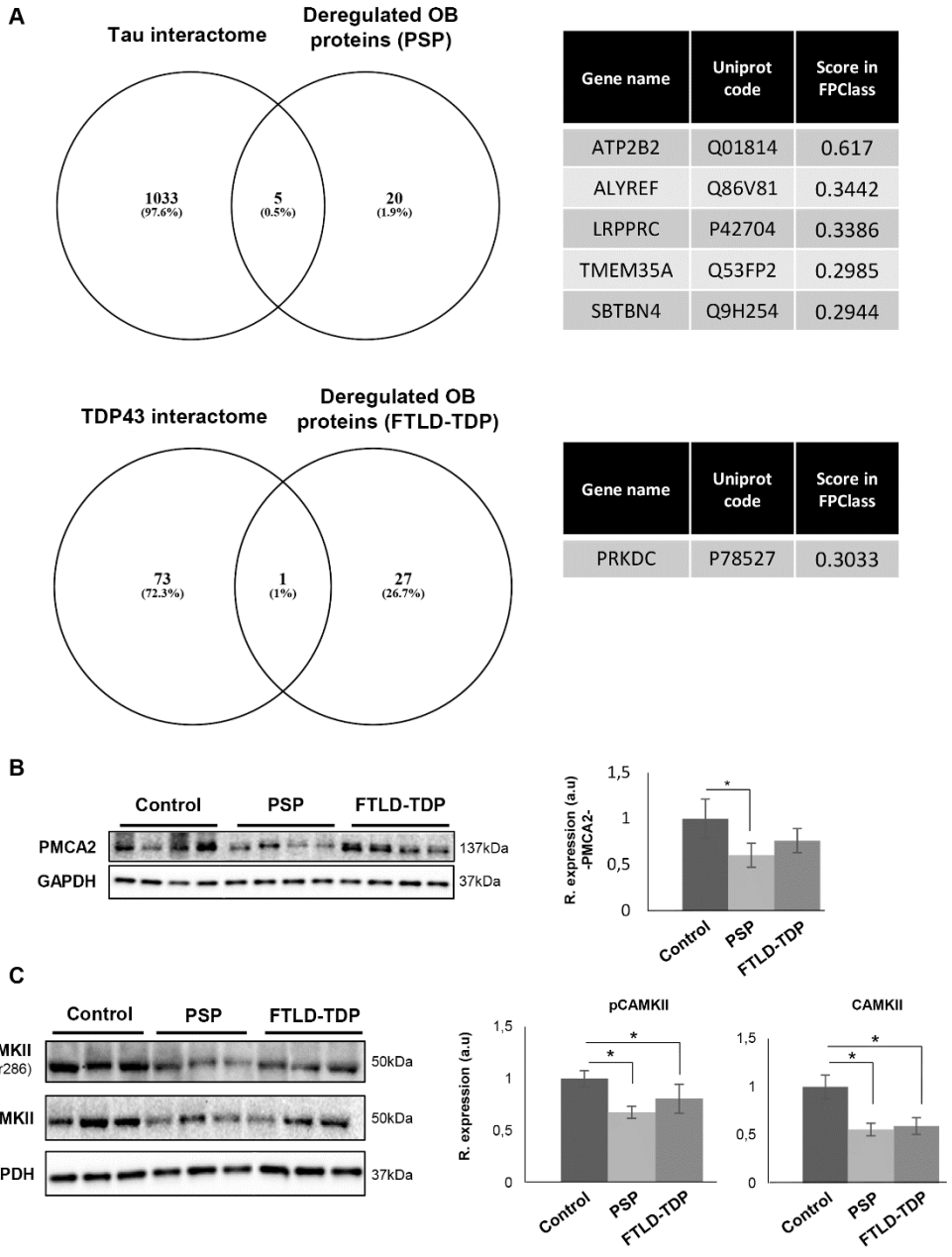

Gene name	Uniprot code	Score in FPClass
ATP2B2	Q01814	0.617
ALYREF	Q86V81	0.3442
LRPPRC	P42704	0.3386
TMEM35A	Q53FP2	0.2985
SBTBN4	Q9H254	0.2944

Gene name	Uniprot code	Score in FPClass
PRKDC	P78527	0.3033

Figure 3. Differential OB proteins as potential interactors of neuropathological substrates. A) Significant representative interactors of Tau and TDP43. B) Levels of PMCA2 in PSP and FTLD-TDP43 OB samples. C) Levels and activation state of OB CaMKII in PSP and FTLD-TDP43 subjects.

Functional pathway analysis for the differential OB proteomic expression profile

Aiming to extract biological information regarding the deregulated proteins in the context of PSP and FTLD-TDP43, we performed a functional pathway analysis using IPA software. As shown in figure 4, concerning PSP analysis, relevant affected processes were related to death and survival (ATP2B2, PSIP1, GLS, HSPB6, PLEKHA7) molecular transport (SPTBN4, ATP2B2, CACNA1E, ALYREF, ATP5L, SLC25A22), behavior (SPTBN4, ATP2B2, CACNA1E, ILF3, GLS), movement disorder (SPTBN4, ATP2B2, ATP5L, ILF3, SLC25A22), sensation (SPTBN4, ATP2B2, CACNA1E), locomotion (SPTBN4, ATP2B2, CACNA1E), and apoptosis (ATP2B2, PSIP1, GLS) (Figure 4A). On the other hand, OB differential proteins in FTLD-TDP43 subjects, depicted common deregulated processes such as death and survival (PRDX6, RPL13A, COL6A1, NEFM, RPS11, GSK3A, VGF, PRKDC, PPP1R1B, RRAS) and movement disorder (PRDX6, APLP1, COL6A3, RPL13A, GPD1, PPP1R1B, BCAS1) and other disease-specific as neuromuscular disease (PRDX6, APLP1, RPL13A, GPD1, PPP1R1B, BCAS1), cell viability (PRDX6, NEFM, GSK3A, VGF, PRKDC, PPP1R1B), learning (SLC8A2, VGF, PPP1R1B), and plasticity (VGF, PPP1R1B) (Figure 4B). These data point out that cell death and survival routes are potentially compromised in both FTD phenotypes.

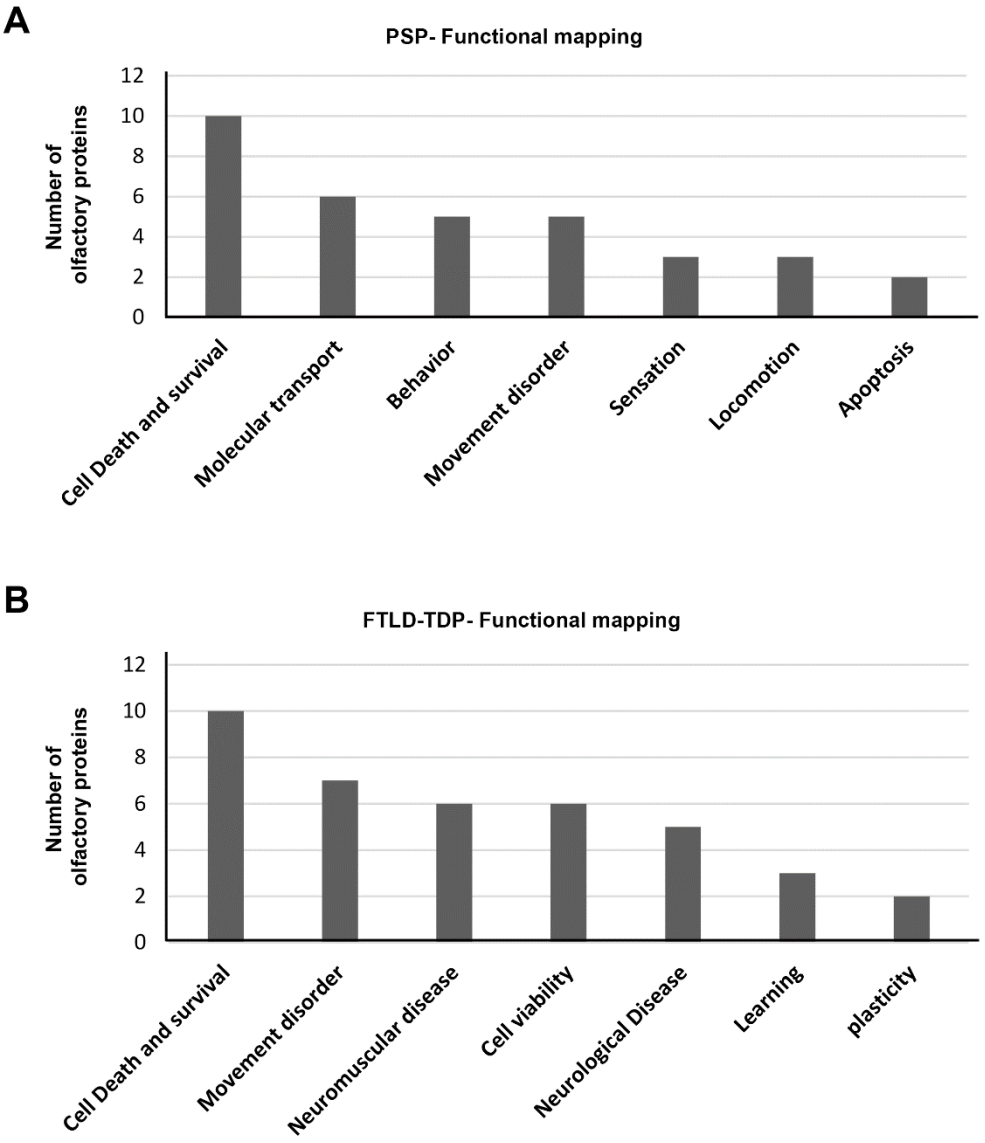

Figure 4. Significantly enriched biofunctions in the OB of PSP and FTLD-TDP43 subjects.

Characterization of OB death and survival routes in PSP and FTLD-TDP43

Within PSP and FTLD-TDP43 much effort has been spent on studying the role of Tau and TDP-43 in human disease pathogenesis but the available information is insufficient to fully understand the neurodegenerative progression at the level of olfactory areas. It has been previously demonstrated that the activation dynamics of specific survival routes is compromised in some

tauopathies and synucleinopathies at the level of OB [32, 33] (However, there is no information about the survival potential of OB neurons in PSP and FTLD-TDP43 disorders. Based on functional analysis (figure 4) and to complement our proteomic workflow, survival and apoptotic pathways were monitored to analyze the impact of both FTD phenotypes on the viability of the olfactory neurons. First, a stepwise characterization of constitutive pro- and anti-apoptotic factors involved in mitochondrial apoptotic pathways was performed. No differences were observed neither in survival protein levels (Bcl-2, Bcl-xL) nor in caspase activation (caspase 3, 9 and 12) between controls and FTD phenotypes (supplementary figure 1). Considering the limited information available regarding the role of survival pathways in the FTD spectrum, subsequent experiments were performed to monitor a panel of survival pathways at the level of OB. Total and residue-specific phosphorylation of MEK/ERK, SEK/SAPK, PDK1, PKC, AKT, p38 MAPK, and PKA were measured by Western-blotting. No appreciable changes were detected in the activation status of AKT, P38 MAPK axis, or PKA across PSP and FTLD-TDP43 (supplementary figure 2). In contrast to data obtained in the OB from AD subjects [47], our findings showed a decrease in the activation state of MEK/ERK axis for both frontotemporal diseases (figure 5). However, activation of ERK has been previously characterized in both neurons and glial cells of cerebral cortex from PSP patients, presenting a close relationship with tau deposits [48, 49], indicating that the activation of MAPK route is region-dependent in PSP. In human brain, the stress-responsive kinase phospho-SAPK is significantly increased in AD over control cases, overlapping with Tau-positive neurofibrillary pathology [50, 51]. In PSP, phospho-SAPK immunoreactive granules have been observed in neurons and astrocytes with abnormal Tau deposition [52], and are considered granulovacuolar degeneration (GVD) bodies at hippocampal level [53]. At the level of OB, the SEK/SAPK axis is specifically disrupted in PSP, indicating that synaptic plasticity and neuronal survival differs at olfactory level between PSP and FTLD-TDP43 (figure 6A) [54]. On the other hand, PDK1 homeostasis was specifically altered in the OB from FTLD-TDP43 subjects (Figure 6B). Interestingly, PDK1 deficiency induces a decrease in OB GABA,

taurine and serotonin levels in mice, being a molecular sensor for behavior indicative for anxiety and depression [55]. The decrease in OB PKC levels concurrently observed in PSP and FTLD-TDP43, may explain the drop (no significant) in PKC activity as measured by a specific antibody against phosphorylated PKC isoforms at a residue homologous to activated Thr514 of human PKCγ (Figure 6B). In accordance, our group has previously detected disarrangements in PKC route in the OB from AD and PD subjects [32, 33], suggesting a clear involvement of this kinase in olfactory dysfunction. The PKC family (composed by 12 isoforms) plays essentially roles in several cognitive processes such as learning and memory, in particular due to its function in synaptic transmission and plasticity, and neurite outgrowth. Immunohistochemical studies have revealed that PKCiota/lambda isoform is present within tau-positive neurofibrillary inclusions in PSP [56]. Although PKC activators have been proposed for the treatment of dementias [57] due to their capacity to restore neurotrophic activity and synaptogenesis reducing Tau hyperphosphorylation [58], the high complexity of PKC signaling needs further exploration at the level of OB, with the aim to reveal the specific role of each PKC isoform during the neurodegenerative process.

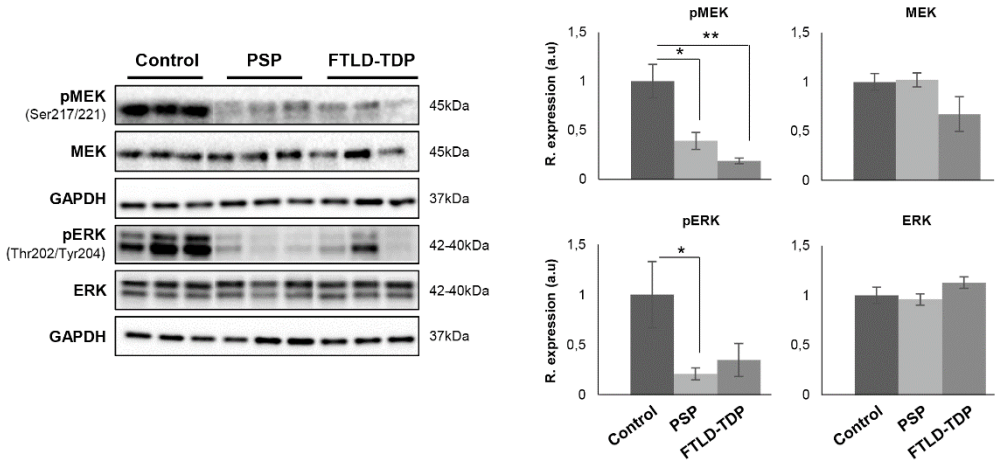

Figure 5. Activation state of MAPK pathway in the OB from PSP and FTLD-TDP43 subjects. Data are presented as mean ± SEM. *P < 0.05 vs control group; **P<0.01 vs control group.

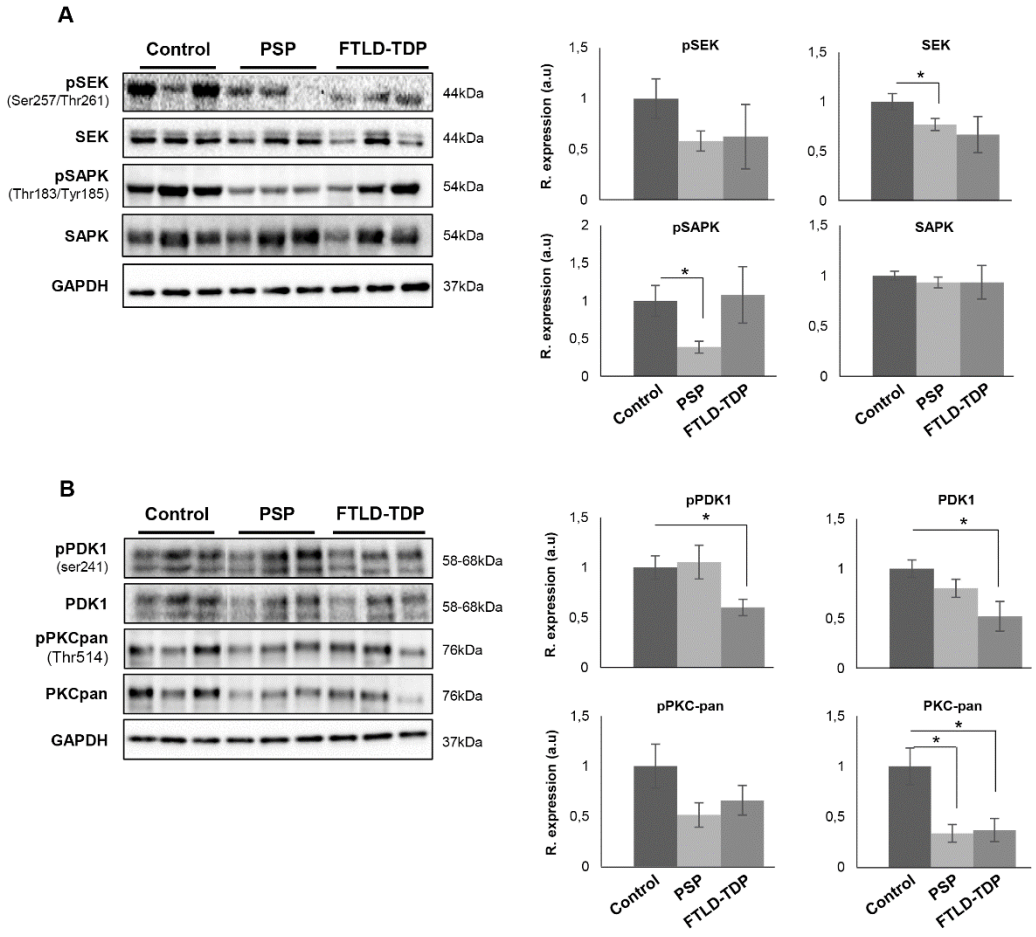

Figure 6. Activation state of SEK/SAPK and PDK1/PKC axis in the OB from PSP and FTLD-TDP43 subjects. Data are presented as mean ± SEM. *P < 0.05 vs control group.

Conclusion

Our data reflect, for the first time, olfactory molecular disarrangements in PSP and FTLD-TDP43, two clinically similar FTD disorders, but with different neuropathological signature. The differential proteomes lie in an imbalance in mitochondrial functionality and calcium homeostasis in PSP, and protein synthesis and vesicle trafficking in FTLD-TDP43. Moreover, besides FTDs present mild olfactory dysfunction and neuropathological substrates are not commonly present in olfactory areas, our findings revealed similarities and differences in the activation dynamics of specific survival routes between PSP and FTLD-TDP43, providing basic information for understanding the implication of the OB in the pathophysiology of FTDs.

References

[1] Attems, J., Walker, L., Jellinger, K. A., Olfactory bulb involvement in neurodegenerative diseases. *Acta Neuropathol* 2014, *127*, 459-475.

[2] Doty, R. L., The olfactory vector hypothesis of neurodegenerative disease: is it viable? *Ann Neurol* 2008, *63*, 7-15.

[3] Rey, N. L., Wesson, D. W., Brundin, P., The olfactory bulb as the entry site for prion-like propagation in neurodegenerative diseases. *Neurobiol Dis*, *109*, 226-248.

[4] Fullard, M. E., Morley, J. F., Duda, J. E., Olfactory Dysfunction as an Early Biomarker in Parkinson's Disease. *Neurosci Bull*, *33*, 515-525.

[5] Doty, R. L., Olfactory dysfunction in Parkinson disease. *Nat Rev Neurol* 2012, *8*, 329-339.

[6] Doty, R. L., Olfactory dysfunction in neurodegenerative diseases: is there a common pathological substrate? *Lancet Neurol* 2017, *16*, 478-488.

[7] Heyanka, D. J., Golden, C. J., McCue, R. B., 2nd, Scarisbrick, D. M.*, et al.*, Olfactory deficits in frontotemporal dementia as measured by the Alberta Smell Test. *Appl Neuropsychol Adult*, *21*, 176-182.

[8] Orasji, S. S., Mulder, J. L., de Bruijn, S. F., Wirtz, P. W., Olfactory dysfunction in behavioral variant frontotemporal dementia. *Clin Neurol Neurosurg*, *141*, 106-110.

[9] Silveira-Moriyama, L., Hughes, G., Church, A., Ayling, H.*, et al.*, Hyposmia in progressive supranuclear palsy. *Mov Disord*, *25*, 570-577.

[10] Li, Y. Q., Tan, M. S., Yu, J. T., Tan, L., Frontotemporal Lobar Degeneration: Mechanisms and Therapeutic Strategies. *Mol Neurobiol*, *53*, 6091-6105.

[11] Mann, D. M. A., Snowden, J. S., Frontotemporal lobar degeneration: Pathogenesis, pathology and pathways to phenotype. *Brain Pathol*, *27*, 723-736.

[12] Mackenzie, I. R., Neumann, M., Molecular neuropathology of frontotemporal dementia: insights into disease mechanisms from postmortem studies. *J Neurochem*, *138 Suppl 1*, 54-70.

[13] Shi, J., Shaw, C. L., Du Plessis, D., Richardson, A. M.*, et al.*, Histopathological changes underlying frontotemporal lobar degeneration with clinicopathological correlation. *Acta Neuropathol* 2005, *110*, 501-512.

[14] Neumann, M., Sampathu, D. M., Kwong, L. K., Truax, A. C.*, et al.*, Ubiquitinated TDP-43 in frontotemporal lobar degeneration and amyotrophic lateral sclerosis. *Science* 2006, *314*, 130-133.

[15] Mackenzie, I. R., Munoz, D. G., Kusaka, H., Yokota, O.*, et al.*, Distinct pathological subtypes of FTLD-FUS. *Acta Neuropathol*, *121*, 207-218.

[16] Luzzi, S., Snowden, J. S., Neary, D., Coccia, M.*, et al.*, Distinct patterns of olfactory impairment in Alzheimer's disease, semantic dementia, frontotemporal dementia, and corticobasal degeneration. *Neuropsychologia* 2007, *45*, 1823-1831.

[17] McLaughlin, N. C., Westervelt, H. J., Odor identification deficits in frontotemporal dementia: a preliminary study. *Arch Clin Neuropsychol* 2008, *23*, 119-123.

[18] Pardini, M., Huey, E. D., Cavanagh, A. L., Grafman, J., Olfactory function in corticobasal syndrome and frontotemporal dementia. *Arch Neurol* 2009, *66*, 92-96.

[19] Kovacs, T., Cairns, N. J., Lantos, P. L., beta-amyloid deposition and neurofibrillary tangle formation in the olfactory bulb in ageing and Alzheimer's disease. *Neuropathol Appl Neurobiol* 1999, *25*, 481-491.

[20] Hubbard, P. S., Esiri, M. M., Reading, M., McShane, R., Nagy, Z., Alpha-synuclein pathology in the olfactory pathways of dementia patients. *J Anat* 2007, *211*, 117-124.

[21] Duda, J. E., Olfactory system pathology as a model of Lewy neurodegenerative disease. *J Neurol Sci*, *289*, 49-54.

[22] Kohl, Z., Schlachetzki, J. C., Feldewerth, J., Hornauer, P.*, et al.*, Distinct Pattern of Microgliosis in the Olfactory Bulb of Neurodegenerative Proteinopathies. *Neural Plast*, *2017*, 3851262.

[23] Mackenzie, I. R., Neumann, M., Baborie, A., Sampathu, D. M.*, et al.*, A harmonized classification system for FTLD-TDP43 pathology. *Acta Neuropathol* 2011, *122*, 111-113.

[24] Litvan, I., Hauw, J. J., Bartko, J. J., Lantos, P. L.*, et al.*, Validity and reliability of the preliminary NINDS neuropathologic criteria for progressive supranuclear palsy and related disorders. *J Neuropathol Exp Neurol* 1996, *55*, 97-105.

[25] Dayon, L., Pasquarello, C., Hoogland, C., Sanchez, J. C., Scherl, A., Combining low- and high-energy tandem mass spectra for optimized peptide quantification with isobaric tags. *J Proteomics*, *73*, 769-777.

[26] Vizcaino, J. A., Deutsch, E. W., Wang, R., Csordas, A.*, et al.*, ProteomeXchange provides globally coordinated proteomics data submission and dissemination. *Nat Biotechnol* 2014, *32*, 223-226.

[27] Lachen-Montes, M., Fernandez-Irigoyen, J., Santamaria, E., Deconstructing the molecular architecture of olfactory areas using proteomics. *Proteomics Clin Appl* 2016.

[28] Mundinano, I. C., Caballero, M. C., Ordonez, C., Hernandez, M.*, et al.*, Increased dopaminergic cells and protein aggregates in the olfactory bulb of patients with neurodegenerative disorders. *Acta Neuropathol* 2011, *122*, 61-74.

[29] Uryu, K., Nakashima-Yasuda, H., Forman, M. S., Kwong, L. K.*, et al.*, Concomitant TAR-DNA-binding protein 43 pathology is present in Alzheimer disease and corticobasal degeneration but not in other tauopathies. *J Neuropathol Exp Neurol* 2008, *67*, 555-564.

[30] Yokota, O., Davidson, Y., Bigio, E. H., Ishizu, H.*, et al.*, Phosphorylated TDP-43 pathology and hippocampal sclerosis in progressive supranuclear palsy. *Acta Neuropathol*, *120*, 55-66.

[31] Bronner, I. F., Bochdanovits, Z., Rizzu, P., Kamphorst, W.*, et al.*, Comprehensive mRNA expression profiling distinguishes tauopathies and identifies shared molecular pathways. *PLoS One* 2009, *4*, e6826.

[32] Lachen-Montes, M., Gonzalez-Morales, A., Zelaya, M. V., Perez-Valderrama, E.*, et al.*, Olfactory bulb neuroproteomics reveals a chronological perturbation of survival routes and a disruption of prohibitin complex during Alzheimer's disease progression. *Sci Rep* 2017, *7*, 9115.

[33] Lachen-Montes, M., Gonzalez-Morales, A., Iloro, I., Elortza, F.*, et al.*, Unveiling the olfactory proteostatic disarrangement in Parkinson's disease by proteome-wide profiling. *Neurobiol Aging* 2018, *73*, 123-134.

[34] Svenningsson, P., Nishi, A., Fisone, G., Girault, J. A.*, et al.*, DARPP-32: an integrator of neurotransmission. *Annu Rev Pharmacol Toxicol* 2004, *44*, 269-296.

[35] Hemmings, H. C., Jr., Greengard, P., Tung, H. Y., Cohen, P., DARPP-32, a dopamine-regulated neuronal phosphoprotein, is a potent inhibitor of protein phosphatase-1. *Nature* 1984, *310*, 503-505.

[36] Albers, D. S., Beal, M. F., Mitochondrial dysfunction in progressive supranuclear palsy. *Neurochem Int* 2002, *40*, 559-564.

[37] Mori, K., Membrane and synaptic properties of identified neurons in the olfactory bulb. *Prog Neurobiol* 1987, *29*, 275-320.

[38] Kotlyar, M., Pastrello, C., Pivetta, F., Lo Sardo, A.*, et al.*, In silico prediction of physical protein interactions and characterization of interactome orphans. *Nat Methods*, *12*, 79-84.

[39] Strehler, E. E., Zacharias, D. A., Role of alternative splicing in generating isoform diversity among plasma membrane calcium pumps. *Physiol Rev* 2001, *81*, 21-50.

[40] Brini, M., Plasma membrane Ca(2+)-ATPase: from a housekeeping function to a versatile signaling role. *Pflugers Arch* 2009, *457*, 657-664.

[41] Di Leva, F., Domi, T., Fedrizzi, L., Lim, D., Carafoli, E., The plasma membrane Ca2+ ATPase of animal cells: structure, function and regulation. *Arch Biochem Biophys* 2008, *476*, 65-74.

[42] Palluzzi, F., Ferrari, R., Graziano, F., Novelli, V., *et al.*, A novel network analysis approach reveals DNA damage, oxidative stress and calcium/cAMP homeostasis-associated biomarkers in frontotemporal dementia. *PLoS One*, *12*, e0185797.

[43] Sochivko, D., Pereverzev, A., Smyth, N., Gissel, C., *et al.*, The Ca(V)2.3 Ca(2+) channel subunit contributes to R-type Ca(2+) currents in murine hippocampal and neocortical neurones. *J Physiol* 2002, *542*, 699-710.

[44] De Koninck, P., Schulman, H., Sensitivity of CaM kinase II to the frequency of Ca2+ oscillations. *Science* 1998, *279*, 227-230.

[45] Nichols, R. A., Sihra, T. S., Czernik, A. J., Nairn, A. C., Greengard, P., Calcium/calmodulin-dependent protein kinase II increases glutamate and noradrenaline release from synaptosomes. *Nature* 1990, *343*, 647-651.

[46] Barria, A., Muller, D., Derkach, V., Griffith, L. C., Soderling, T. R., Regulatory phosphorylation of AMPA-type glutamate receptors by CaM-KII during long-term potentiation. *Science* 1997, *276*, 2042-2045.

[47] Lachen-Montes, M., Gonzalez-Morales, A., de Morentin, X. M., Perez-Valderrama, E., *et al.*, An early dysregulation of FAK and MEK/ERK signaling pathways precedes the beta-amyloid deposition in the olfactory bulb of APP/PS1 mouse model of Alzheimer's disease. *J Proteomics* 2016, *148*, 149-158.

[48] Ferrer, I., Blanco, R., Carmona, M., Ribera, R., *et al.*, Phosphorylated map kinase (ERK1, ERK2) expression is associated with early tau deposition in neurones and glial cells, but not with increased nuclear DNA vulnerability and cell death, in Alzheimer disease, Pick's disease, progressive supranuclear palsy and corticobasal degeneration. *Brain Pathol* 2001, *11*, 144-158.

[49] Ferrer, I., Blanco, R., Carmona, M., Puig, B., Phosphorylated mitogen-activated protein kinase (MAPK/ERK-P), protein kinase of 38 kDa (p38-P), stress-activated protein kinase (SAPK/JNK-P), and calcium/calmodulin-dependent kinase II (CaM kinase II) are differentially expressed in tau deposits in neurons and glial cells in tauopathies. *J Neural Transm (Vienna)* 2001, *108*, 1397-1415.

[50] Ferrer, I., Gomez-Isla, T., Puig, B., Freixes, M., *et al.*, Current advances on different kinases involved in tau phosphorylation, and implications in Alzheimer's disease and tauopathies. *Curr Alzheimer Res* 2005, *2*, 3-18.

[51] Zhu, X., Raina, A. K., Rottkamp, C. A., Aliev, G., *et al.*, Activation and redistribution of c-jun N-terminal kinase/stress activated protein kinase in degenerating neurons in Alzheimer's disease. *J Neurochem* 2001, *76*, 435-441.

[52] Ferrer, I., Blanco, R., Carmona, M., Puig, B., *et al.*, Active, phosphorylation-dependent mitogen-activated protein kinase (MAPK/ERK), stress-activated protein kinase/c-Jun N-terminal kinase (SAPK/JNK), and p38 kinase expression in Parkinson's disease and Dementia with Lewy bodies. *J Neural Transm (Vienna)* 2001, *108*, 1383-1396.

[53] Lagalwar, S., Berry, R. W., Binder, L. I., Relation of hippocampal phospho-SAPK/JNK granules in Alzheimer's disease and tauopathies to granulovacuolar degeneration bodies. *Acta Neuropathol* 2007, *113*, 63-73.

[54] Curtis, J., Finkbeiner, S., Sending signals from the synapse to the nucleus: possible roles for CaMK, Ras/ERK, and SAPK pathways in the regulation of synaptic plasticity and neuronal growth. *J Neurosci Res* 1999, *58*, 88-95.

[55] Ackermann, T. F., Hortnagl, H., Wolfer, D. P., Colacicco, G., *et al.*, Phosphatidylinositide dependent kinase deficiency increases anxiety and decreases GABA and serotonin abundance in the amygdala. *Cell Physiol Biochem* 2008, *22*, 735-744.

[56] Shao, C. Y., Crary, J. F., Rao, C., Sacktor, T. C., Mirra, S. S., Atypical protein kinase C in neurodegenerative disease II: PKCiota/lambda in tauopathies and alpha-synucleinopathies. *J Neuropathol Exp Neurol* 2006, *65*, 327-335.

[57] Sun, M. K., Alkon, D. L., Activation of protein kinase C isozymes for the treatment of dementias. *Adv Pharmacol*, *64*, 273-302.

[58] Sun, M. K., Alkon, D. L., Pharmacology of protein kinase C activators: cognition-enhancing and antidementic therapeutics. *Pharmacol Ther*, *127*, 66-77.

DISCUSSION

The occurrence of olfactory deficits in neurological disorders has been characterized for years, and it is clear that this dysfunction appears early, even preceding mental and motor symptoms [1-3]. Besides, the wide-spread application of standardized olfactory tests has enable to accurately assess and compare the relative degree of olfactory impairment in a wide range of diseases [4]. Consequently, it is well known that olfactory dysfunction occurs in a high degree in AD and PD [5, 6] and in lesser magnitude in patients with amyotrophic lateral sclerosis (ALS), progressive supranuclear palsy (PSP) and frontotemporal dementias (FTD) [4, 7, 8]. However, little is known about the molecular events that are responsible for this common impairment, or why these disorders affect the olfactory system in early stages of the disease.

The neuropathological findings observed in the OB in neurodegenerative diseases (NDs) typically carry depositions/inclusions of misfolded proteins that constitute the hallmark injury of the neurodegenerative disease progression [3]. In this sense, strong evidence suggests that this region serves as the entry point for pathogens and other environmental insults that can trigger neuropathological alterations and then spread throughout the brain via olfactory pathways [9, 10]. Moreover, since the NDs involve pathological protein/s, this pattern is similar to the prion hypothesis, which states that these misfolded proteins spread through the different brain regions as far as the disease progresses. Altogether, it seems that the OB could play a crucial role not only in the appearance, but also in the progression of neurological disorders. With the compilation of articles presented in this thesis, our group has been able to partially characterize the molecular disturbances that occur in the OB during the neurodegenerative process in distinct neurological disorders.

1. Olfactory molecular disturbances in APP/PS1 and Tg2576 mouse models

The incidence of NDs increases with age and considering the life expectancy lengthening of the worldwide population, the prevalence of these disorders is expected to rise in the next decades [11]. Although many efforts have been made to find a treatment for these diseases and

there are ongoing trails evaluating new therapeutic strategies [12], there is still no curative treatment for AD or other NDs. In this sense, an accurate understanding of the etiopathogenic mechanisms underlying the diseases progression is essential for the development of new therapeutic compounds. For this purpose, a series of animal models have been developed. These models partially reproduce the pathological lesions and symptoms of the NDs. Moreover, they represent an indispensable tool for the testing of potential treatments before conducting clinical trials in humans [13].

In this work, two generated transgenic mouse lines expressing mutated genes associated with AD (APP/PS1 and Tg2576) [14, 15] have been employed to study the potential olfactory disturbances occurring in AD progression. Importantly, both models express 695-amino acid isoform of human Alzheimer Aβ precursor protein (APP) containing the Swedish mutation (Lys670 --> Asn and Met671 -->Leu). However, the first one also carries a PS1-dE9 mutation. Interestingly, our findings have demonstrated that either proteomic or proteotranscriptomic variations at olfactory level appear at pre-plaque stages in both APP/PS1 and Tg2576 models at 3 and 2 months of age, respectively. Moreover, those alterations precede memory and cognitive deficits, reinforcing that olfactory impairment is an early event in AD progression [16, 17]. Interestingly, among the differentially expressed proteins in both studies, there are only two proteins commonly deregulated in both models, the intrinsic up-regulated positive control, APP, and *PIP4K2A*. Data mining though revealed that common biological processes were affected, being mainly cell survival-related cascades. However, the olfactory survival kinome profile performed in both models revealed few kinases commonly deregulated. For instance, a sustained dephosphorylation of olfactory FAK in tyr576/577 residues was observed in the APP/PS1 model, while no changes were observed in Tg2576 mice, suggesting that mutations in the family of preselinins may specifically affect the regulation of this molecular axis. In fact, it has been suggested that FAK absence could have an impact in dementia mainly due to its contribution in plasticity events, although its role in AD has not been fully elucidated [18]. On

the other hand, both models showed imbalance in the MAP kinase pathway. Nevertheless, while both activated MEK and ERK levels were deregulated in APP/PS1 model, only ERK was affected in the OB of Tg2576 mice. Accordingly, ERK has been previously associated with APP processing, tau phosphorylation and, cell death [19-21]. Moreover, it has been suggested that the absence of preselinin 1 and 2 enhances ERK activity [19]. Strikingly, our results showed an opposite pattern when checking this pathway in a model carrying presenilin mutations suggesting that, at least at the level of the OB, ERK activity might be affected by phosphatase activities such as PP2A, which levels were, in fact, increased in our dataset.

Although animal models represent an excellent tool to increase the understanding of AD, these models are based on known genetic mutations associated with the disease, while the vast majority of patients (over the 90%) develop the sporadic form of AD, in which the underlying causes are still unknown. That is why, it is important to bear in mind that the animal models used in this thesis do not recapitulate all features of sporadic AD. Hence, we have observed different molecular signatures among the three different approaches that we have used to study the impact of AD in the olfactory system. Although similar cell death and survival-related pathways were affected in the OB of APP/PS1, Tg2576 and human sporadic AD, the patterns of the tangled regulatory mechanisms differed. For instance, the MEK/ERK axis and p38 MAPK showed great disparities between species. As mentioned before, animal models do not completely reflect sporadic AD as they do not cover all factors that may influence the disease progression. Differences in the specie-dependent inflammatory responses [22], in iron homeostasis and glial response [23], the absence of neuronal loss and neurofibrillary tangles and the fastest progression in both models [24-26], may partially explain the disparities observed at the level of the OB. In this sense, clinical trials in NDs based on therapeutics that had showed success in animals, have largely failed, and strategies to improve translatability or developing better animal models for these diseases have been suggested [13]. Nonetheless, it is clear that when appropriately used, these models have provide useful information regarding

neurological disorders and still represent a valid tool for the discovery of new potential biomarkers [27-31] .

2. Integrative analysis of transcriptomic and proteomic data reveals no correlation in the molecular disturbances occurring in the OB

The development of high-throughput screening techniques such as transcriptomics and proteomics has opened a wide field for the search of biomarkers that could lead to early diagnosis and treatment, as well as contribute to understand the pathogenesis of NDs. In the ''Introduction'' headline, it has already been mentioned that both transcriptomic and proteomic studies have attempted to discover the molecular mechanisms underlying AD, PD and FTD pathogenesis [32-39]. In this thesis, a combination of both approaches has been applied in Tg2576 mice and human sporadic AD samples to decipher the OB progressive transcriptome-proteome wide alterations occurring during AD development [17, 40, 41]. Using this dual-omic approach, we were able to observe disruption of multiple molecular pathways during AD progression. Leaving beside the specific results obtained in each set of experiments, it is worth to mention that no correlation was found between the transcriptomic and proteomic data in neither of the two studies. This means that none of the deregulated genes during AD progression in mice and humans, were afterwards deregulated at protein level. Although this might seem quite surprising at first, there are several reasons that may explain these results [42]. For years, it was generally assumed that there was strict correlation between mRNA and protein expression measured from a tissue. Nevertheless, multiple studies failed to show this correspondence [43-49]. Next, a summary of potential events that may explain the absence of correlation in the OB datasets are described:

- First, due to technical reasons, high-throughput proteomic analysis are not able to identify and quantify all the OB mouse or human proteome. In fact, approximately a 10% and 5% of

the mouse and human proteome, respectively, was analyzed in the proteomic approach, while full protein-coding genome was measured through RNA microarrays.

- Due to the shortage of sample, OB RNA and protein were retrieved from different Tg2576 mice.
- Being aware that this is a limitation in our studies performed in mice and human samples, all cellular layers present in the bulk OB were processed. However, as mentioned in the ''Introduction'' headline, the OB is composed by a complex mixture of multiple cell types with different functions in architecture and connectivity. Thus, information regarding the specific-cell mRNA and proteins products is lost in our workflow. Sharma and colleagues generated a parallel RNA-seq profiling and proteome mouse brain map in which while correlation between the biological replicates for both transcriptomic and proteomic analysis were extremely high (Pearson's correlation higher than 0.96 and 0.98, respectively), the correlation between the different cell types in the mouse brain were much lower, from 0.25 to 0.86 in the transcriptome analysis and from 0.48 and 0.84 in the proteome one [50]. In the ''Perspectives'' headline, the implementation of more targeted approaches such as Laser Capture Microdissection (LCM) that might help deepen into the molecular profile of each OB cell type will be discussed [51].
- The large number of transcript isoforms due to alternative splicing of the same gene is another issue to considerate when comparing mRNA and protein levels [52, 53]. The possibility that the identified peptide could be compared to splice isoforms that do not contain their respective peptide sequence may also alter the mRNA/protein correlation. This becomes particularly relevant when using RNA microarrays instead of RNA-seq, where isoforms and differential exon usage can be better quantified [54].
- A delay in the mRNA and protein synthesis during state transition is another issue to take into account. It is not expected that induced transcription, immediately leads to an increase in the protein levels. Maturation, export and translation of mRNA take some time. A study

on mammalian cells has reported that mRNAs are 5 times less stable and 900 times less abundant that proteins and spanned a higher dynamic range [55]. Also post-translational modifications such as ubiquitination and different degradation rates in proteins, may also affect the mRNA/protein correlation [56].

- Finally, effect of the data analysis can also lead to different results bringing extrinsic noise that could influence the results.

Bearing in mind these potential drawbacks, a joint analysis of the transcriptomic and proteomic data can provide useful insights into AD pathogenesis. Several integration data strategies have already been suggested [57]. As previously reported, we have merged the transcriptomic and proteomic data aiming to extract undetected mechanisms when using the individual datasets in the Tg2576 study [58-63]. Although no direct overlap was found between transcripts and proteins, the significant differences found in both approaches partially share functional context. This refers to biological processes in which the significantly expressed genes and proteins are enriched [64]. Figure D1 shows the biological pathways shared when analyzing transcriptomic and proteomic datasets individually in the Tg2576 study. Additionally, the combined dataset helped us to build a complex network of functional related genes and proteins. This integrated cluster analysis allowed us to explore new relationships between genes and proteins, and developing new hypothesis related to the olfactory deficits occurring during AD progression.

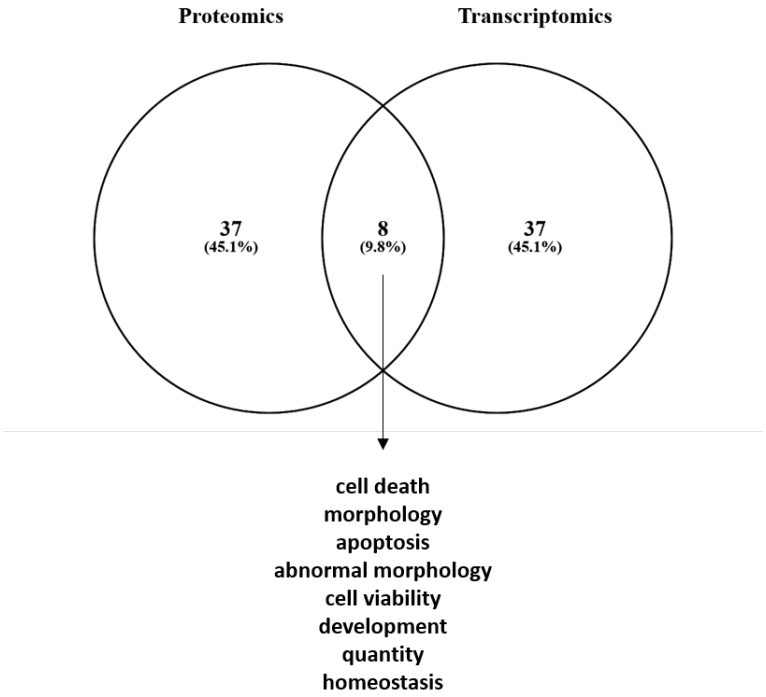

Figure D1: Venn diagram showing the common enriched pathways in both proteomic and transcriptomic studies in the Tg2576 approach (18m).

3. Is there a common pathological mechanism in neurodegeneration? The olfactory bulb as the entry site for prion like propagation

NDs constitute a large set of pathological conditions causing a slow progressive and irreversible loss of neurons and synapses in the nervous system. Although the clinical symptoms across these disorders are very diverse, the pathological accumulation of misfolded proteins plays a central role in the pathogenesis of NDs [65, 66]. In fact, these disorders are also called ''*proteinopathies*'' and include the Aβ plaques in AD, inclusions of the hyperphosphorylated form of tau in different tautopathies such as AD and PSP, α-synuclein aggregates in PD and other synucleinopathies and TDP43 inclusions in ALS and FTD. These abnormal deposits lead to dysfunction and death of neuronal and glial cells disintegrating the neuronal networks [67, 68].

In the olfactory system, these pathological hallmarks have also been found not only in the OB, but also in the OE and olfactory cortex [3, 69, 70]. Indeed, our group has reconfirmed the

detection of some of these pathological aggregates at the level of the OB [71]. These findings clearly mean that a dysregulation in the molecular mechanisms underlying the normal olfactory physiology are happening in several NDs. As previously mentioned, olfactory deficits are a common symptom in patients suffering from NDs. However, this dysfunction occurs in different degrees among the different neurological disorders (Table D1) [4].

Neurodegenerative disorder	N	Age	UPSIT score	% difference from control	p value
Dementia with Lewy bodies	26	77..6	13.6 (NA)	55.7	<0.001
Vascular dementia	13	79.2	12 (19)	50	<0.001
Sporadic Alzheimer's disease	**25**	**69.5**	**18.5 (6.6)**	**46.9**	**<0.001**
Down's syndrome	16	14.3	19.3 (4.7)	46.4	<0.001
Idiopathic Parkison's disease	**50**	**63**	**18.2 (6.8)**	**45.2**	**<0.001**
Parkinsonism-dementia complex of Guam	24	60.5	20.5 (7.3)	43.7	<0.001
Hungtington's disease	12	42	21.2 (7.0)	40.1	<0.001
Vascular parkinsonism	15	73.4	18.3 (4.4)	40	<0.001
Frontotemporal dementia	**14**	**64.9**	**23.3 (3.6)**	**32.7**	**<0.001**
Mild cognitive impairment	21	73.2	24.2 (8.6)	28.8	<0.001
PARK 8 (LRRK2) parkinsonism	14	69.1	21.5 (7.3)	27.6	0.007
REM sleep behaviour disorder	44	70.9	20.4 (6.8)	26.3	<0.001
Multiple system atrophy	29	58.6	26.7 (29)	20.3	<0.001
Incidental Lewy body disease	13	86.2	22.2 (9.1)	19.9	0.004
Cortical degeneration	7	67.1	27.1 (6.6)	19.1	<0.001
Drug-induced parkinsonism	15	65.8	23 (5.3)	14.8	0.072
Spinocerebellar ataxia type 7	28	42.6	24.5 (4.2)	13.2	<0.001
Amyotrophic lateral sclerosis	37	61.7	30.4 (6.3)	12.5	<0.001
X-linked dystonia-parkinsonism	20	44.6	28.7 (5.1)	12.3	0.003
Progressive supranuclear palsy	**21**	**68**	**31 (7.4)**	**12.1**	**0.019**
Multiple sclerosis	25	42.2	33.7 (5.1)	9.3	<0.001
Guacher disease	30	60.9	32.5 (9.3)	8.5	0.01
Essential tremor	29	67.3	31 (4.4)	6.1	Not significant
MPTP-induced parkinsonism	6	26-42	33.9 (2.1)	2.8	Not significant

Table D1: **Olfactory dysfunction in neurodegenerative diseases.** Disorders are ordered in terms of relative differences in UPSIT scores compared with matched controls and are grouped into arbitrary difference categories of >35%, 19-35%, 8-15% and 0-7%. The disorders that constitute the core of this thesis are highlighted in black. Table adapted from *Doty R L, Lancet Neurol 2017; 16: 478-88.*

Accordingly, our findings have shown molecular disturbances in the OB from various NDs and these alterations are more prominent in those disorders with higher clinical olfactory deficits (Figure D2).

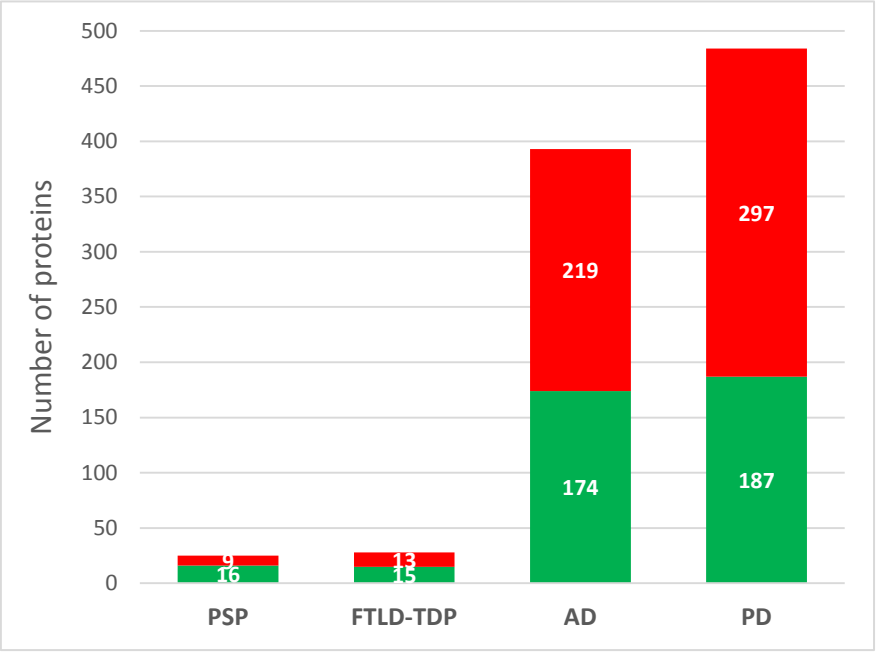

Figure D2: **Differentially expressed proteins in the OB across NDs.** In red: upregulated proteins; in green: downregulated proteins. In accordance to clinical data concerning olfactory deficits, these findings show a strong disruption in olfactory protein mediators in AD and PD. On the other hand the disturbances are much mild in PSP and FTLD-TDP43 subjects. (AD and PD data refer to the total number of differentially expressed protein across the three stages analyzed).

It is important to note that a stage-dependent approach was used in our in AD and PD studies. During the last years, the application of tissue neuroproteomics has been considered an ideal approach to zoom-in where the pathophysiological changes are taking place due to the presence of a proteinopathy. However, most of the workflows focusing on the characterization of human AD and PD neurodegeneration, although informative, have ignored the neuropathological progression of the disease across AD/PD related-brain structures (Table D2).

	Brain area	Subjects	Analytic platform	Reference
AD	Inferior patietal lobule	12 preclinical AD and 12 HC	2D-E-MS/MS	Aluise C D, et al, Neurobiol Dis, 2011
	Cortex	10 AD cases and 10 HC	LC-MS/MS	Andreev V P, et al, J Proteome Res 2012
	Hippocampus	3AD cases and 3 HC	LC-MS/MS	Begcevic I, et al, Clin Proteomics 2013
	Neocortex	10 AD cases and 10 HC	LC-MS/MS	Musunuri S, et al, J Proteome Res, 2014
	Prefrontal cortex	2 AD cases	LC-MS/MS	Drummond E S, et al, Sci Rep, 2015
	Hippocampus	5 AD cases and 5 HC	LC-MS/MS	Kim J H, et al, Sci Rep, 2015
	Hippocampus	35 AD cases and 5 HC	LCM coupled to LC-MS/MS	Hondius D C, et al, Alzheimer & Dementia 2016
	Hippocampus	4 AD cases and 4 HC	LC-MS/MS	Ayyadevara S, et al, Aging Cell 2016
	Prefrontal cortex	59 AD cases and 12 HC	LC-MS/MS	Sweet R A, et al, Mol Cell Proteomics 2016
	Middle frontal gyrus	6 asymptomatic AD, 11 MCI, 13 AD and 5 HC	LC-MS/MS	Hales C M, et al, Proteomics 2016
	Grey matter of frontal gyrus	10 AD cases and 10 HC	LC-MS/MS	Wang S, et al, J Pathol 2017
PD	Substantia nigra	4 PD cases and 4 HC	2D-E MS/MS	Basso M, et al, Proteomics 2004
	Substantia nigra	5 PD cases and 5 HC	2D-E MS/MS	Werner C J, et al, Proteome Science 2008
	Frontal cortex	15 PD cases and 5 HC	2D-E MS/MS	Shi M, et al, J Neuropathol Exp Neurol 2008
	Frontal cortex	12 PD cases and 12 HC	LC-MS/MS	Dumitriu et al, BMC Medical Genomics 2016
	Frontal gyrus	15 PD cases and 5 HC	LCM combined with LC-MS/MS	Shi M et al, AJP 2009
	Substantia nigra	6 PD cases and 4 HC	2D-E MS/MS	Licher V, et al, Journal of Proteomics 2012
	Lenses	3 PD cases and 3 HC	LC-MS/MS	Klettner A et al, Mov Disord, 2017
	Synaptosomal fractions	15 PD cases and 5 HC	Maldi TOF	Shi M, et al, Am J Pathol 2009
	Substantia nigra	5 PD cases and 5 HC	LC-MS/MS	Jin J et al, MCP 2006
	Locus coeruleus	6 PD cases and 6 HC	LC-MS/MS	van Dijk K D et al, Brain Pathology 2011

Table D2: Compilation of recent neuroproteomics research focus on the study of AD and PD pathogenesis. (AD: Alzheimer's disease; HC: healthy controls; MCI: mild cognitive impairment; PD: Parkinson's disease)

In this thesis, the OB sample sets used in AD and PD studies were divided in three groups according to Aβ and LB pathology. We consider that deciphering the progressive proteome-wide alterations that occur in a stage-dependent manner in early-affected OB region, may help to unveil the biochemical pathways affected during the progressive olfactory pathophysiology of AD and PD, identifying potential novel therapeutic targets and biomarkers. Thus, there are some protein subsets commonly deregulated across AD and PD neuropathological stages (24 and 65 proteins in AD and PD, respectively). Moreover, the proteomic workflow used in AD and PD was different from the one used in PSP and FTLD-TDP43 analysis. AD and PD samples were analyzed using a label free approach, this means, without any sample labeling. On the other hand, PSP and FTLD-TDP43 samples were labeled with TMT tags [71]. Although both proteomic approaches differ in the workflow and data analysis, we consider that our findings clearly demonstrate a strong olfactory proteostatic imbalance in AD and PD compared to FTD phenotypes since 20% of the quantified proteome was deregulated in the first two disorders, while only 1% was identified in PSP and FTLD-TDP43. Interestingly, our data obtained at the level of the OB are in

agreement with the current knowledge of olfactory deficits in NDs, demonstrating a clear correlation between molecular and clinical phenotypes.

Given these findings, an important question arises focused on the potential differential disruption of a common neuropathological substrate that could cause these different olfactory deficits [4]. To answer this question, most of the hypothesis have focused on the role of neuropathological hallmarks such as Aβ, and α-synuclein inclusions [3]. However, other hypothesis propose that the exposure to environmental xenobiotics or viruses also represent a potential explanation for olfactory deficits. Although various chemical-metabolizing enzymes are secreted by the Bowman glands to protect brain invasion and epithelial damage by these agents, some of them are still capable of invading the brain via the olfactory receptors, perineural spaces or the lymphatic channels of the neuroepithelium [73]. On the other hand, damages in the neurotransmitter systems that affect olfaction, either directly by influencing neural transmission or microglial function or, indirectly, altering the regeneration in the OE are a potential explanation for the similarities and differences in olfactory function among NDs [4]. For instance, defects in the forebrain cholinergic system have been suggested [74, 75]. Correlations between the odor identification scores and acetylcholinesterase activity within the hippocampal formation, amygdala and neocortex have been found in PD patients [76]. In this sense, as Brain-derived neurotrophic factor (BDNF) signaling is directly involved in the survival of cholinergic neurons, the characterization of the functional BDNF interactome at the level of the OB might provide mechanistic clues in the elucidation of olfactory impairments in AD and PD. In this context, network-driven proteomics has allow to detect some differential functional interactors of BDNF in AD and PD subjects at the level of the OB (Figure D3), suggesting that these protein alterations may differentially compromised the integrity of cholinergic pathways in both neurological syndromes. In addition, other modest correlations have been found between dopamine levels and odor tests scores [77].

AD (Braak I-II)

A

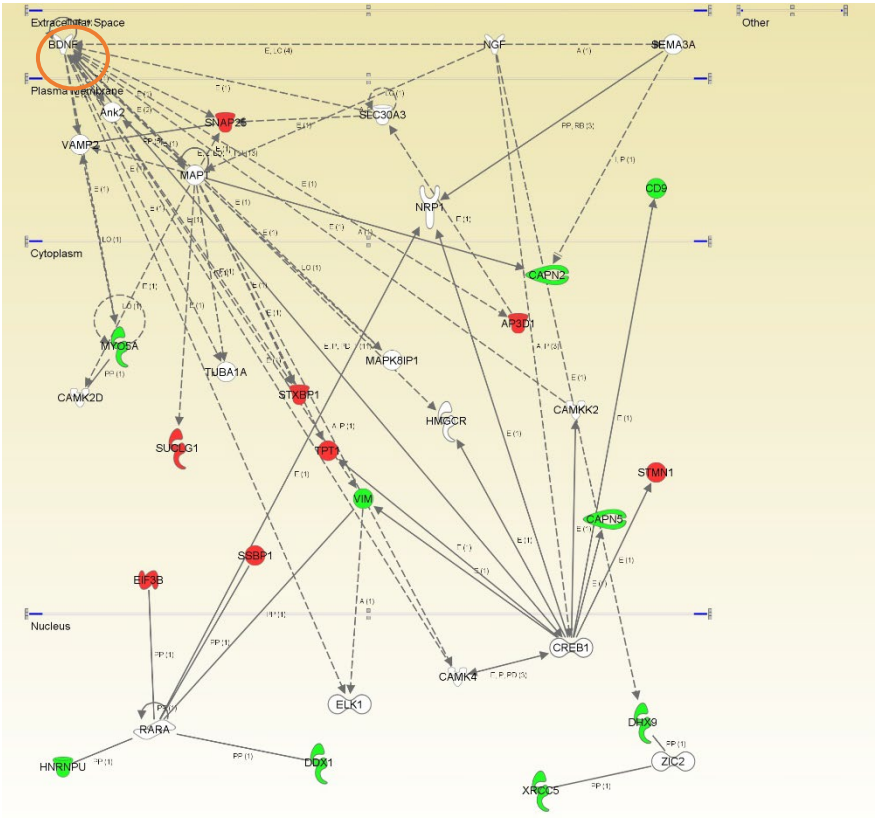

AD (Braak III-IV)

B

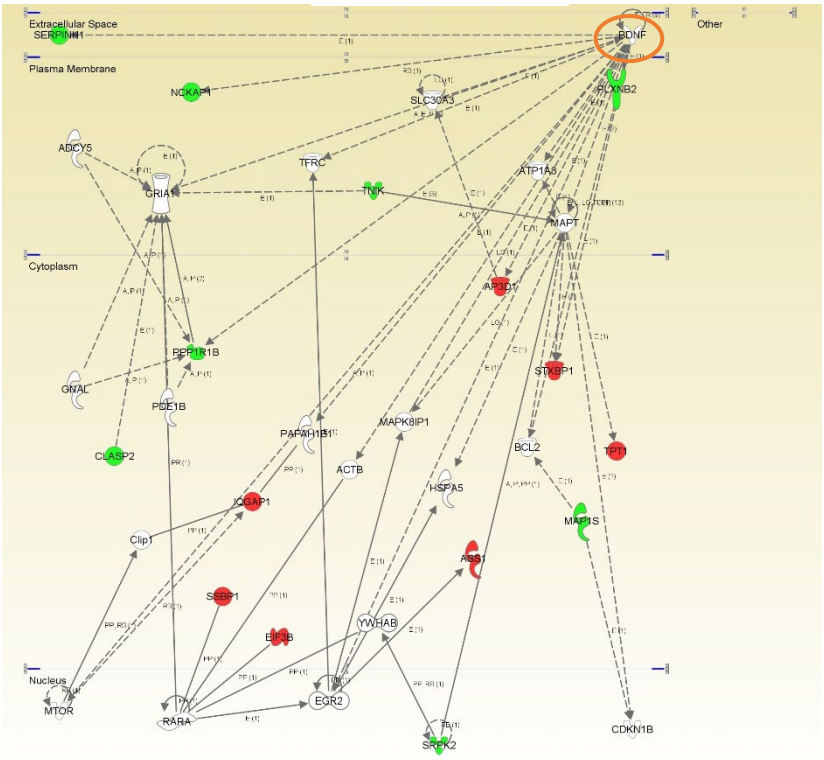

AD (Braak V-VI)

C

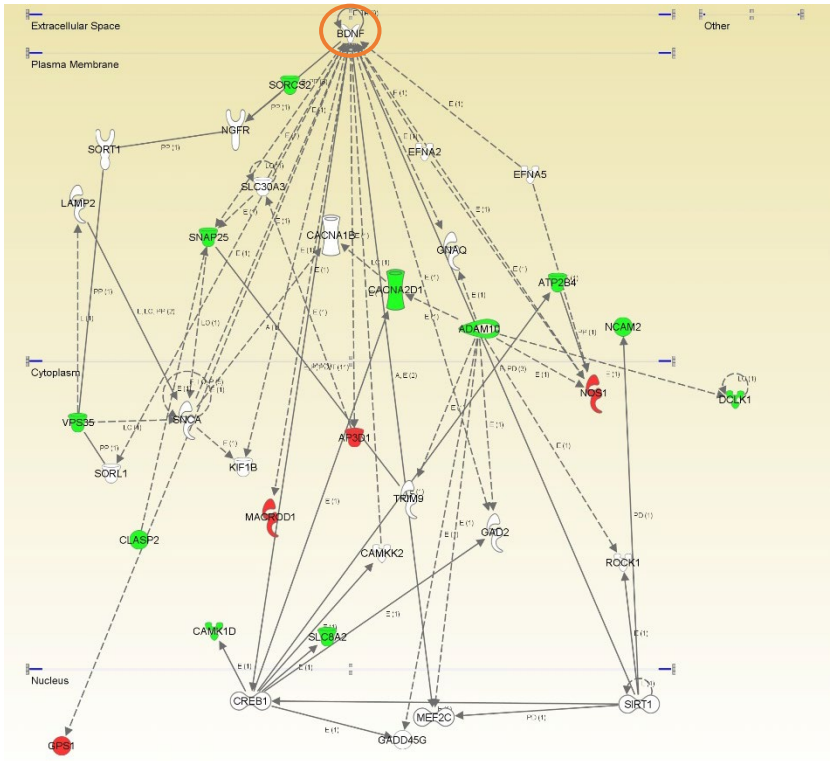

Figure D3: Modulation of the BDNF functional interactome across AD stages at the level of OB. Adaptation of BDNF functional network in initial AD (Braak I-II) (A), intermediate AD (Braak III-IV) (B) and advanced AD (Braak V-VI) (C). Continuous lines represent direct interactions, while discontinuous lines correspond to indirect functional interactions. Up-regulated molecules in red, and down-regulated molecules in green. (See complete legend at: http://ingenuity.force.com/ipa/articles/Feature_Description/Legend).

At this point, data-mining of the results generated in this thesis might help decipher common or specific altered molecular mechanisms occurring in the OB among different NDs. Due to technical and annotation reasons, the most abundant OB proteome has been analyzed in this work and other disturbances than the reported here may be participating in the neurodegenerative process. Interestingly, our wide analysis among 4 different neurological disorders has not shown any common deregulated substrate in this region (Figure D4). Nevertheless, data mining using bioinformatics predicted tools revealed that common molecular

pathways related to cell death and survival were predictively impaired in this olfactory structure across the different NDs (Table D3).

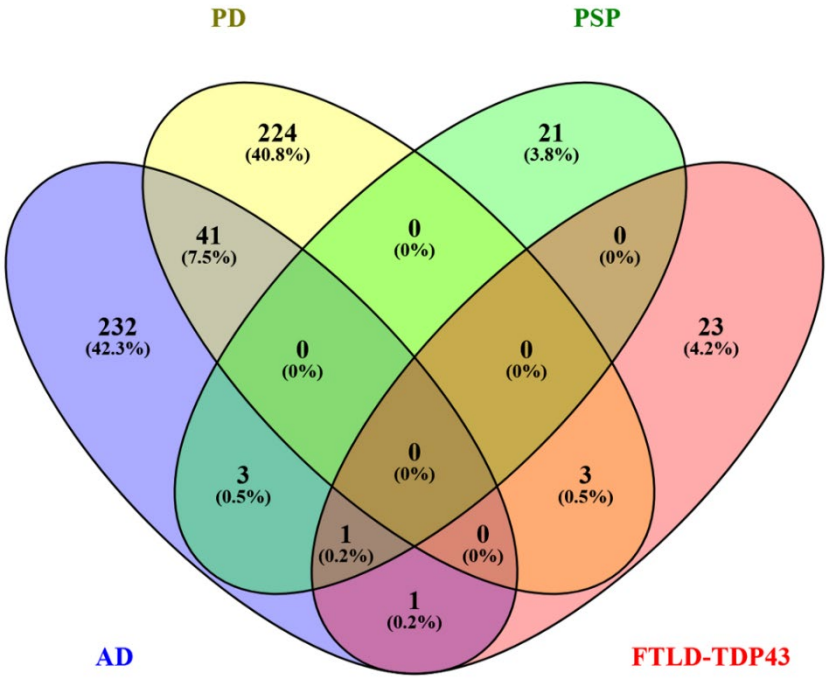

Figure D4: **Venn diagram showing the molecular disturbances occurring at the level of the OB in AD, PD, FTLD-TDP43 and PSP.** No common differences are observed in the 4 neurological syndromes.

Disease	Category	Number of molecules	p value	Molecules
Low AD	Cell death and survival	54	3,07E-09	CD81, EEF1A1, EPHX2, STMN1, RPS7, NSF, USP7, EIF3B, EZR, COMT, JUP, ITGB4, STXBP1, PON2, PSMB5, PPP1R1B, PLEC, RDX, L1CAM, LYPLA2, CDH2, CD9, PSMD12, S100B, SORCS2, SCRIB, CAPN2, CTTN, PTPRA, XRCC5, NOS1, APOE, ARHGEF7, RAB35, DYNC1I1, DMD, ERC1, MYH11, CLIC4, SF3B3, CUL3, TNC, YES1, PHGDH, CD38, DHX9, TPT1, ANXA4, VIM, SNAP25, SF3B2, SERPINH1, COX5A, MSN
Intermediate AD	Cell death and survival	56	4,70E-08	CAMK1D, ASS1, TUBB, STMN1, CACYBP, CTBP1, USP7, SRPK2, EIF3B, MAP1S, GFAP, ANXA7, ITGB4, PRKRA, MIF, STXBP1, PPP1R1B, PHB2, BASP1, TXN2, GNAO1, PSMD12, S100B, SORCS2, PNP, PTPRA, MYH11, FNTA, RAD50, CUL3, TNC, YES1, SERPINB9, ARRB1, HSPE1, CD38, BCAP31, COL18A1, RPS5, PCBP2, NCKAP1, TSTA3, GSTM1, NAE1, TPT1, SOD1, ACLY, OTUB1, CALM1 (includes others), SF3B2, NDUFV2, TUBB6, SERPINH1, COX5A, PIN1, ATP2B4
High AD	Cell death and survival	66	5,77E-08	EHD3, CAMK1D, ELAVL1, GLO1, MYO18A, STMN1, USP7, EIF3B, MAP2K2, COMT, MAP1S, JUP, PSMC2, STXBP1, PON2, PPP1R1B, PHB2, RAC1, RDX, TPM3, GSN, LYPLA2, UBE2L3, CDH2, BASP1, FUS, HNRNPA1, S100B, PSMD12, GNAO1, SORCS2, ALCAM, NOS1, APOE, TOLLIP, DYNC1I1, HYOU1, CUL3, YES1, SERPINB9, ARRB1, CDK5, HSPE1, PCBP2, COL18A1, BCAP31, TSTA3, CD59, DCTN3, TPT1, TRIM28, TRIM2, SOD1, SNAP25, FAH, OTUB1, FDPS, CALM1 (includes others), PRKAR2B, HNRNPH1, COX5A, CD44, PIN1, ATP2B4, LRP1, LANCL2
LBDL	Cell death and survival	49	3,65E-03	GDA, RACK1, PSMC5, ANK1, CACYBP, CSE1L, GPX4, CALB1, HUWE1, MYO6, PON2, EEF2, COPS5, GRIA2, AGAP3, CAPRIN1, XRCC5, DECR1, PA2G4, GPX1, PCMT1, CTNNA1, ILF2, DMD, COL4A2, EIF4G1, MCAM, PSMA3, HNRNPC, STAT1, KYAT1, GMFB, RAD23B, PPP3CA, ABCB1, CALR, RHOC, SNCG, F3, CISD2, ANP32A, LOC102724788/PRODH, LIMS1, CIRBP, NT5E, COX5A, EIF2AK2, CTNND1, LANCL2
LBDE	Cell death and survival	44	1,26E-03	NPM1, EHD3, PA2G4, EEF1A2, GPX1, RACK1, CTNNA1, ILF2, DMD, DNAJB2, COL4A2, EEF1D, ANK1, RPS7, CACYBP, MCAM, EZR, CD38, STAM, GPX4, COL18A1, GMFB, HUWE1, KRT14, EHD1, CALR, PSMB5, EEF2, RHOC, GRIA2, DMTN, SNCG, ADAR, F3, ARHGDIB, ANP32A, LOC102724788/PRODH, LIMS1, ATP1A2, GNAO1, COX5A, AGAP3, EIF5A, EIF2AK2, AKR1B1, PTPRA, ARHGAP1, XRCC5
LBDN	Cell death and survival	69	8,02E-05	MYH9, EHD3, GDA, EEF1A2, RACK1, DNAJB2, PSMC5, RPS7, CACYBP, HDAC6, ALDH1A1, ITIH4, CSE1L, EZR, GPX4, CALB1, HEBP2, PGRMC1, EHD1, PSMB5, PON2, EEF2, GRIA2, DMTN, ARHGDIB, RAP1GAP, PNP, AGAP3, EIF5A, AARS, AGRN, AKR1B1, ARHGAP1, XRCC5, HSD17B10, DECR1, ARMC10, PA2G4, CTNNA1, ILF2, DMD, COL4A2, CD55, ARRB1, COL6A1, NCS1, HNRNPC, STAT1, LONP1, PPP3CA, GMFB, KRT14, CALR, LETM1, RHOC, TRIM28, SNCG, F3, TPP2, LAMB2, ANP32A, LOC102724788/PRODH, HNRNPH1, LIMS1, CIRBP, ATP1A2, COX5A, EIF2AK2, CTNND1
FTLD-TDP43	Cell death and survival	10	0,00699	PRDX6, RPL13A, COL6A1, NEFM, RPS11, GSK3A, VGF, PRKDC, PPP1R1B, RRAS
PSP	Cell death and survival	6	0,00293	PLEKHA7, PSIP1, GLS, ATP2B2, HSPB6

Table D3. OB cell death and survival related molecules altered in the 4 NDs analyzed are shown. (AD: Alzheimer's disease; LBDL: Lewy body disease - Limbic stage; LBDE: Lewy body disease - Early neocortical stage; LBDN: Lewy body disease – Neocortical stage; FTLD-TDP43: frontotemporal lobar degeneration TDP43; PSP: progressive supranuclear palsy).

Moreover, proteome-scale interactome networks based on the differentially expressed proteomes during NDs progression suggested that central functioning of several cell survival-related mediators were impaired at the level of the OB. Interestingly, although PSP and FTLD-TDP disorders carry mild olfactory impairments and OB proteome alterations, we were able to see some disturbances across different cell death and survival-related pathways. Additionally, distinct molecular impairments across specific signaling cascades were observed between NDs. For instance, the behaviour of the MAPK axis activation significantly differed across the different NDs considered in this study. Although it has been well defined as cell survival factor, it has also been demonstrated that ERK is involved in neuronal cell death induction, APP processing, and Tau and TDP43 phosphorylation [19-21, 78, 79]. At the level of the OB, ERK and its upstream

substrate MEK activation levels were decreased in PD, PSP and FTLD-TDP43. On the other hand, in human AD, an increase in the phosphorylated levels was observed. Therefore, these data clearly demonstrate that the neurodegenerative process differentially impacts on the olfactory MAPK pathway across NDs.

Other important cell death-related cascades were suggested as potential mediators of olfactory deficits in neurodegeneration. Again, a different pattern was observed between AD and the rest of NDs in the p38 MAPK axis. While no changes were observed in PSP and FTLD-TDP disorders and only a downregulation of upstream MKK3 and MKK6 levels were detected in PD, a disruption across the entire p38 MAPK axis was observed across AD stages. On the other hand, a similar pattern was observed for the PDK1/PKC cascade, which was mainly inactivated in all NDs analyzed, suggesting a potential common molecular mechanism in olfactory deficits across neurodegenerative phenotypes.

In this sense, it has been recently suggested that a common mechanism involving non-cell autonomous spreading of Aβ and α-synuclein inclusions might play an important role in the pathogenesis of two clinically different disorders such as AD and PD [9]. In addition, as olfactory disturbances are known to appear at very early stages of the neurodegenerative process, it has also been suggested that the OB might be the starting point of the pathology and then, spread through other brain regions [80]. Although we are aware that our earliest neuropathological stages in the AD and PD analysis are probably already late, we have compared the OB proteins differentially expressed in both diseases aiming to discover any common protein mediators between them. Interestingly, as it will be discussed later on in the ‘’Perspectives’’ headline, we did observed some common proteomic alterations between AD and PD in these two apparently clinically different disorders which, as mentioned before, are those who carry the higher olfactory dysfunction (Figure D5). Finally, only two *(Cox5a and Clasp2*) were aberrantly deregulated across the three stages in both diseases. The first one, *Cox5a* (cytochrome c oxidase subunit 5a), constitutes a subunit of the mitochondrial cytochrome oxidase [81]. In this sense,

mitochondrial dysfunction is a well-known pathological hallmark of neurodegeneration [82-84] and in fact, Aβ, tau and α-synuclein have been demonstrated to exert detrimental effects on mitochondria [85]. Here, its deregulation together with other mitochodrial-related proteins reflects an impairment in mitochondrial function and in redox signaling that might directly or indirectly participate in olfactory deficits. On the other hand, *Clasp2* (CLIP-associating protein 2) belongs to the family of cytoplasmic linker-associated proteins (CLASPs) which exert a great number of functions being mainly regulators of microtubule dynamics [86]. Interestingly, there is strong evidence that *Clasp2* is a key regulator of dendrite outgrowth [87, 88], neuronal migration and polarity in neurons [89]. Thus, the drop in *Clasp2* levels might provoque functional alterations in olfactory synaptic activity and formation. Consequently, the decreased levels of this protein in both AD and PD suggest that potential impairments in synaptic transmission are occurring at the level of the OB. Since no research has been focused on the specific role of these two proteins in the olfactory system, it remains to be elucidated whether they could be mediators of the Aβ and α-synuclein inclusions spreading or are secondary manifestations of previous damage associated with olfactory deficits.

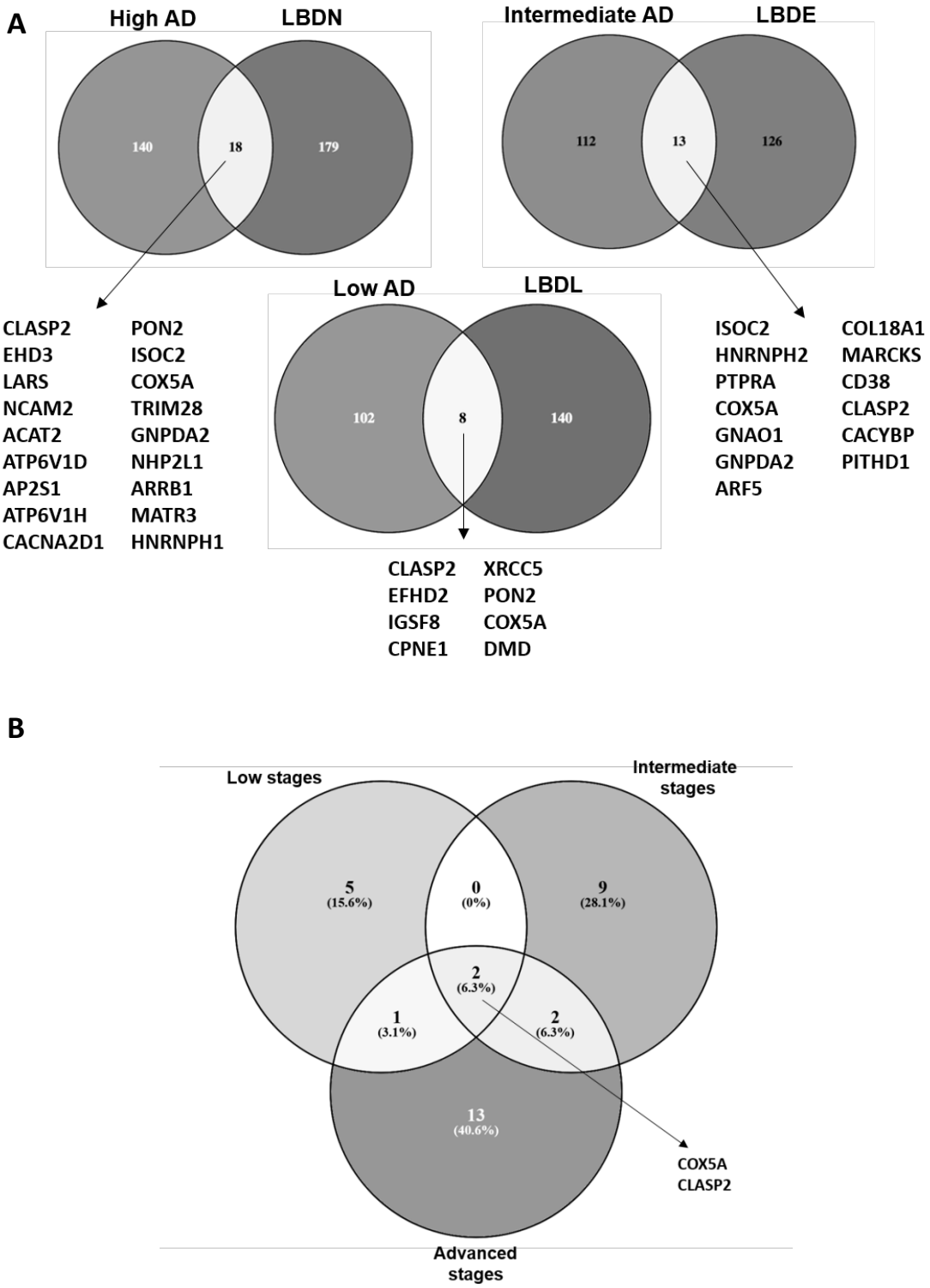

Figure D5: A) Common alterations in AD and PD stages. B) Alterations occuring in both pathologies across the three stages of the disease (*Cox5a and Clasp2*). (LBDL: Lewy body disease - Limbic stage; LBDE: Lewy body disease - Early neocortical stage; LBDN: Lewy body disease – Neocortical stage).

4. GNPDA2 as a potential biomarker of PD

Despite the great efforts and advances aiming to understand the pathological process of NDs, effective treatments are still lacking. This is also due to the relatively late diagnosis of these disorders, meaning that when patients become aware of their symptoms and seek medical advice, the neurodegenerative process is already wide spread through the CNS. There is an urgent need to find early stage biomarkers to define state of a disease condition and thus, give more specific diagnosis. For that, CSF and serum constitute the most valuable samples in terms of availability, although the first one even represents a more faithful source due to its close spatial relation with the CNS [90]. In this sense, an interesting inverse correlation between GNPDA2 and α-synuclein at CSF level has been discovered from olfactory proteomics datasets in PD. GNPDA2 is an allosteric enzyme that catalyzes the reversible reaction converting D-glucosamine-6-phosphate into D-fructose-6-phosphate and ammonia (www.uniprot.org/uniprot/Q8TDQ7). In this sense, ammonia is known to be a potent neurotoxin causing negative effects on the CNS. It has been demonstrated that at high concentration, ammonia produces deleterious effects to the cell such as mitochondrial dysfunction, disruption in cellular energy metabolism or even deffects in neurontransmission [91]. In fact, ammonia is considered a toxic factor with great relevance in AD [92]. In accordance, it has been demonstrated that this product is elevated in the blood and brain from patients suffering from AD [93]. One of the suggested hypothesis to explain this increase in ammonia levels has been the impairment of the glutamine synthetase, which activity is known to decrease with age and also, in AD progression [94]. In mammalian brains, ammonia is mainly derived from the metabolisms of putative neurotransmitters glutamate and asparte, and monoamines. Thus, impairments in metabolic enzymes such as monoamine oxidase A (MAO A) have been also proposed as possible ammonia sources [92]. However, no correlation with the GNPDA2 enzyme has been previously characterized. Our data have shown increased levels of this enzyme at both the level of the OB and CSF from PD subjects, suggesting that the potential elevated ammonia

levels in the OB might be causing negative effects in the CNS of these patients [95]. On the contrary, serum GNPDA2 levels were significantly decreased in PD population. This inverse pattern across fluids has been previously described for other proteins in the PD context [96] and damage in the blood-brain barrier (BBB) may be a potential cause [97]. Finally, despite the well-known damage that ammonia causes in the CNS, such as deficits in excitatory glutamatergic and GABAergic neurotransmission, inflammatory responses, and memory impairments [98], little attention has been paid to this field in NDs, apart from AD. As it will be discussed in the ''Perspectives'' headline, we considered that GNPDA2 constitutes a potential secretable biomarker to be studied in the neurodegenerative process.

References

[1] Huttenbrink, K. B., Hummel, T., Berg, D., Gasser, T., Hahner, A., Olfactory dysfunction: common in later life and early warning of neurodegenerative disease. *Dtsch Arztebl Int* 2013, *110*, 1-7, e1.
[2] Alves, J., Petrosyan, A., Magalhães, R., Olfactory dysfunction in dementia. *World Journal of Clinical Cases : WJCC* 2014, *2*, 661-667.
[3] Attems, J., Walker, L., Jellinger, K. A., Olfactory bulb involvement in neurodegenerative diseases. *Acta Neuropathol* 2014, *127*, 459-475.
[4] Doty, R. L., Olfactory dysfunction in neurodegenerative diseases: is there a common pathological substrate? *Lancet Neurol* 2017, *16*, 478-488.
[5] Doty, R. L., Olfaction in Parkinson's disease and related disorders. *Neurobiol Dis* 2012, *46*, 527-552.
[6] Jellinger, K. A., Attems, J., Alzheimer pathology in the olfactory bulb. *Neuropathol Appl Neurobiol* 2005, *31*, 203.
[7] McLaughlin, N. C., Westervelt, H. J., Odor identification deficits in frontotemporal dementia: a preliminary study. *Arch Clin Neuropsychol* 2008, *23*, 119-123.
[8] Orasji, S. S., Mulder, J. L., de Bruijn, S. F., Wirtz, P. W., Olfactory dysfunction in behavioral variant frontotemporal dementia. *Clin Neurol Neurosurg* 2016, *141*, 106-110.
[9] Goedert, M., NEURODEGENERATION. Alzheimer's and Parkinson's diseases: The prion concept in relation to assembled Abeta, tau, and alpha-synuclein. *Science* 2015, *349*, 1255555.
[10] Rey, N. L., Wesson, D. W., Brundin, P., The olfactory bulb as the entry site for prion-like propagation in neurodegenerative diseases. *Neurobiol Dis* 2018, *109*, 226-248.
[11] Heemels, M. T., Neurodegenerative diseases. *Nature* 2016, *539*, 179.
[12] Cummings, J., Lee, G., Ritter, A., Zhong, K., Alzheimer's disease drug development pipeline: 2018. *Alzheimers Dement (N Y)* 2018, *4*, 195-214.
[13] Dawson, T. M., Golde, T. E., Lagier-Tourenne, C., Animal models of neurodegenerative diseases. *Nat Neurosci* 2018, *21*, 1370-1379.
[14] Borchelt, D. R., Thinakaran, G., Eckman, C. B., Lee, M. K.*, et al.*, Familial Alzheimer's disease-linked presenilin 1 variants elevate Abeta1-42/1-40 ratio in vitro and in vivo. *Neuron* 1996, *17*, 1005-1013.
[15] Hsiao, K., Chapman, P., Nilsen, S., Eckman, C.*, et al.*, Correlative memory deficits, Abeta elevation, and amyloid plaques in transgenic mice. *Science* 1996, *274*, 99-102.
[16] Lachen-Montes, M., Gonzalez-Morales, A., de Morentin, X. M., Perez-Valderrama, E.*, et al.*, An early dysregulation of FAK and MEK/ERK signaling pathways precedes the beta-amyloid deposition in the olfactory bulb of APP/PS1 mouse model of Alzheimer's disease. *J Proteomics* 2016, *148*, 149-158.
[17] Palomino-Alonso, M., Lachen-Montes, M., Gonzalez-Morales, A., Ausin, K.*, et al.*, Network-Driven Proteogenomics Unveils an Aging-Related Imbalance in the Olfactory IkappaBalpha-NFkappaB p65 Complex Functionality in Tg2576 Alzheimer's Disease Mouse Model. *Int J Mol Sci* 2017, *18*.
[18] Armendariz, B. G., Masdeu Mdel, M., Soriano, E., Urena, J. M., Burgaya, F., The diverse roles and multiple forms of focal adhesion kinase in brain. *Eur J Neurosci* 2014, *40*, 3573-3590.
[19] Dehvari, N., Isacsson, O., Winblad, B., Cedazo-Minguez, A., Cowburn, R. F., Presenilin regulates extracellular regulated kinase (Erk) activity by a protein kinase C alpha dependent mechanism. *Neurosci Lett* 2008, *436*, 77-80.
[20] Subramaniam, S., Zirrgiebel, U., von Bohlen Und Halbach, O., Strelau, J.*, et al.*, ERK activation promotes neuronal degeneration predominantly through plasma membrane damage and independently of caspase-3. *J Cell Biol* 2004, *165*, 357-369.
[21] Cheung, E. C., Slack, R. S., Emerging role for ERK as a key regulator of neuronal apoptosis. *Sci STKE* 2004, *2004*, Pe45.

[22] Meadowcroft, M. D., Connor, J. R., Yang, Q. X., Cortical iron regulation and inflammatory response in Alzheimer's disease and APPSWE/PS1DeltaE9 mice: a histological perspective. *Front Neurosci* 2015, *9*, 255.
[23] Baker, M. S., Ahn, S. B., Mohamedali, A., Islam, M. T.*, et al.*, Accelerating the search for the missing proteins in the human proteome. *Nat Commun* 2017, *8*, 14271.
[24] Aso, E., Lomoio, S., Lopez-Gonzalez, I., Joda, L.*, et al.*, Amyloid generation and dysfunctional immunoproteasome activation with disease progression in animal model of familial Alzheimer's disease. *Brain Pathol* 2012, *22*, 636-653.
[25] Irizarry, M. C., McNamara, M., Fedorchak, K., Hsiao, K., Hyman, B. T., APPSw transgenic mice develop age-related A beta deposits and neuropil abnormalities, but no neuronal loss in CA1. *J Neuropathol Exp Neurol* 1997, *56*, 965-973.
[26] Kitazawa, M., Medeiros, R., Laferla, F. M., Transgenic mouse models of Alzheimer disease: developing a better model as a tool for therapeutic interventions. *Curr Pharm Des* 2012, *18*, 1131-1147.
[27] Sasaguri, H., Nilsson, P., Hashimoto, S., Nagata, K.*, et al.*, APP mouse models for Alzheimer's disease preclinical studies. *Embo j* 2017, *36*, 2473-2487.
[28] Blesa, J., Przedborski, S., Parkinson's disease: animal models and dopaminergic cell vulnerability. *Front Neuroanat* 2014, *8*, 155.
[29] Koprich, J. B., Kalia, L. V., Brotchie, J. M., Animal models of alpha-synucleinopathy for Parkinson disease drug development. *Nat Rev Neurosci* 2017, *18*, 515-529.
[30] Philips, T., Rothstein, J. D., Rodent Models of Amyotrophic Lateral Sclerosis. *Curr Protoc Pharmacol* 2015, *69*, 5.67.61-21.
[31] White, M. A., Kim, E., Duffy, A., Adalbert, R.*, et al.*, TDP-43 gains function due to perturbed autoregulation in a Tardbp knock-in mouse model of ALS-FTD. *Nat Neurosci* 2018, *21*, 552-563.
[32] Martiskainen, H., Viswanathan, J., Nykanen, N. P., Kurki, M.*, et al.*, Transcriptomics and mechanistic elucidation of Alzheimer's disease risk genes in the brain and in vitro models. *Neurobiol Aging* 2015, *36*, 1221.e1215-1228.
[33] Annese, A., Manzari, C., Lionetti, C., Picardi, E.*, et al.*, Whole transcriptome profiling of Late-Onset Alzheimer's Disease patients provides insights into the molecular changes involved in the disease. *Sci Rep* 2018, *8*, 4282.
[34] Borrageiro, G., Haylett, W., Seedat, S., Kuivaniemi, H., Bardien, S., A review of genome-wide transcriptomics studies in Parkinson's disease. *Eur J Neurosci* 2018, *47*, 1-16.
[35] Craft, G. E., Chen, A., Nairn, A. C., Recent advances in quantitative neuroproteomics. *Methods* 2013, *61*, 186-218.
[36] Moya-Alvarado, G., Gershoni-Emek, N., Perlson, E., Bronfman, F. C., Neurodegeneration and Alzheimer's disease (AD). What Can Proteomics Tell Us About the Alzheimer's Brain? *Mol Cell Proteomics* 2016, *15*, 409-425.
[37] Hosp, F., Mann, M., A Primer on Concepts and Applications of Proteomics in Neuroscience. *Neuron* 2017, *96*, 558-571.
[38] Bayes, A., Grant, S. G., Neuroproteomics: understanding the molecular organization and complexity of the brain. *Nat Rev Neurosci* 2009, *10*, 635-646.
[39] Scifo, E., Calza, G., Fuhrmann, M., Soliymani, R.*, et al.*, Recent advances in applying mass spectrometry and systems biology to determine brain dynamics. *Expert Rev Proteomics* 2017, *14*, 545-559.
[40] Lachen-Montes, M., Zelaya, M. V., Segura, V., Fernandez-Irigoyen, J., Santamaria, E., Progressive modulation of the human olfactory bulb transcriptome during Alzheimer s disease evolution: novel insights into the olfactory signaling across proteinopathies. *Oncotarget* 2017, *8*, 69663-69679.
[41] Lachen-Montes, M., Gonzalez-Morales, A., Zelaya, M. V., Perez-Valderrama, E.*, et al.*, Olfactory bulb neuroproteomics reveals a chronological perturbation of survival routes and a disruption of prohibitin complex during Alzheimer's disease progression. *Sci Rep* 2017, *7*, 9115.

[42] Liu, Y., Beyer, A., Aebersold, R., On the Dependency of Cellular Protein Levels on mRNA Abundance. *Cell* 2016, *165*, 535-550.
[43] Chen, G., Gharib, T. G., Huang, C. C., Taylor, J. M.*, et al.*, Discordant protein and mRNA expression in lung adenocarcinomas. *Mol Cell Proteomics* 2002, *1*, 304-313.
[44] Pascal, L. E., True, L. D., Campbell, D. S., Deutsch, E. W.*, et al.*, Correlation of mRNA and protein levels: cell type-specific gene expression of cluster designation antigens in the prostate. *BMC Genomics* 2008, *9*, 246.
[45] Gygi, S. P., Rochon, Y., Franza, B. R., Aebersold, R., Correlation between protein and mRNA abundance in yeast. *Mol Cell Biol* 1999, *19*, 1720-1730.
[46] Yeung, E. S., Genome-wide correlation between mRNA and protein in a single cell. *Angew Chem Int Ed Engl* 2011, *50*, 583-585.
[47] Ghazalpour, A., Bennett, B., Petyuk, V. A., Orozco, L.*, et al.*, Comparative analysis of proteome and transcriptome variation in mouse. *PLoS Genet* 2011, *7*, e1001393.
[48] Tian, Q., Stepaniants, S. B., Mao, M., Weng, L.*, et al.*, Integrated genomic and proteomic analyses of gene expression in Mammalian cells. *Mol Cell Proteomics* 2004, *3*, 960-969.
[49] Budnik, B., Levy, E., Harmange, G., Slavov, N., SCoPE-MS: mass spectrometry of single mammalian cells quantifies proteome heterogeneity during cell differentiation. *Genome Biol* 2018, *19*, 161.
[50] Sharma, K., Schmitt, S., Bergner, C. G., Tyanova, S.*, et al.*, Cell type- and brain region-resolved mouse brain proteome. *Nat Neurosci* 2015, *18*, 1819-1831.
[51] Espina, V., Wulfkuhle, J. D., Calvert, V. S., VanMeter, A.*, et al.*, Laser-capture microdissection. *Nature Protocols* 2006, *1*, 586.
[52] Kang, H. J., Kawasawa, Y. I., Cheng, F., Zhu, Y.*, et al.*, Spatio-temporal transcriptome of the human brain. *Nature* 2011, *478*, 483-489.
[53] Wang, E. T., Sandberg, R., Luo, S., Khrebtukova, I.*, et al.*, Alternative isoform regulation in human tissue transcriptomes. *Nature* 2008, *456*, 470-476.
[54] Mortazavi, A., Williams, B. A., McCue, K., Schaeffer, L., Wold, B., Mapping and quantifying mammalian transcriptomes by RNA-Seq. *Nat Methods* 2008, *5*, 621-628.
[55] Schwanhausser, B., Busse, D., Li, N., Dittmar, G.*, et al.*, Global quantification of mammalian gene expression control. *Nature* 2011, *473*, 337-342.
[56] Maier, T., Guell, M., Serrano, L., Correlation of mRNA and protein in complex biological samples. *FEBS Lett* 2009, *583*, 3966-3973.
[57] Ritchie, M. D., Holzinger, E. R., Li, R., Pendergrass, S. A., Kim, D., Methods of integrating data to uncover genotype-phenotype interactions. *Nat Rev Genet* 2015, *16*, 85-97.
[58] Peng, Z., He, S., Gong, W., Xu, F.*, et al.*, Integration of proteomic and transcriptomic profiles reveals multiple levels of genetic regulation of salt tolerance in cotton. *BMC Plant Biol* 2018, *18*, 128.
[59] Delmotte, N., Ahrens, C. H., Knief, C., Qeli, E.*, et al.*, An integrated proteomics and transcriptomics reference data set provides new insights into the Bradyrhizobium japonicum bacteroid metabolism in soybean root nodules. *Proteomics* 2010, *10*, 1391-1400.
[60] McRedmond, J. P., Park, S. D., Reilly, D. F., Coppinger, J. A.*, et al.*, Integration of proteomics and genomics in platelets: a profile of platelet proteins and platelet-specific genes. *Mol Cell Proteomics* 2004, *3*, 133-144.
[61] Sjostedt, E., Sivertsson, A., Hikmet Noraddin, F., Katona, B.*, et al.*, Integration of transcriptomics and antibody-based proteomics for exploration of proteins expressed in specialized tissues. *J Proteome Res* 2018.
[62] Kwon, H. K., Jeong, H., Hwang, D., Park, Z. Y., Comparative proteomic analysis of mouse models of pathological and physiological cardiac hypertrophy, with selection of biomarkers of pathological hypertrophy by integrative Proteogenomics. *Biochim Biophys Acta Proteins Proteom* 2018.

[63] Xiong, Q., Feng, J., Li, S. T., Zhang, G. Y.*, et al.*, Integrated transcriptomic and proteomic analysis of the global response of Synechococcus to high light stress. *Mol Cell Proteomics* 2015, *14*, 1038-1053.
[64] Voillet, V., San Cristobal, M., Pere, M. C., Billon, Y.*, et al.*, Integrated Analysis of Proteomic and Transcriptomic Data Highlights Late Fetal Muscle Maturation Process. *Mol Cell Proteomics* 2018, *17*, 672-693.
[65] Taylor, J. P., Hardy, J., Fischbeck, K. H., Toxic proteins in neurodegenerative disease. *Science* 2002, *296*, 1991-1995.
[66] Gan, L., Cookson, M. R., Petrucelli, L., La Spada, A. R., Converging pathways in neurodegeneration, from genetics to mechanisms. *Nat Neurosci* 2018, *21*, 1300-1309.
[67] Palop, J. J., Chin, J., Mucke, L., A network dysfunction perspective on neurodegenerative diseases. *Nature* 2006, *443*, 768-773.
[68] Seeley, W. W., Crawford, R. K., Zhou, J., Miller, B. L., Greicius, M. D., Neurodegenerative diseases target large-scale human brain networks. *Neuron* 2009, *62*, 42-52.
[69] Duda, J. E., Olfactory system pathology as a model of Lewy neurodegenerative disease. *J Neurol Sci* 2010, *289*, 49-54.
[70] Hubbard, P. S., Esiri, M. M., Reading, M., McShane, R., Nagy, Z., Alpha-synuclein pathology in the olfactory pathways of dementia patients. *J Anat* 2007, *211*, 117-124.
[71] Zelaya, M. V., Perez-Valderrama, E., de Morentin, X. M., Tunon, T.*, et al.*, Olfactory bulb proteome dynamics during the progression of sporadic Alzheimer's disease: identification of common and distinct olfactory targets across Alzheimer-related co-pathologies. *Oncotarget* 2015, *6*, 39437-39456.
[72] Thompson, A., Schafer, J., Kuhn, K., Kienle, S.*, et al.*, Tandem mass tags: a novel quantification strategy for comparative analysis of complex protein mixtures by MS/MS. *Anal Chem* 2003, *75*, 1895-1904.
[73] Doty, R. L., The olfactory vector hypothesis of neurodegenerative disease: is it viable? *Ann Neurol* 2008, *63*, 7-15.
[74] Getchell, M. L., Shah, D. S., Buch, S. K., Davis, D. G., Getchell, T. V., 3-Nitrotyrosine immunoreactivity in olfactory receptor neurons of patients with Alzheimer's disease: implications for impaired odor sensitivity. *Neurobiol Aging* 2003, *24*, 663-673.
[75] Franco, J., Prediger, R. D., Pandolfo, P., Takahashi, R. N.*, et al.*, Antioxidant responses and lipid peroxidation following intranasal 1-methyl-4-phenyl-1,2,3,6-tetrahydropyridine (MPTP) administration in rats: increased susceptibility of olfactory bulb. *Life Sci* 2007, *80*, 1906-1914.
[76] Bohnen, N. I., Muller, M. L., Kotagal, V., Koeppe, R. A.*, et al.*, Olfactory dysfunction, central cholinergic integrity and cognitive impairment in Parkinson's disease. *Brain* 2010, *133*, 1747-1754.
[77] Berendse, H. W., Roos, D. S., Raijmakers, P., Doty, R. L., Motor and non-motor correlates of olfactory dysfunction in Parkinson's disease. *J Neurol Sci* 2011, *310*, 21-24.
[78] Ferrer, I., Blanco, R., Carmona, M., Ribera, R.*, et al.*, Phosphorylated map kinase (ERK1, ERK2) expression is associated with early tau deposition in neurones and glial cells, but not with increased nuclear DNA vulnerability and cell death, in Alzheimer disease, Pick's disease, progressive supranuclear palsy and corticobasal degeneration. *Brain Pathol* 2001, *11*, 144-158.
[79] Li, W., Reeb, A. N., Lin, B., Subramanian, P.*, et al.*, Heat Shock-induced Phosphorylation of TAR DNA-binding Protein 43 (TDP-43) by MAPK/ERK Kinase Regulates TDP-43 Function. *J Biol Chem* 2017, *292*, 5089-5100.
[80] Rey, N. L., Wesson, D. W., Brundin, P., The olfactory bulb as the entry site for prion-like propagation in neurodegenerative diseases. *Neurobiol Dis* 2016.
[81] Balsa, E., Marco, R., Perales-Clemente, E., Szklarczyk, R.*, et al.*, NDUFA4 is a subunit of complex IV of the mammalian electron transport chain. *Cell Metab* 2012, *16*, 378-386.
[82] Arun, S., Liu, L., Donmez, G., Mitochondrial Biology and Neurological Diseases. *Curr Neuropharmacol* 2016, *14*, 143-154.

[83] Smith, E. F., Shaw, P. J., De Vos, K. J., The role of mitochondria in amyotrophic lateral sclerosis. *Neurosci Lett* 2017.
[84] Cabezas-Opazo, F. A., Vergara-Pulgar, K., Perez, M. J., Jara, C.*, et al.*, Mitochondrial Dysfunction Contributes to the Pathogenesis of Alzheimer's Disease. *Oxid Med Cell Longev* 2015, *2015*, 509654.
[85] Briston, T., Hicks, A. R., Mitochondrial dysfunction and neurodegenerative proteinopathies: mechanisms and prospects for therapeutic intervention. *Biochem Soc Trans* 2018, *46*, 829-842.
[86] Lawrence, E. J., Arpag, G., Norris, S. R., Zanic, M., Human CLASP2 specifically regulates microtubule catastrophe and rescue. *Mol Biol Cell* 2018, *29*, 1168-1177.
[87] Beffert, U., Dillon, G. M., Sullivan, J. M., Stuart, C. E.*, et al.*, Microtubule plus-end tracking protein CLASP2 regulates neuronal polarity and synaptic function. *J Neurosci* 2012, *32*, 13906-13916.
[88] Schmidt, N., Basu, S., Sladecek, S., Gatti, S.*, et al.*, Agrin regulates CLASP2-mediated capture of microtubules at the neuromuscular junction synaptic membrane. *J Cell Biol* 2012, *198*, 421-437.
[89] Dillon, G. M., Tyler, W. A., Omuro, K. C., Kambouris, J.*, et al.*, CLASP2 Links Reelin to the Cytoskeleton during Neocortical Development. *Neuron* 2017, *93*, 1344-1358.e1345.
[90] Li, X., Li, T. Q., Andreasen, N., Wiberg, M. K.*, et al.*, The association between biomarkers in cerebrospinal fluid and structural changes in the brain in patients with Alzheimer's disease. *J Intern Med* 2014, *275*, 418-427.
[91] Cooper, A. J., Plum, F., Biochemistry and physiology of brain ammonia. *Physiol Rev* 1987, *67*, 440-519.
[92] Seiler, N., Ammonia and Alzheimer's disease. *Neurochem Int* 2002, *41*, 189-207.
[93] Branconnier, R. J., Dessain, E. C., McNiff, M. E., Cole, J. O., Blood ammonia and Alzheimer's disease. *Am J Psychiatry* 1986, *143*, 1313-1314.
[94] Smith, C. D., Carney, J. M., Starke-Reed, P. E., Oliver, C. N.*, et al.*, Excess brain protein oxidation and enzyme dysfunction in normal aging and in Alzheimer disease. *Proc Natl Acad Sci U S A* 1991, *88*, 10540-10543.
[95] Lachen-Montes, M., Gonzalez-Morales, A., Iloro, I., Elortza, F.*, et al.*, Unveiling the olfactory proteostatic disarrangement in Parkinson's disease by proteome-wide profiling. *Neurobiol Aging* 2018, *73*, 123-134.
[96] Halbgebauer, S., Ockl, P., Wirth, K., Steinacker, P., Otto, M., Protein biomarkers in Parkinson's disease: Focus on cerebrospinal fluid markers and synaptic proteins. *Mov Disord* 2016, *31*, 848-860.
[97] Sweeney, M. D., Sagare, A. P., Zlokovic, B. V., Blood-brain barrier breakdown in Alzheimer disease and other neurodegenerative disorders. *Nat Rev Neurol* 2018, *14*, 133-150.
[98] Adlimoghaddam, A., Sabbir, M. G., Albensi, B. C., Ammonia as a Potential Neurotoxic Factor in Alzheimer's Disease. *Frontiers in Molecular Neuroscience* 2016, *9*, 57.

PERSPECTIVES

This thesis has aimed to analyze the potential molecular disturbances occurring at the level of the OB in view of the widely accepted concept that olfactory dysfunction is one of the earliest symptoms in patients with NDs. Altogether, our results have shown a severe imbalance in the OB proteostasis in AD and PD subjects, while no such important differences where seen in PSP and FTLD-TDP43 ones. These data are hand to hand with the clinical outcomes that these patients have when being subjected to olfactory tests. In this next headline, the drawbacks and future perspectives that this thesis might lead will be discussed.

1. What about other NDs? And, what is happening in the olfactory tract?

As already mentioned before, Doty was able to classify a great number of neurological disorders according to the great or lesser olfactory deficit score when subjecting patients to the UPSIT [1]. Checking the Table D1 in the ''Discussion'' headline, it is worth to note that the disease with greatest olfactory dysfunction is the Dementia with Lewy bodies (DLB). This is one of the most common causes of dementia, although not as common as AD. In fact, the clinical symptoms of DLB can often overlap with those of AD and PD and it is not uncommon to have cases with mixed pathology [2, 3]. Moreover, although LBs are the pathological hallmark of DLB [4], these aggregates may also be found in other pathologies such as PD and multiple systems atrophy (MSA). Still, some distinctions could be made between the deposits in DLB and PD, being the first ones mainly diffusely distributed throughout the cortices of the brain and in PD within the dopaminergic neurons in the substantia nigra [5]. On the other hand, in terms of clinical features, it is sometimes difficult to distinguish between DLB and PD dementia (PDD). Here, the key fact is the temporal relationship between the symptoms. Whereas in DLB, the onset of both parkinsonism and dementia occurs concurrently or within 1 year [6], in PDD the parkinsonism symptoms prior to dementia have been progressing during 10 years [7]. Finally, concerning olfactory deficits, it has been suggested that olfactory testing might be a useful tool for identifying patients with higher risk for developing PD or other LB related disorders [8].

Unfortunately, these tests do not distinguish between PD and DLB. In this sense, we considered that the molecular analysis of the olfactory system of subjects with a post-mortem diagnosis of DLB might help to decipher the potential specific mechanisms occurring at this level in this disease, understanding the pathogenesis of Lewy body-related disorders and leading to the discovery of new biomarkers able to differentiate between DLB, PD and PDD at olfactory level.

On the other hand, it is worth to note that our study has left a considerably important region in the olfactory system to be carefully analyzed. It has been demonstrated that pathological depositions such as Aβ and α-synuclein inclusions are also present in the OT of patients with distinct NDs [9]. As mentioned in the ''Introduction'' headline, the OT is mainly composed by the axons coming from the mitral and tufted cells in the OB. That is why, it may be considered a subcellular fraction of olfactory neurons. This specialized region exerts a very important function being responsible for the connection between the OB and the central brain regions [10]. Thus, the neuronal axons transmit the action potential from the cell body to the synaptic sites of other neuronal cells. Besides, axons are also used as physical channels to transport proteins, lipids or even cellular organelles such as mitochondria or synaptic vesicles. This process is called axonal transport and it is now widely known that is fundamental for the neurons' response to external stimuli [11]. Interestingly, it has recently been demonstrated that mRNAs localize to axons and that translation often occurs in this region to support neuronal functions such as axon growth, maintenance and regeneration after injury. In addition, deficits in axonal transport have recently emerged as a common factor in several NDs [12]. In this sense, we consider that since the OT is the region responsible for the correct transmission of the odor information towards the central brain regions, it is likely that alterations in these processes might be causing part of the deficits in olfaction functionality observed in patients with NDs. One of our next aims is to characterized the OT proteome across different neurological disorders in order to: a) study whether there is a differential mRNA translation rate in this region compared to the one occurring in the OB; b) analyze the potential alterations in protein translation during the neurodegenerative process; c)

assess the existence of commonalities and differences across tauopathies and synucleinopathies; d) discover whether OB deregulated proteome and pathways are also altered in the olfactory axonal bundle.

2. Using Laser Microdissection Capture to describe molecular signatures in the OB cell layers

One of the drawbacks of this study is the loss of information concerning the molecular composition of each OB cell layer. Briefly, it has already been mentioned that the OB is composed by differentiated concentric layers [13]. At this point, it is worth to mention that in whole set of the cases, the samples were obtained from different european brain banks and usually received frozen and placed on an aluminum foil strip aiming to preserve tissue morphology. However, in the majority of cases, OB morphology was lost in the protein extraction phase where mostly the whole tissue was processed. In this sense, the use of LCM, first introduced in 1996 [14], represents a valuable technique for regional or cell specific enrichments. It allows the dissection of small areas of tissue, such as single cells, using a precise laser, leaving the protein content inside the cells intact. Thus, the ability to perform cell-type specific proteomics might help to answer questions about any disease. In fact, this approach has been widely applied in the study of NDs and to characterize the cellular connections in human brain [15-21]. In this case, the application of LCM coupled to MS in the OB would help to further understand the role of olfactory dysfunction in NDs, and even to increase the knowledge about olfactory processing in each OB cell layer. Interestingly, this technique has also been used to specifically isolate the amyloid plaques from human AD brain tissue [22]. In this sense, the presence of amyloid plaques and other pathological protein aggregations has been described in the olfactory system [9]. However, whether those are responsible for olfactory deficits in NDs remains unknown. Altogether, we consider that combining LCM with liquid chromatography (LC) tandem mass spectrometry (MS/MS) might provide useful information about these questions.

3. Using olfactory epithelial cells to understand neurodegeneration. What is happening in peripheral structures prior to the OB?

In the olfactory mucosa, the olfactory neuroepithelium is constituted by olfactory sensory epithelial neurons that are replaced by neurogenesis continuously during adult life. These cells are pluripotent cells that can proliferate in vitro and differentiate into multiple cell types, including neurons and glia [23, 24]. Interestingly, recent research has shown that patients with different types of neuropsychiatric diseases present specific impairments in the functionality of these cells [25, 26]. Hence, it has been suggested that this peripheral tissue might be a useful source of information regarding CNS functionality and about the neuropathology occurring in mental illnesses [27]. In view that olfactory dysfunction occurs in a wide spectrum of NDs, this opens a huge field of research to better understand the neurodegeneration process. In fact, recent evidence suggests that the pathogenesis in PD and other NDs involves trans-synaptic transmission cell to cell via the OB to the substantia nigra and, considering that the olfactory system is one of the gateways to the environment, it seems likely that potential injuries in these OSNs could have an impact in the NDs pathogenesis [28].

Since the OE is accessible for low-risk biopsy [29], our future goal is to study the functionality of the olfactory neuroepithelial cells coming from individuals without underlying neurological disease and from patients suffering from neurological disorders. A simple experiment to compare the intracellular and extracellular proteomes of these cells between healthy and pathological states would give valuable information regarding the cumulative damage gathered in this region during the neurodegenerative process as well as the identification of primary signals of neurodegeneration in life, anticipating potential therapeutic targets for early intervention. In addition, exploring the molecular changes induced by toxic forms of Aβ and α-synuclein in normal cells might also help to understand the aberrant effects that those aggregates produce or not at epithelial level. On the other hand, another interesting approach

would be to analyze what effect has the GNPDA2 chemical reaction involving the formation of ammonia. Since it has already been demonstrated that ammonia exerts a toxic effect in the CNS [30, 31], we consider a relevant approach to study the potential effect that the silencing, under-expression or overexpression of this enzyme, or other common targets discovered in this thesis between AD and PD, might cause in these olfactory cells. In addition, combining these treatments with the Aβ and α-synuclein deposits induction or with the common deregulated protein found in our analysis (*Cox5a and Clasp2*) might help to find common or specific mechanisms across the different NDs. Additionally, ammonia blood levels have been shown to be increased in patients with AD [32]. That is why, next steps will be focused on the study of the levels of this protein in serum samples from AD and other NDs patients by ELISA and/or multiple selection monitoring (MRM). These new findings might help to clarify the sensitivity and selectivity of a potential disease-specific or neurodegeneration biomarker.

Finally, as mentioned in the ''Introduction'' headline, it is worth to remember that the ORs are supposed to reside in these olfactory epithelial cells. The family of ORs is well-known to belong to the largest family of missing proteins [33]. Thus, from a technological point of view, using these cells, we have the opportunity to analyze the biological material where these ORs are expressed at protein level and be able to detect this protein family by MS for the first time, providing new information to the scientific community involved in Human Proteome Project (HPP) [34, 35].

4. A translational point of view: Potential intranasal therapies based on enzyme replacement or specific drug delivery

Although many efforts have been made to understand the pathogenesis of NDs, these remain incurable disorders. In this sense, most of the available treatments for them use either the oral or parenteral route of drug administration. However, the drawback of this kind of administration is the limited accessibility of drug molecules from the blood to the brain [36], in

which the blood-brain barrier (BBB) restricts the entry of almost all the xenobiotics, protein, peptides and other products to protect the brain from any harm [37]. Moreover, the metabolic and degradative processes occurring in these routes also reduce drug availability [38].

In this sense, intranasal (IN) drug delivery is emerging as an alternative route to overpass the BBB and deliver potential therapeutic agents to the brain [39-44]. In fact, the neuroepithelium located in the olfactory region in the nasal cavity is the only portion of the CNS exposed to the external environment [45]. The general mechanism by which a drug is transferred from the nose to the brain, starts in the nasal cavity, where it experiences the mucociliary clearance in the vestibular region [46]. Afterwards, the drug moves to the posterior region of the nasal cavity and then, it is transported to the brain through different pathways including the olfactory nerve pathway, the trigeminal pathway, the lymphatic and vascular pathway and CSF [47]. Although there are some challenges to be faced during IN delivery, such as low membrane permeability or the possibility of enzymatic degradation in the lumen of the nasal cavity, there are already a good number of patents on nose to brain drug delivery systems [48]. Interestingly, concerning NDs, research has focused mainly on AD treatment. In fact, there are lots of studies that have achieved great results in reducing memory impairments and Aβ accumulation in different mouse models [44, 49-54]. Also, in PD mouse models, the IN administration of stem cells has probed to reduce the degenerative effects of rotenone [55] and other drug molecules such as carnosine have attenuated the transcriptomic alterations occurring during PD progression [56]. At this point, it is important to note that a few clinical trials have tested the IN delivery for the treatment NDs. For instance, IN insulin administration has proved to be effective for improving cognition in patients with AD [57]. On the other hand, the IN administration of glutathione, although proved to be safe and tolerable for PD patients, did not cause any differential effect between the healthy and the diseased population [58]. Thus, the treatment of these group of disorders remains a significant challenge. As mentioned before, current drugs act only by reducing the symptoms of the disease and that is why, the research

and the development of drugs acting on the pathological factors of NDs are urgently needed. With our high-throughput analysis, we have been able to detect pathological olfactory substrates that might have an important role in the neurodegenerative process. We consider that this data contribute to increase the list of potential therapeutic agents (protein or peptides) that might be afterwards tested for IN delivery in animal models of neurodegeneration and thus, help to treat or decrease the neurodegenerative process acting in the olfactory system.

References

[1] Doty, R. L., Olfactory dysfunction in neurodegenerative diseases: is there a common pathological substrate? *Lancet Neurol* 2017, *16*, 478-488.
[2] Capouch, S. D., Farlow, M. R., Brosch, J. R., A Review of Dementia with Lewy Bodies' Impact, Diagnostic Criteria and Treatment. *Neurol Ther* 2018.
[3] Toledo, J. B., Cairns, N. J., Da, X., Chen, K.*, et al.*, Clinical and multimodal biomarker correlates of ADNI neuropathological findings. *Acta Neuropathol Commun* 2013, *1*, 65.
[4] Spillantini, M. G., Schmidt, M. L., Lee, V. M., Trojanowski, J. Q.*, et al.*, Alpha-synuclein in Lewy bodies. *Nature* 1997, *388*, 839-840.
[5] Tsuboi, Y., Uchikado, H., Dickson, D. W., Neuropathology of Parkinson's disease dementia and dementia with Lewy bodies with reference to striatal pathology. *Parkinsonism Relat Disord* 2007, *13 Suppl 3*, S221-224.
[6] McKeith, I. G., Boeve, B. F., Dickson, D. W., Halliday, G.*, et al.*, Diagnosis and management of dementia with Lewy bodies: Fourth consensus report of the DLB Consortium. *Neurology* 2017, *89*, 88-100.
[7] Aarsland, D., Kurz, M. W., The epidemiology of dementia associated with Parkinson's disease. *Brain Pathol* 2010, *20*, 633-639.
[8] Driver-Dunckley, E., Adler, C. H., Hentz, J. G., Dugger, B. N.*, et al.*, Olfactory dysfunction in incidental Lewy body disease and Parkinson's disease. *Parkinsonism Relat Disord* 2014, *20*, 1260-1262.
[9] Attems, J., Walker, L., Jellinger, K. A., Olfactory bulb involvement in neurodegenerative diseases. *Acta Neuropathol* 2014, *127*, 459-475.
[10] Sarnat, H. B., Yu, W., Maturation and Dysgenesis of the Human Olfactory Bulb. *Brain Pathol* 2016, *26*, 301-318.
[11] Hirokawa, N., Niwa, S., Tanaka, Y., Molecular motors in neurons: transport mechanisms and roles in brain function, development, and disease. *Neuron* 2010, *68*, 610-638.
[12] Millecamps, S., Julien, J. P., Axonal transport deficits and neurodegenerative diseases. *Nat Rev Neurosci* 2013, *14*, 161-176.
[13] Mori, K., Nagao, H., Yoshihara, Y., The olfactory bulb: coding and processing of odor molecule information. *Science* 1999, *286*, 711-715.
[14] Emmert-Buck, M. R., Bonner, R. F., Smith, P. D., Chuaqui, R. F.*, et al.*, Laser capture microdissection. *Science* 1996, *274*, 998-1001.
[15] Drummond, E. S., Nayak, S., Ueberheide, B., Wisniewski, T., Proteomic analysis of neurons microdissected from formalin-fixed, paraffin-embedded Alzheimer's disease brain tissue. *Sci Rep* 2015, *5*, 15456.
[16] Hondius, D. C., van Nierop, P., Li, K. W., Hoozemans, J. J.*, et al.*, Profiling the human hippocampal proteome at all pathologic stages of Alzheimer's disease. *Alzheimers Dement* 2016, *12*, 654-668.
[17] Mastroeni, D., Sekar, S., Nolz, J., Delvaux, E.*, et al.*, ANK1 is up-regulated in laser captured microglia in Alzheimer's brain; the importance of addressing cellular heterogeneity. *PLoS One* 2017, *12*, e0177814.
[18] Mastroeni, D., Nolz, J., Sekar, S., Delvaux, E.*, et al.*, Laser-captured microglia in the Alzheimer's and Parkinson's brain reveal unique regional expression profiles and suggest a potential role for hepatitis B in the Alzheimer's brain. *Neurobiol Aging* 2018, *63*, 12-21.
[19] Andre, E. M., Daviaud, N., Sindji, L., Cayon, J.*, et al.*, A novel ex vivo Huntington's disease model for studying GABAergic neurons and cell grafts by laser microdissection. *PLoS One* 2018, *13*, e0193409.
[20] Tan, Y., Delvaux, E., Nolz, J., Coleman, P. D.*, et al.*, Upregulation of histone deacetylase 2 in laser capture nigral microglia in Parkinson's disease. *Neurobiol Aging* 2018, *68*, 134-141.

[21] Tagliafierro, L., Bonawitz, K., Glenn, O. C., Chiba-Falek, O., Gene Expression Analysis of Neurons and Astrocytes Isolated by Laser Capture Microdissection from Frozen Human Brain Tissues. *Front Mol Neurosci* 2016, *9*, 72.
[22] Nijholt, D. A., Stingl, C., Luider, T. M., Laser capture microdissection of fluorescently labeled amyloid plaques from Alzheimer's disease brain tissue for mass spectrometric analysis. *Methods Mol Biol* 2015, *1243*, 165-173.
[23] Leung, C. T., Coulombe, P. A., Reed, R. R., Contribution of olfactory neural stem cells to tissue maintenance and regeneration. *Nat Neurosci* 2007, *10*, 720-726.
[24] Matigian, N., Abrahamsen, G., Sutharsan, R., Cook, A. L*., et al.*, Disease-specific, neurosphere-derived cells as models for brain disorders. *Dis Model Mech* 2010, *3*, 785-798.
[25] Mackay-Sim, A., Concise review: Patient-derived olfactory stem cells: new models for brain diseases. *Stem Cells* 2012, *30*, 2361-2365.
[26] Benitez-King, G., Valdes-Tovar, M., Trueta, C., Galvan-Arrieta, T*., et al.*, The microtubular cytoskeleton of olfactory neurons derived from patients with schizophrenia or with bipolar disorder: Implications for biomarker characterization, neuronal physiology and pharmacological screening. *Mol Cell Neurosci* 2016, *73*, 84-95.
[27] Lavoie, J., Sawa, A., Ishizuka, K., Application of olfactory tissue and its neural progenitors to schizophrenia and psychiatric research. *Curr Opin Psychiatry* 2017, *30*, 176-183.
[28] Godoy, M. D., Voegels, R. L., Pinna Fde, R., Imamura, R., Farfel, J. M., Olfaction in neurologic and neurodegenerative diseases: a literature review. *Int Arch Otorhinolaryngol* 2015, *19*, 176-179.
[29] Feron, F., Perry, C., McGrath, J. J., Mackay-Sim, A., New techniques for biopsy and culture of human olfactory epithelial neurons. *Arch Otolaryngol Head Neck Surg* 1998, *124*, 861-866.
[30] Seiler, N., Ammonia and Alzheimer's disease. *Neurochem Int* 2002, *41*, 189-207.
[31] Albrecht, J., in: Lajtha, A., Oja, S. S., Schousboe, A., Saransaari, P. (Eds.), *Handbook of Neurochemistry and Molecular Neurobiology: Amino Acids and Peptides in the Nervous System*, Springer US, Boston, MA 2007, pp. 261-276.
[32] Jin, Y. Y., Singh, P., Chung, H. J., Hong, S. T., Blood Ammonia as a Possible Etiological Agent for Alzheimer's Disease. *Nutrients* 2018, *10*.
[33] Baker, M. S., Ahn, S. B., Mohamedali, A., Islam, M. T*., et al.*, Accelerating the search for the missing proteins in the human proteome. *Nat Commun* 2017, *8*, 14271.
[34] Legrain, P., Aebersold, R., Archakov, A., Bairoch, A*., et al.*, The human proteome project: current state and future direction. *Mol Cell Proteomics* 2011, *10*, M111.009993.
[35] Deutsch, E. W., Orchard, S., Binz, P. A., Bittremieux, W*., et al.*, Proteomics Standards Initiative: Fifteen Years of Progress and Future Work. *J Proteome Res* 2017, *16*, 4288-4298.
[36] Lochhead, J. J., Wolak, D. J., Pizzo, M. E., Thorne, R. G., Rapid transport within cerebral perivascular spaces underlies widespread tracer distribution in the brain after intranasal administration. *J Cereb Blood Flow Metab* 2015, *35*, 371-381.
[37] van Sorge, N. M., Doran, K. S., Defense at the border: the blood-brain barrier versus bacterial foreigners. *Future Microbiol* 2012, *7*, 383-394.
[38] Bitter, C., Suter-Zimmermann, K., Surber, C., Nasal drug delivery in humans. *Curr Probl Dermatol* 2011, *40*, 20-35.
[39] Chapman, C. D., Frey, W. H., 2nd, Craft, S., Danielyan, L*., et al.*, Intranasal treatment of central nervous system dysfunction in humans. *Pharm Res* 2013, *30*, 2475-2484.
[40] Vaka, S. R. K., Sammeta, S. M., Day, L. B., Murthy, S. N., Delivery of Nerve Growth Factor to brain via intranasal administration and enhancement of brain uptake. *Journal of pharmaceutical sciences* 2009, *98*, 3640-3646.
[41] Chen, X. Q., Fawcett, J. R., Rahman, Y. E., Ala, T. A., Frey, I. W., Delivery of Nerve Growth Factor to the Brain via the Olfactory Pathway. *J Alzheimers Dis* 1998, *1*, 35-44.
[42] Lochhead, J. J., Thorne, R. G., Intranasal delivery of biologics to the central nervous system. *Adv Drug Deliv Rev* 2012, *64*, 614-628.

[43] Wu, S., Li, K., Yan, Y., Gran, B.*, et al.*, Intranasal Delivery of Neural Stem Cells: A CNS-specific, Non-invasive Cell-based Therapy for Experimental Autoimmune Encephalomyelitis. *Journal of clinical & cellular immunology* 2013, *4*, 10.4172/2155-9899.1000142.
[44] Cheng, Y. S., Chen, Z. T., Liao, T. Y., Lin, C.*, et al.*, An intranasally delivered peptide drug ameliorates cognitive decline in Alzheimer transgenic mice. *EMBO Mol Med* 2017, *9*, 703-715.
[45] Haque, S., Md, S., Fazil, M., Kumar, M.*, et al.*, Venlafaxine loaded chitosan NPs for brain targeting: pharmacokinetic and pharmacodynamic evaluation. *Carbohydr Polym* 2012, *89*, 72-79.
[46] Vyas, T. K., Babbar, A. K., Sharma, R. K., Singh, S., Misra, A., Intranasal mucoadhesive microemulsions of clonazepam: preliminary studies on brain targeting. *J Pharm Sci* 2006, *95*, 570-580.
[47] Agrawal, M., Saraf, S., Antimisiaris, S. G., Chougule, M. B.*, et al.*, Nose-to-brain drug delivery: An update on clinical challenges and progress towards approval of anti-Alzheimer drugs. *J Control Release* 2018, *281*, 139-177.
[48] Pardeshi, C. V., Belgamwar, V. S., Direct nose to brain drug delivery via integrated nerve pathways bypassing the blood-brain barrier: an excellent platform for brain targeting. *Expert Opin Drug Deliv* 2013, *10*, 957-972.
[49] De Rosa, R., Garcia, A. A., Braschi, C., Capsoni, S.*, et al.*, Intranasal administration of nerve growth factor (NGF) rescues recognition memory deficits in AD11 anti-NGF transgenic mice. *Proc Natl Acad Sci U S A* 2005, *102*, 3811-3816.
[50] Capsoni, S., Marinelli, S., Ceci, M., Vignone, D.*, et al.*, Intranasal "painless" Human Nerve Growth Factors Slows Amyloid Neurodegeneration and Prevents Memory Deficits in App X PS1 Mice. *PLoS ONE* 2012, *7*, e37555.
[51] Zheng, X., Shao, X., Zhang, C., Tan, Y.*, et al.*, Intranasal H102 Peptide-Loaded Liposomes for Brain Delivery to Treat Alzheimer's Disease. *Pharm Res* 2015, *32*, 3837-3849.
[52] Guo, C., Wang, T., Zheng, W., Shan, Z. Y.*, et al.*, Intranasal deferoxamine reverses iron-induced memory deficits and inhibits amyloidogenic APP processing in a transgenic mouse model of Alzheimer's disease. *Neurobiol Aging* 2013, *34*, 562-575.
[53] Fine, J. M., Renner, D. B., Forsberg, A. C., Cameron, R. A.*, et al.*, Intranasal deferoxamine engages multiple pathways to decrease memory loss in the APP/PS1 model of amyloid accumulation. *Neurosci Lett* 2015, *584*, 362-367.
[54] Lin, C. Y., Cheng, Y. S., Liao, T. Y., Lin, C.*, et al.*, Intranasal Administration of a Polyethylenimine-Conjugated Scavenger Peptide Reduces Amyloid-beta Accumulation in a Mouse Model of Alzheimer's Disease. *J Alzheimers Dis* 2016, *53*, 1053-1067.
[55] Salama, M., Sobh, M., Emam, M., Abdalla, A.*, et al.*, Effect of intranasal stem cell administration on the nigrostriatal system in a mouse model of Parkinson's disease. *Exp Ther Med* 2017, *13*, 976-982.
[56] Bermudez, M. L., Skelton, M. R., Genter, M. B., Intranasal carnosine attenuates transcriptomic alterations and improves mitochondrial function in the Thy1-aSyn mouse model of Parkinson's disease. *Mol Genet Metab* 2018.
[57] Craft, S., Baker, L. D., Montine, T. J., Minoshima, S.*, et al.*, Intranasal insulin therapy for Alzheimer disease and amnestic mild cognitive impairment: a pilot clinical trial. *Arch Neurol* 2012, *69*, 29-38.
[58] Mischley, L. K., Leverenz, J. B., Lau, R. C., Polissar, N. L.*, et al.*, A randomized, double-blind phase I/IIa study of intranasal glutathione in Parkinson's disease. *Mov Disord* 2015, *30*, 1696-1701.

CONCLUSIONS

1. The OB proteomic signature performed at AD early stages in APP/PS1 and Tg2576 mice revealed imbalance in processes such as cytoskeletal rearrangement, mitochondrial homeostasis and synaptic plasticity together with disarrangements in cell-death and survival routes, prior to the appearance of Aβ plaques and memory impairment.
2. A progressive modulation of the OB transcriptome signature was demonstrated during AD progression, revealing EGFR, CREB1, TGF-beta, c-JUN and STAT3 as a specific olfactory transducer panel that significantly differs across proteinopathies.
3. A stage-dependent proteostatic derangement has been observed during AD evolution at the level of OB, revealing an early disruption in the p38 MAPK cascade and a subsequent impairment in the PDK1/PKC signaling axis, suggesting Phb complex as a differential driver in neurodegeneration at olfactory level.
4. In the case of PD, the stage-dependent OB proteome modulation pointed out an alteration in the activation dynamics of ERK1/2, MKK3/6 and PDK/PKC signaling axis. The survival potential of olfactory neurons clearly differs between AD and PD phenotypes.
5. The cross-disease study performed across AD and PD staging revealed different protein derangements in the modulation of SCGN, CACYBP and GNPDA2, indicating differences in olfactory processing, cytoskeletal dynamics and glucose metabolism.
6. The combination of alpha-synuclein and GNPDA2 biofluid protein profile may be considered as a potential biomarker candidate of PD.
7. A mild modulation in the OB proteomic signature was observed across the FTLD spectrum, suggesting impairments in calcium homeostasis and mitochondrial functionality in PSP and protein synthesis and vesicle trafficking in FTLD-TDP43, as well as highlighting cross-disease similarities and differences in the regulation of survival pathways.

CONCLUSIONES

1. El estudio proteómico realizado en el bulbo olfatorio de dos modelos murinos de la EA, APP/PS1 y Tg2576 ha demostrado alteraciones en procesos relacionados con el reordenamiento del citoesqueleto, la homeostasis mitocondrial y la plasticidad neuronal, junto con desajustes en rutas de muerte y supervivencia celular, antes de la aparición de placas amiloides y deterioro cognitivo.
2. Se ha demostrado la existencia de una modulación progresiva del transcriptoma del bulbo olfatorio durante la progresión de la EA. Además, se ha podido observar un comportamiento significativamente diferente en el panel de transductores EGFR, CREB1, TGF-beta, c-JUN y STAT3 entre distintas proteinopatías.
3. Se ha demostrado una alteración en la proteostasis del bulbo olfatorio estadio-dependiente durante la progresión de la EA, incluyendo desequilibrios tempranos en la cascada de p38 MAPK y posteriores en el eje PDK1/PKC. Además, se sugiere el papel diferencial del complejo Phb en procesos neurodegenerativos a nivel olfatorio.
4. En el caso de la EP, el análisis estadio-dependiente ha revelado una alteración en la activación de los ejes de señalización ERK1/2, MKK3/6 y PDK1/PKC. Además, el patrón en las cascadas de supervivencia neuronal difiere entre la EA y la EP.
5. El estudio cruzado realizado a través del estadiaje de la EA y la EP ha permitido identificar diferentes desequilibrios en los niveles de SCGN, CACYBP y GNPDA2 entre ambas enfermedades, indicando por tanto diferencias en el procesamiento de la información olfatoria, en la dinámica del citoesqueleto y el metabolismo de la glucosa.
6. La combinación de los perfiles de α-synucleína y GNPDA2 en fluidos biológicos puede considerarse un potencial biomarcador de la EP.
7. Se ha demostrado la existencia de una modulación leve del proteoma del bulbo olfatorio en enfermedades pertenecientes al espectro de degeneración lobar fronto-temporal. En concreto, se han observado desequilibrios relacionados con la homeostasis del calcio y la funcionalidad mitocondrial en PSP y en la síntesis de proteínas y el tráfico de vesículas en

FTLD-TDP43, así como similitudes y diferencias en la regulación de cascadas de supervivencia celular.

ANNEXES

- The supplementary information of each of the manuscripts is available in the CD located at the back of the thesis book.
- The original manuscripts already published are also available in the CD.
- Finally, the submission letters regarding the research articles that have not been published yet are also available.